Quantum electrodynamic shifts of mass and magnetic moment near dielectric or conducting surfaces

Robert Bennett

Submitted for the degree of Doctor of Philosophy

Department of Physics & Astronomy

School of Mathematical and Physical Sciences

University of Sussex

May 2013

Declaration

I hereby declare that this thesis has not been and will not be submitted in whole or in part to another University for the award of any other degree.

Signature:

Robert Bennett

"God made the bulk; surfaces were invented by the devil."

- Wolfgang Pauli

UNIVERSITY OF SUSSEX

Robert Bennett, Doctor of Philosophy

Quantum electrodynamic shifts of mass and magnetic moment near dielectric or conducting surfaces

Summary

Quantum electrodynamics is the spectacularly successful theory of the interaction of light and matter. Its consequences are well-understood, and have been experimentally verified to extreme precision. What is not generally known is how these predictions change when the theory is considered in anything other than free space – near a surface, for example. A material boundary causes vacuum fluctuations of the electromagnetic field to be different from their counterparts in free space, causing the electromagnetic environment of a microscopic system sitting near the boundary to differ from that if the surface were not present. This causes a variety of surface-dependent shifts in the properties of the microscopic system – this work investigates these shifts for a free electron. First using explicit normal mode expansion and analytic continuation of the wave-vector in the complex plane, and then using a semi-phenomenological 'noise current' approach, the work presents derivations of formulae for the shifts in the mass and magnetic moment of an electron near a dispersive and absorbing surface. The formalism is also extended to the case where the electron is subject to a harmonic potential. It is noted that results for different models of the surface do not agree in the expected limiting cases due to their differing behaviour at low frequency, which leads to the conclusion that one must be very careful to use an appropriate model of a particular surface when considering quantum electrodynamic surface effects. Analysis of the results shows that use of a realistic model of the surface can make these shifts orders of magnitude larger than previous calculations had suggested, since they all relied on the somewhat unrealistic assumption that the surface is perfectly reflecting. This is shown to be particularly relevant to experiments which aim to measure the anomalous magnetic moment of an electron.

Acknowledgements

It is a pleasure to thank Dr. Claudia Eberlein for helping me learn enough to write this thesis, and for numerous suggestions and guidance along the way. I would also like to thank Dr. Robert Zietal for regular encouragement and advice, as well as for numerous cups of coffee.

Contents

Chapter 1

Thesis outline

Quantum electrodynamics is the extraordinarily successful theory of the interaction of light and matter – its predictions are well-understood and have been experimentally verified to extreme precision. Perhaps surprising is that the interaction of quantum electrodynamic systems with objects in their vicinity is relatively poorly understood, even though this is an unavoidable scenario in any real experiment. Such objects modify the quantum-mechanical fluctuations of the electromagnetic vacuum field that exists throughout space, meaning that any quantum system coupled to that field will experience effects that are due to the presence of objects in its vicinity.

This thesis aims to quantify some of these effects for a free electron near a surface. We will begin by discussing the general properties of the quantum-mechanical vacuum state in Chapter 2, before moving on to a discussion of the quantization of the electromagnetic vacuum field. Following this we will outline the challenges one faces when trying to describe the quantized electromagnetic field in the presence of dielectric materials. In Chapter 3 we will detail two specific models of the surface which allow one to derive an explicit mode expansion for the quantized electromagnetic field in its vicinity, and then in Chapter 4 we will use this to calculate the shift in the mass of an electron near such surfaces. We will then extend our model to arbitrary surfaces, and discuss the experimental relevance of our calculation.

The mass shift acts as an introduction to the methods that we will employ – a more involved and physically relevant calculation is that of the shift in the magnetic moment of an electron near a surface. In Chapter 5 we will use perturbation theory in the Dirac equation to derive an expression that delivers the shift in the magnetic moment in terms of the normal modes of the quantized electromagnetic field near an interface. We will then use our explicit expressions for the mode expansions near various materials to calculate the

magnetic moment shift of an electron near a selection of surfaces. We will then generalize our results to arbitrary surfaces and discuss the experimental consequences thereof, with particular reference to precision measurements of the anomalous magnetic moment of the electron. We will show that under favorable conditions a measurement of the surface-dependent part of the magnetic moment may be on the verge of experimental viability, which is of distinct importance because of the anomalous magnetic moment's role as one of the most accurately measured quantities in all of physics. In Chapter 6 we will bring our work closer to experiment by considering surface-induced shifts in the properties of an electron subject to harmonic confinement near an interface, which is a common scenario in real experiments that aim to measure the anomalous magnetic moment of the electron.

Finally, in Chapter 7 we will dispense with the mode expansion and use an entirely different method based on the so-called 'noise-current' description of quantum electrodynamics in media to calculate the same quantities as in Chapters 4 and 5, namely the mass and magnetic moment of an electron near a surface. These noise-current calculations were done because much of the work in Chapters 4 and 5 is based on entirely new methods, so comparison with an existing formalism is of obvious importance. We will show that the results of Chapters 4 and 5 can be reproduced using the noise-current approach, and provide some insight into its relationship with the mode expansion method.

Chapter 2

Introduction

2.1 Vacuum fluctuations

The origin of the present understanding of the vacuum is largely the pioneering work of Max Planck in the first years of the 20th century, in which he resurrected Newton's idea that light exists only in discrete lumps (called 'quanta') in order to develop a theory which successfully explained the experimentally observed spectrum of black body radiation. Planck did not immediately realize that this represented a revolution in physics, dubbing it "a purely formal assumption" [1]. Each quantum was defined to possess energy $h\nu = \hbar\omega$, where $\hbar$ is now known as the reduced Planck's constant $h/2\pi$ and ω is the angular frequency of radiation with frequency ν. In order to recover the continuous, classical theory from a quantized theory, one should take the limit of large quantum numbers, which is mathematically equivalent to taking $\hbar \to 0$. A 1913 paper of Einstein and Stern [2] noted that average energy of a harmonic oscillator of frequency ω at temperature T in Planck's theory is

$$E = \frac{\hbar\omega}{e^{\hbar\omega/k_B T} - 1} \approx k_B T - \frac{1}{2}\hbar\omega + \mathcal{O}(\hbar^2) \tag{2.1}$$

as $\hbar \to 0$. The equipartition theorem states that the above energy should be equal to $k_B T$, so we must add an energy of $\frac{1}{2}\hbar\omega$ in order to satisfy the theorem to first order in $\hbar$. They named this addition the *Nullpunktsenergie* ("zero-point energy"). Einstein and Stern concluded their paper by stating that "the existence of zero-point energy of magnitude $\frac{1}{2}\hbar\omega$ is probable".

The development of quantum mechanics in the 1920s culminated in Schrödinger's famous equation, which is succinctly represented as

$$i\hbar\frac{\partial}{\partial t}\Psi(x,t) = \hat{H}\Psi(x,t)\ , \tag{2.2}$$

where $\hat{H}$ is the Hamiltonian operator which acts on the state $\Psi(x,t)$ and whose eigenvalue

for a stationary state $\Psi(x)$ is the energy of that state. For a particle of mass m moving in potential in one dimension, the (classical) Hamiltonian reads

$$H = \frac{p^2}{2m} + V(x) \ . \tag{2.3}$$

Position x and momentum p are canonically conjugate variables. The Poisson bracket for functions of f and g of the canonical variables p and q is defined as

$$\{f, g\} = \frac{\partial f}{\partial q}\frac{\partial g}{\partial p} - \frac{\partial f}{\partial p}\frac{\partial g}{\partial q} \ . \tag{2.4}$$

It is clear that if f and g are themselves canonically conjugate co-ordinate and momentum ($f = q$, $g = p$), their Poisson bracket will be unity. In particular, we have for the harmonic oscillator described by (2.3):

$$\{x, p\} = 1 \ . \tag{2.5}$$

Canonical quantization consists of promoting the canonical variables to operators and replacing the Poisson bracket (2.5) with the commutator

$$[\hat{x}, \hat{p}] = i\hbar, \tag{2.6}$$

so that the Hamiltonian H becomes the Hamiltonian operator $\hat{H}$

$$\hat{H} = \frac{\hat{p}^2}{2m} + V(\hat{x}) \ . \tag{2.7}$$

The commutator (2.6) leads to the famous Heisenberg uncertainty relation

$$\Delta x \Delta p \geq \frac{\hbar}{2}, \tag{2.8}$$

where Δx and Δp are the standard deviations of position and momentum, respectively. This shows that one cannot simultaneously observe the position and momentum of a quantum system to arbitrary accuracy, or, equivalently, very accurate measurement of the position of a particle introduces significant uncertainty into its momentum. In fact, the relation holds for any pair of conjugate variables [3], for example energy E and time t

$$\Delta E \Delta t \geq \frac{\hbar}{2} \ . \tag{2.9}$$

Since, in quantum mechanics, time is a actually a parameter not a variable, the interpretation of Δt above is not without controversy (see, for example [4]). However, the relation provides a heuristic justification of the way in which quantum mechanics predicts the existence of vacuum fluctuations – if a process happens over a very short timescale, a significant uncertainty is introduced into its energy. Or, very loosely, processes which happen over

very short timescales have a 'fuzziness' in their energy, meaning that conservation of energy is not strictly imposed.

The next question is how, if at all, these heuristic discussions can be formalized in such a way as to lead to the zero-point energy that Einstein and Stern postulated. The answer is provided by solution of the Schrödinger equation for a single particle moving in a one-dimensional harmonic potential, for which the (classical) Hamiltonian is

$$H = \frac{p^2}{2m} + \frac{1}{2}m\omega^2 x^2, \tag{2.10}$$

where ω is the angular frequency of the harmonic motion. The position and momentum are of course still the canonically conjugate variables, as can be easily verified by checking that Eq. (2.10) satisfies Hamilton's equations of motion. Thus we may immediately canonically quantize to give

$$\hat{H} = \frac{\hat{p}^2}{2m} + \frac{1}{2}m\omega^2\hat{x}^2 \ . \tag{2.11}$$

The Schrödinger equation (2.2) with this Hamiltonian can be solved relatively easily by using an analytical method, with the resulting wave functions being expressed in terms of Hermite polynomials (see, for example, [5]), from which one can extract the energy eigenvalues. However, it is in fact possible to extract these eigenvalues purely algebraically, i.e. without solving the differential equation. To do this, one uses Dirac's 'ladder operator' method. Since this method is of huge utility in the more complex problems considered later (as well as across all of physics), it is the approach we follow here. We begin by introducing the following non-Hermitian operators

$$\hat{a} = \frac{1}{\sqrt{2\hbar m\omega}}(\hat{p} - im\omega\hat{x}), \tag{2.12a}$$

$$\hat{a}^\dagger = \frac{1}{\sqrt{2\hbar m\omega}}(\hat{p} + im\omega\hat{x}), \tag{2.12b}$$

which, as a consequence of (2.6), have the commutator

$$[\hat{a}, \hat{a}^\dagger] = 1 \ . \tag{2.13}$$

These can be used to write the Hamiltonian as

$$\hat{H} = \hbar\omega\left(\hat{a}^\dagger\hat{a} + \frac{1}{2}\right). \tag{2.14}$$

The energy levels are specified by the eigenvalues $n \in \mathbb{N}$ of the (Hermitian) operator $\hat{a}^\dagger\hat{a}$ acting upon the state $|n\rangle$. It is well-known that acting the operators $\hat{a}$ and $\hat{a}^\dagger$ on a state, defining a ground state $\hat{a}\,|0\rangle = 0$ and enforcing a normalization gives the following algebra

for the operators

$$\hat{a}\,|n\rangle = \sqrt{n}\,|n-1\rangle\,, \tag{2.15a}$$

$$\hat{a}^\dagger\,|n\rangle = \sqrt{n+1}\,|n+1\rangle\,, \tag{2.15b}$$

which immediately gives the energy levels as

$$E_n = \hbar\omega\left(n+\frac{1}{2}\right), \qquad n = 0, 1, 2, ... \tag{2.16}$$

which, of course, is the same result one gets from explicitly solving the Schrödinger equation. In the lowest state ($n = 0$), we have non-zero energy $\frac{\hbar\omega}{2}$, just as Einstein and Stern predicted. We have reached this conclusion by beginning from a classical model (2.10), identifying the canonically conjugate position and momentum (which was trivial in this case) and promoting these to operators that obey the canonical commutation relation (2.6). The same approach will be taken in discussion of electromagnetism in the next section.

2.2 The electromagnetic vacuum

To demonstrate the real world consequences of vacuum fluctuations, we explore their role in electromagnetism. An obvious starting point is to write down Maxwell's equations in vacuum without any charges or currents

$$\begin{aligned} \nabla\cdot\mathbf{E}(\mathbf{r},t) &= 0, & \nabla\times\mathbf{E}(\mathbf{r},t) &= -\frac{\partial}{\partial t}\mathbf{B}(\mathbf{r},t), \\ \nabla\cdot\mathbf{B}(\mathbf{r},t) &= 0, & \nabla\times\mathbf{B}(\mathbf{r},t) &= \frac{\partial}{\partial t}\mathbf{E}(\mathbf{r},t), \end{aligned} \tag{2.17}$$

from which we hope to identify canonically conjugate variables so that we may quantize the free electromagnetic field along the same lines as in the previous section. From here onwards we work in a system of natural units where c, $\hbar$ and ϵ_0 are all equal to 1. Introducing the usual electromagnetic potentials $\mathbf{A}$ and ϕ as the objects that satisfy

$$\mathbf{B}(\mathbf{r},t) = \nabla\times\mathbf{A}(\mathbf{r},t), \qquad \mathbf{E}(\mathbf{r},t) = -\frac{\partial\mathbf{A}(\mathbf{r},t)}{\partial t} - \nabla\phi(\mathbf{r},t), \tag{2.18}$$

eqs. (2.17) can be reduced to a pair of coupled differential equations

$$\nabla\times[\nabla\times\mathbf{A}(\mathbf{r},t)] + \frac{\partial^2}{\partial t^2}\mathbf{A}(\mathbf{r},t) - \frac{\partial\nabla\phi(\mathbf{r},t)}{\partial t} = 0\,, \tag{2.19a}$$

$$\frac{\partial}{\partial t}\nabla\cdot\mathbf{A}(\mathbf{r},t) + \nabla\cdot\nabla\phi(\mathbf{r},t) = 0\,. \tag{2.19b}$$

These may be decoupled by astute choice of gauge. In this section we choose the Coulomb gauge, $\nabla\cdot\mathbf{A} = 0$. It is easy to see on inspection of eq. (2.19b) that this gauge condition means $\phi(\mathbf{r},t)$ may be set to zero, meaning that eq. (2.19a) becomes

$$\nabla\times[\nabla\times\mathbf{A}(\mathbf{r},t)] + \frac{\partial^2}{\partial t^2}\mathbf{A}(\mathbf{r},t) = 0, \tag{2.20}$$

and we note in particular from eqs. (2.18) that

$$\mathbf{E}(\mathbf{r},t) = -\frac{\partial \mathbf{A}(\mathbf{r},t)}{\partial t} \,. \tag{2.21}$$

Using a vector identity and the Coulomb gauge condition to simplify eq. (2.20), we obtain a wave equation for the vector potential $\mathbf{A}$:

$$\nabla^2 \mathbf{A}(\mathbf{r},t) - \frac{\partial^2}{\partial t^2}\mathbf{A}(\mathbf{r},t) = 0, \tag{2.22}$$

The solutions to this equation are monochromatic waves, which for a single field mode are given by

$$\mathbf{A}_\mathbf{k}(\mathbf{r},t) = \alpha(0)e^{-i\omega t}\mathbf{f}_\mathbf{k}(\mathbf{r}) + \alpha^*(0)e^{i\omega t}\mathbf{f}^*_\mathbf{k}(\mathbf{r}), \tag{2.23}$$

where $\mathbf{f}_\mathbf{k}(\mathbf{r})$ satisfies the Helmholtz equation

$$\left(\nabla^2 + \omega^2\right)\mathbf{f}_\mathbf{k}(\mathbf{r}) = 0 \,. \tag{2.24}$$

Defining

$$q(t) = i\left[N\alpha(t) - N^*\alpha^*(t)\right], \tag{2.25a}$$

$$p(t) = k\left[N\alpha(t) + N^*\alpha^*(t)\right], \tag{2.25b}$$

where N is a normalization constant, the Hamiltonian for this single electromagnetic field mode satisfies

$$H_\mathbf{k} = \frac{1}{2}\int d^3\mathbf{r}(\mathbf{E}^2 + \mathbf{B}^\mathbf{2}) = \frac{|N|^2}{2}(p(t)^2 + \omega^2 q(t)^2) \,. \tag{2.26}$$

The Hamilton equations that follow from this are

$$\dot{q}(t) = p(t), \qquad \dot{p}(t) = -\omega^2 q(t) \,. \tag{2.27}$$

These can also be derived from eqs. (2.25), showing that q and p are canonically conjugate co-ordinate and momentum variables, meaning that on promotion to operators they obey the canonical commutation relation

$$[\hat{q}(t), \hat{p}(t)] = i, \tag{2.28}$$

with $\hat{q}(t)$ and $\hat{p}(t)$ representing operator-valued versions of eqs (2.25)

$$\hat{q}(t) = i\left[N\hat{a}(t) - N^*\hat{a}^\dagger(t)\right], \tag{2.29a}$$

$$\hat{p}(t) = k\left[N\hat{a}(t) + N^*\hat{a}^\dagger(t)\right], \tag{2.29b}$$

The single-mode classical vector potential $\mathbf{A}_\mathbf{k}$ becomes the operator $\hat{\mathbf{A}}_\mathbf{k}$

$$\hat{\mathbf{A}}_\mathbf{k}(\mathbf{r},t) = N\hat{a}(0)e^{-i\omega t}\mathbf{f}_\mathbf{k}(\mathbf{r}) + N^*\hat{a}^\dagger(0)e^{i\omega t}\mathbf{f}^*_\mathbf{k}(\mathbf{r}), \tag{2.30}$$

and the Hamiltonian H for the electromagnetic field becomes the Hamiltonian operator $\hat{H}$

$$\hat{H}_{\mathbf{k}} = \frac{|N|^2}{2}(\hat{p}(t)^2 + \omega^2 \hat{q}(t)^2) \, . \tag{2.31}$$

We now choose a normalization such that this Hamiltonian can be written in the canonical form

$$\hat{H}_{\mathbf{k}} = \hbar\omega \left(\hat{a}^\dagger \hat{a} + \frac{1}{2} \right), \tag{2.32}$$

which corresponds to choosing $N = 1/\sqrt{2\omega}$. The commutation relation becomes

$$\left[\hat{a}(t), \hat{a}^\dagger(t) \right] = 1 \, , \tag{2.33}$$

completing the quantum description of a single mode of the electromagnetic field.

The extension of this to a multi-mode field is straightforward. The multi-mode field must satisfy the Helmholtz equation (2.24), and the Coulomb gauge condition $\nabla \cdot \mathbf{A}$. The simplest choice of $\mathbf{f}_{\mathbf{k}}(\mathbf{r})$ that satisfies these is

$$\mathbf{f}_{\mathbf{k}}(\mathbf{r}) = \hat{\mathbf{e}}_\lambda(\mathbf{k}) e^{i\mathbf{k}\cdot\mathbf{r}}, \tag{2.34}$$

where $\hat{\mathbf{e}}_\lambda(\mathbf{k})$ is some vector that obeys

$$\mathbf{k} \cdot \hat{\mathbf{e}}_\lambda(\mathbf{k}) = 0 \, . \tag{2.35}$$

This has two independent solutions corresponding to the two possible polarizations of the electromagnetic field, other than that the choice of $\hat{\mathbf{e}}_\lambda(\mathbf{k})$ is arbitrary. A convenient choice, used throughout this thesis, is the TE (transverse-electric) and TM (transverse-magnetic) polarization vectors listed appendix A.1.1. The linearity of Maxwell's equations means that we can simply sum over all the modes to find the expression in the Heisenberg picture for the electromagnetic field in Coulomb gauge:

$$\hat{\mathbf{A}}(\mathbf{r}, t) = \frac{1}{(2\pi)^{3/2}} \sum_\lambda \int d^3\mathbf{k} \frac{1}{\sqrt{2\omega}} \left[\hat{a}_{\mathbf{k}\lambda} e^{-i\omega_k t} e^{i\mathbf{k}\cdot\mathbf{r}} + \hat{a}^\dagger_{\mathbf{k}\lambda} e^{i\omega_k t} e^{-i\mathbf{k}\cdot\mathbf{r}} \right] \hat{\mathbf{e}}_{\mathbf{k}\lambda}(\mathbf{k}) \, , \tag{2.36}$$

where $\hat{a}_{\mathbf{k}\lambda} \equiv \hat{a}_{\mathbf{k}\lambda}(0)$ and $\lambda = \text{TE}, \text{TM}$. The operators $\hat{a}_{\mathbf{k}\lambda}$ and $\hat{a}^\dagger_{\mathbf{k}\lambda}$ represent creation and annihilation operators for the harmonic oscillator corresponding to each Fourier mode of the electromagnetic field. The normalization is obtained by demanding that the electromagnetic field Hamiltonian (2.26) is written in the canonical form

$$\hat{H}_{\text{EM}} = \sum_\lambda \int d^3\mathbf{k} \, \omega \left(\hat{a}_{\mathbf{k}\lambda} \hat{a}^\dagger_{\mathbf{k}\lambda} + \frac{1}{2} \right). \tag{2.37}$$

This corresponds to an infinite continuum of *uncoupled* harmonic oscillators, meaning that the different modes of the field are independent and obey the commutation relation

$$\left[\hat{a}_{\mathbf{k}\lambda}, \hat{a}^\dagger_{\mathbf{k}'\lambda'} \right] = \delta^{(3)}(\mathbf{k} - \mathbf{k}')\delta_{\lambda\lambda'} \, , \tag{2.38}$$

where $\delta^{(3)}(\mathbf{k}-\mathbf{k}') \equiv \delta(k_x-k_x')\delta(k_y-k_y')\delta(k_z-k_z')$. For our purposes it proves convenient to rewrite (2.36) as

$$\hat{\mathbf{A}}(\mathbf{r},t) = \sum_{\lambda} \int d^3\mathbf{k} \left[\hat{a}_{\mathbf{k}\lambda} e^{-i\omega_k t} \mathbf{f}_{\mathbf{k}\lambda}(\mathbf{r},\omega) + \hat{a}^{\dagger}_{\mathbf{k}\lambda} e^{i\omega_k t} \mathbf{f}^{*}_{\mathbf{k}\lambda}(\mathbf{r},\omega) \right], \tag{2.39}$$

with

$$\mathbf{f}_{\mathbf{k}\lambda}(\mathbf{r},\omega) = \frac{1}{(2\pi)^{3/2}} \frac{1}{\sqrt{2\omega}} e^{i\mathbf{k}\cdot\mathbf{r}} \hat{\mathbf{e}}_{\mathbf{k}\lambda}, \tag{2.40}$$

which is called a mode function. The expression (2.40) is the mode function for free space – throughout this thesis we will consider analogues of (2.40) for systems that impose boundary conditions on the electromagnetic field.

An important property of the mode functions is their completeness. To see that they are complete, we rewrite eq. (2.20) in frequency space

$$\nabla \times [\nabla \times \mathbf{A}(\mathbf{r},\omega)] = \omega^2 \mathbf{A}(\mathbf{r},\omega) \, . \tag{2.41}$$

The operator $\nabla \times \nabla \times$ is Hermitian, so this is a Hermitian eigenvalue problem. This means that the vector potential $\mathbf{A}$ may be expanded into mode functions, and those mode functions must be complete. The completeness relation is

$$\int d^3\mathbf{k} \; (2\omega) f^{i}_{\mathbf{k}\lambda}(\mathbf{r},\omega) f^{j*}_{\mathbf{k}\lambda}(\mathbf{r}',\omega) = \delta^{\perp}_{ij}(\mathbf{r}'-\mathbf{r}), \tag{2.42}$$

where $\delta^{\perp}_{ij}(\mathbf{r}'-\mathbf{r})$ is the transverse delta function, expressed through its Fourier transform as

$$\delta^{\perp}_{ij}(\mathbf{r}'-\mathbf{r}) = \int \frac{d^3\mathbf{k}}{(2\pi)^3} e^{i\mathbf{k}\cdot(\mathbf{r}-\mathbf{r}')} \left(\delta_{ij} - \frac{k_i k_j}{k^2} \right). \tag{2.43}$$

This is the unit operator in the space of transverse vector functions. The transverse δ function also appears in the equal-time commutation relations for the fields, for example

$$[A_i(\mathbf{r}), E_k(\mathbf{r})] = -i\delta^{\perp}_{ik}(\mathbf{r}-\mathbf{r}') \, . \tag{2.44}$$

Finally, we note that the orthogonality and normalization relation is

$$\int d^3\mathbf{r} \; \mathbf{f}_{\mathbf{k}\lambda}(\mathbf{r},\omega) \cdot \mathbf{f}^{*}_{\mathbf{k}'\lambda'}(\mathbf{r},\omega) = \frac{1}{2\omega} \delta_{\lambda\lambda'} \delta^{(3)}(\mathbf{k}'-\mathbf{k}) \, . \tag{2.45}$$

The normalization is fixed by our stipulation that the electromagnetic field Hamiltonian should be written in the canonical form (2.37).

We began this section with the goal of demonstrating the real-world consequences of vacuum fluctuations. We have from (2.37) that the vacuum energy is the sum over the zero-point energies of all the modes of the electromagnetic field

$$E_{\text{vac}} = \sum_{\text{all modes}} \frac{\omega_k}{2} \, , \tag{2.46}$$

which is of course infinite. It seems as if this energy must be irrelevant to observations since no absolute energy measurement can be made[1], we can only measure energies relative to some reference which one might as well take as the vacuum energy. However, this is not the case – the vacuum energy *is* relevant to observations. The reason for this is that the zero point energy (2.46) depends on the mode *structure*, not simply the magnitude of the corresponding energy. Thus altering the mode structure of the vacuum will have real, observable consequences, even though we can only measure energy differences. One way that this alteration can be actually realized is by the introduction of macroscopic objects which modify the electromagnetic field by imposing boundary conditions upon it. In the next section we discuss the most famous way that this alteration can be observed – the Casimir effect. We will also discuss a related fluctuation-induced force known as the Casimir-Polder effect.

2.3 Observing the vacuum

2.3.1 The Casimir effect

The usual example of the 'reality' of vacuum fluctuations is the experimental confirmation of the Casimir effect – the attraction between two material bodies due to the restrictions they place upon the electromagnetic vacuum. If we consider two parallel, perfectly conducting plates separated by vacuum we can avoid many of the complications associated with field quantization in real media. The only way the electromagnetic field 'sees' the plates is via the boundary conditions they impose upon it, which are that the parallel electric field and perpendicular magnetic fields both vanish. Following [6], we begin by decomposing the $\mathbf{k}$ vector into components parallel to the surface ($\mathbf{k}_\parallel$) and perpendicular to it (k_z), giving for the vacuum energy

$$E_{\text{vac}} = \frac{1}{2} \sum_{\text{all modes}} |\mathbf{k}| = \frac{1}{2} \sum_{\text{all modes}} \sqrt{k_\parallel^2 + k_z^2}, \tag{2.47}$$

The boundary conditions mean that the modes are restricted, in particular k_z may only take on values $n\pi/a$, where a is the separation of the plates and $n = 0, 1, 2, \ldots$. Thus the energy E_C contained between plates of area L^2 for one polarization of the electromagnetic field becomes

$$E_{\text{C}}(\text{single polarization}) = \frac{L^2}{2} \sum_{n=0}^{\infty} \int \frac{d^2\mathbf{k}_\parallel}{(2\pi)^2} \sqrt{k_\parallel^2 + \left(\frac{n\pi}{a}\right)^2}, \tag{2.48}$$

[1] An exception is in general relativity, where energies can be inferred by measurement of the curvature of spacetime.

If n is zero only one polarization survives, so we may write for the sum of the two polarizations

$$E_{\rm C} = \frac{L^2}{2}\int \frac{d^2\mathbf{k}_\parallel}{(2\pi)^2}\left[k_\parallel + 2\sum_{n=1}^{\infty}\sqrt{k_\parallel^2 + \left(\frac{n\pi}{a}\right)^2}\right] . \tag{2.49}$$

This is infinite, so we renormalize by a process which is repeated many times in this thesis – we subtract the energy that *would* have been in the system if the bounding surfaces were not present. In this case, this is the electromagnetic vacuum energy contained within in a simple box of volume L^2a. This is

$$E_0 = \frac{L^2 a}{2}\int \frac{d^2\mathbf{k}_\parallel}{(2\pi)^2}\int_{-\infty}^{\infty}\frac{dk_z}{(2\pi)} 2\sqrt{k_\parallel^2 + k_z^2} . \tag{2.50}$$

Changing variables to $k_z = n\pi/a$, this becomes

$$E_0 = \frac{L^2}{2}\int \frac{d^2\mathbf{k}_\parallel}{(2\pi)^2}\int_0^{\infty} dn\, 2\sqrt{k_\parallel^2 + \left(\frac{n\pi}{2}\right)^2} , \tag{2.51}$$

giving the energy per unit area as

$$\Delta E_C = \frac{E_C - E_0}{L^2} = \frac{1}{2\pi}\int_0^{\infty} dk_\parallel k_\parallel \left[\frac{k_\parallel}{2} + \sum_{n=1}^{\infty}\sqrt{k_\parallel^2 + \left(\frac{n\pi}{a}\right)^2} - \int_0^{\infty} dn\sqrt{k_\parallel^2 + \left(\frac{n\pi}{2}\right)^2}\right] , \tag{2.52}$$

where we have transformed to spherical polar co-ordinates and carried out the trivial angular integration. This expression is still divergent at large $k_\parallel$ and must be regularized, which we achieve by introducing a smooth cutoff function $f(k_\parallel)$, where

$$f(k_\parallel) = \begin{cases} 1 & \text{if } k_\parallel \lesssim k_\parallel^{\rm crit} \\ 0 & k_\parallel \gg k_\parallel^{\rm crit} . \end{cases} \tag{2.53}$$

Changing variables to $u = a^2k_\parallel^2/\pi$, this leads to:

$$\Delta E_C = \frac{\pi^2}{4a^3}\left[\frac{1}{2}F(0) + \sum_{n=1}^{\infty}F(n) - \int_0^{\infty} dn F(n)\right] , \tag{2.54}$$

with

$$F(n) = \int_{n^2}^{\infty} du\sqrt{u} f(\pi\sqrt{u}/a) . \tag{2.55}$$

Equation (2.54) is convergent. Using the Euler-MacLaurin summation formula (see, for example, [7] sec. 23.1.30) and the properties of $f(k_\parallel)$, the energy evaluates to

$$\Delta E_C = -\frac{\pi^2}{720a^3} , \tag{2.56}$$

where it should be noted that all reference to the regulator has disappeared. Taking the negative gradient of this and restoring factors of $\hbar$ and c finally gives the pressure

$$\frac{F}{L^2} = -\frac{\hbar c\pi^2}{240a^4} \approx 0.001(\mu\text{m})^{-4}\text{Pa} . \tag{2.57}$$

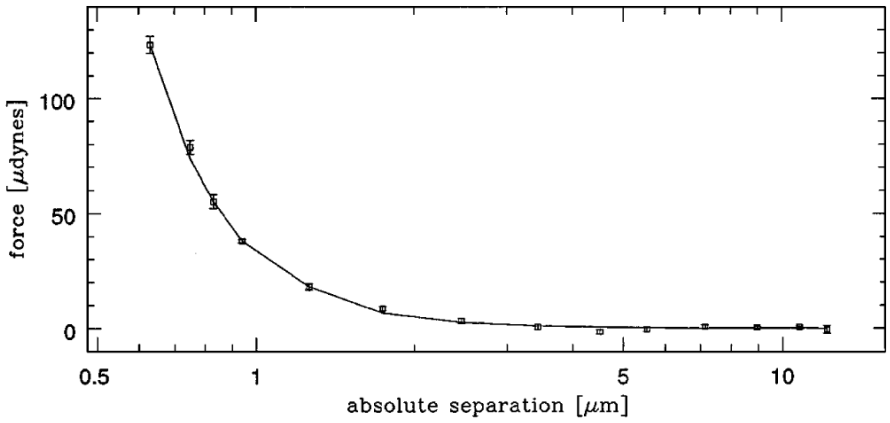

Figure 2.1: (Reproduced from [8]) Measurements of the Casimir effect using a torsion pendulum showing good agreement with theoretical predictions (solid line). However, later analyses showed that at separations below 1μm the error bars are significantly underestimated [9].

as found in Casimir's original paper [10]. So, we have a measurable attraction between the plates which originates from their modification of the mode structure between them, namely restricting the wave vector in the direction perpendicular to the plates to discrete values. The result has been rederived in a wide variety of other ways, most notably in the generalization to bulk dielectrics accomplished by by Landau and Lifshitz [11]. Other approaches include scattering theory [12], geometrical optics [13] and consideration of the plates as δ function potentials [14], amongst numerous others.

It is clear from (2.57) that even for micrometer separations the effect is small. However, a pioneering experiment attempting to measure the Casimir effect was undertaken as early as 1958 by Sparnaay [15], who found results which "do not contradict Casimir's theoretical prediction", although this experiment had significant problems due to stray charges on the plates. The first modern experiment which measured the effect to reasonable accuracy was done by Lamoreaux [8, 16, 17] as shown in fig. 2.1. The extreme difficulty of such measurements has led to continuing controversy [9] over the validity of these results. Later measurements by Decca et. al are shown in fig. 2.2.

The serious experimental problems encountered with measurements of the Casimir effect have meant that it is worthwhile considering a family of closely related phenomena, chiefly the Casimir-Polder effect.

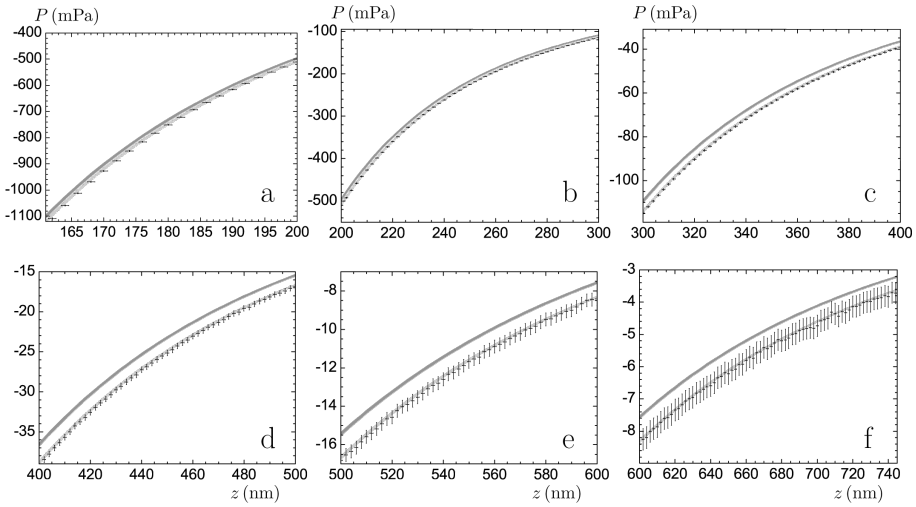

Figure 2.2: (Reproduced from [18]) Measurements of the Casimir pressure at various separations using a micromachined mechanical oscillator compared to two theoretical models of the surfaces. The horizontal error bars represent uncertainty in the measurement of the distance between the surfaces, and the vertical error bars represent uncertainty in the measurement of the pressure.

2.3.2 The Casimir-Polder effect

It is well-known that in free space the degeneracy of the $^2S_{1/2}$ and $^2P_{1/2}$ hydrogen orbitals is lifted due to the interaction of the atomic electron with the quantized electromagnetic vacuum field. This is known as the Lamb shift, and was discovered in a 1947 experiment of Lamb and Rutherford [19]. It stands to reason that modification of the vacuum field by imposition of external boundary conditions (such as those applied by a material surface) should produce a further shift in the transition frequency between atomic orbitals. This 'shift in the Lamb shift' was first described in 1948 by Casimir and Polder [20], and is now known as the Casimir-Polder effect.

Calculation of the effect is most conveniently done by in the multipolar coupling approach to QED, where the sources appearing in Maxwell's equations are replaced by the polarization $\mathbf{P}(\mathbf{r})$ and magnetization $\mathbf{M}(\mathbf{r})$ that the atomic electron generates. For example, the polarization for an atom with its nucleus at $\mathbf{r}$ and an electron at $\mathbf{q}$ is:

$$\mathbf{P}(\mathbf{r}) = -e\mathbf{q}\int_0^1 d\lambda\delta^{(3)}(\mathbf{r}-\lambda\mathbf{q})\,. \tag{2.58}$$

Assuming that the electron co-ordinate q is by far the smallest length scale in the problem, this may be approximated to

$$\mathbf{P}(\mathbf{r}) = -e\mathbf{q}\int_0^1 d\lambda\delta^{(3)}(\mathbf{r}-\lambda\mathbf{q}) \approx -\mathbf{x}\,\delta^{(3)}(\mathbf{r}), \tag{2.59}$$

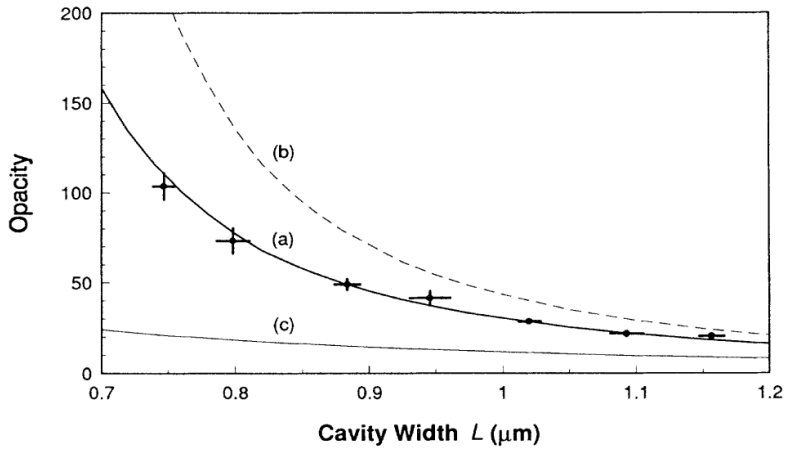

Figure 2.3: (Reproduced from [21]) Measurements of the Casimir-Polder shift in the micrometer regime

where $\mathbf{x} = -e\mathbf{q}$ is the electric dipole moment of the electron. This is known as the dipole approximation. For neutral atoms one can the apply the Power-Zienau transformation [22] which allows the Hamiltonian describing the interaction of the atomic electron and the quantized field to be written in a very simple form, namely

$$H_{\text{int}} = -\mathbf{x} \cdot \mathbf{E} \,. \tag{2.60}$$

Casimir and Polder's original calculation [20] was somewhat complicated due to the fact that it was done without the aid of the multipolar coupling technique. More modern calculations are in agreement with Casimir and Polder's, and proceed much more simply using the dipole approximation. The now well-known dependence of the frequency shift $\Delta\nu$ from the ground state to the first excited state in two asymptotic cases (known as the 'non-retarded' and 'retarded' regimes) as

$$\Delta\nu \propto \frac{1}{z^3} \qquad \text{for } \tau_\gamma \ll \tau_a, \qquad\qquad \Delta\nu \propto \frac{1}{z^4} \qquad \text{for } \tau_\gamma \gg \tau_a, \tag{2.61}$$

where τ_γ is the typical time needed for a virtual photon to make the round trip from the atom to the surface and back, and τ_a is the time associated with the atomic transition under consideration. The shift was measured in the 1990s [21, 23], and, as shown in fig. 2.3, found good agreement with experiment.

2.4 Free electron vs atom

The main limiting factor on precise measurements of the Lamb shift (and consequently the Casimir-Polder shift) is the large uncertainty in the charge radius r_p of the proton

[24]. The current accepted CODATA value obtained by precision spectroscopy of atomic hydrogen is $r_p = 0.8775(51)$fm [25] – the error is around 0.6%, which is extremely large compared to that for other fundamental quantities. The consequences of this for the Lamb shift $\delta\nu$ are that its error is relatively large, for example the best theoretical estimate of the 2S Lamb shift in hydrogen based on the CODATA proton radius is $\delta\nu = 1.045003(4)$kHz [26], which is an error of around 4 parts per million. Further to this, the method used to obtain the CODATA radius relies on bound-state QED calculations, and thus is vulnerable to insufficiencies in these – the results of some two-loop effects in hydrogen have recently been questioned [27]. A recent experiment [28] found a proton radius which differs from the CODATA value by five standard deviations. Since a free electron is, by definition, not in a bound state, no such errors can arise in measurements of its properties. In fact, the magnetic moment of the electron is one of the most accurately known quantities in all of physics. The latest value has an uncertainty of 0.76 parts per trillion [29] – the uncertainty in the magnetic moment of an electron is around a million times less than that of the Lamb shift of atomic energy levels. This shows that measurements of the properties of a free electron can provide much more stringent tests of QED than the analogous measurements of an atom (although with extra experimental complications due to the electron's non-zero net charge). This why we choose to investigate the effects of a surface upon a free electron – even tiny shifts caused by the influence of the environment can be of importance in measurements of the electron's properties.

The most closely analogous quantity to the Lamb shift of an atom for a free electron is its self-energy – the difference is that the electron's excitation spectrum is continuous rather than defined by discrete atomic energy levels. However, any attempt at calculating the self-energy in the same manner as the Casimir-Polder shift breaks down almost immediately since one cannot apply the Power-Zienau transformation to a free electron since it is not neutral. Then we will move on to the magnetic moment, precision knowledge of which is important because of its role as the most stringent test of QED. We will tackle these problems by finding a representation of the medium-dependent quantized electromagnetic field (a task which is non-trivial, as discussed in the next section) and then allow this field to interact with the electron. We consider the interaction as a perturbation, which allows us to calculate the shifts that are due to the interaction of the electron with the surface.

2.5 Approaches to electromagnetic field quantization in the presence of media

The given examples of the Casimir and Casimir-Polder effects both relied on vast oversimplification of the influence that a medium can have upon the quantized electromagnetic field. The assumption of perfect reflector boundary conditions meant that we never needed to consider the form of the fields inside the plates themselves, meaning that all we had to do was apply boundary conditions to the vacuum field in-between. In fact, the process of electromagnetic field quantization in the presence of a dielectric or conducting material turns out to be much more complicated and nuanced than its counterpart in free space (or indeed with perfect reflector boundary conditions). The problem seems simple – one needs to consider the interactions of the electromagnetic field with the ensemble of atoms that makes up the material. However, the material is necessarily made up of an astronomically large number of these. To 'exactly' investigate the field even in a small sample of the medium one would have to consider its interaction with $\sim 10^{23}$ interacting atomic systems – this is not computationally possible, not even approximately. Thus, the usual approach to this problem is to define a macroscopic response function $\epsilon(\omega)$ known as the permittivity[2], which multiplies the electric field. The resulting quantity is known as the electric displacement $\mathbf{D}(\mathbf{r},\omega)$ and satisfies

$$\mathbf{D}(\mathbf{r},\omega) = \epsilon(\mathbf{r},\omega)\mathbf{E}(\mathbf{r},\omega), \tag{2.62}$$

Maxwell's equations in frequency space in terms of this quantity are

$$\begin{aligned} \nabla\cdot\mathbf{D}(\mathbf{r},\omega) &= 0, & \nabla\times\mathbf{E}(\mathbf{r},\omega) &= i\omega\mathbf{B}(\mathbf{r},\omega), \\ \nabla\cdot\mathbf{B}(\mathbf{r},\omega) &= 0, & \nabla\times\mathbf{B}(\mathbf{r},\omega) &= -i\omega\mathbf{D}(\mathbf{r},\omega)\,. \end{aligned} \tag{2.63}$$

Introducing the scalar potentials $\mathbf{A}$ and ϕ in an analogous way to eqs. (2.18) means eqs. (2.63) reduce to

$$\nabla\times[\nabla\times\mathbf{A}(\mathbf{r},\omega)] - \omega^2\epsilon(\mathbf{r},\omega)\mathbf{A}(\mathbf{r},\omega) + i\omega\epsilon(\mathbf{r},\omega)\nabla\phi = 0, \tag{2.64a}$$

$$-i\omega\nabla\cdot[\epsilon(\mathbf{r},\omega)\mathbf{A}(\mathbf{r},\omega)] + \nabla\cdot[\epsilon(\mathbf{r},\omega)\nabla\phi] = 0\,. \tag{2.64b}$$

For a spatially homogenous permittivity $\epsilon(\mathbf{r},\omega) = \epsilon(\omega)$, we choose the Coulomb gauge $\nabla\cdot\mathbf{A} = 0$ which means we can combine these into a single equation in terms of the vector

[2] In principle one also needs to define a permeability $\mu(\omega)$, but here and throughout we limit ourselves to non-magnetic media $\mu(\omega) = \mu_0$.

potential $\mathbf{A}(\mathbf{r},\omega)$ in the same way as was done to obtain eq. (2.20)

$$\nabla \times [\nabla \times \mathbf{A}(\mathbf{r},\omega)] - \omega^2 \epsilon(\omega)\mathbf{A}(\mathbf{r},\omega) = 0 \,, \tag{2.65}$$

which, as with eq. (2.22), reduces to the wave equation

$$\nabla^2 \mathbf{A}(\mathbf{r},\omega) + \omega^2 \epsilon(\omega)\mathbf{A}(\mathbf{r},\omega) = 0 \,. \tag{2.66}$$

The precise form of $\epsilon(\omega)$ can be determined empirically, or by the use of simple models of the response the atoms in the material to an electromagnetic field. Beginning from a general response relation in real space and Fourier transforming, it can be shown that $\epsilon(\omega)$ must be a complex-valued function which satisfies the well-known Kramers-Kronig relations

$$\mathrm{Re}\,\epsilon(\omega) = 1 + \frac{2}{\pi}\mathcal{P}\int_0^\infty \frac{\omega' \,\mathrm{Im}\,\epsilon(\omega')}{\omega'^2 - \omega^2} d\omega' \,, \tag{2.67a}$$

$$\mathrm{Im}\,\epsilon(\omega) = -\frac{2\omega}{\pi}\mathcal{P}\int_0^\infty \frac{\omega' \,\mathrm{Re}\,\epsilon(\omega') - 1}{\omega'^2 - \omega^2} d\omega' \,, \tag{2.67b}$$

where $\mathcal{P}$ denotes the Cauchy principal value.

All that then remains is to quantize the field that obeys (2.66). This seemingly simple task is in fact quite complicated due to the fact that the permittivity is complex and frequency dependent, meaning that the procedure of canonical quantization cannot proceed in the usual way [30, 31, 32, 33, 34]. The reason for this is related to the fact that canonical quantization makes use of equal-time commutation relations, but the response of a medium necessarily depends on the electric field at previous times.

This thesis avoids this issue in different two ways. The first of these is to approximate real materials as non-absorbing, which corresponds to ignoring the imaginary part of the permittivity. This approach has the advantage that for some simple choices of $\epsilon(\omega)$ the electromagnetic field can be explicitly canonically quantized through its decomposition into normal modes, meaning that we can use the resulting quantized field to produce physically transparent and rigorous calculations of radiative corrections near surfaces. The results of this method are amenable to *a posteriori* extension to more complicated choices of $\epsilon(\omega)$, as we will explain later. This approach forms the basis of the mass shift and magnetic moment calculations found in Chapters 3 to 6, which are the main work presented here.

The second way of avoiding these issues with canonical quantization is to introduce a source term corresponding to the current that is induced in the material by the propagation of a damped electromagnetic wave [35, 36, 37, 38]. Introduction of this term produces the correct field commutator (2.44), but cannot be regarded as a rigorous canonical quantization.

However, the advantage of this approach is that it explicitly includes absorption from the start of the calculation, but relies upon the introduction of quantities with no clear physical interpretation and so does not have the same intuitive qualities as the mode expansion method. This approach will be investigated in Chapter 7, in which the results for the mass shift and magnetic moment are rederived so that the two methods can be compared.

Chapter 3

Field quantization in the presence of surfaces

3.1 Introduction

The process of electromagnetic field quantization in free space detailed in the previous chapter is elementary and well-understood, and even the presence of a perfectly reflecting boundary does not complicate matters too much. A derivation of the normal mode expansion of the electromagnetic field near such an idealized surface is straightforward [39], meaning that it is often used as an initial test-case in calculations of surface-induced corrections. However, the physical relevance of this model is somewhat limited. Its first major deficiency is that it does not exhibit high-frequency transparency like any real material would. On top of this it completely ignores modes which are evanescent (exponentially damped) outside the material. As we shall explain, the latter issue can be remedied by modeling a material as non-dispersive with a finite refractive index $\epsilon(\omega) = n^2 > 1$. This model is superior to the perfect reflector, but is still highly simplified. However, we will show that use of this simple model demonstrates that the perfect reflector model is not even a 'good-enough' approximation to any real material. In this chapter we will determine the explicit normal modes for a non-dispersive dielectric, and then add an additional level of realism by doing the same for the simplest dispersive material – an undamped plasma.

3.2 Non-dispersive dielectric

A non-dispersive medium is characterized by a single number $n > 1$, defined through $\epsilon(\omega) = n^2$. We would like to determine the quantized electromagnetic field in a system

where such a medium fills the region $z > 0$, and $z < 0$ is vacuum. The dielectric function $\epsilon(\mathbf{r}, \omega) = n^2(\mathbf{r})$ for this geometry reads

$$n^2(\mathbf{r}) = 1 + \Theta(z)(n^2 - 1), \tag{3.1}$$

where $\Theta(z)$ is the Heaviside step function. We will determine the quantized electromagnetic field in a similar way to that found in our general discussion of field quantization in dielectric media in section 2.5, with one crucial difference relating to a choice of gauge.

Maxwell's equations which a general frequency and space-dependent dielectric function $\epsilon(\mathbf{r}, \omega)$ are given by eqs. (2.64)

$$\nabla \times [\nabla \times \mathbf{A}(\mathbf{r}, \omega)] - \omega^2 \epsilon(\mathbf{r}, \omega)\mathbf{A}(\mathbf{r}, \omega) + i\omega\epsilon(\mathbf{r})\nabla\phi = 0 \,, \tag{3.2a}$$

$$-i\omega\nabla \cdot [\epsilon(\mathbf{r}, \omega)\mathbf{A}(\mathbf{r}, \omega)] + \nabla \cdot [\epsilon(\mathbf{r}, \omega)\nabla\phi] = 0 \,. \tag{3.2b}$$

In section 2.5 we simplified these by assuming that the permittivity was not spatially varying. Clearly, our use of the dielectric function for a non-dispersive half space $\epsilon(\mathbf{r}, \omega) = n^2(\mathbf{r})$ shown in (3.1) means that we cannot make that assumption here. However, we would still like to eliminate the scalar field ϕ in a similar way to that done for the homogenous case in section 2.5. Previously we achieved this by choosing Coulomb gauge $\nabla \cdot \mathbf{A}(\mathbf{r}, \omega) = 0$, however eqs. (3.2) clearly show that this is not an appropriate choice when the permittivity varies with space. To effect the elimination of ϕ we must choose a different gauge – we choose the *generalized* Coulomb gauge, defined by

$$\nabla \cdot [\epsilon(\mathbf{r}, \omega)\mathbf{A}(\mathbf{r}, \omega)] = 0, \tag{3.3}$$

which, via (3.2b), allows us to dispense with ϕ as required. Using this gauge condition we can simplify eq. (3.2a) to

$$\nabla \times [\nabla \times \mathbf{A}(\mathbf{r}, \omega)] = \omega^2 n^2(\mathbf{r})\mathbf{A}(\mathbf{r}, \omega), \tag{3.4}$$

where we have also used the fact that $\epsilon(\mathbf{r}, \omega) = n^2(\mathbf{r})$ for the non-dispersive half-space. Using a vector calculus identity, (3.4) becomes

$$\nabla [\nabla \cdot \mathbf{A}(\mathbf{r}, \omega)] - \nabla^2 \mathbf{A}(\mathbf{r}, \omega) = \omega^2 n^2(\mathbf{r})\mathbf{A}(\mathbf{r}, \omega) \,. \tag{3.5}$$

In Coulomb gauge, the first term on the left hand side of (3.5) would be eliminated and we would have a wave equation as usual, but now we are in generalized Coulomb gauge so we cannot make this simplification. Using the half-space dielectric function (3.1) the generalized Coulomb gauge condition becomes

$$\begin{aligned} \nabla \cdot \left[n^2(\mathbf{r})\mathbf{A}(\mathbf{r}, \omega)\right] &= n^2(\mathbf{r})\nabla \cdot \mathbf{A}(\mathbf{r}, \omega) + A_z(\mathbf{r}, \omega)\frac{\partial}{\partial z} n^2(\mathbf{r}) \\ &= n^2(\mathbf{r})\nabla \cdot \mathbf{A}(\mathbf{r}, \omega) + (n^2 - 1)A_z(\mathbf{r}, \omega)\delta(z), \end{aligned} \tag{3.6}$$

so that the generalized Coulomb gauge differs from standard Coulomb gauge by a surface term. This means that the two gauge conditions coincide only if $z \neq 0$. Thus, we may simplify eq. (3.5) to

$$\nabla^2 \mathbf{A}(\mathbf{r},\omega) + n^2(\mathbf{r})\frac{\partial^2}{\partial t^2}\mathbf{A}(\mathbf{r},\omega) = 0 \qquad \text{for } z \neq 0, \tag{3.7}$$

so that we can work with the wave equation as long as we are away from the interface. This suffices for our purposes since we will consider each side of the interface separately and then match solutions across the boundary using the well-known Maxwell boundary conditions. The subtle differences between Coulomb gauge and generalized Coulomb gauge are considered in depth in [40].

Restating eq. (3.4),

$$\nabla \times [\nabla \times \mathbf{A}(\mathbf{r},\omega)] = \omega^2 n^2(\mathbf{r})\mathbf{A}(\mathbf{r},\omega), \tag{3.8}$$

and following our previous approach of writing the quantized field in terms of mode functions $\mathbf{f}_{\mathbf{k}\lambda}(\mathbf{r},\omega)$ via eq. (2.39), we have

$$\nabla \times [\nabla \times \mathbf{f}(\mathbf{r},\omega)] = \omega^2 n^2(\mathbf{r})\mathbf{f}(\mathbf{r},\omega)\ . \tag{3.9}$$

This is *not* a Hermitian eigenvalue problem, so the modes $\mathbf{f}_{\mathbf{k}\lambda}(\mathbf{r},\omega)$ do not form an orthogonal and complete set, meaning that to quantize the field we cannot simply repeat the analysis found in section 2.2. We note from [41] that if we substitute $\mathbf{f}_{\mathbf{k}\lambda}(\mathbf{r},\omega) = \mathbf{g}_{\mathbf{k}\lambda}(\mathbf{r},\omega)/n(\mathbf{r})$ into (3.9) we have

$$\frac{1}{n(\mathbf{r})}\nabla \times \left[\nabla \times \frac{\mathbf{g}(\mathbf{r},\omega)}{n(\mathbf{r})}\right] = \omega^2 \mathbf{g}(\mathbf{r},\omega)\ . \tag{3.10}$$

This *is* a Hermitian eigenvalue problem, so the functions $\mathbf{g}_{\mathbf{k}\lambda}(\mathbf{r},\omega) = n(\mathbf{r})\mathbf{f}_{\mathbf{k}\lambda}(\mathbf{r},\omega)$ necessarily form an orthogonal and complete set. This means that if we want to continue to write the field through (2.39) we need to weight the functions $\mathbf{f}_{\mathbf{k}\lambda}(\mathbf{r},\omega)$ by appropriate factors of n in order for them to satisfy orthogonality and completeness relations. The explicit form of the completeness relation is [40][1]

$$\int d^3\mathbf{k}\ (2\omega) n(\mathbf{r}) f^i_{\mathbf{k}\lambda}(\mathbf{r},\omega) n(\mathbf{r}') f^{j*}_{\mathbf{k}\lambda}(\mathbf{r}',\omega) = \delta^{\epsilon}_{ij}(\mathbf{r},\mathbf{r}')\ , \tag{3.11}$$

where $\delta^{\epsilon}_{ij}(\mathbf{r},\mathbf{r}')$ is a version of the transverse delta function relevant to generalized Coulomb gauge, defined as

$$\delta^{\epsilon}_{ij}(\mathbf{r},\mathbf{r}') = (\delta_{ij} + \nabla_i \nabla'_j \nabla^{-2})\delta^{(3)}(\mathbf{r}-\mathbf{r}')\ . \tag{3.12}$$

[1] The factor of 2ω in our completeness relation (3.11) does not appear in the expressions found in ref. [40] due to the use of differing conventions in eq. (2.39). As we shall see later, the choices made in this work are much more convenient for calculations which are undertaken for several different models of the surface, which is to be contrasted to ref. [40]'s restriction to the non-dispersive case.

The inversion of the operator ∇^{-2} provides the Green's function of the scalar potential in the particular system described by $\epsilon(\mathbf{r},\omega)$. The orthogonality relation is

$$\int d^3\mathbf{r}\, n^2(\mathbf{r})\mathbf{f}_{\mathbf{k}\lambda}(\mathbf{r},\omega)\mathbf{f}^*_{\mathbf{k}'\lambda'}(\mathbf{r},\omega) = \frac{1}{2\omega}\delta_{\lambda\lambda'}\delta^{(3)}(\mathbf{k}'-\mathbf{k})\,, \tag{3.13}$$

where we have chosen a normalization that ensures the electromagnetic Hamiltonian is written in its canonical form

$$H_{\text{rad}} = \frac{1}{2}\int d^3\mathbf{r}\left[n^2(\mathbf{r})\dot{\mathbf{A}}^2 + (\nabla\times\mathbf{A})^2\right] = \frac{1}{2}\sum_\lambda \int d^3\mathbf{k}\,\omega\left(\hat{a}_{\mathbf{k}\lambda}\hat{a}^\dagger_{\mathbf{k}\lambda} + \hat{a}^\dagger_{\mathbf{k}\lambda}\hat{a}_{\mathbf{k}\lambda}\right)\,. \tag{3.14}$$

Later on we will see that generalizations of eq. (3.9) allow one to determine which models of the surface admit an explicit mode expansion.

The fact that eq. (3.7) is the usual Helmholtz equation as long as $z \neq 0$ means that we can solve it separately on either side of the interface and then stitch the solutions together using the Maxwell boundary conditions at the interface of two non-magnetic materials

$$n^2(\mathbf{r})\mathbf{E}_\perp(\mathbf{r})|_{z=0^-} = n^2(\mathbf{r})\mathbf{E}_\perp(\mathbf{r})|_{z=0^+} \tag{3.15a}$$

$$\mathbf{E}_\parallel(\mathbf{r})|_{z=0^-} = \mathbf{E}_\parallel(\mathbf{r})|_{z=0^+} \tag{3.15b}$$

$$\mathbf{B}(\mathbf{r})|_{z=0^-} = \mathbf{B}(\mathbf{r})|_{z=0^+}. \tag{3.15c}$$

We envisage incident (i), reflected (r) and transmitted (t) modes for each direction, which form the so-called 'triplet' modes [42]. Decomposing the wave vector into its z component k_z and its component parallel to the interface $\mathbf{k}_\parallel$, one can derive a set of reflection and transmission coefficients that multiply plane waves for each incidence direction L or R and polarization λ, as shown in fig. 3.1. These turn out to be the well-known Fresnel

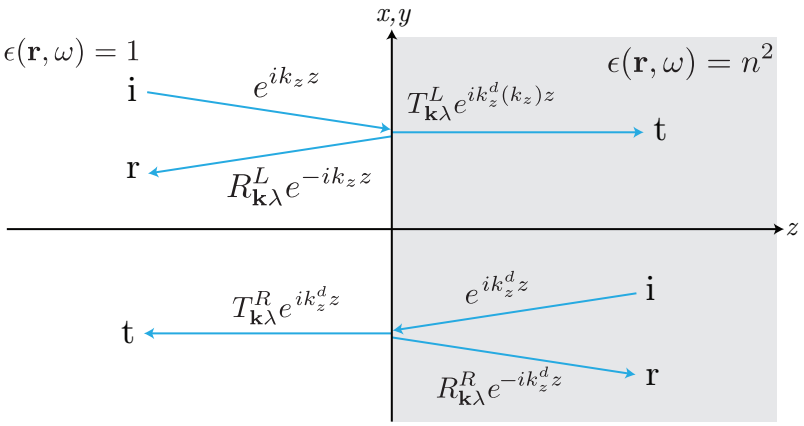

Figure 3.1: Non-dispersive half-space geometry with mode labelling prescription.

coefficients $R^{L/R}_{\mathbf{k}\lambda}[\epsilon(k_z,k_\parallel)]$ and $T^{L/R}_{\mathbf{k}\lambda}[\epsilon(k_z,k_\parallel)]$ for radiation incident on a planar interface

listed in appendix A.2 [42]. The modes that satisfy the normalization relation (3.13) are:

$$\mathbf{f}^L_{\mathbf{k}\lambda}(\mathbf{r},\omega) = \frac{1}{(2\pi)^{3/2}}\frac{1}{\sqrt{2\omega}}\Big[\Theta(-z)\left(e^{i\mathbf{k}\cdot\mathbf{r}}\hat{\mathbf{e}}_{\mathbf{k}\lambda} + R^L_{\mathbf{k}\lambda}(n^2)e^{i\bar{\mathbf{k}}\cdot\mathbf{r}}\hat{\mathbf{e}}_{\mathbf{k}\lambda}\right) + \Theta(z)T^L_{\mathbf{k}\lambda}(n^2)e^{i\mathbf{k}^d\cdot\mathbf{r}}\hat{\mathbf{e}}_{\mathbf{k}^d\lambda}\Big], \tag{3.16a}$$

$$\mathbf{f}^R_{\mathbf{k}\lambda}(\mathbf{r},\omega) = \frac{1}{(2\pi)^{3/2}}\frac{1}{n}\frac{1}{\sqrt{2\omega}}\Big[\Theta(z)\left(e^{i\mathbf{k}^d\cdot\mathbf{r}}\hat{\mathbf{e}}_{\mathbf{k}^d\lambda} + R^R_{\mathbf{k}\lambda}(n^2)e^{i\bar{\mathbf{k}}^d\cdot\mathbf{r}}\hat{\mathbf{e}}_{\mathbf{k}^d\lambda}\right) + \Theta(-z)T^R_{\mathbf{k}\lambda}(n^2)e^{i\mathbf{k}\cdot\mathbf{r}}\hat{\mathbf{e}}_{\mathbf{k}\lambda}\Big], \tag{3.16b}$$

where we have abbreviated

$$R^L_{\mathbf{k}\lambda}\left[\epsilon(k_z,k_\parallel)\to n^2\right] \equiv R^L_{\mathbf{k}\lambda}(n^2)\,, \tag{3.17}$$

and similar for the remaining Fresnel coefficients. A superscript d denotes k vectors that belong to modes that exist inside the medium, and barred quantities have undergone a reflection so the sign of their z component is reversed. The constraint $\mathrm{sgn}(k_z) = \mathrm{sgn}(k_z^d)$ is applied to ensure that each triplet mode has a consistent direction of propagation. The vector potential is obtained from these via:

$$\hat{\mathbf{A}}^L(\mathbf{r},t) = \sum_\lambda \int d^2\mathbf{k}_\parallel \int_0^\infty dk_z \left[\hat{a}_{\mathbf{k}\lambda}e^{i\omega_k t}\mathbf{f}_{\mathbf{k}\lambda}(\mathbf{r},\omega) + \hat{a}^\dagger_{\mathbf{k}\lambda}e^{-i\omega_k t}\mathbf{f}^*_{\mathbf{k}\lambda}(\mathbf{r},\omega)\right], \tag{3.18}$$

$$\hat{\mathbf{A}}^R(\mathbf{r},t) = \sum_\lambda \int d^2\mathbf{k}_\parallel \int_{-\infty}^0 dk_z^d \left[\hat{a}_{\mathbf{k}\lambda}e^{i\omega_k t}\mathbf{f}_{\mathbf{k}\lambda}(\mathbf{r},\omega) + \hat{a}^\dagger_{\mathbf{k}\lambda}e^{-i\omega_k t}\mathbf{f}^*_{\mathbf{k}\lambda}(\mathbf{r},\omega)\right]. \tag{3.19}$$

The restriction of the range of the $k_z^{(d)}$ integrals ensures the modes are counted correctly. Eqs. (3.16) are known as 'triplet' modes, and can be explicitly shown to satisfy eq. (3.13), but the derivation is somewhat tedious [42, 43].

The main new feature of this model as compared to the perfect reflector is the possibility of medium-incident modes being totally internally reflected at the interface, resulting in exponentially decaying (evanescent) modes on the vacuum side. That this can happen is easily seen by noting that Snell's law dictates

$$\omega = |\mathbf{k}| \qquad \text{in vacuum,} \qquad \omega = \frac{|\mathbf{k}|}{n} \qquad \text{in the medium,} \tag{3.20}$$

which, alongside the requirement from conservation of energy that ω be continuous means

$$k_z^2 + k_\parallel^2 = \frac{k_z^{d2} + k_\parallel^2}{n^2}\,, \tag{3.21}$$

where we have also noted that $k_\parallel$ must also be continuous as demonstrated by the boundary condition (3.15b). From (3.21) we derive the useful relations

$$k_z = \frac{1}{n}\sqrt{k_z^{d2} - k_\parallel^2(n^2-1)}\,, \tag{3.22a}$$

$$k_z^d = \sqrt{n^2k_z^2 + k_\parallel^2(n^2-1)}\,. \tag{3.22b}$$

Using fact that $n > 1$ it is easy to see from (3.22a) that k_z may become imaginary for certain values of k_z^d – this leads to total internal reflection and the production of a mode which is evanescent on the vacuum side. Naive inspection of (3.22a) in isolation would lead one to suggest that if k_z^d is imaginary then so is k_z. This is true, but such a combination of k_z and k_z^d in fact violates the Maxwell boundary condition (3.15a), as will be shown explicitly in section 3.3.2 where we will discuss this as a counterexample to a situation where k_z and k_z^d *can* be simultaneously imaginary without violating the boundary conditions. Thus, the conclusion of our discussion of (3.22a) is that for k_z and k_z^d consistent with the boundary conditions, there is a range of k_z^d for which k_z is imaginary, and all such values of k_z^d are real.

Similarly, it follows from (3.22b) that for k_z and k_z^d consistent with the boundary conditions, there is *not any* value of k_z for which k_z^d is imaginary, meaning that vacuum-incident modes cannot become evanescent on the medium side. The consequences of eqs. (3.22a) and (3.22b) are shown schematically in fig. 3.2.

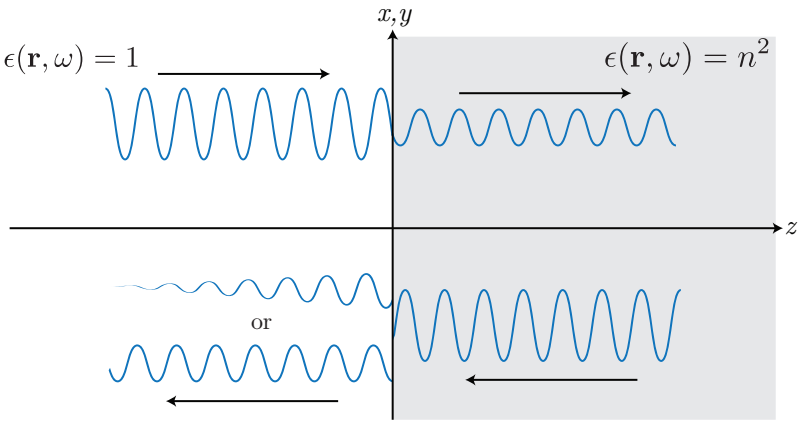

Figure 3.2: Schematic illustration of evanescent modes for a non-dispersive surface

3.3 Plasma

The idea of a non-dispersive dielectric represents a significant step up in realism compared to the perfect reflector, but is still somewhat idealized due to, for example, its exclusion of dispersion. In this section we will remedy this by deriving the normal mode expansion of the quantized electromagnetic field near a half-space consisting of the simplest dispersive material – an undamped plasma. We will see that the field is made up of TE and TM modes, just as in previous sections, but that we also have an additional type of mode – the surface plasmon.

The dielectric function for this type of material can be derived microscopically by considering the equation of motion of electrons within the medium to be

$$m\ddot{\mathbf{x}}(\omega,t) = -e\mathbf{E}(\omega,t). \tag{3.23}$$

where $\mathbf{x}$ is the electron's displacement away from its parent nucleus. Assuming harmonic time-dependence $\mathbf{E}(\omega,t) = \mathbf{E}_0(\omega)e^{-i\omega t}$, we have a polarization $\mathbf{P}(\omega,t) = \mathbf{P}_0(\omega)e^{-i\omega t} = -Ne\mathbf{x}_0(\omega)e^{-i\omega t}$ given by

$$\mathbf{P}_0(\omega) = -\frac{Ne^2}{m\omega^2}\mathbf{E}_0(\omega), \tag{3.24}$$

where N is the number density of electrons in the material. Using the general relation $\mathbf{P}_0(\omega) = (\epsilon(\omega)-1)\mathbf{E}_0(\omega)$ we have for the plasma dielectric function $\epsilon_p(\omega)$

$$\epsilon_p(\omega) = 1 + \frac{\mathbf{P}_0(\omega)}{\mathbf{E}_0(\omega)} = 1 - \frac{Ne^2}{m\omega^2} \equiv 1 - \frac{\omega_p^2}{\omega^2}\ , \tag{3.25}$$

where the plasma frequency $\omega_p^2 \equiv Ne^2/m$ has been defined. Thus a system with plasma filling the region $z > 0$ and vacuum otherwise has the dielectric function

$$\epsilon_p(\mathbf{r},\omega) = 1 - \Theta(z)\frac{\omega_p^2}{\omega^2}\ . \tag{3.26}$$

Using this dielectric function Maxwell's equations (2.63) we find

$$\nabla\times[\nabla\times\mathbf{A}(\mathbf{r},\omega)] = \omega^2\epsilon_p(\mathbf{r},\omega)\mathbf{A}(\mathbf{r},\omega)\ , \tag{3.27}$$

which follows directly from eq. (2.65). Just as in the non-dispersive case, we must carefully consider which gauge we wish to work in. The determination of this is much more complicated than for the non-dispersive half space, however it has been shown [44] that one may use the generalized Coulomb gauge and, via a suitable unitary transformation, eliminate the scalar field ϕ. This is precisely the result of our discussion of the non-dispersive dielectric in section (3.2), which means that we can write the wave equation for a plasma surface in the same way as (3.7) for the non-dispersive dielectric, giving

$$\nabla^2\mathbf{A}(\mathbf{r},t) + \omega^2\mathbf{A}(\mathbf{r},t) = \Theta(z)\omega_p^2\mathbf{A}(\mathbf{r},t) \qquad \text{for } z \neq 0, \tag{3.28}$$

which we will henceforth write as

$$\nabla^2\mathbf{A}(\mathbf{r},t) + \omega^2\mathbf{A}(\mathbf{r},t) = \begin{cases} 0 & \text{if } z < 0 \\ \omega_p^2\mathbf{A}(\mathbf{r},t) & \text{if } z > 0, \end{cases} \tag{3.29}$$

where, we emphasize, $z = 0$ is specifically excluded.

3.3.1 TE and TM modes

We begin by considering the analog of wave equation (3.9) with the plasma permittivity $\epsilon_p(\mathbf{r},\omega)$ given by (3.26):

$$\left[\nabla\times\nabla\times+\omega_p^2\Theta(z)\omega_p^2\right]\mathbf{f}_{\mathbf{k}\lambda}(\mathbf{r},t)=\mathbf{f}_{\mathbf{k}\lambda}(\mathbf{r},t)\ . \tag{3.30}$$

The left hand side is a Hermitian operator acting on $\mathbf{f}(\mathbf{r},t)$. This means that in contrast to the non-dispersive case we do *not* need to apply a weighting to satisfy the completeness relation (2.42). This means that the choice of normalization that ensures the Hamiltonian is written in the canonical form (3.14) is

$$\int d^3\mathbf{r}\,\mathbf{f}_{\mathbf{k}\lambda}(\mathbf{r},t)\mathbf{f}^*_{\mathbf{k}'\lambda'}(\mathbf{r},t)=\frac{1}{2\omega}\delta_{\lambda\lambda'}\delta^{(3)}(\mathbf{k}'-\mathbf{k})\ . \tag{3.31}$$

The reflection and transmission coefficients derived via the Maxwell boundary conditions (3.15) are all identical to the non-dispersive case, except of course with $n^2\to\epsilon_p(\omega)$. Thus, the only difference between the plasma modes and the non-dispersive modes is that those for the plasma do not require the overall factor $1/\sqrt{\epsilon_p(\omega)}$ in the right-incident part. Their explicit form is then

$$\mathbf{f}^L_{\mathbf{k}\lambda}(\mathbf{r},\omega)=\frac{1}{(2\pi)^{3/2}}\frac{1}{\sqrt{2\omega}}\left[\Theta(-z)\left(e^{i\mathbf{k}\cdot\mathbf{r}}\hat{\mathbf{e}}_{\mathbf{k}\lambda}+R^L_{\mathbf{k}\lambda}(\epsilon_p)e^{i\bar{\mathbf{k}}\cdot\mathbf{r}}\hat{\bar{\mathbf{e}}}_{\mathbf{k}\lambda}\right)+\Theta(z)T^L_{\mathbf{k}\lambda}(\epsilon_p)e^{i\mathbf{k}^d\cdot\mathbf{r}}\hat{\mathbf{e}}_{\mathbf{k}^d\lambda}\right], \tag{3.32a}$$

$$\mathbf{f}^R_{\mathbf{k}\lambda}(\mathbf{r},\omega)=\frac{1}{(2\pi)^{3/2}}\frac{1}{\sqrt{2\omega}}\left[\Theta(z)\left(e^{i\mathbf{k}^d\cdot\mathbf{r}}\hat{\mathbf{e}}_{\mathbf{k}^d\lambda}+R^R_{\mathbf{k}\lambda}(\epsilon_p)e^{i\bar{\mathbf{k}}^d\cdot\mathbf{r}}\hat{\bar{\mathbf{e}}}_{\mathbf{k}^d\lambda}\right)+\Theta(-z)T^R_{\mathbf{k}\lambda}(\epsilon_p)e^{i\mathbf{k}\cdot\mathbf{r}}\hat{\mathbf{e}}_{\mathbf{k}\lambda}\right], \tag{3.32b}$$

where we have abbreviated

$$R^L_{\mathbf{k}\lambda}\left[\epsilon(k_z,k_\parallel)\to\epsilon_p(k_z,k_\parallel)\right]\equiv R^L_{\mathbf{k}\lambda}(\epsilon_p)\ , \tag{3.33}$$

and similar for the transmission coefficients.

We now explore the circumstances under which modes may be evanescent using the same method we used for the equivalent discussion for the non-dispersive dielectric. The same continuity conditions which produced eq. (3.21) for the non-dispersive dielectric produce for the plasma surface

$$k_z^2+k_\parallel^2=\frac{k_z^{d2}+k_\parallel^2}{\epsilon_p(k_z,k_\parallel)}\ . \tag{3.34}$$

Using the explicit plasma dielectric function (3.26), this can be rearranged to

$$k_z^{d2}=k_z^2-\omega_p^2\ . \tag{3.35}$$

Since ω_p is real, this relation tells us that it is possible for modes incident from the vacuum to be evanescent on the material side (k_z^d imaginary, k_z real), but it is not possible for medium-incident modes to become evanescent on the vacuum side (k_z imaginary, k_z^d real), which is the opposite of what was found for the non-dispersive surface. Just as in the corresponding relations (3.22a) and (3.22b) for the non-dispersive surface, equation (3.35) also shows that k_z and k_z^d can in principle be simultaneously imaginary. However, as we shall show in the next section, for the plasma surface this does *not* result in a violation of the boundary condition (3.15b). This is the origin of the previously mentioned additional type of mode – the surface plasmon.

3.3.2 Surface plasmon modes

In order to investigate the solutions of (3.35) with k_z and k_z^d both imaginary, we write down an ansatz for a mode which decays exponentially on both sides of the interface. To ensure the right asymptotic behavior far from the interface, we must specify the signs of the imaginary parts of the wave-vector in such a way that the modes decay away from the interface, rather than exponentially rise. Defining $\kappa, \kappa^d > 0$, our ansatz is

$$\mathbf{f}_\tau^{\mathrm{sp}} = \Theta(-z) N^L(k) e^{i\mathbf{k}_\parallel \cdot \mathbf{r}_\parallel + \kappa z} \mathbf{e}^L(\kappa) + \Theta(z) N^R(k) e^{i\mathbf{k}_\parallel \cdot \mathbf{r}_\parallel - \kappa^d z} \mathbf{e}^R(\kappa^d), \tag{3.36}$$

where N^L and N^R are normalization constants, $\mathbf{e}(\kappa^{(d)})$ are as-yet undetermined polarization vectors. The vector potential corresponding to this is

$$\hat{\mathbf{A}}_{\mathrm{sp}}(\mathbf{r}, t) = \sum_{\text{all modes}} \left[\hat{a}_\tau^{\mathrm{sp}} e^{i\omega_{\mathrm{sp}} t} \mathbf{f}_\tau^{\mathrm{sp}}(\mathbf{r}, \omega) + \hat{a}_\tau^{\mathrm{sp}\dagger} e^{-i\omega_{\mathrm{sp}} t} \mathbf{f}_\tau^{\mathrm{sp}*}(\mathbf{r}, \omega) \right], \tag{3.37}$$

where $\hat{a}_\tau^{\mathrm{sp}}$ and its conjugate are the annihilation and creation operators for a surface plasmon τ of frequency ω_{sp}. Our task is then to determine the normalization constants and the polarization vectors, while ensuring that the boundary conditions (3.15) are obeyed at the interface. The overall normalization is taken care of by N^L and N^R, so the choice of normalization for the polarization vectors is arbitrary. We choose

$$\mathbf{e}(\kappa^{(d)}) = \frac{1}{k_\parallel} (\mathbf{k}_\parallel + \lambda^{(d)} \hat{z}). \tag{3.38}$$

Letting $k_z^{(d)2} = -\kappa^{(d)2}$, we have

$$\omega_{\mathrm{sp}}^2 = k_\parallel^2 - \kappa^2, \tag{3.39a}$$

$$\omega_{\mathrm{sp}}^2 = k_\parallel^2 - \kappa^{d2} + \omega_p^2, \tag{3.39b}$$

where $\omega_{\rm sp}$ is the frequency of the surface plasmon. We can use the Coulomb gauge condition[2] $\nabla \cdot \mathbf{A}$ to derive

$$\lambda = -i\frac{k_\parallel^2}{\kappa}, \qquad \lambda^d = i\frac{k_\parallel^2}{\kappa^d}, \tag{3.40}$$

giving

$$\mathbf{e}^L(\kappa) = \hat{\mathbf{k}}_\parallel - i\frac{k_\parallel}{\kappa}\hat{z}, \qquad \mathbf{e}^R(\kappa^d) = \hat{\mathbf{k}}_\parallel + i\frac{k_\parallel}{\kappa^d}\hat{z}. \tag{3.41}$$

The boundary condition (3.15b) states that the parallel component of $\mathbf{E} = -\dot{\mathbf{A}}$ must be continuous across the interface. This sets $N^L(k) = N^R(k) \equiv N(k)$.

The dispersion relation for the surface plasmon modes can be found from the boundary condition (3.15a), which states that $\epsilon(\omega)\mathbf{A}_z$ should be continuous across the surface. Using this condition in eqs. (3.36) and (3.37) we find

$$\frac{1}{\kappa} + \frac{\epsilon_p(\omega_{\rm sp})}{\kappa^d} = 0, \tag{3.42}$$

which is known as the surface plasmon condition. This equation only has a solution if the system at hand admits a surface plasmon excitation. For example, if one takes $\epsilon(\omega_{\rm sp}) \to n^2$ in (3.42), it is easy to see that this requires κ and κ^d to have different signs – a restriction which contradicts the way they were defined in eq. (3.36). This shows that a non-dispersive surface does not admit a surface plasmon mode, proving the assertion in the discussion following eqs. (3.22). Using eqs. (3.39) the surface plasmon condition can be written

$$k_\parallel^2 - \epsilon_p(\omega_{\rm sp})\omega_{\rm sp}^2 = \epsilon_p^2(\omega_{\rm sp})(k_\parallel^2 - \omega_{\rm sp}^2)\ . \tag{3.43}$$

The solution of this with the plasma permittivity (3.25) is

$$\omega_{\rm sp}^2 = k_\parallel^2 + \frac{\omega_p^2}{2} - \sqrt{k_\parallel^4 + \frac{\omega_p^4}{4}}\ , \tag{3.44}$$

where the sign of the square root term is a consequence of the fact that $\kappa, \kappa^d > 0$. This relation shows an important property of the surface plasmon modes, which is that their frequency depends only on their momentum parallel to the surface. This means that the sum over all surface plasmon modes consists of an integral over $d^2\mathbf{k}_\parallel$, and that the arbitrary plasmon label τ can be replaced by $k_\parallel$. The surface plasmon vector potential is then given by

$$\hat{\mathbf{A}}_{\rm sp}(\mathbf{r}, t) = \int d^2\mathbf{k}_\parallel \left[\hat{a}_{k_\parallel}^{\rm sp} e^{i\omega_{\rm sp}t}\mathbf{f}_{k_\parallel}^{\rm sp}(\mathbf{r}, \omega) + \hat{a}_{k_\parallel}^{\rm sp\dagger} e^{-i\omega_{\rm sp}t}\mathbf{f}_{k_\parallel}^{\rm sp*}(\mathbf{r}, \omega)\right]\ . \tag{3.45}$$

[2] We remind the reader that while we are in generalized Coulomb gauge $\nabla \cdot [\epsilon(\mathbf{r}, \omega)\mathbf{A}(\mathbf{r}, \omega)] = 0$, in the present geometry this coincides with the standard Coulomb gauge $\nabla \cdot \mathbf{A}(\mathbf{r}, \omega) = 0$ provided $z \neq 0$, which is satisfied here since we are considering each side of the interface separately.

We normalize the modes by ensuring that their electromagnetic energy $H_{\rm sp}$ is written in the canonical form

$$H_{\rm sp} = \frac{1}{2}\int d^3\mathbf{r}\left[\epsilon_p(\mathbf{r},\omega)\dot{\mathbf{A}}^2 + (\nabla\times\mathbf{A})^2\right] \stackrel{!}{=} \frac{1}{2}\int d^2\mathbf{k}_\parallel\,\omega_{\rm sp}\left(\hat{a}^{\rm sp}_{k_\parallel}\hat{a}^{\rm sp\dagger}_{k_\parallel} + \hat{a}^{\rm sp\dagger}_{k_\parallel}\hat{a}^{\rm sp}_{k_\parallel}\right) . \tag{3.46}$$

The normalization $N(k) = N(k_\parallel)$ is most easily found by using the harmonic time-dependence of $\mathbf{A}$ and the explicit plasma dielectric function (3.26), giving for the field Hamiltonian

$$H_{\rm sp} = \frac{1}{2}\int d^3\mathbf{r}\left[\dot{\mathbf{A}}^2 + \omega_p^2\Theta(z)\mathbf{A}^2 + (\nabla\times\mathbf{A})^2\right] . \tag{3.47}$$

The explicit vector potential (3.45) is then inserted into this equation, and the spatial integration carried out. The resultant expressions contain various products of the polarisation vectors $\mathbf{e}(\kappa^{(d)})$, listed in appendix A.1.2. One eventually finds

$$\begin{aligned} H_{\rm sp} =& (2\pi)^2\int d^2\mathbf{k}_\parallel |N^2(k_\parallel)|\left(\hat{a}^{\rm sp}_{k_\parallel}\hat{a}^{\rm sp\dagger}_{k_\parallel} + \hat{a}^{\rm sp\dagger}_{k_\parallel}\hat{a}^{\rm sp}_{k_\parallel}\right)\omega_{\rm sp}^2 \\ &\times\left[\frac{1+k_\parallel^2/\kappa^2}{2\kappa} + \frac{1+k_\parallel^2/\kappa^{d2}}{2\kappa^d} + \left(1+\frac{k_\parallel^2}{\kappa^{d2}}\right)\frac{\omega_p^2}{\omega_{\rm sp}^2 2\kappa^d} + \frac{\omega_{\rm sp}^2}{2\kappa^3} + \frac{(\omega_{\rm sp}^2-\omega_p^2)^2}{2\omega_{\rm sp}^2\kappa^{d3}}\right] \\ =& (2\pi)^2\int d^2\mathbf{k}_\parallel N^2(\mathbf{k}_\parallel)\left(\hat{a}^{\rm sp}_{k_\parallel}\hat{a}^{\rm sp\dagger}_{k_\parallel} + \hat{a}^{\rm sp\dagger}_{k_\parallel}\hat{a}^{\rm sp}_{k_\parallel}\right)\omega_{\rm sp}\frac{\epsilon_p^2(\omega_{\rm sp})\sqrt{-(1+\epsilon_p^2(\omega_{\rm sp}))}}{\epsilon_p^4(\omega_{\rm sp})-1}, \end{aligned} \tag{3.48}$$

where the second line follows from the first via simple but tedious algebra. Comparing with (3.46), it is easy to see that the correct normalization is given by

$$|N^2(k_\parallel)| = \frac{1}{(2\pi)^2}\frac{\epsilon_p^4(\omega_{\rm sp})-1}{\epsilon_p^2(\omega_{\rm sp})\sqrt{-(1+\epsilon_p^2(\omega_{\rm sp}))}} \equiv \frac{1}{(2\pi)^2}\frac{1}{p(\mathbf{k}_\parallel)} , \tag{3.49}$$

giving for the final expression of the surface plasmon modes

$$\begin{aligned} \mathbf{f}^{\rm sp}_{k_\parallel} = \frac{1}{2\pi}\frac{1}{\sqrt{p(\mathbf{k}_\parallel)}}\Big[&\Theta(-z)\left(\hat{\mathbf{k}}_\parallel - i(k_\parallel/\kappa)\hat{z}\right)e^{i\mathbf{k}_\parallel\cdot\mathbf{r}_\parallel+\kappa z} \\ &+\Theta(z)\left(\hat{\mathbf{k}}_\parallel + i(k_\parallel/\kappa^d)\hat{z}\right)e^{i\mathbf{k}_\parallel\cdot\mathbf{r}_\parallel-\kappa^d z}\Big] . \end{aligned} \tag{3.50}$$

Thus the entire quantized electromagnetic field in the plasma half-space geometry is given by eqs. (3.50) and (3.32).

3.4 Summary and conclusions

In this chapter we have described explicit mode expansions for the quantized electromagnetic field subject to the boundary conditions imposed by a non-dispersive dielectric, given by eq. (3.16). We then extended this to the corresponding description of an undamped plasma, with the results give by eqs. (3.50) and (3.32). These expressions completely describe the quantized electromagnetic field in the two situations, so we are now ready to investigate the consequences of their coupling to an electron in the vicinity of the interface.

Chapter 4

Mass Shift

4.1 Introduction

The first and simplest radiative correction that we wish to investigate is the shift in the mass of the electron caused by its interaction with the quantized electromagnetic field (known as the self-energy)[1]. This effect is relatively straightforward to calculate, and paves the way for our calculation of the shift in the magnetic moment in Chapter 5. We will see that its physical relevance lies in accurate prediction of the cyclotron frequency of a trapped electron.

The effect arises due to the analytic structure of the two-point correlation function for an electron, which represents the probability for an electron to travel from y to x. For an electron with with spinor ψ this is

$$\langle 0|\, \top \psi(x)\bar{\psi}(y)\, |0\rangle =$$

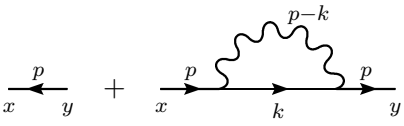

(4.1)

where $\top$ is the time-ordering symbol[2], and, as usual, and represent electrons and photons respectively, each with four-momentum p. Using the Fourier-space version of the two point function, the contribution from each diagram may be written down using the standard Feynman rules for quantum electrodynamics (see, for example, [45] app. A.1.). If

[1] The mass shift is usually described in field-theoretic terms as a renormalization of the electron mass, however we use the term 'mass shift' to avoid confusion with discussion of our unrelated approach to renormalization.

[2] For fermion fields the time-ordering symbol is defined as

$$\top(\psi(x)\bar{\psi}(y) = \begin{cases} \psi(x)\bar{\psi}(y) & \text{for } x^0 > y^0 \\ -\bar{\psi}(y)\psi(x) & \text{for } x^0 < y^0. \end{cases} \tag{4.2}$$

we consider the electron as non-interacting, the whole series is given by the bare propagator

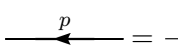

$$= \frac{i(\not{p} + m)}{p^2 - m^2 + i\epsilon} \,, \tag{4.3}$$

where m is the mass of the electron. In the non-interacting theory, the 'bare' mass and the observed mass are the same thing since there are no extra interactions to take into account. This expression has a simple pole at $p^2 = m^2$ – the position of this pole is the observed mass of the electron. If we now let the electron interact with the photon field, each term in the perturbation series will shift the pole slightly, so to find the observed mass we must sum all the terms, which corresponds to summing all the diagrams. This means we must make the distinction between the mass we observe resulting from an infinite series of diagrams, and the mass that appears in the first diagram. We term the former m and the latter m_0 (often called the 'bare' mass), giving the bare propagator for the interacting theory

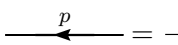

$$= \frac{i(\not{p} + m_0)}{p^2 - m_0^2 + i\epsilon} \,. \tag{4.4}$$

Applying the Feynman rules, the one-loop diagram is

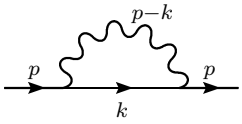

$$= \frac{i(\not{p} + m_0)}{p^2 - m_0^2} \left[-i\Sigma_2(p)\right] \frac{i(\not{p} + m_0)}{p^2 - m_0^2} \,, \tag{4.5}$$

with

$$-i\Sigma_2(p) = (-ie)^2 \int \frac{d^4k}{(2\pi)^4} \gamma^\mu \frac{i(\not{K} + m)}{k^2 - m_0^2 + i\epsilon} \gamma_\mu \frac{-i}{(p-k)^2 + i\epsilon} \,. \tag{4.6}$$

This can be simplified using a Feynman parameterization, the resulting dimensionally regularized expression is [45]

$$\Sigma_2(p) = \frac{\alpha}{2\pi} \int_0^1 dx (2m_0 - x\not{p}) \ln\left(\frac{x\Lambda^2}{(1-x)m_0^2 + x\mu^2 - x(1-x)p^2}\right) , \tag{4.7}$$

where Λ and μ are fictitious masses used in the regularization procedure, and α is the fine structure constant. The mass is delivered by the pole of the propagator, the position of which (to one loop) is not obvious from (4.7). To find the position of this pole, we employ the an elegant way of summing the entire series.

First we let $-i\Sigma(p)$ be equal to the sum of all one-particle irreducible diagrams with two external electron lines:

$-i\Sigma(p) =$ 

$=$ 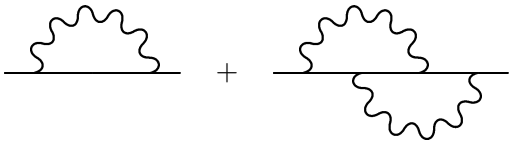

The momentum-space two point function can now be written as:

$$\int d^4x \, \langle 0| \top \psi(x)\bar{\psi}(y) |0\rangle \, e^{ip\cdot x} = \text{———} + \text{———●———} + \text{———●———●———} + \cdots$$

$$= \frac{i(\not{p} + m_0)}{p^2 - m_0^2} + \frac{i(\not{p} + m_0)}{p^2 - m_0^2}(-i\Sigma(p))\frac{i(\not{p} + m_0)}{p^2 - m_0^2} + \cdots \tag{4.8}$$

$$= \frac{i}{\not{p} - m_0} + \frac{i}{\not{p} - m_0}(-i\Sigma(\not{p}))\frac{i}{\not{p} - m_0} + \cdots \tag{4.9}$$

which follows since $(\not{p})^2 = p^2$ and $\Sigma(p)$ commutes with $\not{p}$. This is a geometric series of the form:

$$\frac{i}{a-b} = \frac{i}{a} + \frac{ib}{a^2} + \frac{ib^2}{a^3} + \cdots \tag{4.10}$$

with $a = \not{p} - m_0$ and $b = \Sigma(p)$. This means the entire series can be written as

$$\int d^4x \, \langle 0| \top \psi(x)\bar{\psi}(y) |0\rangle \, e^{ip\cdot x} = \frac{i}{\not{p} - m_0 - \Sigma(\not{p})} \, , \tag{4.11}$$

which *does* display the expected property of containing a simple pole shifted away from m_0. Thus, the interaction of the electron with the quantized electromagnetic field produces a shift in the mass, which is identified as the solution of the equation

$$[\not{p} - m_0 - \Sigma(\not{p})]_{\not{p}=m} = 0 \, . \tag{4.12}$$

Thus we may find the mass shift to one-loop order by evaluating $\Sigma_2(\not{p} = m_0)$, which from (4.7) is

$$\Sigma_2(\not{p} = m_0) = \frac{\alpha}{2\pi} m_0 \int_0^1 dx (2-x) \ln\left[\frac{x\Lambda^2}{(1-x)^2 m_0^2 + x\mu^2}\right] \, , \tag{4.13}$$

which contains a divergent term of the form

$$\lim_{\Lambda\to\infty} \frac{3\alpha}{4\pi} m_0 \ln\left(\frac{\Lambda^2}{m_0^2}\right) \, . \tag{4.14}$$

Thus the physical mass differs from the bare mass by an infinite quantity. This is not surprising from the viewpoint of classical electrodynamics due to the energy of a point charge also being divergent

$$E_{\text{cl}} \sim \int_{\text{all space}} d^3\mathbf{r} |\mathbf{E}|^2 \sim \int_0^\infty \frac{dr}{r^2} \, . \tag{4.15}$$

where **E** is the electric field of the charge. The divergent self-energy (4.14) is best studied through the use of renormalized perturbation theory, which we shall not discuss here. For our purposes it is enough to note that

1. The interaction of the electron and the photon field produces a shift in the mass of the electron.

2. The shift in the mass contains infinite quantities which must be carefully dealt with.

Bearing these two facts in mind, the question is then how should one proceed to modify the above analysis to a calculation of the mass shift near a surface. This was done for a non-dispersive dielectric in [46], where the authors calculate the mass shift by determining the modified photon propagator. Their approach was to compare the terms of the half-space propagator with those of the free-space propagator, in order to determine a correction to the propagator that is solely attributable to the surface. This sidesteps the need to deal with regularization and renormalization since these are already taken care of by the free-space part of the photon field, and the calculation is also simplified by restriction to the dipole approximation whereby the electromagnetic field is assumed not to vary over the position of the electron[3]. Even with these simplifications, the calculation still contains significant technical hurdles, largely stemming from the loss of translation invariance in the direction perpendicular to the interface. Another complication is that one needs to enforce a localization upon the electron in order to have a meaningful idea of its position relative to the interface.

For these reasons we will dispense with the usual field-theoretic description of radiative corrections and borrow some of the techniques of quantum optics in order to produce an intuitive and manageable calculation of the mass shift[4]. The method that we will describe is relatively easily generalizable to realistic surfaces, and can be extended to calculations of other radiative corrections besides the mass shift.

[3]Henceforth the terms 'dipole', 'quadrupole', 'multipole' etc. refer to approximations made about the variation of the photon field across the position of the electron, *not* those mentioned when describing the multipolar coupling approach to QED in section 2.3.2, which deal with the variation of the field across the electron-nucleus separation.

[4]The calculation presented in the following sections is an expanded version of the published work [47].

4.2 Interaction with a surface

The fundamental physical assumption we make in our calculation of the surface-dependent mass shift (and throughout this thesis) is that the electron is localized well away from the surface – there is no wave function overlap. The lifting of this assumption would require a treatment which describes the specific atomic structure of the interface, which would lead a wholly different type of calculation since our approach to field quantization relies upon the material being adequately described by its bulk properties. In field-theoretic terms the assumption means that to leading order the electron line does not gain a boundary dependence, so that its propagator coincides with that for an electron in free space. The one-loop diagram and a selected two-loop diagram are shown in figure 4.1 where double

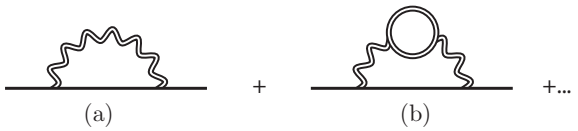

Figure 4.1

lines indicates boundary dependent quantities. We will consider a first-quantized electron sitting in a second-quantized electromagnetic field, which loosely corresponds to considering a non-relativistic analogue of diagram 4.1a. This simplification breaks down if one looks for effects like that shown in figure 4.1b, which are of quadratic or higher order in the fine structure constant α, we will not consider these. The non-relativistic Hamiltonian for such a system is

$$H = \frac{(\mathbf{p} - e\mathbf{A})^2}{2m} + e\Phi = \frac{\mathbf{p}^2}{2m} + \frac{e^2}{2m}\mathbf{A}^2 - \frac{e}{m}\mathbf{p}\cdot\mathbf{A} + e\Phi, \tag{4.16}$$

where we have neglected the electron's spin. The electron 'sees' the surface in two ways. These are via the boundary-dependent quantized field $\mathbf{A}$ and the electrostatic image potential $V_{\text{image}} = e\Phi$. The term in $\mathbf{A}^2$ contributes the same energy to every state of the electron because it appears in first-order perturbation theory only. Thus it does not affect observable frequency shifts, so can be ignored. So the interaction Hamiltonian which delivers the boundary-dependent shift is

$$H_{\text{int}} = -\frac{e}{m}\mathbf{p}\cdot\mathbf{A} + V_{\text{image}} \,. \tag{4.17}$$

Taking as an example the case where the electron's motion is perpendicular to the interface $\mathbf{p} \to p_\perp \hat{z}$ and excluding the (infinite) term in $\frac{e^2}{2m}\mathbf{A}^2$, the energy of the system is

$$E + V_{\text{image}} = \frac{\langle p_\perp^2 \rangle}{2m} + \Delta E_\perp + V_{\text{image}} \,, \tag{4.18}$$

where $\Delta E_\perp$ is the energy shift due to the coupling $p_\perp A_z$. This may be rewritten as

$$E + V_{\text{image}} = \langle p_\perp^2 \rangle \left(\frac{1}{2m} + \frac{\Delta E}{\langle p_\perp^2 \rangle} \right) + V_{\text{image}} = \frac{\langle p_\perp^2 \rangle}{2(m + \Delta m_\perp)} + V_{\text{image}} \, . \tag{4.19}$$

The quantity $\Delta m_\perp$ is the shift in the mass, and is given by[5]

$$\Delta m_\perp = -\frac{2m^2 \Delta E}{\langle p_\perp^2 \rangle + 2m\Delta E} = -\frac{2m^2 \Delta E}{\langle p_\perp^2 \rangle} + \mathcal{O}(\Delta E)^2 \, . \tag{4.20}$$

with a similar relation for motion parallel to the surface $\mathbf{p} \to p_\parallel \hat{r}_\parallel$ (where $\hat{r}_\parallel$ is a unit vector parallel to the surface).

To evaluate $\Delta E = \Delta E_\perp + \Delta E_\parallel$, we write a one-photon state of momentum $\mathbf{k}$ and polarization λ as $|1_{\mathbf{k}\lambda}\rangle$ and the momentum state of the electron as $|\mathbf{p}_{\text{int}}\rangle$, then calculate the energy shift due to vacuum-vacuum transitions via a one-photon intermediate composite state $|\mathbf{p}_{\text{int}}\rangle \otimes |1_{\mathbf{k}\lambda}\rangle = |\mathbf{p}_{\text{int}}; 1_{\mathbf{k}\lambda}\rangle$. Writing the vacuum state as $|\mathbf{p}; 0\rangle$, the expression for this energy shift in second-order perturbation theory is

$$\Delta E = \frac{e^2}{m^2} \sum_{k,\lambda} \sum_{p_{\text{int}}} \frac{|\langle \mathbf{p}_{\text{int}}; 1_{\mathbf{k}\lambda}| \, \mathbf{p} \cdot \mathbf{A} \, |\mathbf{p}; 0\rangle|^2}{\frac{\mathbf{p}^2}{2m} - \left(\frac{\mathbf{p}_{\text{int}}^2}{2m} + \omega \right)} \, . \tag{4.21}$$

The matrix element in the numerator is the non-relativistic analogue of diagram 4.1a, as shown in figure 4.2. We make the no-recoil approximation, which entails taking the

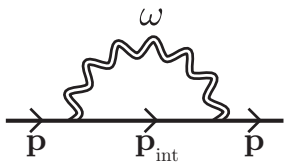

Figure 4.2

electron's momentum in the intermediate state p_{int} to be equal to its initial and final momenta p. This is a reasonable assumption because we are dealing with a low energy effect, so the mass of the electron is by far the largest quantity in the calculation. This assumption simplifies the expression to

$$\Delta E = -\frac{e^2}{m^2} \langle p_i^2 \rangle \sum_{k,\lambda} \frac{1}{\omega} |\langle 1_{\mathbf{k}\lambda}| \, A_i \, |0\rangle|^2 \, . \tag{4.22}$$

Substituting the quantised field $\mathbf{A}$ as given by eq. (2.39), this becomes

$$\Delta E = -\frac{e^2}{m^2} \langle p_i^2 \rangle \sum_{\text{all modes}} \frac{1}{\omega} \left| \langle 1_{\mathbf{k}\lambda}| \, \hat{a}_{\mathbf{k}\lambda} e^{i\omega_k t} f_{\mathbf{k}\lambda,i}(\mathbf{r}, \omega) + \hat{a}_{\mathbf{k}\lambda}^\dagger e^{-i\omega_k t} f_{\mathbf{k}\lambda,i}^*(\mathbf{r}, \omega) \, |0\rangle \right|^2 . \tag{4.23}$$

We have that $\hat{a}_{\mathbf{k}\lambda} |0\rangle = 0$, so on application of the operators we have

$$\Delta E = -\frac{e^2}{m^2} \langle p_i^2 \rangle \sum_{\text{all modes}} \frac{1}{\omega} \left| f_{\mathbf{k}\lambda,i}^*(\mathbf{r}, \omega) \right|^2 . \tag{4.24}$$

[5] ΔE will of course turn out to be proportional to $\langle p_\perp^2 \rangle$ so that m^* is independent of the momentum

4.2.1 Non-Dispersive

For a non-dispersive dielectric, we have TE and TM modes only, so the sum over all modes is given simply by

$$\sum_{\text{all modes}} \to \int d^3\mathbf{k} \sum_{\lambda=\text{TE,TM}} \tag{4.25}$$

We wish to calculate the mass shift for an electron localized in the $z < 0$ region of a system described by the following dielectric function

$$\epsilon(\mathbf{r},\omega) = 1 + \Theta(z)(n^2 - 1), \tag{4.26}$$

with $n^2 > 1$. This is a non-dispersive material that fills the entire space $z > 0$, with $z < 0$ being vacuum, as shown in figure 4.3. We first calculate the contribution proportional to

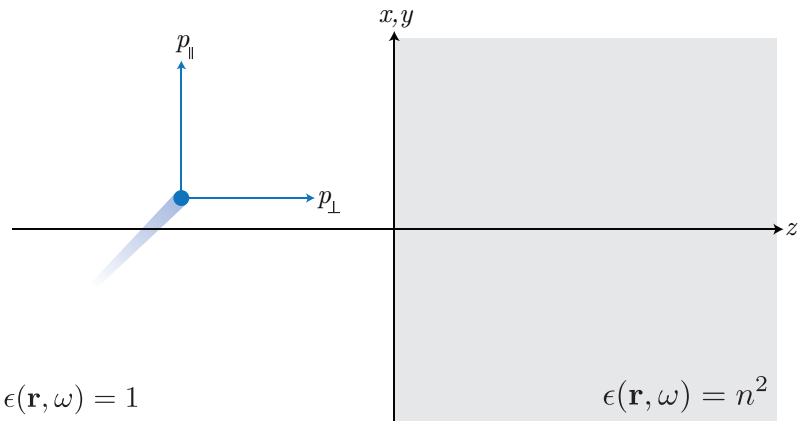

Figure 4.3: Physical setup for calculation of the surface dependence of the mass shift of an electron near a non-dispersive half-space.

$\langle p_\perp^2 \rangle$, given by

$$\Delta E_\perp = -\frac{e^2}{m^2}\langle p_\perp^2\rangle \int d^3\mathbf{k} \sum_\lambda \frac{1}{\omega} \left| f^*_{\mathbf{k}\lambda,z}(\mathbf{r},\omega)\right|^2. \tag{4.27}$$

The vector character of the mode functions is inherited from $\mathbf{A}$, and ultimately $\mathbf{E}$. Since TE modes are defined by the lack of a z component of electric field in the direction of propagation, it is expected that the z component of the TE mode function will vanish. This is seen explicitly in our choice for the polarization vectors (A.1). Thus, eq. (4.27) may be evaluated by considering TM modes only. The modes for this system were determined in section 3.2, and are given by equations (3.16). Substituting these into eq. (4.27) and specializing to the region $z < 0$ we have for the energy shift near a non-dispersive dielectric

$$\Delta E_\perp^{\text{nondisp}} = -\frac{1}{(2\pi)^3}\frac{e^2}{m^2}\langle p_\perp^2\rangle \int d^2\mathbf{k}_\parallel \Bigg[\int_0^\infty dk_z \left| e^{i\mathbf{k}\cdot\mathbf{r}} + R^L_{\mathbf{k},\text{TM}}(n^2) e^{i\bar{\mathbf{k}}\cdot\mathbf{r}}\right|^2 + \frac{1}{n^2}\int_0^\infty dk_z^d \left| T^R_{\mathbf{k},\text{TM}}(n^2) e^{i\mathbf{k}\cdot\mathbf{r}}\right|^2 \Bigg] \underbrace{\frac{k_\parallel^2}{2k^4}}_{\text{coeff.}}, \tag{4.28}$$

where the polarization vectors specified in eqs. (A.1) have been used, $k = |\mathbf{k}| = \omega$ and we have highlighted part of the expression for later use. The wave vector $\mathbf{k} = \mathbf{k}_\parallel + k_z\hat{z}$ appearing in the k_z^d integral depends on k_z^d via

$$k_z = \frac{1}{n}\sqrt{k_z^{d2} - k_\parallel^2(n^2-1)}, \tag{4.29}$$

where $k_\parallel = |\mathbf{k}_\parallel|$. As discussed in section 3.2, this shows that there exists a certain range of k_z^d for which k_z is imaginary, corresponding to modes which are totally internally reflected and thus become evanescent on the vacuum side. The critical value of k_z^d below which the modes are totally internally reflected is

$$k_{z,\mathrm{crit}}^d = k_\parallel\sqrt{n^2-1} \equiv \Gamma\ , \tag{4.30}$$

meaning we can rewrite the shift as

$$\begin{aligned}\Delta E_\perp^{\mathrm{nondisp}} = &-\frac{1}{(2\pi)^3}\frac{e^2}{m^2}\langle p_\perp^2\rangle\int d^2\mathbf{k}_\parallel \\ &\times\left\{\int_0^\infty dk_z\Big[1 + R^L_{\mathbf{k},\mathrm{TM}}(n^2)(e^{2ik_zz} + e^{-2ik_zz}) + |R^L_{\mathbf{k},\mathrm{TM}}(n^2)|^2\Big]\right. \\ &\left. + \frac{1}{n^2}\int_{-\Gamma}^0 dk_z^d|T^R_{\mathbf{k},\mathrm{TM}}(n^2)|^2e^{i(k_z-k_z^*)z} + \frac{1}{n^2}\int_{-\infty}^{-\Gamma} dk_z^d|T^R_{\mathbf{k},\mathrm{TM}}(n^2)|^2\right\}\frac{k_\parallel^2}{2k^4}\ .\end{aligned} \tag{4.31}$$

Using eq. (4.29) we can change variables from k_z^d to k_z in the final term to obtain an integral which runs over $k_z = 0..\infty$. Additionally, we can combine the integrals over the two exponentials in the term proportional to $R^L_{\mathbf{k},\mathrm{TM}}(n^2)$ by changing variables $k_z \to -k_z$ in one of them. Noting that for k_z purely imaginary, $k_z - k_z^* = 2k_z$ and rearranging, we have:

$$\begin{aligned}\Delta E_\perp^{\mathrm{nondisp}} = &-\frac{1}{(2\pi)^3}\frac{e^2}{m^2}\langle p_\perp^2\rangle\int d^2\mathbf{k}_\parallel\left\{\int_0^\infty dk_z\left[1 + |R^L_{\mathbf{k},\mathrm{TM}}(n^2)|^2 + \frac{k_z}{k_z^d}|T^R_{\mathbf{k},\mathrm{TM}}(n^2)|^2\right]\right. \\ &\left. + \int_{-\infty}^\infty dk_z R^L_{\mathbf{k},\mathrm{TM}}(n^2)e^{2ik_zz} + \frac{1}{n^2}\int_{-\Gamma}^0 dk_z^d|T^R_{\mathbf{k},\mathrm{TM}}(n^2)|^2e^{2ik_zz}\right\}\frac{k_\parallel^2}{2k^4}\ .\end{aligned} \tag{4.32}$$

In order to evaluate the final term we need to choose which branch of the square root function we take in eq. (4.29). The physical requirement that the energy shift should vanish as $z \to -\infty$ means $\mathrm{Im}(k_z) < 0$ is the appropriate choice. We can now change variables from k_z to k_z^d in the final term, giving

$$\int_0^{-i\Gamma/n} dk_z\frac{k_z}{k_z^d}|T^R_{\mathbf{k},\mathrm{TM}}(n^2)|^2e^{2ik_zz}\ . \tag{4.33}$$

It is very useful to note that the following relation holds for either polarization λ for imaginary k_z

$$R^L_{\mathbf{k}\lambda}(n^2)|_{k_z^d=-K} - R^L_{\mathbf{k}\lambda}(n^2)|_{k_z^d=K} = \frac{k_z}{k_z^d}T^R_{\mathbf{k}\lambda}(n^2)T^{R*}_{\mathbf{k}\lambda}(n^2)|_{k_z^d=-K}. \tag{4.34}$$

where $K > 0$. This means we can manipulate eq. (4.33) into

$$\lim_{\delta\to 0}\left[\int_{-\delta}^{-i\Gamma/n-\delta} dk_z R^L_{\mathbf{k},\mathrm{TM}}(n^2)e^{2ik_z z} + \int_{-i\Gamma/n+\delta}^{\delta} dk_z R^L_{\mathbf{k},\mathrm{TM}}(n^2)e^{2ik_z z}\right], \tag{4.35}$$

where we have introduced $\delta > 0$ to displace the integration paths either side of the imaginary axis branch cut in order to fulfill the constraint $\mathrm{sgn}(k_z) = \mathrm{sgn}(k_z^d)$. This can be combined with the term proportional to R^L_{TM} in eq. (4.32) to give

$$\Delta E_\perp^{\mathrm{nondisp}} = -\frac{1}{(2\pi)^3}\frac{e^2}{m^2}\langle p_\perp^2\rangle \int d^2\mathbf{k}_\parallel \left\{ \int_0^\infty dk_z \left[1 + |R^L_{\mathbf{k},\mathrm{TM}}(n^2)|^2 + \frac{k_z}{k_z^d}|T^R_{\mathbf{k},\mathrm{TM}}(n^2)|^2\right] + \int_C dk_z R^L_{\mathbf{k},\mathrm{TM}}(n^2)e^{2ik_z z}\right\}\frac{k_\parallel^2}{2k^4}\,. \tag{4.36}$$

with the contour C shown in fig. 4.4.

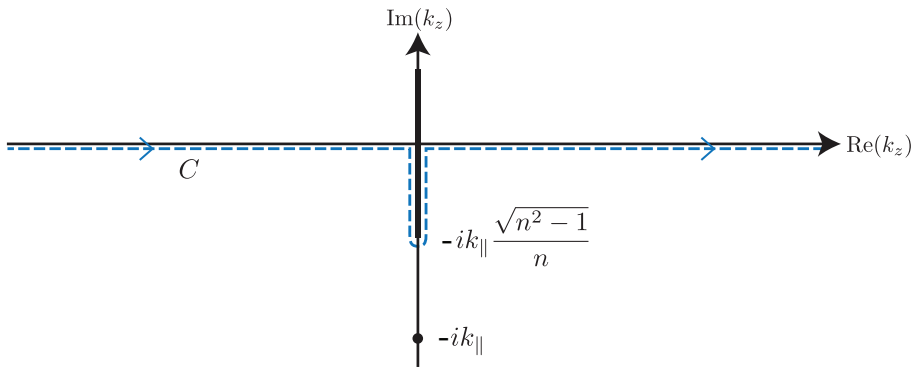

Figure 4.4: Integration contour in the complex k_z plane required to evaluate the mass shift near a non-dispersive surface.

We now turn our attention to the first term in eq. (4.36). It is not hard to show that the following relation holds for either polarization λ for real k_z

$$|R^L_{\mathbf{k}\lambda}(n^2)|^2 + \frac{k_z}{k_z^d}|T^R_{\mathbf{k}\lambda}(n^2)|^2 = 1 \tag{4.37}$$

so that

$$\int d^2\mathbf{k}_\parallel \int_0^\infty dk_z \left[1 + |R^L_{\mathbf{k},\mathrm{TM}}(n^2)|^2 + \frac{k_z}{k_z^d}|T^R_{\mathbf{k},\mathrm{TM}}(n^2)|^2\right] = 2\int d^2\mathbf{k}_\parallel \int_0^\infty dk_z\,. \tag{4.38}$$

which is manifestly infinite. This is not surprising based on the discussion of the free space contribution in section 4.1, but is not a problem for our purposes. This is because we only seek the shift in the magnetic moment that is attributable to the surface, *not* its absolute value. To isolate surface-dependent quantities we remove the surface by letting reflection and transmission coefficients go to zero and unity respectively, and see which parts of the shift remain. These will be the boundary-independent parts of the energy shift, so can be

dropped. In this case, it is clear that the term shown in eq. (4.38) is the only one which remains, so this is discarded. Thus, the renormalized shift is given by

$$\Delta E_{\perp\text{ren}}^{\text{nondisp}} = -\frac{1}{8\pi^2}\frac{e^2}{m^2}\langle p_\perp^2\rangle \int_0^\infty dk_\parallel \int_C dk_z \, \frac{k_\parallel^3}{(k_z^2+k_\parallel^2)^2} R_{\mathbf{k}.\text{TM}}^L(n^2) e^{2ik_z z}. \tag{4.39}$$

where we have introduced polar co-ordinates defined by $k_x = k_\parallel \sin\phi$, $k_y = k_\parallel \cos\phi$ and carried out the trivial ϕ integral. The mass shift attributable to motion parallel to the interface is found in exactly the same way, the result is

$$\Delta E_{\parallel\text{ren}}^{\text{nondisp}} = \frac{1}{16\pi^2}\frac{e^2}{m^2}\langle p_\parallel^2\rangle \int_0^\infty dk_\parallel \int_C dk_z \, \frac{k_\parallel k_z^2}{(k_z^2+k_\parallel^2)^2} \times \left[R_{\mathbf{k},\text{TM}}^L(n^2) + (k_z^2+k_\parallel^2) R_{\mathbf{k},\text{TE}}^L(n^2)\right] e^{2ik_z z}. \tag{4.40}$$

It is worth noting that none of the preceding analysis relied on the specific form (aside from its analyticity along the contour) of the quantity labelled 'coeff.' in eq. (4.28), and that all of the manipulations done inside the square brackets of eq. (4.28) are valid for both TE and TM modes. This observation will be used later in evaluating shifts which are given by the sum of several integrals of the form (4.27).

The integral (4.39) is most conveniently evaluated by the method of residues. We close the contour in the lower half-plane using a semicircle with a large radius. By Jordan's lemma the contribution from this semicircle vanishes as its radius is sent to infinity, meaning the desired integral is found by summing over the residues of all the poles in the lower half-plane. The reflection coefficients have no poles because of the constraint $\text{sgn}(k_z) = \text{sgn}(k_z^d)$, so the only contribution to integrals (4.39) and (4.40) is from the (double) pole at $k_z = -ik_\parallel$. The residue theorem gives the energy shift as

$$\Delta E_{\perp\text{ren}}^{\text{nondisp}} = \frac{i}{4\pi}\frac{e^2}{m^2}\langle p_\perp^2\rangle \int_0^\infty dk_\parallel \operatorname*{Res}_{k_z\to -ik_\parallel} \frac{k_\parallel^3}{(k_z^2+k_\parallel^2)^2} R_{\mathbf{k}.\text{TM}}^L(n^2) e^{2ik_z z}, \tag{4.41}$$

$$\Delta E_{\parallel\text{ren}}^{\text{nondisp}} = -\frac{i}{8\pi}\frac{e^2}{m^2}\langle p_\parallel^2\rangle \int_0^\infty dk_\parallel \operatorname*{Res}_{k_z\to -ik_\parallel} \frac{k_\parallel k_z^2}{(k_z^2+k_\parallel^2)^2} \times \left[R_{\mathbf{k},\text{TM}}^L(n^2) + (k_z^2+k_\parallel^2) R_{\mathbf{k},\text{TE}}^L(n^2)\right] e^{2ik_z z}. \tag{4.42}$$

Evaluating the residues, we find for our final results for the mass shift near a non-dispersive

surface

$$\Delta E^{\text{nondisp}}_{\perp\text{ren}} = -\frac{e^2}{16\pi m^2}\langle p_\perp^2\rangle \int_0^\infty dk_\parallel k_\parallel e^{2k_\parallel z}\left[i\frac{dR^L_{\text{TM}}(n^2)}{dk_z} + R^L_{\text{TM}}(n^2)\left(\frac{1}{k_\parallel} - 2z\right)\right]_{k_z\to -ik_\parallel}, \tag{4.43}$$

$$\Delta E^{\text{nondisp}}_{\parallel\text{ren}} = -\frac{e^2}{32\pi m^2}\langle p_\parallel^2\rangle \int_0^\infty dk_\parallel k_\parallel e^{2k_\parallel z}\left[\frac{2R^L_{\text{TE}}(n^2)}{k_\parallel} + i\frac{dR^L_{\text{TM}}(n^2)}{dk_z} - R^L_{\text{TM}}(n^2)\left(2z + \frac{1}{k_\parallel}\right)\right]_{k_z\to -ik_\parallel}, \tag{4.44}$$

with

$$R^L_{\mathbf{k},\text{TE}}(n^2) = \frac{k_z - \sqrt{n^2k_z^2 + k_\parallel^2(n^2-1)}}{k_z + \sqrt{n^2k_z^2 + k_\parallel^2(n^2-1)}}, \quad R^L_{\mathbf{k},\text{TM}}(n^2) = \frac{n^2k_z - \sqrt{n^2k_z^2 + k_\parallel^2(n^2-1)}}{n^2k_z + \sqrt{n^2k_z^2 + k_\parallel^2(n^2-1)}}, \tag{4.45}$$

as shown in appendix A.2. We have also utilized the explicit form of k_z^d shown in eq. (3.22b). As an initial check on our results, we take the $n\to\infty$ limit of the reflection coefficients ($R^L_{TE} = -1$, $R^L_{TM} = 1$) *before* the limit $k_z \to -ik_\parallel$, which corresponds to taking the 'perfect mirror' limit of the dielectric model. The derivative terms all vanish and the remaining integrals are trivial, giving for the total energy shift $\Delta E^{\text{PM}}_{\text{ren}} = \Delta E^{\text{nondisp}}_{\perp\text{ren}}(n\to\infty) + \Delta E^{\text{nondisp}}_{\parallel\text{ren}}(n\to\infty)$ of an electron near a perfect reflector as

$$\Delta E^{\text{PM}}_{\text{ren}} = -\frac{e^2}{32m^2\pi z}\langle p_\parallel^2\rangle + \frac{e^2}{16\pi m^2 z}\langle p_\perp^2\rangle\,. \tag{4.46}$$

For finite n the integrals (4.43) and (4.44) are also trivial, the shift $\Delta E^{\text{nondisp}}_{\text{ren}} = \Delta E^{\text{nondisp}}_{\perp\text{ren}} + \Delta E^{\text{nondisp}}_{\parallel\text{ren}}$ for an electron near a non-dispersive interface is

$$\Delta E^{\text{nondisp}}_{\text{ren}} = \frac{e^2}{32m^2\pi z}\frac{n^2\left(n^2-1\right)}{\left(1+n^2\right)^2}\langle p_\parallel^2\rangle + \frac{e^2}{16\pi m^2 z}\frac{2n^4-n^2-1}{(n^2+1)^2}\langle p_\perp^2\rangle. \tag{4.47}$$

The $n\to\infty$ limit of this is

$$\Delta E^{\text{nondisp}}_{\text{ren}}(n\to\infty) = \frac{e^2}{32m^2\pi z}\langle p_\parallel^2\rangle + \frac{e^2}{8\pi m^2 z}\langle p_\perp^2\rangle \neq \Delta E^{\text{PM}}_{\text{ren}}, \tag{4.48}$$

which is *not* in agreement with the perfect reflector result (4.46). Eqs. (4.46) and (4.47) together reproduce the result of the far more involved calculation found in [46, 48], where the reason for the discrepancy between the dielectric and perfect reflector results is discussed in detail. We postpone such a discussion until dispersive models have been considered because the inclusion of dispersion turns out to clarify the issue that causes the discrepancy.

4.2.2 Plasma

We now calculate the magnetic moment of an electron near a plasma surface, for which we derived the mode expansion of the quantized electromagnetic field in section (3.3). Here we have three types of mode; TE, TM and surface plasmon (SP), so the mode sum is

$$\sum_{\text{all modes}} \to \int d^3\mathbf{k} \sum_{\lambda=\text{TE,TM}} + \int d^2\mathbf{k}_\parallel \sum_{\lambda=\text{SP}} , \tag{4.49}$$

where the modes are given by eqs (3.50) and (3.32). The energy shift that is attributable to the surface plasmon is

$$\Delta E^{\text{sp}} = -\frac{e^2}{m^2}\langle p_i^2\rangle \int d^2\mathbf{k}_\parallel \frac{1}{\omega_{\text{sp}}} \left| f^{\text{sp}*}_{\mathbf{k}_\parallel,i}(\mathbf{r},\omega)\right|^2 , \tag{4.50}$$

which can easily be derived by repeating the analysis that takes eq. (4.21) to eq. (4.24) but instead acting with the surface plasmon field operator (3.45) on the vacuum state to produce a one-surface plasmon state $|1^{\text{sp}}_{k_\parallel}\rangle$. Combining this with the bulk contribution (4.27), the component of the plasma mass shift that is proportional to $\langle p_\perp^2\rangle$ is given by:

$$\begin{aligned}\Delta E_\perp^{\text{plasma}} &= -\frac{e^2}{m^2}\langle p_\perp^2\rangle \left\{ \int d^3\mathbf{k} \sum_\lambda \frac{1}{\omega} \left| f^*_{\mathbf{k}\lambda,z}(\mathbf{r},\omega)\right|^2 + \int d^2\mathbf{k}_\parallel \frac{1}{\omega_{\text{sp}}} \left| f^{\text{sp}*}_{k_\parallel,z}(\mathbf{r},\omega)\right|^2 \right\} \\ &= \Delta E_\perp^{\text{bulk}} + \Delta E_\perp^{\text{SP}} .\end{aligned} \tag{4.51}$$

where we have split the energy shift into bulk and surface-plasmon contributions given by the first and second terms of (4.51), respectively. Inserting the bulk modes (3.32) into $\Delta E_\perp^{\text{bulk}}$ and again localizing the electron in the region $z<0$ we have

$$\begin{aligned}\Delta E_\perp^{\text{bulk}} = -\frac{1}{(2\pi)^3}\frac{e^2}{m^2}\langle p_\perp^2\rangle \int d^2\mathbf{k}_\parallel \Bigg(&\int_0^\infty dk_z \left| e^{i\mathbf{k}\cdot\mathbf{r}} + R^L_{\mathbf{k},\text{TM}}(\epsilon_p) e^{i\bar{\mathbf{k}}\cdot\mathbf{r}}\right|^2 \\ &+ \int_0^\infty dk_z^d \left| T^R_{\mathbf{k},\text{TM}}(\epsilon_p) e^{i\mathbf{k}\cdot\mathbf{r}}\right|^2 \Bigg) \frac{k_\parallel^2}{2k^4} .\end{aligned} \tag{4.52}$$

From eq. (3.35) we have

$$k_z = \sqrt{k_z^{d2} + \omega_p^2} . \tag{4.53}$$

In contrast to the corresponding relation (4.29) for the non-dispersive dielectric, this relation shows that for real k_z^d, k_z must also be real. So, in a similar fashion to eq. (4.32), we rewrite the second term of (4.52) by changing variables from k_z to k_z^d, giving

$$\begin{aligned}\Delta E_\perp^{\text{bulk}} = -\frac{1}{(2\pi)^3}\frac{e^2}{m^2}\langle p_\perp^2\rangle \int d^2\mathbf{k}_\parallel \Bigg\{ &\int_0^\infty dk_z \left[1 + |R^L_{\mathbf{k},\text{TM}}(\epsilon_p)|^2 + \frac{k_z}{k_z^d} |T^R_{\mathbf{k},\text{TM}}(\epsilon_p)|^2 \right] \\ &+ \int_{-\infty}^\infty dk_z R^L_{\mathbf{k},\text{TM}}(\epsilon_p) e^{2ik_z z} \Bigg\} \frac{k_\parallel^2}{2k^4} ,\end{aligned} \tag{4.54}$$

where eq. (4.53) has been used to change variables in the transmission term. Appeal to eq. (4.38) shows that the first term is that which would remain if there were no surface present, so is dropped. This leaves simply

$$\Delta E^{\text{bulk}}_{\perp\text{ren}} = -\frac{1}{8\pi^2}\frac{e^2}{m^2}\langle p_\perp^2\rangle \int_0^\infty dk_\parallel \int_{-\infty}^\infty dk_z \frac{k_\parallel^3}{k^4} R^L_{\mathbf{k},\text{TM}}(\epsilon_p) e^{2ik_z z} \,. \tag{4.55}$$

Again we evaluate the integral through the residue theorem, however this time the TM reflection coefficient has a simple pole on the imaginary k_z axis at $k_{z,\text{sp}} = \sqrt{\omega_{\text{sp}}^2 - k_\parallel^2}$. Consequently we split the energy shift into the contribution $\Delta E^{\text{bulk}}_{\perp,0}$ from the pole at $-ik_\parallel$, and $\Delta E^{\text{bulk}}_{\perp,R}$ from the pole in the TM reflection coefficient;

$$\Delta E^{\text{bulk}}_{\perp\text{ren}} = \Delta E^{\text{bulk}}_{\perp,0} + \Delta E^{\text{bulk}}_{\perp,\text{R}} \,. \tag{4.56}$$

Evaluation of $\Delta E^{\text{bulk}}_{\perp,0}$ proceeds in exactly the same way as (4.41) and (4.42) were obtained from (4.40) in the calculation for the non-dispersive surface, namely by evaluation of the residue at $k_z = -ik_\parallel$, giving

$$\Delta E^{\text{bulk}}_{\perp,0} = \frac{i}{4\pi}\frac{e^2}{m^2}\langle p_\perp^2\rangle \int_0^\infty dk_\parallel \operatorname*{Res}_{k_z\to -ik_\parallel} \frac{k_\parallel^3}{(k_z^2+k_\parallel^2)^2} R^L_{\mathbf{k}.\text{TM}}(\epsilon_p) e^{2ik_z z}, \tag{4.57}$$

$$\Delta E^{\text{bulk}}_{\parallel,0} = -\frac{i}{8\pi}\frac{e^2}{m^2}\langle p_\parallel^2\rangle \int_0^\infty dk_\parallel \operatorname*{Res}_{k_z\to -ik_\parallel} \frac{k_\parallel k_z^2}{(k_z^2+k_\parallel^2)^2} \times \left[R^L_{\mathbf{k},\text{TM}}(n^2) + (k_z^2+k_\parallel^2) R^L_{\mathbf{k},\text{TE}}(\epsilon_p)\right] e^{2ik_z z}. \tag{4.58}$$

Moving on to the contribution $\Delta E^{\text{bulk}}_{\perp,\text{R}}$ from the pole in the TM reflection coefficient, we find for the residue of the reflection coefficient at $k_{z,\text{sp}}$

$$\operatorname*{Res}_{k_z\to k_{z,\text{sp}}} \left[R^L_{\mathbf{k},\text{TM}}(\epsilon_p)\right] = -2i\frac{\omega_{\text{sp}}^2}{\omega_p^2}\frac{(\omega_p^2-\omega_{\text{sp}})^2\sqrt{\omega_p^2-2\omega_{\text{sp}}^2}}{\omega_{\text{sp}}^4+(\omega_p^2-\omega_{\text{sp}}^2)^2} \equiv -i\mathcal{S} \,, \tag{4.59}$$

so that the contribution from the pole at $k_{z,\text{sp}}$ is

$$\Delta E^{\text{bulk}}_{\perp,\text{R}} = \frac{1}{4\pi}\frac{e^2}{m^2}\langle p_\perp^2\rangle \int_0^\infty dk_\parallel \frac{k_\parallel^3}{\omega_{\text{sp}}^4}\mathcal{S} e^{2\kappa z} \,. \tag{4.60}$$

This completes the evaluation of the the bulk contribution (4.56) to the mass shift (4.51), so we now move on to the surface plasmon part.

From eq. (4.51) we have for the surface plasmon part of the energy shift

$$\Delta E^{\text{SP}}_\perp = -\frac{e^2}{m^2}\langle p_\perp^2\rangle + \int d^2\mathbf{k}_\parallel \frac{1}{\omega_{\text{sp}}} \left| f^{\text{sp}*}_{k_\parallel,z}(\mathbf{r},\omega)\right|^2 \,. \tag{4.61}$$

Recalling that our electron is localized in the region $z<0$, we substitute the $z<0$ part of the surface plasmon modes (3.50) into this to find

$$\Delta E^{\text{SP}}_\perp = -\frac{1}{2\pi}\frac{e^2}{m^2}\langle p_\perp^2\rangle \int_0^\infty dk_\parallel \frac{1}{p(\mathbf{k}_\parallel)}\frac{k_\parallel^3}{\kappa^2\omega_{\text{sp}}} e^{2\kappa z} = \Delta E^{\text{SP}}_{\perp\text{ren}} \,, \tag{4.62}$$

where we note that the renormalization of this term is trivial since the surface plasmon has no counterpart in free space.

We have now evaluated the entire energy shift of an electron near a plasma surface

$$\begin{aligned}\Delta E_{\perp\text{ren}}^{\text{plasma}} &= \Delta E_{\perp\text{ren}}^{\text{bulk}} + \Delta E_{\perp\text{ren}}^{\text{SP}} \\ &= \Delta E_{\perp,0}^{\text{bulk}} + \Delta E_{\perp,\text{R}}^{\text{bulk}} + \Delta E_{\perp\text{ren}}^{\text{SP}} \,. \end{aligned} \tag{4.63}$$

The crucial observation is that contributions (4.60) and (4.62) exactly cancel each other

$$\Delta E_{\perp,\text{R}}^{\text{bulk}} + \Delta E_{\perp}^{\text{sp}} = 0 \,. \tag{4.64}$$

This type of cancellation has been noted in a similar calculation [49], and is a consequence of the fact that the modes form a complete set. It is also seen to happen in the corresponding calculation for motion parallel to the surface. This means that our final results for for the total energy shifts arising from motion in both directions are

$$\Delta E_{\perp\text{ren}}^{\text{plasma}} = \Delta E_{\perp,0}^{\text{bulk}} \,, \qquad\qquad \Delta E_{\parallel\text{ren}}^{\text{plasma}} = \Delta E_{\parallel,0}^{\text{bulk}} . \tag{4.65}$$

The right hand sides of the above two expressions are given by explicitly by eqs. (4.57) and (4.58), so we finally have

$$\Delta E_{\perp\text{ren}}^{\text{plasma}} = \frac{i}{4\pi}\frac{e^2}{m^2}\langle p_\perp^2\rangle \int_0^\infty dk_\parallel \operatorname*{Res}_{k_z\to -ik_\parallel} \frac{k_\parallel^3}{(k_z^2+k_\parallel^2)^2} R^L_{\mathbf{k},\text{TM}}(\epsilon_p) e^{2ik_z z} \,, \tag{4.66}$$

$$\begin{aligned}\Delta E_{\parallel\text{ren}}^{\text{plasma}} = -\frac{i}{8\pi}\frac{e^2}{m^2}\langle p_\parallel^2\rangle \int_0^\infty dk_\parallel \operatorname*{Res}_{k_z\to -ik_\parallel} \frac{k_\parallel k_z^2}{(k_z^2+k_\parallel^2)^2} \\ \times \left[R^L_{\mathbf{k},\text{TM}}(\epsilon_p) + (k_z^2+k_\parallel^2) R^L_{\mathbf{k},\text{TE}}(\epsilon_p)\right] e^{2ik_z z}. \end{aligned} \tag{4.67}$$

Comparison of eqs. (4.41) and (4.42) which give the mass shift near a non-dispersive surface with eqs. (4.66) and (4.67) which give the mass shift near a plasma surface shows that results for the two models can be obtained from the *same* expressions, just with the appropriate dielectric function inserted into the reflection coefficients. The fact that our calculations have this quality is of particular use later on, when we consider more complex models of the surface.

Proceeding with our calculation for the plasma, we now evaluate the integrals (4.66) and (4.67) which deliver the mass shift near a plasma surface. We begin by evaluating the residues, which give expressions identical to (4.43) and (4.44) but with $n^2 \to \epsilon_p$. Noting that the $k_z \to -ik_\parallel$ limits of the plasma reflection coefficients coincide with those for the perfect mirror, we find that we can write the plasma shifts as corrections to the perfect

mirror shifts via

$$\Delta E^{\text{plasma}}_{\perp\text{ren}} = \Delta E^{\text{PM}}_{\perp\text{ren}} + \Delta_\perp \,, \tag{4.68a}$$

$$\Delta E^{\text{plasma}}_{\parallel\text{ren}} = \Delta E^{\text{PM}}_{\parallel\text{ren}} + \Delta_\parallel \,, \tag{4.68b}$$

with

$$\Delta_\perp = -\frac{e^2}{4\pi m^2\omega_p^2}\langle p_\perp^2\rangle \int_0^\infty dk_\parallel k_\parallel \sqrt{k_\parallel^2+\omega_p^2}\, e^{2k_\parallel z} \,, \tag{4.69a}$$

$$\Delta_\parallel = -\frac{e^2}{4\pi m^2\omega_p^2}\langle p_\parallel^2\rangle \int_0^\infty dk_\parallel k_\parallel \left(\sqrt{k_\parallel^2+\omega_p^2} - \frac{k_\parallel}{2}\right) e^{2k_\parallel z} \,. \tag{4.69b}$$

The integrals $\Delta_{\perp,\parallel}$ can be evaluated analytically in MATHEMATICA, the results for $\Delta_\perp$ is

$$\Delta_\perp = -\frac{e^2\langle p_z^2\rangle}{48m^2\pi\omega_p^2 z^3}\Big\{3J_0(2\omega_p z) + 2\omega_p z\left[3J_1(2\omega_p z) - \omega_p z(2\omega_p z - 3J_2(2\omega_p z)\ln(-\omega_p z))\right] + 3\omega_p^2\pi z^2 H_2(2\omega_p z) + 6\frac{\partial}{\partial a}\left[{}_0F_1(-a,-\omega_p^2 z^2)/\Gamma(-a)\right]\Big|_{a=1}\Big\} \,, \tag{4.70}$$

where ${}_0F_1(a,z)$ is a confluent hypergeometric function (see, for example, section 9.14 of [50]), defined by

$${}_0F_1(a,x) = \sum_{n=0}^{\infty}\frac{z^n}{(a)_n n!} \tag{4.71}$$

where $(a)_n$ is the nth Pochhammer symbol $\Gamma(a+n)/\Gamma(a)$. $J_n(x)$ is the nth Bessel function of the second kind, and $H_n(x)$ is the nth Struve function. Doing the elementary integral given by the second term of (4.69b), we have that $\Delta_\parallel$ can be obtained from $\Delta_\perp$ through

$$\Delta_\parallel = \langle p_\parallel^2\rangle\left[-\frac{e^2}{32m^2\pi\omega_p^2 z^3} + \frac{\Delta_\perp}{\langle p_\perp^2\rangle}\right] \,. \tag{4.72}$$

The form of these functions is shown in fig. 4.5, which indicates that the $|\omega_p z|\to\infty$ limit of both $\Delta_\parallel$ and $\Delta_\perp$ is zero. To prove this from the expression (4.70) is not a simple matter, so we go back to the integral form of $\Delta_\perp$ (4.69a) and change variables to $x = -k_\parallel z$, giving

$$\Delta_\perp = \frac{e^2}{4\pi m^2 z}\frac{\langle p_\perp^2\rangle}{(\omega_p z)^2}\int_0^\infty dk_\parallel x\sqrt{x^2+(\omega_p z)^2}\, e^{-2x} \,. \tag{4.73}$$

The integrand may then be expanded for small $|\omega_p z|$ and integrated term-by-term. The result is

$$\Delta_\perp(|\omega_p z|\gg 1) = -\frac{e^2}{4\pi m^2 z}\langle p_\perp^2\rangle\left[\frac{1}{\omega_p z} + \mathcal{O}\left(1/z^3\right)\right] \,, \tag{4.74}$$

which, in combination with the relation (4.72) linking $\Delta_\perp$ and $\Delta_\parallel$, confirms that

$$\lim_{|\omega_p z|\to\infty}\Delta_\perp = 0 \,, \qquad \lim_{|\omega_p z|\to\infty}\Delta_\parallel = 0 \,. \tag{4.75}$$

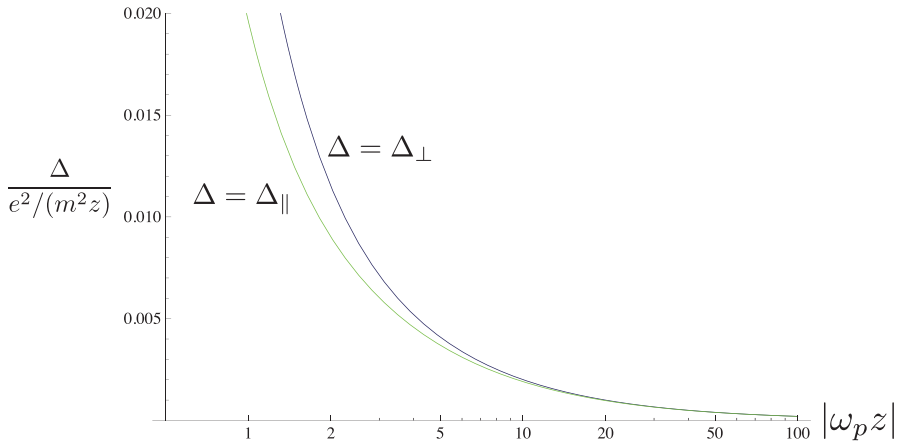

Figure 4.5: The functions $\Delta_\perp$ and $\Delta_\parallel$ as a function of $|\omega_p z|$ (note the log scale on the horizontal axis).

Inserting these into eqs. (4.68a) and (4.68b) to find the large $|\omega_p z|$ approximation of the mass shift near plasma, we see that that the plasma and perfect mirror results agree at $|\omega_p z| \to \infty$, which is expected because both models have $|\epsilon(\omega)| \to \infty$ at this point. Both of the models exclude evanescent modes, in contrast to the non-dispersive dielectric. Thus, we are beginning to see that evanescent modes play a decisive role in the calculation of radiative corrections near a surface – a phenomenon which will be discussed in detail after the consideration of some more realistic models of the response of the surface.

4.2.3 More realistic models of the surface

The use of the plasma model represents a significant advance over previous perfect-reflector and non-dispersive calculations. However, real surfaces have more complicated dielectric functions. Writing a general dielectric function for a vacuum-medium half space in terms of the susceptibility of the medium $\chi(\omega) = \epsilon(\omega) - 1$, we have

$$\epsilon(\mathbf{r}, \omega) = 1 + \Theta(z)\chi(\omega) \; . \tag{4.76}$$

Inserting this into Maxwell's equations (2.64) we find in generalized Coulomb gauge $\nabla \cdot [\epsilon(\mathbf{r}, \omega)\mathbf{A}(\mathbf{r}, \omega)] = 0$

$$\nabla \times [\nabla \times \mathbf{A}(\mathbf{r}, \omega)] = \omega^2 \epsilon(\mathbf{r}, \omega)\mathbf{A}(\mathbf{r}, \omega) \; . \tag{4.77}$$

Writing this in terms of general mode functions $\mathbf{f}_{\mathbf{k}\lambda}(\mathbf{r}, \omega)$ defined by (2.39)

$$\mathbf{A}(\mathbf{r}, \omega) = \sum_\lambda \int d^3\mathbf{k} \left[\hat{a}_{\mathbf{k}\lambda} e^{-i\omega_k t} \mathbf{f}_{\mathbf{k}\lambda}(\mathbf{r}, \omega) + \hat{a}^\dagger_{\mathbf{k}\lambda} e^{i\omega_k t} \mathbf{f}^*_{\mathbf{k}\lambda}(\mathbf{r}, \omega) \right] \; , \tag{4.78}$$

and using the explicit half space dielectric function (4.76), we find

$$\nabla \times [\nabla \times \mathbf{f}_{\mathbf{k}\lambda}(\mathbf{r}, \omega)] - \Theta(z)\omega^2 \chi(\omega) \mathbf{f}_{\mathbf{k}\lambda}(\mathbf{r}, \omega) = \omega^2 \mathbf{f}_{\mathbf{k}\lambda}(\mathbf{r}, \omega) \; . \tag{4.79}$$

It is well known that if the wave equation is a Hermitian eigenvalue problem, the modes necessarily form a complete set, which means that one can write down a mode expansion and choose a normalization such that the field is canonically quantized. Since our approach relies on being able to explicitly work with the mode expansion, it is worth investigating under what conditions (4.79) represents a Hermitian eigenvalue problem. This happens if $\chi(\omega)$ obeys one of two conditions

- $\chi(\omega)$ is independent of ω, so that $\chi(\omega)$ may be written in the form $\chi(\omega) = n^2 - 1$ (with $n > 1$) and (4.79) rearranged to coincide with eq. (3.9),

or,

- $\omega^2\chi(\omega)$ is independent of ω, so that the second term on the left hand side of eq. (4.79) becomes independent of ω.

The non-dispersive model discussed in section 4.2.1 satisfies the first condition, and the plasma model discussed in section 4.2.2 satisfies the second. Combining the second condition with the definition that $\chi(\omega) = \epsilon(\omega) - 1$, we have that the only permissible dielectric function for the half-space is of the form

$$\epsilon(\omega) = 1 + \frac{\text{constant}}{\omega^2} \,, \tag{4.80}$$

which shows that the plasma is the *only* dispersive model that admits a mode expansion (with, of course, the constant being equal to $-\omega_p^2$). Since our method is reliant on the existence of an explicit mode expansion, it seems that this sets a limit of the applicability of our approach.

However, we obtain results for surfaces which do not admit a mode expansion by taking what seems like an unjustified leap of faith and consider our formulae (4.43) and (4.44) as being correct for any choice of dielectric function $\epsilon(\omega)$ for the half space. In Chapter 7 we approach this and related problems from a different direction in such a way as to explicitly justify this step, but for now we note several indications that hint towards the validity of this procedure. The first is of course that the non-dispersive and plasma results can both be obtained by insertion of the relevant dielectric function into (4.43) and (4.44), so it is not unreasonable to expect that other models will work in the same way. The second is that the electromagnetic Green's function for the half-space geometry can be written entirely in terms of the reflection coefficients of a surface with arbitrary dielectric function [51], so that if one worked with the Green's function one would necessarily get the same formulae (4.43) and (4.44) for the mass shift. In Chapter 7 we use a completely different

approach based on a so-called 'noise current' as a final and explicit justification for this step.

Proceeding, we write eqs. (4.66) and (4.67) with an arbitrary dielectric function $\epsilon(k_z, k_\parallel)$,

$$\Delta E_{\perp\text{ren}} = \frac{i}{4\pi}\frac{e^2}{m^2}\langle p_\perp^2\rangle \int_0^\infty dk_\parallel \operatorname*{Res}_{k_z\to -ik_\parallel} \frac{k_\parallel^3}{(k_z^2+k_\parallel^2)^2} R^L_{\mathbf{k},\text{TM}}\left[\epsilon(k_z,k_\parallel)\right] e^{2ik_z z}, \tag{4.81a}$$

$$\Delta E_{\parallel\text{ren}} = -\frac{i}{8\pi}\frac{e^2}{m^2}\langle p_\parallel^2\rangle \int_0^\infty dk_\parallel \operatorname*{Res}_{k_z\to -ik_\parallel} \frac{k_\parallel k_z^2}{(k_z^2+k_\parallel^2)^2} \times \left\{R^L_{\mathbf{k},\text{TM}}\left[\epsilon(k_z,k_\parallel)\right] + (k_z^2+k_\parallel^2) R^L_{\mathbf{k},\text{TE}}\left[\epsilon(k_z,k_\parallel)\right]\right\} e^{2ik_z z}. \tag{4.81b}$$

Using the explicit forms of the reflection coefficients (A.5), we find upon evaluation of the residues show in the integrands of (4.81a) and (4.81b)

$$\Delta E_{\perp\text{ren}} = \frac{e^2}{16\pi m^2}\langle p_\perp^2\rangle \int_0^\infty dk_\parallel \frac{e^{2k_\parallel z}}{\left[1+\epsilon(-ik_\parallel,k_\parallel)\right]^2}\Big[1-2k_\parallel z + 2\epsilon(-ik_\parallel,k_\parallel) + (2k_\parallel z-3)\epsilon^2(-ik_\parallel,k_\parallel) - 2ik_\parallel \epsilon'(-ik_\parallel,k_\parallel)\Big], \tag{4.82a}$$

$$\Delta E_{\parallel\text{ren}} = -\frac{e^2}{32\pi m^2}\int_0^\infty dk_\parallel \frac{e^{2k_\parallel z}}{\left[1+\epsilon(-ik_\parallel,k_\parallel)\right]^2}\Big[1+2k_\parallel z - 2\epsilon(-ik_\parallel,k_\parallel) + (1-2k_\parallel z)\epsilon^2(-ik_\parallel,k_\parallel) + 2ik_\parallel \epsilon'(-ik_\parallel,k_\parallel)\Big], \tag{4.82b}$$

where $\epsilon'(k_z, k_\parallel)$ denotes the derivative[6] of ϵ with respect to k_z. These equations reproduce the non-dispersive and plasma results (4.47) and (4.68) upon insertion of the appropriate dielectric functions.

Using the loose *a priori* (and strong *a posteriori*) justification detailed at the start of this section, we are now free to insert any dielectric function into into eqs. (4.82) and evaluate the shift. But what should we use as the dielectric function which best captures the physics of dispersion? For a non-magnetic substance the equation of motion for the electrons within the material is (see, for example, sec. 7.5 of [52])

$$m(\ddot{\mathbf{x}} + \gamma\dot{\mathbf{x}} + \omega_T^2\mathbf{x}) = -e\mathbf{E}(\mathbf{x},t)\ , \tag{4.83}$$

where $\mathbf{x}$ is the position of an atomic electron relative to its parent nucleus, γ is a damping parameter and ω_T describes a restoring force. These two parameters respectively define the position and width of an absorption resonance of the medium. If the amplitude of the oscillation is small enough to permit the use of the dipole approximation, and the field varies harmonically with time, we can use identical steps to those which took eq. (3.23) to

[6] Here and throughout we use primes to denote derivatives of ϵ – this should not be confused with the common notation $\epsilon' = \operatorname{Re}\epsilon$ and $\epsilon'' = \operatorname{Im}\epsilon$.

eq. (3.26) in our derivation of the dielectric function for a plasma half-space to derive the corresponding dielectric function for this model, giving

$$\epsilon(\mathbf{r},\omega) = 1 - \Theta(z)\frac{\omega_p^2}{\omega^2 - \omega_T^2 + i\omega\gamma} \equiv \epsilon_\gamma(\mathbf{r},\omega)\ . \tag{4.84}$$

The dielectric function to be inserted into eqs. (4.81a) and (4.81b) is $\epsilon_\gamma(\mathbf{r},\omega)$ in terms of k_z and $k_\parallel$, which is

$$\epsilon_\gamma(k_z,k_\parallel) = 1 - \Theta(z)\frac{\omega_p^2}{k_z^2 + k_\parallel^2 - \omega_T^2 + i\gamma\sqrt{k_z^2+k_\parallel^2}}\ . \tag{4.85}$$

We initially consider the case $\gamma = 0$, a model which will we will refer to as the 'undamped dispersive dielectric', with dielectric function $\epsilon_{\text{disp}}(k_z,k_\parallel)$ given by

$$\epsilon_{\text{disp}}(k_z,k_\parallel) \equiv \epsilon_\gamma(k_z,k_\parallel,\gamma\to 0)\ . \tag{4.86}$$

The validity of the use of this particular dielectric function in our formulae (4.82) is reinforced by the fact that the introduction of the parameter ω_T does not affect the post-deformation contour in the k_z plane, as shown in figure 4.6, where the positions of the various poles and branch points are given by

$$K_{z,\pm} = \frac{1}{\sqrt{2}}\sqrt{\omega_p^2+\omega_T^2-k_\parallel^2 \pm \sqrt{k_\parallel^4 + 2k_\parallel^2\left(\omega_p^2-\omega_T^2\right)+\left(\omega_p^2+\omega_T^2\right)^2}}\ , \tag{4.87a}$$

$$k_{z,\pm} = \sqrt{\frac{1}{2}(\omega_p^2+\omega_T^2) \pm \sqrt{k_\parallel^4 - k_\parallel^2\omega_T^2 + \frac{1}{4}\left(\omega_p^2+\omega_T^2\right)^2}}\ . \tag{4.87b}$$

Proceeding, we insert the dielectric function (4.86) into our formulae (4.82), which leads to integrals which are, surprisingly, much simpler than for the plasma case. The result is

$$\Delta E_{\text{ren}}^{\text{disp}} = \frac{e^2}{16\pi m^2}\frac{\omega_p^2}{\left(\omega_p^2+2\omega_T^2\right)^2}\left\{\left[\frac{1}{2z^3}+\frac{1}{2z}\left(\omega_p^2+\omega_T^2\right)\right]\langle p_\parallel^2\rangle + \left[\frac{1}{z^3}+\frac{1}{z}(2\omega_p^2+3\omega_T^2)\right]\langle p_\perp^2\rangle\right\}. \tag{4.88}$$

The $\omega_p\to\infty$ ('perfect reflector') limit of this is

$$\Delta E_{\text{ren}}^{\text{disp}}(\omega_p\to\infty) = \frac{e^2}{32m^2\pi z}\langle p_\parallel^2\rangle + \frac{e^2}{8\pi m^2 z}\langle p_\perp^2\rangle\ . \tag{4.89}$$

Comparing this with eqs. (4.46), (4.48) and (4.68), we have that

$$\left\{\Delta E_{\text{ren}}^{\text{disp}}(\omega_p\to\infty) = \Delta E_{\text{ren}}^{\text{nondisp}}(n\to\infty)\right\} \neq \left\{\Delta E_{\text{ren}}^{\text{plasma}}(\omega_p\to\infty) = \Delta E_{\text{ren}}^{\text{PM}}\right\}. \tag{4.90}$$

which shows that the models of the surface naturally separate into two classes, as discussed in the next section.

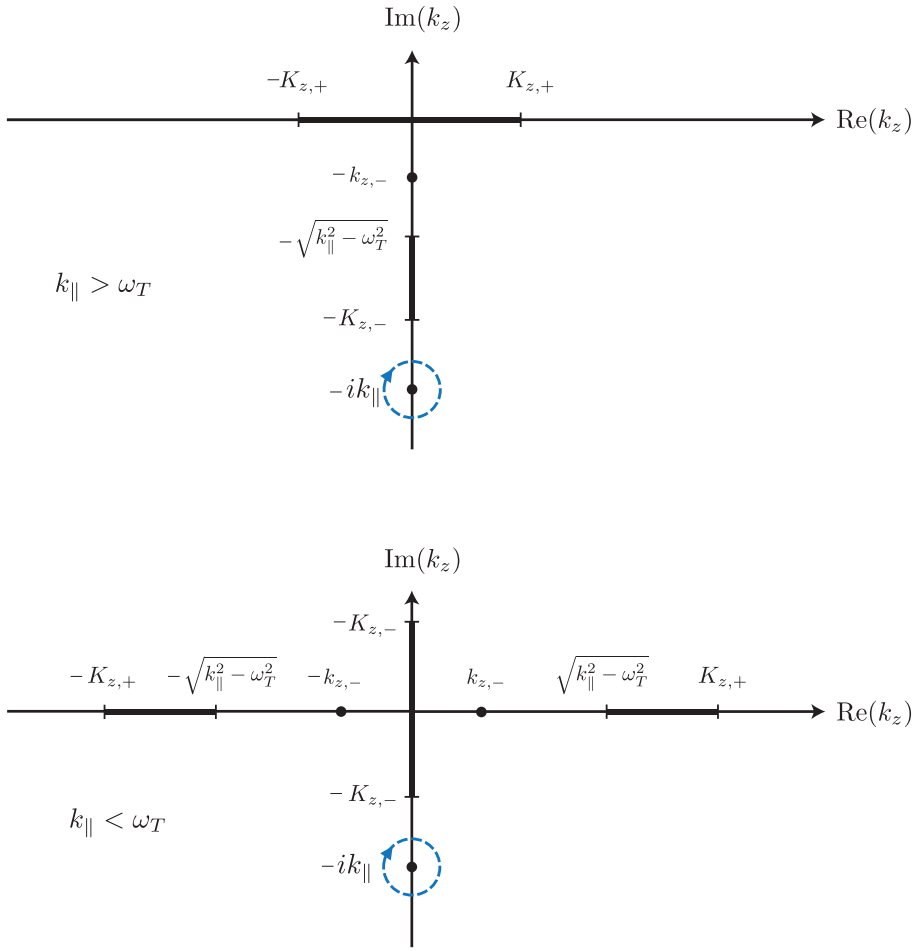

Figure 4.6: Complex k_z plane for $1/\omega^2$ multiplied by the dispersive dielectric reflection coefficient, with labels as defined in eqs (4.87). The energy shifts $\Delta E_{\perp \mathrm{ren}}$ and $\Delta E_{\parallel \mathrm{ren}}$ are given by the residue around $k_z = -ik_\parallel$

4.2.4 Comparison of results

In order to better investigate the disagreements between each model, we characterize each in terms of its static susceptibility $\chi(\omega \to 0) \equiv \chi(0)$

$$\chi(0) \equiv \epsilon(0) - 1 = \begin{cases} \infty & \text{(perfect mirror, plasma)} \\ n^2 - 1 & \text{(non-dispersive dielectric)} \\ \omega_p^2/\omega_T^2 & \text{(undamped dispersive dielectric)} \end{cases}$$

so that, for example, the perpendicular component of the mass shift for the undamped dispersive dielectric is given by

$$\Delta E_{\perp \mathrm{ren}}^{\mathrm{disp}} = \frac{e^2}{16\pi m^2 z} \frac{\chi(0)}{(\omega_T z)^2} \frac{1 + (\omega_T z)^2 (3 + 2\chi(0))}{(2 + \chi(0))^2} \langle p_\perp^2 \rangle. \tag{4.91}$$

The results for three of the four models considered so far are shown in fig. (4.7) The plasma result cannot be shown in fig. (4.7) since its static susceptibility is infinite; however it can

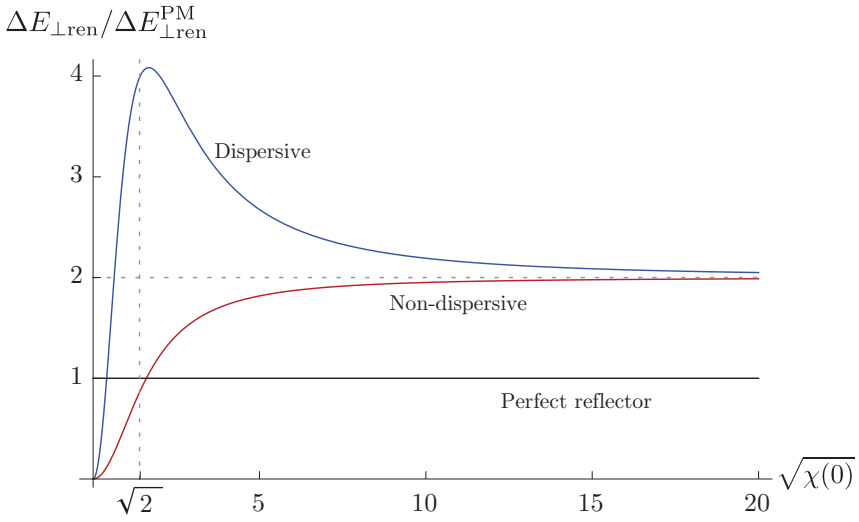

Figure 4.7: Energy shift vs static susceptibility for various models in units of the perfect reflector shift. The dispersive dielectric is shown for $\omega_T z = 0.2$

be compared to the dispersive shift via a plot against the dimensionless parameter $\omega_p z$, as shown in fig. (4.8). In both plots we show energy shifts in units of the perfect reflector shift.

A notable feature of fig. (4.7) is the peak near $\chi(0) = 2$ in the dispersive model. By differentiating the dispersive energy shift (4.91) with respect to $\omega_T z$, it is easy to show that the peak emerges only when $|\omega_T z| < 1/\sqrt{5}$. It moves towards $\chi(0) = 2$ for decreasing $|\omega_T z|$, and its height scales as $(\omega_T z)^{-2}$. Thus, for small values of $|\omega_T z|$ we see that the shift can be made considerably larger than in the previously considered perfect reflector model. We note in particular that the shape of the peak shown in fig. (4.7) would not be easily measurable in a single experiment since it would require the parameters describing the surface to be continuously varied. The peak simply shows which types of material should give a large shift. The experimental consequences of such a large shift in the mass turn out to be to the cyclotron frequency of the electron, which we discuss in section 4.3. Here we focus on the reasons for the apparent discrepancies between the models.

Mathematically, the disagreements arise because of non-commutation of limits in the reflection coefficients (or their derivatives), namely $k_z \to -ik_\parallel$ (required for finding the residue at this point) and whatever limit one has to take to get from dielectric function to another. For example, the $\omega_T \to 0$ limit of the result for the dispersive dielectric should take us to the plasma result, but it does not. This is because the $\omega_T \to 0$ and $k_z \to -ik_\parallel$ limits of the derivative of the dispersive TM reflection coefficient do not commute. A similar problem causes the perfect reflector and non-dispersive results to disagree in the

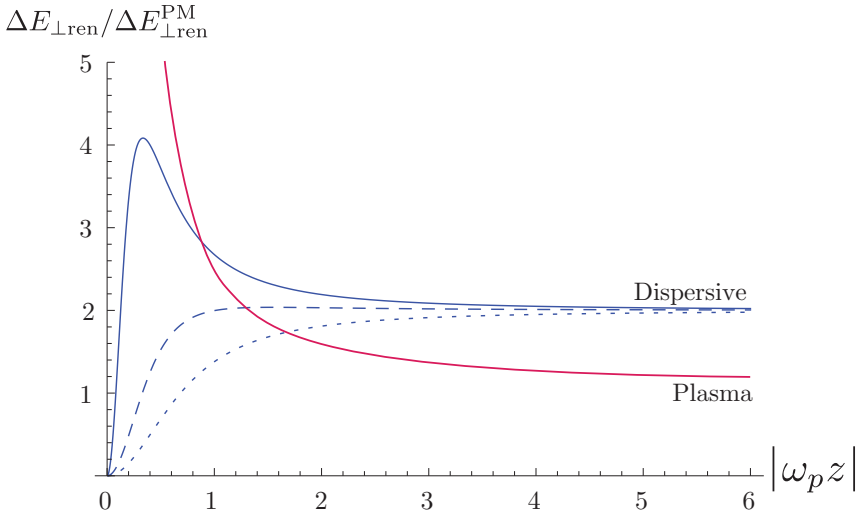

Figure 4.8: Energy shift in units of the perfect reflector shift vs the dimensionless parameter $\omega_p z$ for the plasma and dispersive dielectric models for various $\omega_T z$. The values of $\omega_T z$ shown are 0.2 (solid line), 0.4 (dashed), and 0.6 (dotted).

limit $n \to \infty$; namely that the $n \to \infty$ and $k_z \to -ik_\parallel$ limits of the non-dispersive TE reflection coefficient listed in Appendix A.2 do not commute, as can be easily seen via

$$\begin{aligned} \lim_{n\to\infty}\left[R^L_{\mathbf{k},\mathrm{TE}}(n^2)\right] = -1 \quad &\to \quad \lim_{k_z\to -ik_\parallel}\left[\lim_{n\to\infty}\left[R^L_{\mathbf{k},\mathrm{TE}}(n^2)\right]\right] = -1 \\ \lim_{k_z\to -ik_\parallel}\left[R^L_{\mathbf{k},\mathrm{TE}}(n^2)\right] = 0 \quad &\to \quad \lim_{n\to\infty}\left[\lim_{k_z\to -ik_\parallel}\left[R^L_{\mathbf{k},\mathrm{TE}}(n^2)\right]\right] = 0\,, \end{aligned} \tag{4.92}$$

This issue has been encountered in previous work [46, 48], we confirm this in the context of a dispersive medium. A summary of the various commutation properties of the reflection coefficients for the considered models is shown in fig. (4.9).

Physically, the differences between models that disagree with each other are down to a number of reasons. One of them is the exclusion of part of the photon phase-space, namely the evanescent modes. Previous workers have shown that exclusion of evanescent modes is not an adequate approximation to real materials [46, 48], again we have confirmed this conclusion for a dispersive medium. The other main reason for the discrepancies is the different response of conductors and dielectrics to electric fields at low frequencies: $\varepsilon(\omega)$ has a pole at $\omega = 0$ for a conductor but not for a dielectric. The discrepancies between the results for the mass shift show that one has to decide whether the material at hand should be modelled as a metal (no restoring force for the charge carriers) or as a dielectric (with a restoring force parametrized by ω_T), since these two classes of model for the surface are not obtainable as limiting cases of one another, demonstrating the different nature of the electromagnetic response of conductors and dielectrics.

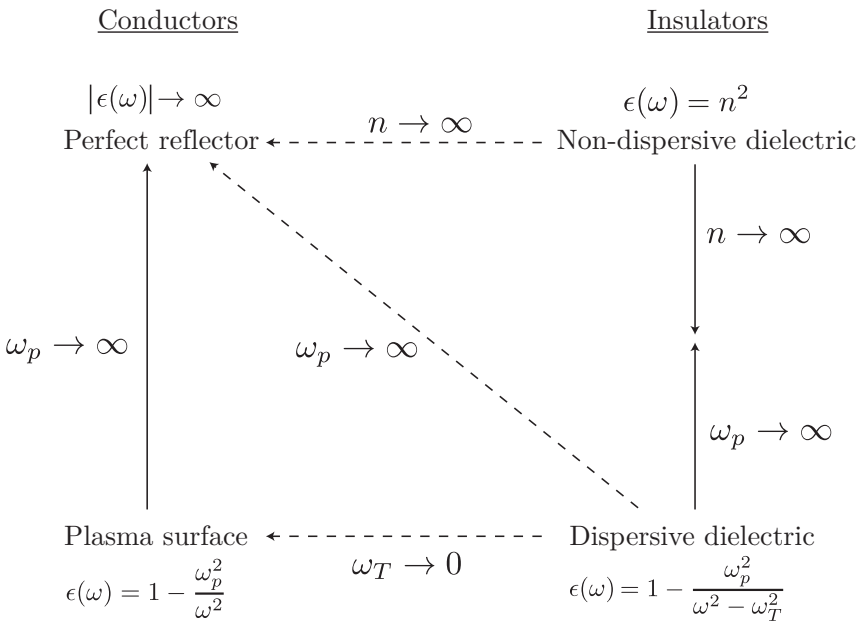

Figure 4.9: Commutation properties of the various models discussed here. Each arrow indicates a limit which takes one dielectric function to another. Solid (dashed) arrows indicate a limit that, when applied the reflection coefficients, commutes (does not commute) with the limit $k_z \to -ik_\parallel$. The consequence of this is that the mass shift results for two models connected by solid (dashed) arrows are (are not) obtainable as limiting cases of one another.

To find conductors and dielectrics giving rise to different results on account of their different response to electromagnetic fields is of course not surprising – different models should give different results. This is, however, in contrast to what one might have expected from the closely related Casimir-Polder energy shift in an atom close to a conducting or dielectric boundary, which was briefly discussed in section 2.3.2. In both the retarded and non-retarded regimes the Casimir-Polder shift of an atom in front of a dielectric [53] reproduces the original result for an atom close to a perfect reflector [54] in the limit of infinite dielectric constant, and so does the level shift for an atom near a plasma surface [49] in the limit of infinite plasma frequency, $\omega_p \to \infty$. The crucial difference between an atom and a free particle in this context is that the excitation spectrum of a bound electron has a gap at low frequencies corresponding to the nearest energy level whereas a free particle admits excitations of arbitrarily low frequency. As a consequence, the low-frequency behavior of the electromagnetic response of the material, in particular the pole at $\omega = 0$ in the dielectric function of a conductor, play a decisive role for the mass shift of a free particle, but not for the Casimir-Polder shift of an atom. An interesting

intermediate case would be an electron that is weakly bound in a Rydberg atom, but any investigation would have to ensure that our assumption of there being no wave function overlap between the surface and the (highly delocalized) atomic wave function remains valid.

The decisive importance of the pole at $\omega = 0$ in the dielectric function of a conductor is made obvious by the fact that the energy shifts (4.68a) and (4.68b) do not vanish in the limit $\omega_p \to 0$, despite $\epsilon(\omega)$ reducing to the vacuum value of 1 in that case. The limit $\omega_p \to 0$ is non-analytic because the choice of a dielectric function of the form (3.26) necessarily describes freely moving charge carriers at $\omega = 0$, which is obviously not true for vacuum with $\epsilon \equiv 1$. Mathematically speaking, eq. (3.26) is ill-defined if both $\omega \to 0$ and $\omega_p \to 0$; in line with the physical interpretation, the fact that $\epsilon(\omega)$ has a pole at $\omega = 0$ is more important than the strength of this pole.

4.2.5 Damping

The final step in the investigation of the effect for realistic materials is to take $\gamma \neq 0$ in eq. (4.85)

$$\epsilon_\gamma(k_z, k_\parallel) = 1 - \Theta(z)\frac{\omega_p^2}{k_z^2 + k_\parallel^2 - \omega_T^2 + i\gamma\sqrt{k_z^2 + k_\parallel^2}}\,. \tag{4.93}$$

This introduces the additional complication that the reflection coefficient has branch points at $k_z = \pm i k_\parallel$, causing the formulae (4.81a) and (4.81b) to become ambiguous, which is why we have separated our discussion of it from the previous (undamped) models. As we will show in Chapter 7, we can obtain unambiguous results for a damped dielectric by using a Green's function approach to the whole problem. One of the differences between the mode expansion calculation and the Green's function calculation is that the latter is naturally done in terms of ω and $k_\parallel$ rather than k_z and $k_\parallel$, so it stands to reason that transforming our mode expansion integrals over k_z and $k_\parallel$ to be over ω and $k_\parallel$ may remove the ambiguity introduced by the branch points in the reflection coefficient. To do this, we go back a few steps and consider eqs. (4.81a) and (4.81a) with any *undamped* dielectric function $\epsilon_{\gamma\to 0}(k_z, k_\parallel)$ inserted into the reflection coefficients.

$$\Delta E_{\perp\text{ren}} = -\frac{1}{8\pi^2}\frac{e^2}{m^2}\langle p_\perp^2\rangle \int_0^\infty dk_\parallel \int_{C'} dk_z \, \frac{k_\parallel^3}{(k_z^2 + k_\parallel^2)^2} R^L_{\mathbf{k},\text{TM}}\left[\epsilon_{\gamma\to 0}(k_z, k_\parallel)\right] e^{2ik_z z}, \tag{4.94}$$

$$\begin{aligned}\Delta E_{\parallel\text{ren}} = \frac{1}{16\pi}\frac{e^2}{m^2}\langle p_\parallel^2\rangle \int_0^\infty dk_\parallel \int_{C'} dk_z \, \frac{k_\parallel k_z^2}{(k_z^2 + k_\parallel^2)^2} \\ \times \left\{ R^L_{\mathbf{k},\text{TM}}\left[\epsilon_{\gamma\to 0}(k_z, k_\parallel)\right] + (k_z^2 + k_\parallel^2) R^L_{\mathbf{k},\text{TE}}\left[\epsilon_{\gamma\to 0}(k_z, k_\parallel)\right] \right\} e^{2ik_z z},\end{aligned} \tag{4.95}$$

where the contour C' is that shown in fig. 4.10. These formulae are unambiguous because

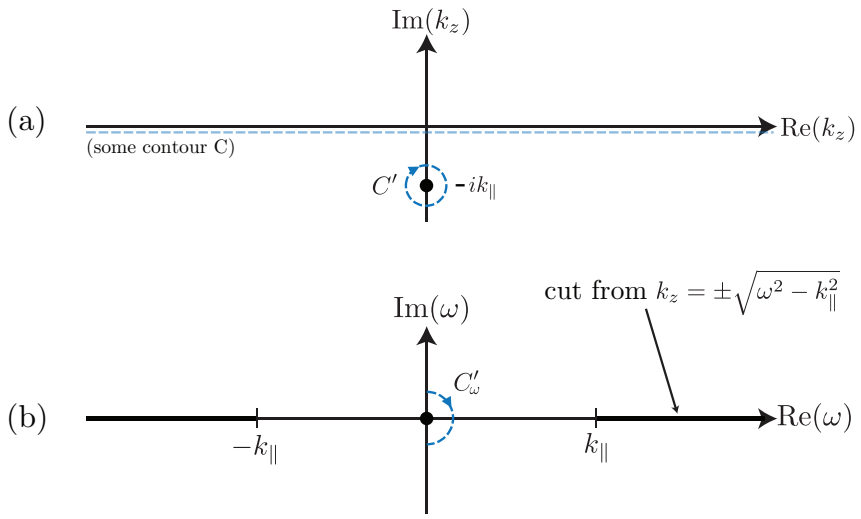

Figure 4.10: Transformation of the contour C' in the k_z plane to the contour C'_ω in the ω plane

the dielectric function has been specifically chosen to be undamped. Transforming the k_z integral from (4.94) to be over ω via $k_z = \sqrt{\omega^2 - k_\parallel^2}$ gives

$$\Delta E_{\perp \text{ren}} = -\frac{e^2}{8\pi^2 m^2}\langle p_\perp^2 \rangle \int_0^\infty dk_\parallel \int_{C'_\omega} d\omega \, \frac{k_\parallel^3}{\omega^3\sqrt{\omega^2 - k_\parallel^2}} R^L_{\mathbf{k},\text{TM}}\left[\epsilon_{\gamma\to 0}(\omega)\right] e^{2i\sqrt{\omega^2-k_\parallel^2}z}, \quad (4.96a)$$

$$\Delta E_{\parallel \text{ren}} = \frac{e^2}{16\pi^2 m^2}\langle p_\parallel^2 \rangle \int_0^\infty dk_\parallel \int_{C'_\omega} d\omega \frac{k_\parallel(\omega^2 - k_\parallel^2)}{\omega^3\sqrt{\omega^2 - k_\parallel^2}}$$
$$\times \left\{R^L_{\mathbf{k},\text{TM}}\left[\epsilon_{\gamma\to 0}(\omega)\right] + \omega^2 R^L_{\mathbf{k},\text{TE}}\left[\epsilon_{\gamma\to 0}(\omega)\right]\right\} e^{2ik_z z}, \quad (4.96b)$$

where the contour is that shown in is shown in fig. 4.10b. The only contribution to eqs. (4.96) is from the pole at $\omega = 0$, which we evaluate using the residue theorem, reproducing our previous results that were found in the k_z plane. Crucially, we find that on replacing $\epsilon_{\gamma\to 0}(\omega)$ with $\epsilon_\gamma(\omega)$, the integral does not gain any new behavior near $\omega = 0$ (unlike in the k_z plane where one introduces an additional branch cut). So what we are seeing is that if we had undertaken our calculation in the ω plane from the start, we would have extended our results beyond the non-dispersive and plasma models with the same justification as shown in section 4.2.3, and that the inclusion of damping would not have caused any extra problems. Thus, our reasoning that making the replacement $\epsilon_{\gamma\to 0}(\omega) \to \epsilon_\gamma(\omega)$ in eqs. (4.96) gives the correct results is of the same strength as our reasoning making the argument that extension past the plasma model is valid. Moreover, we shall see in Chapter 7 that this result is reproduced using an entirely different method.

We now evaluate (4.96) using the residue theorem to find results for the mass shift near a surface described by $\epsilon_\gamma(\omega)$. Expressing this in terms of the static susceptibility $\chi(0)$ and

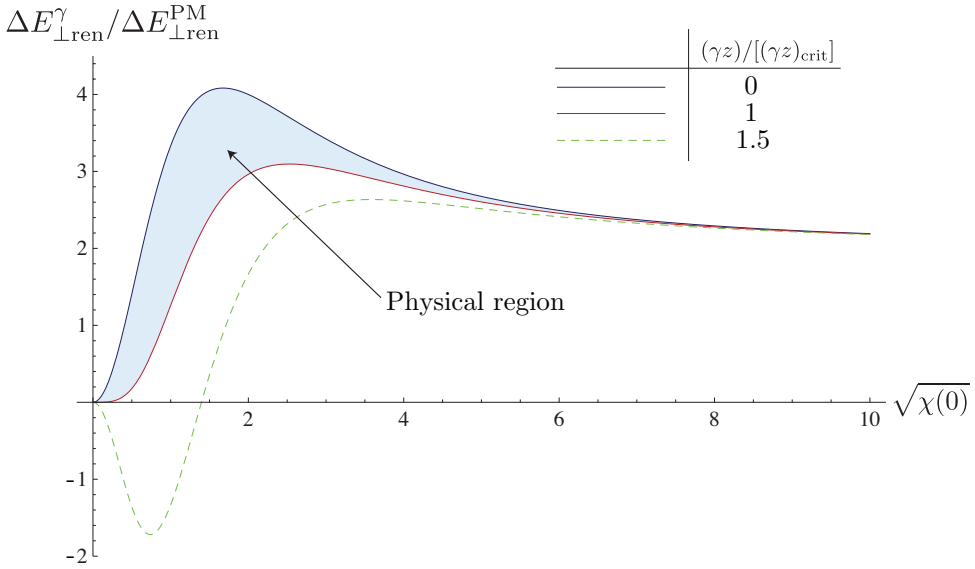

Figure 4.11: Mass shift in units of the perfect reflector shift vs the dimensionless parameter $\sqrt{\chi(0)}$ for a damped surface. The plot takes $|\omega_T z| = 0.2$ in order to facilitate comparison with fig. 4.8. The region corresponding to physically reasonable choices of γz has been labelled.

in units of the respective perfect reflector shifts (4.46), eqs. (4.96) give

$$\frac{\Delta E^{\gamma}_{\perp}}{\Delta E^{\mathrm{PM}}_{\perp}} = \frac{\chi(0)\left[1+(\omega_T z)^2(3+2\chi(0))\right]}{(\omega_T z)^2(2+\chi(0))^2} - \frac{2(\gamma z)^2\chi(0)}{[2+\chi(0)]^3(\omega_T z)^4}\,, \tag{4.97a}$$

$$\frac{\Delta E^{\gamma}_{\parallel}}{\Delta E^{\mathrm{PM}}_{\parallel}} = -\frac{\chi(0)\left[1+(\omega_T z)^2(1+\chi(0))\right]}{[2+\chi(0)]^2(\omega_T z)^2} + \frac{2(\gamma z)^2\chi(0)}{[2+\chi(0)]^3(\omega_T z)^4}\,. \tag{4.97b}$$

From these it is easy to show that if $\gamma z > \omega_T z\sqrt{1+3(\omega_T z)^2} = (\gamma z)_{\mathrm{crit}}$ the shift may change sign and become much larger, as shown by the dashed curve in figure 4.11. This seems to suggest that damping introduces a new peak of the type discussed in section 4.2.4, although of the opposite sign. However, the model underlying the damped dielectric function (4.84) is only sensible if γ is small relative to ω_T. This is because ω_T represents the frequency of an absorption line of the material, while γ represents its linewidth. This only makes physical sense if $\gamma \ll \omega_T$, which in practice places us in the region $(\gamma z) \ll (\gamma z)_{\mathrm{crit}}$, as indicated in fig. 4.11. Thus damping has no dramatic effect, but only serves to slightly reduce the height of the peak shown in figure 4.7.

4.3 Cyclotron Shifts

Our results are intimately related to the shift in the cyclotron frequency of an electron near a surface. As shown in Appendix C, if the external magnetic field is directed perpendicular to the surface the calculations coincide, so that a measurement of the cyclotron frequency

is in effect a measurement of the mass shift of an electron moving parallel to the surface. We can use our formula (4.97b) to provide rough estimates of the magnitude of the effect. In S.I. units, the shift (4.97b) is

$$\Delta E_{\parallel}^{\gamma} = \frac{e^2}{32m^2\epsilon_0 c^2\pi z}\left[\frac{\chi(0)\left[1+(\omega_T z/c)^2(1+\chi(0))\right]}{[2+\chi(0)]^2(\omega_T z/c)^2} - \frac{2(\gamma z/c)^2\chi(0)}{[2+\chi(0)]^3(\omega_T z/c)^4}\right]\langle p_{\parallel}^2\rangle, \quad (4.98)$$

where the shift in the mass is given by

$$\frac{\Delta m_{\parallel}}{m} = -\frac{2m\Delta E^{\gamma}}{\langle p_{\parallel}^2\rangle + 2m\Delta E^{\gamma}} = -\frac{2m\Delta E^{\gamma}}{\langle p_{\parallel}^2\rangle} + \mathcal{O}(\Delta E^{\gamma})^2 \, . \quad (4.99)$$

Taking gold as an example, we have for the parameters [55, 56]

$$\omega_p \approx 1.3\times 10^{16}\ \text{Hz} \qquad \omega_T \approx 4\times 10^{15}\ \text{Hz} \qquad \gamma \approx 1.3\times 10^{14}\ \text{Hz} \quad (4.100)$$

which corresponds to $\chi(0) = \omega_p^2/\omega_T^2 \approx 10.5$. For distances of around of a micron, this gives $\omega_T z/c \approx 13$ and $\gamma z/c \approx 0.4$. Inserting all these values into (4.98) gives for (4.99)

$$\left|\frac{\Delta m_{\parallel}}{m}\right| \approx 2m\Delta E_{\parallel}^{\gamma}/\langle p_{\parallel}^2\rangle \approx 5\times 10^{-10} \, , \quad (4.101)$$

so that the mass and the shifted mass differ from each other by approximately one part in ten billion. Later on we will see that this shift is actually more relevant to measurements of the magnetic moment than the magnetic moment shift itself because of the specific techniques used in contemporary $g-2$ experiments, so we postpone discussion of the experimental relevance of this shift until then. We also note that for these parameters the peak height discussed in the previous section becomes

$$(\gamma z/c)_{\text{crit}} = (\omega_T z/c)\sqrt{1+3(\omega_T z/c)^2} \approx 293 \, . \quad (4.102)$$

In order for there to be a peak like that shown in fig. 4.11, we need $\gamma z/c \gg (\gamma z/c)_{\text{crit}}$, so it is evident that for gold this condition is nowhere near being satisfied.

Finally we note from Appendix C that for magnetic fields directed parallel to the surface, the additional electrostatic interaction skews the orbit, and much more so than the mass anisotropy [39]. Thus, a measurement of the cyclotron frequency in a parallel field does not deliver the mass shift.

4.4 Summary and conclusions

We have calculated the mass shift of an electron near various different kinds of surface. It is cumbersome to quote all the final results here again, so the reader is directed to their location via table 4.1. We have explicitly shown that the perfect reflector, non-dispersive and plasma results can be obtained from precisely the same formulae (4.96) consisting of a contour integral in the complex ω plane. We have provided strong justification of the validity of our formula for a dispersive dielectric, and then extended this to damped surfaces. We will provide further justification for this generalization in Chapter 7, where we shall reproduce all the above results using a different method that is suited from the outset to include both dispersion and absorption.

Model	**Result**
Perfect reflector	(4.46)
Non-dispersive dielectric	(4.47)
Plasma surface	(4.68)
Dispersive dielectric	(4.88)
Damped dispersive dielectric	(4.97)

Table 4.1: Locations of mass shift results.

We have shown that is it crucial that one decides whether the material that induces the mass shift should be modeled as a metal or a dielectric, since the results for the two classes of material are not obtainable as limiting cases of one another in the final results. We have also demonstrated that measurement of the surface-dependent mass of an electron coincides with a measurement of its cyclotron frequency for a magnetic field directed perpendicular to the interface, and undertaken an initial investigation into the experimental relevance of such an effect.

Chapter 5

Magnetic moment

Chapter 4 provided an introduction to the calculational methods needed to find radiative corrections near surfaces. However, while the mass shift is important in its own right, a much more obviously physically relevant calculation is that for the magnetic moment of the electron[1], or indeed the muon. Measurements of the electron's magnetic moment represent one of the most accurate precision tests of QED, while the muon's larger mass means that measurement of its magnetic moment is a potential low-energy route to new physics [57]. The magnetic moment's importance across physics means that any systematic effects in experiments which aim to measure it must be carefully enumerated. In this chapter we will calculate one of these, namely the surface-dependence of the magnetic moment of a spin $1/2$ particle.

5.1 Introduction

5.1.1 Interaction of the photon field with a spin $1/2$ particle

We are interested in the interaction of the quantized photon field with an electron, or other spin $1/2$ particles. In order to include spin, we must begin from the Dirac equation

$$(i\gamma^\mu \partial_\mu - m)\,\psi(x) = 0\ , \tag{5.1}$$

where γ^μ are matrices satisfying $\{\gamma^\mu, \gamma^\nu\} = 2\eta^{\mu\nu}\mathbb{I}_4$ where $\eta^{\mu\nu}$ is the metric tensor and $\mathbb{I}_4$ is a four-dimensional unit matrix. This equation describes an isolated electron, however we will need to couple it to the photon field. This is done via the minimal coupling prescription

$$\partial_\mu \to \partial_\mu + ieA_\mu(x)\ , \tag{5.2}$$

[1] The calculation presented in this chapter is a combination of the short account already published in [58] and an extended paper [59] currently in review.

which describes all electromagnetic interactions. This gives us the Dirac equation coupled to a field $A_\mu(x)$

$$[-i\gamma^\mu(\partial_\mu + ieA_\mu) + m]\,\psi = 0\,. \tag{5.3}$$

5.1.2 The Dirac magnetic moment

The existence of a magnetic moment for the electron can be inferred by taking a non-relativistic expansion of the Dirac equation for an electron coupled to a field $A_\mu = (\Phi, -\mathbf{A})$. We begin by writing (5.1.2) in its non-covariant form via $\gamma^0 = \beta$, $\gamma^i = \beta\alpha_i$

$$i\frac{\partial}{\partial t}\psi = [\boldsymbol{\alpha}\cdot(\mathbf{p} - e\mathbf{A})] + e\Phi + \beta m]\psi, \tag{5.4}$$

where α_i and β may be represented as

$$\alpha_i = \begin{pmatrix} 0 & \sigma_i \\ \sigma_i & 0 \end{pmatrix}, \qquad \beta = \begin{pmatrix} \mathbb{1}_2 & 0 \\ 0 & -\mathbb{1}_2 \end{pmatrix}, \tag{5.5}$$

where σ_i are the Pauli matrices. Splitting the 4-spinor ψ into two 2-spinors ϕ and χ and solving the resulting pair of coupled differential equations yields in the non-relativistic approximation

$$\chi \approx \frac{\boldsymbol{\sigma}\cdot(\mathbf{p} - e\mathbf{A})}{2m}\phi, \tag{5.6}$$

where, since the non-relativistic approximation entails m being much larger than any other energy, χ and ϕ are known as the 'small' and 'large' components respectively. This implies the following non-relativistic approximation of the Dirac equation:

$$i\frac{\partial}{\partial t}\phi = \left(\frac{[\boldsymbol{\sigma}\cdot(\mathbf{p} - e\mathbf{A})]^2}{2m} + e\Phi\right)\phi\,. \tag{5.7}$$

Multiplying out the factor $[\boldsymbol{\sigma}\cdot(\mathbf{p} - e\mathbf{A})]^2$ (noting that $\mathbf{p}$ does not commute with $\mathbf{A}$) gives the Pauli equation

$$i\frac{\partial}{\partial t}\phi = \left(\frac{(\mathbf{p} - e\mathbf{A})^2}{2m} - \frac{e}{2m}\boldsymbol{\sigma}\cdot\mathbf{B} + e\Phi\right)\phi, \tag{5.8}$$

where $\mathbf{B} = \nabla \times \mathbf{A}$ is the magnetic field. Through the definition of the magnetic moment $\Delta E = -\boldsymbol{\mu}\cdot\mathbf{B}$, we have in the non-relativistic approximation:

$$\boldsymbol{\mu} = \frac{e}{2m}\boldsymbol{\sigma} = \frac{g}{2}\frac{e}{2m}\boldsymbol{\sigma}\,, \tag{5.9}$$

where g is exactly 2. However, it is well-known that the value of the g-factor is shifted slightly away from 2 by the interaction of the electron with the quantized electromagnetic field. The leading correction to g was calculated by Schwinger in 1948 [60, 61] and found

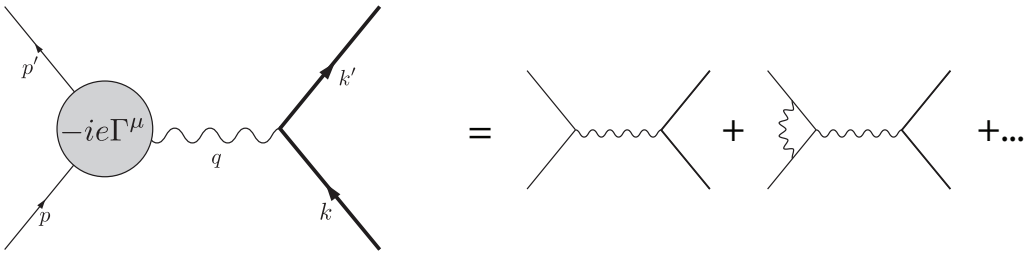

Figure 5.1: Electron scattering from a heavy particle

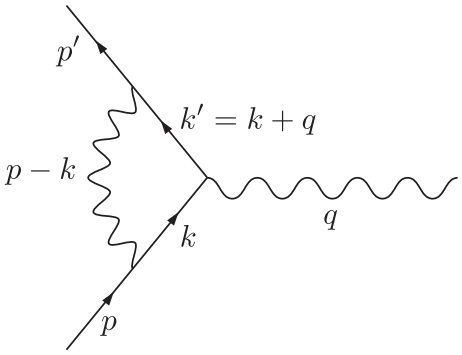

Figure 5.2: Electron-photon one-loop vertex

to be equal to $\frac{\alpha}{2\pi}$. The usual formalism for calculating these corrections does not lend itself to surface-induced effects. To see why, we briefly outline the (relatively) straightforward free-space calculation of the leading order correction $\frac{\alpha}{2\pi}$.

5.1.3 The anomalous magnetic moment

Following the general approach of [45], we consider electron scattering from a very heavy particle, as shown in fig. 5.1. where the grey circle represents the sum of all electron-photon vertices. The form of the vertex function Γ^μ can be deduced from general considerations, namely Lorentz invariance and the Ward identity [62]. This allows one to write:

$$\Gamma^\mu(p', p) = \gamma^\mu F_1(q^2) + \frac{i\sigma^{\mu\nu}q_\nu}{2m} F_2(q^2) \,, \tag{5.10}$$

where $\sigma^{\mu\nu} = \frac{i}{2}[\gamma^\mu, \gamma^\mu]$ and F_1 and F_2 are known as the form factors. Viewing the process as scattering from an applied classical field it can be shown that the g factor is given by

$$g = 2 + 2F_2(0), \tag{5.11}$$

Then, direct consideration of the one-loop diagram (fig. 5.2) using the Feynman rules of quantum electrodynamics (see, for example, [45]) allows one to derive

$$F_2(q^2 = 0) = \frac{\alpha}{2\pi}. \tag{5.12}$$

as required.

5.1.4 Surface dependence

The obvious way to extend this method to calculate a surface-dependent correction is to simply replace the free-space photon propagator entering into the Feynman rules with the boundary-dependent photon propagator (see, for example, [63]). However, this approach runs into significant technical and conceptual difficulties. The principle difficulty is the loss of translation invariance, which, amongst other effects, destroys the simple structure of the vertex in terms of form factors. Further to this, mass and charge renormalization are usually taken into account by using renormalized parameters. However, as we saw in Chapter 4, the mass is subject to additional renormalization in the presence of a surface. Charge renormalization is usually effected by summing an infinite series of vacuum polarization diagrams, but at two-loop and higher these contain internal photon lines, meaning that charge is also subject to additional renormalization in the presence of a surface.

These problems were a source of great confusion in the literature, causing early calculations to go wrong in a wide variety of ways. Early attempts all produced a distance dependence of $1/z$, either by trying to directly consider the vertex diagram as one does in free space [64, 65], or by calculating the shift in energy of the lowest Landau level [49, 66][2]. These calculations were later shown to be incorrect [39, 67]. Vertex calculations yielded answers which were later found to be gauge dependent [68, 69, 70], and Landau level calculations fell foul of an elementary mistake whereby a term was wrongly identified as being linear in the applied magnetic field [39]. These errors were largely cleared up by [71], who showed that the distance dependence should be $1/z^2$.

The state-of-the-art calculation for a surface-dependent magnetic moment at time of writing was Barton and Fawcett's 1988 paper [39], where the authors calculate a variety of surface dependent quantities for an electron near a perfect reflector, as well as repeating the calculations for parallel mirrors. Their results are shown in fig. 5.3, where the 'spin-precession shift' has been highlighted since this corresponds to the magnetic moment we wish to calculate. The inverse quadratic distance dependence predicted in [71] does indeed appear. It is worth noting that Barton and Fawcett's results are categorized into 'retarded' and 'non-retarded' regimes, corresponding to, essentially, the relative sizes of the distance z and an applied magnetic field B_0. Loosely speaking, the retarded regime is when a photon takes long enough to make a round electron-mirror trip that the electron's state may have changed by the time it is reabsorbed, with non-retarded corresponding the photon

[2] Additionally, the Landau level calculation found in [66] assumes a distance dependence of $1/z$ from the outset, so was always doomed to fail

Table 1
Summary of the main results for a single mirror, which appear in the equations indicated. Natural units: $\hbar = 1 = c$, $e^2 \approx 1/137$; $\beta_0 \equiv |e|B_0/m$. The subscripts $\perp$ ($\parallel$) indicate $\boldsymbol{B}_0$ normal (parallel) to the mirror. In eqs. (8.14, 8.15), $\mathscr{E}1$ ($\mathscr{M}1$) identify the frequency shifts of allowed electric-dipole (magnetic-dipole) transitions between Landau states. Magnetic-moment shifts strictly speaking can be defined only in the nonretarded regime, where $\delta\mu/\mu = \delta\omega_s/\beta_0$

	Nonretarded regime $\beta_0 z \ll 1$		Retarded regime $\beta_0 z \gg 1$	
Cyclotron frequency shifts	$\delta\omega_{c\perp}/\beta_0 = \frac{1}{4}\frac{e^2}{mz}$	(6.15)	$\delta\omega^*_{c\perp}/\beta_0 = 2\delta\omega^*_{c\parallel}/\beta_0$	
	$\delta\omega_{c\parallel}/\beta_0 = -\frac{1}{4}\frac{e^2}{mz}\frac{1}{(\beta_0 z)^2}$	(6.18)	$= \frac{1}{2}\frac{e^2}{mz}\cos(2\beta_0 z)$	(6.23, 6.26)
Spin-precession frequency shifts (Dirac electron)	$\delta\omega_{s\perp}/\beta_0 = -\delta\omega_{s\parallel}/\beta_0$ $= \frac{1}{4\pi}\frac{e^2}{mz}\frac{1}{mz}$	(7.12)	$\delta\omega^*_{s\perp}(\mathscr{E}1)/\beta_0 = 2\delta\omega^*_{s\parallel}(\mathscr{E}1)/\beta_0$ $= (2s_3)\frac{1}{4}\frac{e^2}{mz}\frac{\beta_0}{m}\cos(2\beta_0 z)$	(8.14)
			$\delta\omega^*_{s\perp}(\mathscr{M}1)/\beta_0 = 2\delta\omega^*_{s\perp}(\mathscr{M}1)/\beta_0$ $= (2\nu - 1)\frac{1}{4}\frac{e^2}{mz}\frac{\beta_0}{m}\cos(2\beta_0 z)$	(8.15)

Figure 5.3: Direct reproduction of the summary of results of [39], with the magnetic moment shift highlighted.

returning so quickly that the electron's state has not changed. Since, as noted above the table, magnetic moment shifts are only properly defined in the latter, it is assumed from here onwards that our system is in the non-retarded regime, which manifests itself in the calculation as the restriction to the weak-field limit.

Our calculation will differ from [39] in many respects, not least of which is the avoidance of the approach that the authors term the 'Paris Method'. This consists of a unitary transformation which gives an effective Hamiltonian suitable for the calculation of the effects of high-frequency modes upon the electron. As we saw in section 4.2, low frequency (evanescent) modes turn out to be important to these kinds of shifts when the surface is imperfectly reflecting, so this approach is not suitable for our purposes.

For this reason we take a more generally applicable approach. In section 5.1.2 we calculated the leading-order term in the magnetic moment of the electron by finding a non-relativistic approximation of the Dirac equation that decoupled the 'small' and 'large' components χ and ϕ. An obvious approach to finding the same shift for a surface-dependent electromagnetic field $\mathbf{A}$ is to simply substitute the modified $\mathbf{A}$ into eq. (5.3), take a non-relativistic approximation and extract the coefficient of $\boldsymbol{\sigma} \cdot \mathbf{B}_0$. However, the leading-order distance-dependent effects only appear in terms of higher order in e/m than that obtained in section 5.1.2, meaning that it is necessary to include some higher order terms to investigate the distance dependence of the magnetic moment. If one takes the same approach as in section 5.1.2 but to a higher order, the calculation runs into a variety of problems, including the fact that the quantity that would be identified as the Hamiltonian

turns out to be non-Hermitian [72].

A superior way to proceed is via the unitary Foldy-Wouthuysen (FW) transformation [72] which, via repeated application, can systematically produce the non-relativistic expansion of the Dirac equation to any desired order in e/m. Our calculations will eventually require terms up to e^3/m^3, meaning that the FW transformation needs to be applied twice, which makes the calculation somewhat lengthy and prone to errors (see Appendix D). Additionally, since the only previous comparable literature [39] takes the FW-transformed Hamiltonian and then applies *another* unitary transformation to move into the regime specified by the 'Paris Method', using the FW Hamiltonian does not even provide a useful point of contact with previous work. Consequently, in this chapter we completely dispense with applying any kind of unitary transformation, and simply work directly with the Dirac equation by using the Dirac eigenstates of an electron in a constant magnetic field, which can be obtained from the corresponding Schrödinger eigenstates as detailed in the next section. However, we do not completely eschew the FW transformation – in Chapter 6 we consider a confined electron where we will use the FW transformation since the Dirac eigenstates for the situation we consider there are not known.

Once the Schrödinger eigenstates are known, we can find an energy shift using standard second-order perturbation theory by treating the quantized field as a perturbation. This will enable us to extract the terms that cause the energy difference between the two spin states to change – these give us the spin magnetic moment. Then, subtracting the free-space value of the magnetic moment we will find the shift that is solely due to the presence of the surface.

5.2 Schrödinger and Dirac equations for a particle in a constant magnetic field

In order to derive the eigenstates of the Dirac equation for a particle in a constant classical magnetic field $\mathbf{B}_0$ one first solves the corresponding Schrödinger problem and then uses its solutions to generate the Dirac eigenstates [73]. The Schrödinger Hamiltonian for a particle of charge $e = -|e|$ coupled to a classical vector potential $\mathbf{A}_0$ is

$$H_S = \frac{(\mathbf{p} - e\mathbf{A}_0)^2}{2m} \,. \tag{5.13}$$

In Coulomb gauge a constant magnetic field $\mathbf{B}_0$ can be generated by a vector potential

$$\mathbf{A}_0 = -\frac{1}{2}(\mathbf{r} \times \mathbf{B}_0) \qquad A_{0i} = -\frac{1}{2}\epsilon_{ijk} r_j B_{0k}, \tag{5.14}$$

which may easily be checked by showing that the conditions $\nabla \cdot \mathbf{A}_0 = 0$ and $\nabla \times \mathbf{A}_0 = \mathbf{B}_0$ are satisfied. We choose to set the magnetic field along the $\hat{z}$ direction so that $\mathbf{B}_0 = B_0 \hat{z}$, which means we can set $B_{0x} = 0 = B_{0y}$, giving

$$A_{0i} = -\frac{1}{2}\epsilon_{ijz} r_j B_{0z} \qquad \mathbf{A} = \frac{B_0}{2}(-y\hat{x} + x\hat{y}) \,. \tag{5.15}$$

Thus the Hamiltonian may be written as:

$$H_S = \frac{(p_x + \frac{eB_0}{2} y)^2}{2m} + \frac{(p_y - \frac{eB_0}{2} x)^2}{2m} + \frac{p_z^2}{2m} \,. \tag{5.16}$$

One can reduce this to a harmonic oscillator by introducing annihilation and creation operators and rewriting the positions and momenta in terms of those. Following [74], we write

$$\begin{aligned} x &= \frac{1}{\beta_0\sqrt{2}}(\hat{b}_x + \hat{b}_x^\dagger), & p_x &= \frac{i\beta_0}{\sqrt{2}}(\hat{b}_x^\dagger - \hat{b}_x), \\ y &= \frac{1}{\beta_0\sqrt{2}}(\hat{b}_y + \hat{b}_y^\dagger), & p_y &= \frac{i\beta_0}{\sqrt{2}}(\hat{b}_y^\dagger - \hat{b}_y), \end{aligned} \tag{5.17}$$

where $\beta_0 = \sqrt{-eB_0/2}$. The operators $\hat{b}_x, \hat{b}_x^\dagger, \hat{b}_y$ and $\hat{b}_y^\dagger$ are then combined to form creation and annihilation operators for right and left-circular quanta

$$\begin{aligned} \hat{b}_R &= \frac{1}{\sqrt{2}}(\hat{b}_x - i\hat{b}_y) \,, \quad \hat{b}_R^\dagger = \frac{1}{\sqrt{2}}(\hat{b}_x^\dagger + i\hat{b}_y^\dagger) \,, \\ \hat{b}_L &= \frac{1}{\sqrt{2}}(\hat{b}_x + i\hat{b}_y) \,, \quad \hat{b}_L^\dagger = \frac{1}{\sqrt{2}}(\hat{b}_x^\dagger - i\hat{b}_y^\dagger) \,. \end{aligned} \tag{5.18}$$

In terms of these the canonical momenta are then given by

$$\hat{\pi}_x = \hat{p}_x + \frac{eB_0}{2}\hat{y} = i\beta_0(\hat{b}_R^\dagger - \hat{b}_R), \tag{5.19a}$$

$$\hat{\pi}_y = \hat{p}_y - \frac{eB_0}{2}\hat{x} = \beta_0(\hat{b}_R^\dagger + \hat{b}_R), \tag{5.19b}$$

$$\hat{\pi}_z = \hat{p}_z, \tag{5.19c}$$

so that the Hamiltonian reads

$$H_S = -\frac{eB_0}{m}\left(\hat{b}_R^\dagger \hat{b}_R + \frac{1}{2}\right) + \frac{p_z^2}{2m} \,. \tag{5.20}$$

Thus the Hamiltonian is equivalent to a harmonic oscillator of right-circular excitations and possesses infinite degeneracy with respect to the left-circular quanta. Eigenstates $|\nu\rangle$ of the Schrödinger Hamiltonian H_S can therefore be generated by repeated application of the creation operator $\hat{b}_R^\dagger$ to the ground state $|\nu = 0\rangle$ which is defined by $\hat{b}_R|\nu = 0\rangle = 0$. The states $|\nu\rangle$ are known as the Landau states.

We can now use the Schrödinger eigenstates to derive the corresponding Dirac eigenstates. Following [73], we start by noting that eigenfunctions of the Dirac equation

$$(\boldsymbol{\alpha}\cdot\boldsymbol{\pi} + \beta m)\psi \equiv H_0\psi = E_\nu\psi, \tag{5.21}$$

may be obtained from solutions of

$$(H_0^2 - E_\nu^2)X = (H_0 - E_\nu)(H_0 + E_\nu)X = 0 \,. \tag{5.22}$$

If a state X satisfies the above equation, then

$$\psi = (H_0 + E_\nu)X, \tag{5.23}$$

is a solution of eq. (5.21). To find the eigenvalues E_ν^2 of H_0^2 we calculate H_0^2. Using $(\boldsymbol{\alpha}\cdot\boldsymbol{\pi})^2 = \boldsymbol{\pi}^2 - e\sigma_z B_0$ and $\{\alpha_i, \beta\} = 0$ one finds

$$H_0^2 = \boldsymbol{\pi}^2 - e\sigma_z B_0 + m^2 \,. \tag{5.24}$$

This means we can express H_0^2 in terms of the Schrödinger Hamiltonian H_S as

$$H_0^2 = 2mH_S - e\sigma_z B_0 + m^2 \,. \tag{5.25}$$

The eigenvalues E_ν^2 of H_0^2 are found from eq. (5.20), and from the eigenvalues s of the spin operator $S_z = \sigma_z/2$,

$$E_\nu^2 = m^2 + p_z^2 - 2eB_0\left(\nu + s + \frac{1}{2}\right) \,. \tag{5.26}$$

We now choose the states X in such a way that they distinguish spin-up and spin-down states, and particle and anti-particle states, i.e. we choose them to be eigenfunctions of σ_z with eigenvalues $s = \pm 1/2$, and of β with eigenvalues 1 for a particle and -1 for an antiparticle. Equation (5.25) implies that the Dirac eigenstates can be expressed in terms of a product state of the non-relativistic eigenstates $|\nu\rangle$ and the spin state $|s\rangle$, which we choose to write as $|\nu, s\rangle \equiv |\nu\rangle \otimes |s\rangle$,

$$|\Psi_e\rangle = \frac{H_0 + E_\nu}{\sqrt{2E_\nu(E_\nu + m)}}\,|\nu\rangle\,\chi^{(\uparrow,\downarrow)} \quad \text{for } s = \pm 1/2, \tag{5.27}$$

where $\chi^{(\uparrow)\dagger} = (1,0,0,0)$, $\chi^{(\downarrow)\dagger} = (0,1,0,0)$. For antiparticle eigenstates the negative root of (5.26) applies, the normalization factor in the denominator of eq. (5.27) turns into $\sqrt{-2E_\nu(-E_\nu + m)}$, and we use $\chi^{(\uparrow)\dagger} = (0,0,1,0)$, $\chi^{(\downarrow)\dagger} = (0,0,0,1)$.

For calculations it is useful to express momentum components in terms of

$$\pi_+ = \pi_x + i\pi_y = 2i\beta_0 \hat{b}_R^\dagger \,, \tag{5.28a}$$

$$\pi_- = \pi_x - i\pi_y = -2i\beta_0 \hat{b}_R \,. \tag{5.28b}$$

Thus, for a general vector $\mathbf{Q}$ we have

$$\mathbf{Q}\cdot\boldsymbol{\pi} = i\beta_0 Q^{(-)}\hat{b}_R^\dagger - i\beta_0 Q^{(+)}\hat{b}_R + Q_z p_z \,, \tag{5.29}$$

with

$$Q^{(+)} = Q_x + iQ_y, \tag{5.30a}$$

$$Q^{(-)} = Q_x - iQ_y \,. \tag{5.30b}$$

5.3 Shift in terms of mode functions

5.3.1 Setup

The Dirac Hamiltonian for an electron coupled to a classical field $\mathbf{A}_0$ is

$$H_0 = \boldsymbol{\alpha} \cdot (\mathbf{p} - e\mathbf{A}_0) + \beta m + e\Phi, \tag{5.31}$$

and the Hamiltonian for the interaction with the quantized field $\mathbf{A}_Q$ is

$$H_{\text{int}} = -e\boldsymbol{\alpha} \cdot \mathbf{A}_Q \ , \tag{5.32}$$

with $\mathbf{A}_Q$ given by eq. (2.39). The scalar potential $e\Phi$ shifts all states uniformly, meaning it has no impact on the magnetic moment. So we do second order perturbation theory on H_{int} only

$$\Delta E_{\text{int}} = e^2 \sum_{j'_k,\nu',s'} \sum_{\lambda} \int d^3\mathbf{k} \frac{|\langle 1_{k\lambda}, \Psi'_e| \, \alpha \cdot \mathbf{A}_Q \, |0, \Psi_e\rangle|^2}{E - E' - \omega} \ . \tag{5.33}$$

Since the spin magnetic moment is obtained from the coefficient of terms linear in $\sigma_z B_0$, one must carefully account for all the possible effects which may generate additional B_0 dependence. Bearing this in mind, we find that in some terms we have to go beyond the dipole approximation for the field $\mathbf{A}_Q$

$$\mathbf{A}_Q(\mathbf{r}) = \mathbf{A}_Q(\mathbf{r_0}) + [(\mathbf{r} - \mathbf{r}_0) \cdot \nabla]\mathbf{A}_Q(\mathbf{r_0}) + \frac{1}{2}(\mathbf{r} - \mathbf{r}_0)_i(\mathbf{r} - \mathbf{r}_0)_j \frac{\partial^2 \mathbf{A}_Q(\mathbf{r_0})}{\partial r_i \partial r_j} + ... \tag{5.34}$$

since the position operator $(\mathbf{r} - \mathbf{r}_0)$ generates additional factors of B_0, as shown in appendix B eqs (B.5). Each term in the multipole expansion of $\mathbf{A}_Q(\mathbf{r})$ is given by

$$\sum_{\alpha=0}^{\rho} \frac{1}{\alpha!} \left[(\mathbf{r} - \mathbf{r}_0)^i (\mathbf{r} - \mathbf{r}_0)^j ... (\mathbf{r} - \mathbf{r}_0)^\alpha\right] \frac{\partial^\alpha \mathbf{A}_Q(\mathbf{r_0})}{\partial r_i \partial r_j ... \partial r_\alpha} \equiv D^\rho \mathbf{A}_Q(\mathbf{r}) \ , \tag{5.35}$$

then the sum over ρ gives the full multipole expansion. Henceforth we absorb the operator D^ρ into the mode functions $\mathbf{f}_{\mathbf{k}\lambda}$, taking

$$D^\rho \mathbf{A}_Q(\mathbf{r}, t) = \sum_{\rho=0}^{\infty} \sum_{\lambda} \int d^3\mathbf{k} \left[\mathbf{f}^\rho_{\mathbf{k}\lambda}(\mathbf{r}, \omega) \hat{a}_{\mathbf{k}\lambda} e^{-i\omega t} + \mathbf{f}^\rho_{\mathbf{k}\lambda}(\mathbf{r}, \omega) \hat{a}^\dagger_{\mathbf{k}\lambda} e^{i\omega t}\right] \ . \tag{5.36}$$

Each term in the multipole expansion contains a term $(\mathbf{r} - \mathbf{r}_0)^\rho$, so we have that

$$\langle \nu' | \, (\mathbf{r} - \mathbf{r}_0)^\rho \, | \nu \rangle \propto 1/\beta^\rho \propto B_0^{-\rho/2}. \tag{5.37}$$

Since $\rho \geq 0$, we have that it is only possible for the multipole expansion to preserve or reduce order in B_0. Rewriting ΔE_{int} in terms of mode functions rather than fields

$$\Delta E_{\text{int}} = e^2 \sum_{\nu',s'} \sum_{\lambda} \int d^3\mathbf{k} \frac{|\langle \Psi_e| \, \boldsymbol{\alpha} \cdot \mathbf{f}^\rho_{\mathbf{k}\lambda} \, |\Psi'_e\rangle \langle \Psi'_e| \, \boldsymbol{\alpha} \cdot \mathbf{f}^{\rho *}_{\mathbf{k}\lambda} \, |\Psi_e\rangle|^2}{E - E' - \omega}, \tag{5.38}$$

and substituting $|\Psi_e\rangle$ as given by eq. (5.27) into ΔE_{int} we find

$$\Delta E_{\text{int}} = e^2 \sum_{\nu' s'} \sum_{\lambda} \int d^3\mathbf{k} \frac{|\langle \nu, s| (H_0 + E_\nu)\boldsymbol{\alpha} \cdot \mathbf{f}^\rho_{\mathbf{k}\lambda} (H_0 + E_{\nu'}) |\nu', s'\rangle|^2}{(E_\nu - E_{\nu'} - \omega) 2E_\nu (E_\nu + m) 2E_{\nu'} (E_{\nu'} + m)}. \tag{5.39}$$

Using the explicit form of the matrix $\boldsymbol{\alpha}$ shown in eq. (5.5), the unperturbed Hamiltonian is

$$H_0 = \boldsymbol{\alpha} \cdot \boldsymbol{\pi} + \beta m = \begin{pmatrix} m & \boldsymbol{\alpha} \cdot \boldsymbol{\pi} \\ \boldsymbol{\alpha} \cdot \boldsymbol{\pi} & -m \end{pmatrix}. \tag{5.40}$$

which gives

$$(H + E_{\nu'})(\boldsymbol{\alpha} \cdot \mathbf{f}^\rho_{\mathbf{k}\lambda})(H + E_\nu) = \begin{pmatrix} H_{ee} & H_{e\bar{e}} \\ H_{e\bar{e}} & H_{\bar{e}\bar{e}} \end{pmatrix}, \tag{5.41}$$

where

$$H_{ee} = (E_{\nu'} + m)(\boldsymbol{\sigma} \cdot \mathbf{f}^\rho_{\mathbf{k}\lambda})(\boldsymbol{\sigma} \cdot \boldsymbol{\pi}) + (E_\nu + m)(\boldsymbol{\sigma} \cdot \boldsymbol{\pi})(\boldsymbol{\sigma} \cdot \mathbf{f}^\rho_{\mathbf{k}\lambda}), \tag{5.42a}$$

$$H_{e\bar{e}} = (\boldsymbol{\sigma} \cdot \boldsymbol{\pi})(\boldsymbol{\sigma} \cdot \mathbf{f}^\rho_{\mathbf{k}\lambda})(\boldsymbol{\sigma} \cdot \boldsymbol{\pi}) + (E_{\nu'} - m)(E_\nu + m)(\boldsymbol{\sigma} \cdot \mathbf{f}^\rho_{\mathbf{k}\lambda}), \tag{5.42b}$$

$$H_{\bar{e}\bar{e}} = (E_\nu - m)(\boldsymbol{\sigma} \cdot \boldsymbol{\pi})(\boldsymbol{\sigma} \cdot \mathbf{f}^\rho_{\mathbf{k}\lambda}) + (E_{\nu'} - m)(\boldsymbol{\sigma} \cdot \mathbf{f}^\rho_{\mathbf{k}\lambda})(\boldsymbol{\sigma} \cdot \boldsymbol{\pi}). \tag{5.42c}$$

The subscripts e and $\bar{e}$ distinguish particle or antiparticle transitions. Here, only particle-particle and particle-antiparticle transitions are required because our initial state is that of an electron, so $H_{\bar{e}\bar{e}}$ can be discarded. Finally we remind the reader that since we consider the electron to be in vacuum, the generalized Coulomb gauge $\nabla \cdot [\epsilon(\mathbf{r}, \omega)\mathbf{A}(\mathbf{r}, \omega)] = 0$ and standard Coulomb gauge $\nabla \cdot [\mathbf{A}(\mathbf{r}, \omega)] = 0$ are identical for the purposes of this part of the calculation. Consequently, we use the Coulomb gauge condition to simplify expressions found in throughout the remainder of section 5.3.

5.3.2 Particle-particle transitions

Using the fact that the Pauli matrices satisfy $\sigma_i \sigma_j = \delta_{ij} + i\epsilon_{ijk}\sigma_k$ and the Coulomb gauge condition in terms of mode functions ($\nabla \cdot \mathbf{f}_{\mathbf{k}\lambda} = 0$) we can simplify eq. (5.42a) to

$$(\boldsymbol{\sigma} \cdot \mathbf{f}^\rho_{\mathbf{k}\lambda})(\boldsymbol{\sigma} \cdot \boldsymbol{\pi}) = \mathbf{f}^\rho_{\mathbf{k}\lambda} \cdot \boldsymbol{\pi} + i\boldsymbol{\sigma} \cdot (\mathbf{f}^\rho_{\mathbf{k}\lambda} \times \boldsymbol{\pi}), \tag{5.43a}$$

$$(\boldsymbol{\sigma} \cdot \boldsymbol{\pi})(\boldsymbol{\sigma} \cdot \mathbf{f}^\rho_{\mathbf{k}\lambda}) = \mathbf{f}^\rho_{\mathbf{k}\lambda} \cdot \boldsymbol{\pi} + \boldsymbol{\sigma} \cdot (\nabla \times \mathbf{f}^\rho_{\mathbf{k}\lambda}) - i\boldsymbol{\sigma} \cdot (\mathbf{f}^\rho_{\mathbf{k}\lambda} \times \boldsymbol{\pi}). \tag{5.43b}$$

Substituting this into H_{ee} and rearranging:

$$H_{ee} = (E_\nu + E_{\nu'} + 2m)\mathbf{f}^\rho_{\mathbf{k}\lambda} \cdot \boldsymbol{\pi} + (E_{\nu'} - E_\nu) i\boldsymbol{\sigma} \cdot (\mathbf{f}^\rho_{\mathbf{k}\lambda} \times \boldsymbol{\pi}) + (E_{\nu'} + m)\boldsymbol{\sigma} \cdot (\nabla \times \mathbf{f}^\rho_{\mathbf{k}\lambda}), \tag{5.44}$$

Using eq. (5.29), this becomes

$$\begin{aligned} H_{ee} = & b_R^\dagger \Big\{ i\beta_0 (E_\nu + E_{\nu'} + 2m) f^{\rho}_{\mathbf{k}\lambda}{}^{(-)} - (E_{\nu'} - E_\nu)\beta_0 (\boldsymbol{\sigma} \times \mathbf{f}^{\rho}_{\mathbf{k}\lambda})^{(-)} \Big\} \\ & + b_R \Big\{ - i\beta_0 (E_\nu + E_{\nu'} + 2m) f^{\rho}_{\mathbf{k}\lambda}{}^{(+)} + (E_{\nu'} - E_\nu)\beta_0 (\boldsymbol{\sigma} \times \mathbf{f}^{\rho}_{\mathbf{k}\lambda})^{(+)} \Big\} \\ & + (E_\nu + E_{\nu'} + 2m) f^{\rho}_{\mathbf{k}\lambda,z} p_z + (E_{\nu'} - E_\nu)(\boldsymbol{\sigma} \times \mathbf{f}^{\rho}_{\mathbf{k}\lambda})_z + (E_{\nu'} + m)\boldsymbol{\sigma} \cdot (\nabla \times \mathbf{f}^{\rho}_{\mathbf{k}\lambda}) \, . \end{aligned} \tag{5.45}$$

The expression we need to consider in order to evaluate the contribution of H_{ee} to the energy shift is

$$\Delta E^{ee}_{\text{int}} = e^2 \sum_{\nu',s'} \sum_{\lambda} \int d^3k \frac{|\langle \nu, s| H_{ee} |\nu', s'\rangle|^2}{4(E_\nu - E_{\nu'} - \omega) E_\nu (E_\nu + m) E_{\nu'} (E_{\nu'} + m)} \, . \tag{5.46}$$

The fact that (5.45) is made up of terms which are of zeroth or first order in a creation or annihilation operators $b_R^{(\dagger)}$ suggests that one should proceed by splitting H_{ee} into three parts, one for each of $\nu' = \nu - 1, \nu$ and $\nu + 1$. But, the mode functions $\mathbf{f}^{\rho}_{\mathbf{k}\lambda}$ in H_{ee} contain the multipole operator D^ρ, which itself contains any number of operators b_R and $b_R^\dagger$. Attempting to immediately isolate terms linear in B_0 is dangerous on account of equations (5.37). The only simplification we can unambiguously make is to take a large m expansion and discard terms of order $1/m^4$ or higher. We find that on multiplying out the constants in the expression $\langle \nu, s| H_{ee} |\nu', s'\rangle \langle \nu', s;| H_{ee} |\nu, s\rangle$ and dividing by the energy denominator that any term that originates from any of the terms proportional to $(E_{\nu'} - E_\nu)$ in eq. (5.45) cannot contribute due to its order in $1/m$. All the terms in eq. (5.45) that are proportional to $(E_\nu + E_{\nu'} + 2m)$ are spin-independent, so these multiplied by each other also cannot contribute. These considerations together yield three spin-dependent terms which are of the correct order in $1/m$, meaning that we writ the energy shift as

$$\mathcal{E}^D_{ee} = \Delta E^{\text{int}}_{q-} + \Delta E^{\text{int}}_{q+} + \Delta E^{\text{int}}_{s} + \mathcal{O}(1/m^4), \tag{5.47}$$

where

$$\begin{aligned} \Delta E^{\text{int}}_{q-} = & \sum_{\nu' s'} \sum_{\lambda} \int d^3\mathbf{k} \frac{e^2}{\mathcal{E}^D_{ee}} \langle \nu, s| b_R^\dagger i\beta_0 (E_\nu + E_{\nu'} + 2m) f^{\rho}_{\mathbf{k}\lambda}{}^{(-)} |\nu', s'\rangle \\ & \times \langle \nu', s'| (E_{\nu'} + m)(\boldsymbol{\sigma} \cdot (\nabla \times \mathbf{f}^{*\rho'}_{\mathbf{k}\lambda})) |\nu, s\rangle + \text{H.c.}, \end{aligned} \tag{5.48a}$$

$$\begin{aligned} \Delta E^{\text{int}}_{q+} = & \sum_{\nu' s'} \sum_{\lambda} \int d^3\mathbf{k} \frac{e^2}{\mathcal{E}^D_{ee}} \langle \nu, s| b_R (-i\beta_0) (E_\nu + E_{\nu'} + 2m) f^{\rho}_{\mathbf{k}\lambda}{}^{(+)} |\nu', s'\rangle \\ & \times \langle \nu', s'| (E_{\nu'} + m)(\boldsymbol{\sigma} \cdot (\nabla \times \mathbf{f}^{*\rho'}_{\mathbf{k}\lambda})) |\nu, s\rangle + \text{H.c.}, \end{aligned} \tag{5.48b}$$

$$\Delta E^{\text{int}}_{s} = \sum_{\nu' s'} \sum_{\lambda} \int d^3\mathbf{k} \frac{e^2}{\mathcal{E}^D_{ee}} |\langle \nu, s| (E_{\nu'} + m)(\boldsymbol{\sigma} \cdot (\nabla \times \mathbf{f}^{\rho}_{\mathbf{k}\lambda})) |\nu', s'\rangle|^2, \tag{5.48c}$$

where we have defined

$$\mathcal{E}^D_{ee} \equiv 4(E_\nu - E_{\nu'} - \omega)E_\nu(E_\nu + m)E_{\nu'}(E_{\nu'} + m)\ . \tag{5.49}$$

The reason for the choice of labels in eqs. (5.48) will become clear later on. We have immediately set set $p_z = 0$ in eqs. (5.48), which corresponds to dropping terms proportional to $\langle p_z \rangle$ and $\langle p_z^2 \rangle$. The former is easily justified because we have $\langle p_z \rangle = 0$ due to our electron being localized a fixed distance from the interface. There is no *a priori* reason for dropping the terms in $\langle p_z^2 \rangle$, but these all turn out give spin-independent contributions. Explicit inclusion of such terms proves quite cumbersome, so we do not quote them here.

We are now ready to extract terms proportional to B_0 from eqs. (5.48). First considering the large m expansion of $\Delta E^{\text{int}}_{q-}$,

$$\begin{aligned}
\Delta E^{\text{int}}_{q-} &= ie^2 \sum_{\nu' s'} \sum_{\lambda} \int d^3\mathbf{k} \sqrt{\frac{-eB_0}{2}} \frac{(E_\nu + E_{\nu'} + 2m)(E_{\nu'} + m)}{4(E_\nu - E_{\nu'} - \omega)E_\nu(E_\nu + m)E_{\nu'}(E_{\nu'} + m)} \\
&\qquad \times \langle \nu, s |\, b_R^\dagger f_{\mathbf{k}\lambda}^{\rho\ (-)} \,|\nu', s'\rangle \,\langle \nu', s' |\, \boldsymbol{\sigma} \cdot (\nabla \times \mathbf{f}^{*\rho'}_{\mathbf{k}\lambda}) \,|\nu, s\rangle + \text{H.c.}, \\
&= -ie^2 \sum_{\nu' s'} \sum_{\lambda} \int d^3\mathbf{k} \sqrt{\frac{-eB_0}{2}} \left(\frac{1}{2m^2\omega} - \frac{eB_0}{2m^3\omega^2}(n - n' + s - s') + \mathcal{O}\left(\frac{B_0}{m^4}\right) \right) \\
&\qquad \times \langle \nu, s |\, b_R^\dagger f_{\mathbf{k}\lambda}^{\rho\ (-)} \,|\nu', s'\rangle \,\langle \nu', s' |\, \boldsymbol{\sigma} \cdot (\nabla \times \mathbf{f}^{*\rho'}_{\mathbf{k}\lambda}) \,|\nu, s\rangle + \text{H.c.}\ .
\end{aligned} \tag{5.50}$$

Since the multipole operator either preserves or reduces order in B_0, it can never cause the first term of (5.50) to become linear in B_0, so this term is discarded. Equation (5.37) tells us that the second term can become linear in B_0 if the $\rho = 1$ ('quadrupole') term in the multipole operator is present in *one* of the multipole-expanded mode functions entering into the matrix element, so we have a contribution for either $\{\rho = 1, \rho' = 0\}$ or $\{\rho = 0, \rho = 1\}$. For $\rho + \rho' \geq 2$, eq. (5.37) tells us that contribution of the multipole operator is to reduce order in B_0 by at least a factor of B_0, so the first and second terms of (5.50) do not contribute, and no other terms contribute because they are order $1/m^4$ or higher. First considering the case $\rho = 1$, $\rho' = 0$, we have for the second term in $\Delta E^{\text{int}}_{q-} \equiv \Delta E^{\text{int}}_{q-}(\rho, \rho')$

$$\begin{aligned}
\Delta E^{\text{int}}_{q-}(1,0) =& ie^2 \sum_{\nu' s'} \sum_{\lambda} \int d^3\mathbf{k} \sqrt{\frac{-eB_0}{2}} \frac{eB_0}{2m^3\omega^2}(\nu - \nu' + s - s') \\
&\times \langle \nu, s |\, b_R^\dagger(\mathbf{r} - \mathbf{r}_0) \cdot \nabla f_{\mathbf{k}\lambda}^{\ (-)} \,|\nu', s'\rangle \,\langle \nu', s' |\, \boldsymbol{\sigma} \cdot (\nabla \times \mathbf{f}^*_{\mathbf{k}\lambda}) \,|\nu, s\rangle + \text{H.c.}
\end{aligned} \tag{5.51}$$

The matrix elements found in Appendix B.1 tell us that $\langle \nu, s |\, b_R^\dagger(\mathbf{r} - \mathbf{r}_0) \cdot \nabla f_{\mathbf{k}\lambda}^{\ (-)} \,|\nu', s'\rangle$ is only non-zero when $\nu = \nu'$ and $s = s'$. However, whole term is proportional to $\nu - \nu' + s - s'$ so integral (5.51) does not contribute to the magnetic moment.

Now considering $\rho = 0$, $\rho' = 1$, we have

$$\Delta E^{\text{int}}_{q-}(0,1) = ie^2 \sum_{\nu' s'} \sum_{\lambda} \int d^3\mathbf{k} \sqrt{\frac{-eB_0}{2}} \frac{eB_0}{2m^3\omega^2} (\nu - \nu' + s - s') \langle \nu, s | \, a_R^\dagger f_{\mathbf{k}\lambda}{}^{(-)} \, | \nu', s' \rangle \\ \times \langle \nu', s' | \, (\mathbf{r} - \mathbf{r}_0) \cdot \nabla (\boldsymbol{\sigma} \cdot (\nabla \times \mathbf{f}^*_{\mathbf{k}\lambda})) \, | \nu, s \rangle + \text{H.c.}$$

The matrix element is only non-zero when $\nu' = \nu - 1$ and $s = s'$. The prefactor $(\nu - \nu' + s - s')$ is $\neq 0$ at these values, so on substitution of the explicit matrix elements (B.5) we have a contribution

$$\Delta E^{\text{int}}_{\mu,q-}(0,1) = ie^2 \sum_{\lambda} \int d^3\mathbf{k} \frac{eB_0}{4m^3\omega^2} \nu f_{\mathbf{k}\lambda}{}^{(-)} \left(\frac{\partial}{\partial x} + i \frac{\partial}{\partial y} \right) (\boldsymbol{\sigma} \cdot (\nabla \times \mathbf{f}^*_{\mathbf{k}\lambda})) + \text{H.c.} \,, \quad (5.52)$$

where the subscript μ reflects the fact that this is an energy shift from which the magnetic moment can be directly extracted. Since we are only interested in terms proportional to σ_z we can let

$$\boldsymbol{\sigma} \cdot (\nabla \times \mathbf{f}^*_{\mathbf{k}\lambda}) \to \sigma_z \left(\frac{\partial}{\partial x} f^*_{\mathbf{k}\lambda, y} - \frac{\partial}{\partial y} f^*_{\mathbf{k}\lambda, x} \right) \,, \quad (5.53)$$

which means eq. (5.52) can be expressed as

$$\Delta E^{\text{int}}_{\mu,q-}(0,1) = \frac{e^3 \sigma_z B_0}{4m^3} \nu \sum_{\lambda} \int d^3\mathbf{k} \frac{1}{\omega^2} (f_y + i f_x) \\ \times \left(\frac{\partial^2}{\partial x^2} f^*_{\mathbf{k}\lambda, y} - \frac{\partial^2}{\partial x \partial y} f^*_{\mathbf{k}\lambda, x} + i \frac{\partial^2}{\partial x \partial y} f^*_{\mathbf{k}\lambda, y} - i \frac{\partial^2}{\partial y^2} f^*_{\mathbf{k}\lambda, x} \right) + \text{H.c.} \quad (5.54)$$

The simplification of $\Delta E^{\text{int}}_{q+}$ works in exactly the same way, the result is

$$\Delta E^{\text{int}}_{\mu,q+}(0,1) = -\frac{e^3 \sigma_z B_0}{4m^3} (\nu + 1) \sum_{\lambda} \int d^3\mathbf{k} \frac{1}{\omega^2} (f_y - i f_x) \\ \times \left(\frac{\partial^2}{\partial x^2} f^*_{\mathbf{k}\lambda, y} - \frac{\partial^2}{\partial x \partial y} f^*_{\mathbf{k}\lambda, x} - i \frac{\partial^2}{\partial x \partial y} f^*_{\mathbf{k}\lambda, y} + i \frac{\partial^2}{\partial y^2} f^*_{\mathbf{k}\lambda, x} \right) + \text{H.c.} \quad (5.55)$$

Further simplification can be achieved by noticing that, for plane wave mode functions, some terms are zero under $\int d^3\mathbf{k}$. The mode functions get their vector character from the polarisation vectors specified in eq. (A.1), writing these in spherical polar co-ordinates defined by $k_x = k \sin\theta \cos\varphi$, $k_y = k \sin\theta \sin\varphi$

$$\mathbf{e}_{TE} = \begin{pmatrix} \sin\varphi \\ -\cos\varphi \\ 0 \end{pmatrix}, \qquad \mathbf{e}_{TM} = \cos\theta \begin{pmatrix} \cos\varphi \\ -\sin\varphi \\ -\tan\theta \end{pmatrix}, \quad (5.56)$$

and using an integral identity for integers m and n

$$\int_0^{2\pi} d\varphi \sin^n\varphi \cos^m\varphi = 0 \quad \text{if either } n \text{ or } m \text{ are are odd}, \quad (5.57)$$

it is easy to show that the only terms surviving are those where the sum of the number of factors of $f^{(*)}_{\mathbf{k}\lambda,x}$ and $\frac{\partial}{\partial x}$ is even[3]. In light of this, the sum of $\Delta E^{\text{int}}_{\mu,q} = \Delta E^{\text{int}}_{\mu,q-}(0,1) + \Delta E^{\text{int}}_{\mu,q+}(0,1)$ can be simplified to

$$\Delta E^{\text{int}}_{\mu,q} = -\frac{e^3\sigma_z B_0}{4m^3}\sum_\lambda \int d^3\mathbf{k}\frac{1}{\omega^2}\left(f_{\mathbf{k}\lambda,y}\frac{\partial^2 f^*_{\mathbf{k}\lambda,y}}{\partial x^2} - f_{\mathbf{k}\lambda,y}\frac{\partial^2 f^*_{\mathbf{k}\lambda,x}}{\partial x\partial y} + f_{\mathbf{k}\lambda,x}\frac{\partial^2 f^*_{\mathbf{k}\lambda,x}}{\partial y^2} - f_{\mathbf{k}\lambda,x}\frac{\partial^2 f^*_{\mathbf{k}\lambda,y}}{\partial x\partial y}\right) + \text{H.c.} \tag{5.58}$$

where it is worth noting that the result is independent of the Landau level ν due to a cancellation between eqs (5.54) and (5.55).

Moving on to ΔE^{int}_s as specified in eq. (5.48c)

$$\Delta E^{\text{int}}_s = e^2\sum_{\nu' s'}\sum_\lambda \int d^3\mathbf{k}\frac{(E_{\nu'}+m)^2}{E^D_{ee}} |\langle \nu, s|\left(\boldsymbol{\sigma}\cdot(\nabla\times\mathbf{f}^\rho_{\mathbf{k}\lambda})\right)|\nu', s'\rangle|^2 , \tag{5.59}$$

and expanding for large m, we find

$$\Delta E^{\text{int}}_s = e^2\sum_{\nu' s'}\sum_\lambda \int d^3\mathbf{k}\left[-\frac{1}{4m^2\omega} + \frac{eB_0(n-n'+s-s')}{4m^3\omega^2} + \mathcal{O}\left(\frac{B_0}{m^4}\right)\right] \times |\langle \nu, s|\left(\boldsymbol{\sigma}\cdot(\nabla\times\mathbf{f}^\rho_{\mathbf{k}\lambda})\right)|\nu', s'\rangle|^2. \tag{5.60}$$

Since the multipole operator can only reduce order in B_0, the first term of (5.60) cannot be proportional to B_0. Thus, the only contribution is from the second term, and only for $\rho = 0 = \rho'$. The factor of $(\nu - \nu' + s - s')$ removes any $\nu' = \nu$, $s' = s$ contribution, and the fact that the operator $\boldsymbol{\sigma}\cdot(\nabla\times\mathbf{f}^\rho_{\mathbf{k}\lambda})$ in the dipole approximation cannot change ν removes any $\nu' \neq \nu$ terms. So the only contribution is from the second term in eq. (5.60) with $\nu = \nu'$, $s \neq s'$.

$$\Delta E^{\text{int}}_{\mu,s} = \frac{e^3 B_0}{4m^3}(s-s')\sum_{s'}\sum_\lambda \int d^3\mathbf{k}\frac{1}{\omega^2}|\langle s|\,\boldsymbol{\sigma}\cdot(\nabla\times\mathbf{f}_{\mathbf{k}\lambda})\,|s'\rangle|^2 . \tag{5.61}$$

Since we necessarily have $s \neq s'$, this part of the shift is due to spin flips (hence the label 's'), which makes physical sense as the curl of the mode function corresponds to the quantized magnetic field (not to be confused with the applied classical field B_0). Using eq. (5.29) we can rewrite the operator as:

$$\boldsymbol{\sigma}\cdot(\nabla\times\mathbf{f}_{\mathbf{k}\lambda}) = \frac{1}{2}\left[\sigma^{(-)}(\nabla\times\mathbf{f}_{\mathbf{k}\lambda})^{(+)} + \sigma^{(+)}(\nabla\times\mathbf{f}_{\mathbf{k}\lambda})^{(-)}\right] + \sigma_z f_{\mathbf{k}\lambda,z} , \tag{5.62}$$

with the spin operators having non-zero matrix elements

$$\langle s'|\,\sigma^{(+)}\,|s\rangle = 2 \quad \text{for } s = -1/2, \tag{5.63a}$$

$$\langle s'|\,\sigma^{(-)}\,|s\rangle = 2 \quad \text{for } s = +1/2. \tag{5.63b}$$

[3]This of course implies that the sum of the number of factors of f_y and $\frac{\partial}{\partial y}$ is also even since there are four such factors per term.

Substituting these into eq. (5.61) gives for $s' = 1/2$:

$$\Delta E^{\text{int}}_{\mu,s}(s' = 1/2) = -\frac{e^3 B_0}{4m^3} \sum_\lambda \int d^3\mathbf{k} \frac{1}{\omega^2} |(\nabla \times \mathbf{f}_{\mathbf{k}\lambda})^{(+)}|^2, \tag{5.64}$$

and for $s' = -1/2$:

$$\Delta E^{\text{int}}_{\mu,s}(s' = -1/2) = \frac{e^3 B_0}{4m^3} \sum_\lambda \int d^3\mathbf{k} \frac{1}{\omega^2} |(\nabla \times \mathbf{f}_{\mathbf{k}\lambda})^{(-)}|^2 \,. \tag{5.65}$$

So, defining $\Delta E^{\text{int}}_{\mu,s}(\sigma_z) = \frac{\sigma_z}{2}\left[\Delta E^{\text{int}}_{\mu,s}(s' = -1/2) - \Delta E^{\text{int}}_{\mu,s}(s' = 1/2)\right]$ we arrive at

$$\Delta E^{\text{int}}_{\mu,s}(\sigma_z) = \frac{e^3 \sigma_z B_0}{8m^3} \sum_\lambda \int d^3\mathbf{k} \frac{1}{\omega^2} \left[|(\nabla \times \mathbf{f}_{\mathbf{k}\lambda})^{(-)}|^2 + |(\nabla \times \mathbf{f}_{\mathbf{k}\lambda})^{(+)}|^2\right] \,. \tag{5.66}$$

Using the definitions (5.29), this finally reduces to[4] :

$$\Delta E^{\text{int}}_{\mu,s}(\sigma_z) = \frac{e^3 \sigma_z B_0}{8m^3} \sum_\lambda \int d^3\mathbf{k} \frac{1}{\omega^2} \left[|(\nabla \times \mathbf{f}_{\mathbf{k}\lambda})_x|^2 + |(\nabla \times \mathbf{f}_{\mathbf{k}\lambda})_y|^2\right] \,. \tag{5.67}$$

5.3.3 Particle-antiparticle transitions

We begin by restating the term for particle-antiparticle transitions as given by eq. (5.42b)

$$H_{e\bar{e}} = (\boldsymbol{\sigma} \cdot \boldsymbol{\pi})(\boldsymbol{\sigma} \cdot \mathbf{f}^\rho_{\mathbf{k}\lambda})(\boldsymbol{\sigma} \cdot \boldsymbol{\pi}) + (E_{\nu'} - m)(E_\nu + m)(\boldsymbol{\sigma} \cdot \mathbf{f}^\rho_{\mathbf{k}\lambda}) \,. \tag{5.68}$$

This expression contains a $\boldsymbol{\pi}$ operator acting upon another $\boldsymbol{\pi}$ operator, so contains considerable hidden structure stemming from the fact that the canonical momentum $\boldsymbol{\pi}$ is a function of the physical momentum $\mathbf{p}$, whose quantum-mechanical operator is a derivative. Using the properties of the Pauli matrices and a permutation tensor identity, the first term can be written component-wise as

$$(\boldsymbol{\sigma} \cdot \boldsymbol{\pi})(\boldsymbol{\sigma} \cdot \mathbf{f}^\rho)(\boldsymbol{\sigma} \cdot \boldsymbol{\pi}) = (\delta_{ij}\sigma_k + i\epsilon_{ijk} - \delta_{ik}\sigma_j + \delta_{jk}\sigma_i)\pi_i f_j \pi_k \,, \tag{5.69}$$

where the subscript $\mathbf{k}\lambda$ has been dropped from the mode function for notational convenience. Using the definition (5.19) of $\boldsymbol{\pi}$ and the commutator $[\nabla_i, f_j] = (\nabla_i f_j)$ one can derive

$$\pi_i f_j \pi_k = -i(\nabla_i f_j)\pi_k + f_j \pi_i \pi_k \,. \tag{5.70}$$

Substituting this into (5.69) and using the Coulomb gauge condition $\nabla \cdot \mathbf{f}^\rho = 0$ gives

$$\begin{aligned}(\boldsymbol{\sigma} \cdot \boldsymbol{\pi})(\boldsymbol{\sigma} \cdot \mathbf{f}^\rho)(\boldsymbol{\sigma} \cdot \boldsymbol{\pi}) =& (\mathbf{f}^\rho \cdot \boldsymbol{\pi})(\boldsymbol{\sigma} \cdot \boldsymbol{\pi}) - (\boldsymbol{\sigma} \cdot \mathbf{f})\boldsymbol{\pi}^2 + f_j(\boldsymbol{\sigma} \cdot \boldsymbol{\pi})\pi_j - i\mathbf{f}^\rho \cdot (\boldsymbol{\pi} \times \boldsymbol{\pi}) \\ &+ i(\nabla_i f_j)\sigma_j \pi_i - i\sigma_i \nabla_i f_j \pi_j + (\nabla \times \mathbf{f}^\rho) \cdot \boldsymbol{\pi} \,. \end{aligned} \tag{5.71}$$

[4] Energy shifts depend on the state being spin-up or spin-down. Here and throughout we abbreviate this dependence by writing energy shifts as proportional to the Pauli spin matrix σ_z which should be understood as a shorthand for $\langle s| \sigma_z |s\rangle$.

Some terms in (5.71) can be simplified further. Using

$$[\pi_i, \pi_j] = ie(\nabla_i A_{0j} - \nabla_j A_{0i}),$$

we can simplify the third term of eq. (5.71) to

$$f_j(\sigma_i\pi_i)\pi_j = ie\boldsymbol{\sigma}\cdot(\mathbf{f}^\rho \times \mathbf{B}_0) + (\mathbf{f}^\rho\cdot\boldsymbol{\pi})(\boldsymbol{\sigma}\cdot\boldsymbol{\pi})\ . \tag{5.72}$$

Again using the definition (5.19) of $\boldsymbol{\pi}$, the fourth term of eq. (5.71) can be simplified to:

$$(\boldsymbol{\pi}\times\boldsymbol{\pi}) = ie\mathbf{B_0}. \tag{5.73}$$

We can also combine the first two terms in the second line of (5.71)

$$(\nabla_i f_j)\sigma_j\pi_i - i\sigma_i\nabla_i f_j\pi_j = \boldsymbol{\sigma}\times(\nabla\times\mathbf{f}^\rho)\cdot\boldsymbol{\pi}. \tag{5.74}$$

Inserting the simplifications (5.72), (5.73) and (5.74) into eq. (5.71) finally gives

$$\begin{aligned}(\boldsymbol{\sigma}\cdot\boldsymbol{\pi})(\boldsymbol{\sigma}\cdot\mathbf{f}^\rho_{\mathbf{k}\lambda})(\boldsymbol{\sigma}\cdot\boldsymbol{\pi}) =& 2(\mathbf{f}^\rho\cdot\boldsymbol{\pi})(\boldsymbol{\sigma}\cdot\boldsymbol{\pi}) - (\boldsymbol{\sigma}\cdot\mathbf{f}^\rho)\boldsymbol{\pi}^2 + ie\boldsymbol{\sigma}\cdot(\mathbf{f}^\rho\times\mathbf{B}_0) + e(\mathbf{f}^\rho\cdot\mathbf{B_0})\\ &+ i[\boldsymbol{\sigma}\times(\nabla\times\mathbf{f}^\rho)\cdot\boldsymbol{\pi}] + (\nabla\times\mathbf{f}^\rho)\cdot\boldsymbol{\pi}\ .\end{aligned} \tag{5.75}$$

The terms of the form $\mathbf{Q}\cdot\boldsymbol{\pi}$ can be rewritten using eq. (5.29) and the relations $\hat{b}_R\hat{b}_R^\dagger = 1 + \hat{b}_R^\dagger\hat{b}_R$ and ${f^\rho_{\mathbf{k}\lambda}}^{(-)}\sigma^{(+)} + {f^\rho_{\mathbf{k}\lambda}}^{(+)}\sigma^{(-)} = 2(f_x\sigma_x + f_y\sigma_y)$. The first term becomes:

$$\begin{aligned}(\mathbf{f}^\rho_{\mathbf{k}\lambda}\cdot\boldsymbol{\pi})(\boldsymbol{\sigma}\cdot\boldsymbol{\pi}) =\ & -\hat{b}_R^\dagger\hat{b}_R^\dagger\beta_0^2{f^\rho_{\mathbf{k}\lambda}}^{(-)}\sigma^{(-)} - \hat{b}_R\hat{b}_R\beta_0^2{f^\rho_{\mathbf{k}\lambda}}^{(+)}\sigma^{(+)}\\ &+ 2\hat{b}_R^\dagger\hat{b}_R\beta_0^2(f_x\sigma_x + f_y\sigma_y) + \beta_0^2{f^\rho_{\mathbf{k}\lambda}}^{(+)}\sigma^{(-)} + f_{\mathbf{k}\lambda,z}\sigma_z p_z^2\\ &+ i\hat{b}_R^\dagger\beta_0 p_z(\sigma_z{f^\rho_{\mathbf{k}\lambda}}^{(-)} + f_{\mathbf{k}\lambda,z}\sigma^{(-)}) + i\hat{b}_R\beta_0 p_z(-\sigma_z{f^\rho_{\mathbf{k}\lambda}}^{(+)} - f_{\mathbf{k}\lambda,z}\sigma^{(+)}),\end{aligned} \tag{5.76}$$

and the two terms in the second line of eq. (5.75) become

$$(\nabla\times\mathbf{f}^\rho_{\mathbf{k}\lambda})\cdot\boldsymbol{\pi} = i\beta_0(\nabla\times\mathbf{f}^\rho_{\mathbf{k}\lambda})^{(-)}\hat{b}_R^\dagger - i\beta_0(\nabla\times\mathbf{f}^\rho_{\mathbf{k}\lambda})^{(+)}\hat{b}_R + (\nabla\times\mathbf{f}^\rho_{\mathbf{k}\lambda})_z p_z, \tag{5.77}$$

$$\begin{aligned}i[\boldsymbol{\sigma}\times(\nabla\times\mathbf{f}^\rho_{\mathbf{k}\lambda})]\cdot\boldsymbol{\pi} =& -\beta_0[\boldsymbol{\sigma}\times(\nabla\times\mathbf{f}^\rho_{\mathbf{k}\lambda})]^{(-)}\hat{b}_R^\dagger + \beta_0[\boldsymbol{\sigma}\times(\nabla\times\mathbf{f}^\rho_{\mathbf{k}\lambda})]^{(+)}\hat{b}_R\\ &+ i[\boldsymbol{\sigma}\times(\nabla\times\mathbf{f}^\rho_{\mathbf{k}\lambda})]_z p_z\ .\end{aligned} \tag{5.78}$$

These simplifications allow $H_{e\bar{e}}$ to be written in the form

$$H_{e\bar{e}} = H^{(+)}_{(+)} + H^{(-)}_{(-)} + H^{(+)} + H^{(-)} + H^{(+)}_{(-)} + H_E, \tag{5.79}$$

where

$$H^{(+)}_{(+)} = -2\hat{b}^\dagger_R \hat{b}^\dagger_R \beta_0^2 f^{\rho\,(-)}_{\mathbf{k}\lambda} \sigma^{(-)}, \tag{5.80a}$$

$$H^{(-)}_{(-)} = -2\hat{b}_R \hat{b}_R \beta_0^2 f^{\rho\,(+)}_{\mathbf{k}\lambda} \sigma^{(+)}, \tag{5.80b}$$

$$H^{(+)} = \hat{b}^\dagger_R \beta_0 \left\{ i(\nabla \times \mathbf{f}^\rho_{\mathbf{k}\lambda})^{(-)} - [\boldsymbol{\sigma} \times (\nabla \times \mathbf{f}^\rho_{\mathbf{k}\lambda})]^{(-)} \right\}, \tag{5.80c}$$

$$H^{(-)} = \hat{b}_R \beta_0 \left\{ -i(\nabla \times \mathbf{f}^\rho_{\mathbf{k}\lambda})^{(+)} + [\boldsymbol{\sigma} \times (\nabla \times \mathbf{f}^\rho_{\mathbf{k}\lambda})]^{(+)} \right\}, \tag{5.80d}$$

$$\begin{aligned} H^{(+)}_{(-)} = {} & 4\beta_0^2 \hat{b}^\dagger_R \hat{b}_R (f_x \sigma_x + f_y \sigma_y) + 2\beta_0^2 f^{\rho\,(+)}_{\mathbf{k}\lambda} \sigma^{(-)} \\ & - (\boldsymbol{\sigma} \cdot \mathbf{f}^\rho_{\mathbf{k}\lambda})\pi^2 + e\mathbf{f}^\rho_{\mathbf{k}\lambda} \cdot \mathbf{B}_0 + ie\boldsymbol{\sigma} \cdot (\mathbf{f}^\rho_{\mathbf{k}\lambda} \times \mathbf{B}_0), \end{aligned} \tag{5.80e}$$

$$H_E = (\boldsymbol{\sigma} \cdot \mathbf{f}^\rho_{\mathbf{k}\lambda})(E_{\nu'} - m)(E_\nu + m), \tag{5.80f}$$

where p_z has been set to zero for the same reasons as detailed just after (5.49). Since we are considering an intermediate antiparticle state, we must take $E_{\nu'} \to -E_{\nu'}$ in the energy denominator, so that

$$\mathcal{E}^D_{e\bar{e}} = 4(E_\nu - E_{\nu'} - \omega)E_\nu(E_\nu + m)E_{\nu'}(E_{\nu'} - m)] = \mathcal{O}(m^5)\ . \tag{5.81}$$

Noting that eqs. (5.80a)-(5.80e) do not contain any factors of m, the fact that $\mathcal{E}^D_{e\bar{e}} = \mathcal{O}(m^5)$ means that the only contributions to

$$\Delta E^{\text{int}}_{e\bar{e}} = e^2 \sum_{\nu' s'} \sum_\lambda \int d^3\mathbf{k} \frac{|\langle \nu, s| H_{e\bar{e}} |\nu', s'\rangle|^2}{\mathcal{E}^D_{e\bar{e}}}. \tag{5.82}$$

with the correct order in m are those that include H_E, as given by eq. (5.80f), meaning that the only contributions to the magnetic moment must come from

$$\Delta E^{\text{int}}_{e\bar{e},E^2} = e^2 \sum_{\nu' s'} \sum_\lambda \int d^3\mathbf{k} \frac{|\langle \nu, s| H_E |\nu', s'\rangle|^2}{\mathcal{E}^D_{e\bar{e}}}, \tag{5.83}$$

and

$$\Delta E^{\text{int}}_{e\bar{e},E\pm} = e^2 \sum_{\nu' s'} \sum_\lambda \int d^3\mathbf{k} \frac{|\langle \nu, s| H_E |\nu', s'\rangle \langle \nu', s'| H^{(+)}_{(-)} |\nu, s\rangle}{\mathcal{E}^D_{e\bar{e}}} + \text{H.c.} \tag{5.84}$$

On expansion for large m, the first of these becomes

$$\begin{aligned} \Delta E^{\text{int}}_{e\bar{e},E^2} = e^2 \sum_{\nu' s'} \sum_\lambda \int d^3\mathbf{k} \Bigg[\frac{1}{2m} + \frac{\omega}{4m^2} + \frac{eB_0(1 + \nu + \nu' + s + s')}{2m^3} + \frac{\omega^2}{8m^3} + \mathcal{O}\left(\frac{1}{m^4}\right) \Bigg] \\ \times \langle \nu, s| \boldsymbol{\sigma} \cdot \mathbf{f}^\rho_{\mathbf{k}\lambda} |\nu', s'\rangle \langle \nu', s'| \boldsymbol{\sigma} \cdot \mathbf{f}^{\rho *}_{\mathbf{k}\lambda} |\nu, s\rangle\ . \end{aligned} \tag{5.85}$$

Eq. (5.37) tells us that we must have $\rho = 0 = \rho'$, and that only the third term of the expansion contributes to the magnetic moment. The lack of higher multipole powers means

we can set $\nu = \nu'$ since, in the dipole approximation, the operator $\mathbf{f}^{\rho}_{\mathbf{k}\lambda}$ cannot change the Landau level. Using eq. (5.29) we write this as

$$\Delta E^{\text{int}}_{e\bar{e},E^2} = \frac{e^3 B_0}{4m^3} \sum_{s'} \sum_{\lambda} \int d^3\mathbf{k} (1+2\nu+s+s') |\langle s| \sigma^{(-)} f_{\mathbf{k}\lambda}{}^{(+)} + \sigma^{(+)} f_{\mathbf{k}\lambda}{}^{(-)} + 2\sigma_z f_{\mathbf{k}\lambda,z} |s'\rangle|^2, \tag{5.86}$$

The spin matrix elements given in eqs. (5.63) can be used to evaluate the contributions for $s' = \pm 1/2$.

$$\Delta E^{\text{int}}_{e\bar{e},E^2}(s' = +1/2) = \frac{e^3 B_0}{4m^3} \sum_{\lambda} \int d^3\mathbf{k} \left[(1+2\nu) |f_{\mathbf{k}\lambda}{}^{(-)}|^2 + (2+2\nu) |f_{\mathbf{k}\lambda,z}|^2 \right] , \tag{5.87a}$$

$$\Delta E^{\text{int}}_{e\bar{e},E^2}(s' = -1/2) = \frac{e^3 B_0}{4m^3} \sum_{\lambda} \int d^3\mathbf{k} \left[(1+2\nu) |f_{\mathbf{k}\lambda}{}^{(+)}|^2 + 2\nu |f_{\mathbf{k}\lambda,z}|^2 \right] . \tag{5.87b}$$

Using the same reasoning that took the spin-up and spin-down contributions (5.64) and (5.65) to the corresponding energy shift (5.66), we have

$$\Delta E^{\text{int}}_{e\bar{e},E^2} = \frac{e^3 \sigma_z B_0}{8m^3} \sum_{\lambda} \int d^3\mathbf{k} \left[(1+2\nu)(|f_{\mathbf{k}\lambda}{}^{(-)}|^2 - |f_{\mathbf{k}\lambda}{}^{(+)}|^2) + 2|f_{\mathbf{k}\lambda,z}|^2 \right] . \tag{5.88}$$

Using definition (5.29) and the fact that some terms vanish under $\int d^3\mathbf{k}$ [see discussion between eqs. (5.55) and (5.58)], this simplifies to

$$\Delta E^{\text{int}}_{e\bar{e},E^2} = \frac{e^3 \sigma_z B_0}{2m^3} \sum_{\lambda} \int d^3\mathbf{k} |f_{\mathbf{k}\lambda,z}|^2 . \tag{5.89}$$

Now considering $\Delta E^{\text{int}}_{e\bar{e},E\pm}$, we have from have eq. (5.84)

$$\begin{aligned} \Delta E^{\text{int}}_{e\bar{e},E\pm} =& e^2 \sum_{\nu' s'} \sum_{\lambda} \int d^3\mathbf{k} \left[-\frac{1}{8m^3} + \mathcal{O}(1/m^4) \right] \Big\{ \langle \nu, s| \, 4\beta_0^2 \hat{b}_R^\dagger \hat{b}_R (f_x \sigma_x + f_y \sigma_y) \\ &+ 2\beta_0^2 f^{\rho}_{\mathbf{k}\lambda}{}^{(+)} \sigma^{(-)} - (\boldsymbol{\sigma} \cdot \mathbf{f}^{\rho}_{\mathbf{k}\lambda}) \pi^2 + e \mathbf{f}^{\rho}_{\mathbf{k}\lambda} \cdot \mathbf{B}_0 + ie \boldsymbol{\sigma} \cdot (\mathbf{f}^{\rho}_{\mathbf{k}\lambda} \times \mathbf{B}_0) \, |\nu', s'\rangle \\ &\times \langle \nu', s'| \, \boldsymbol{\sigma} \cdot \mathbf{f}^{\rho *}_{\mathbf{k}\lambda} \, |\nu, s\rangle \Big\} + \text{H.c.} \end{aligned} \tag{5.90}$$

Appeal to eq. (5.37) shows us that we must have $\rho = 0 = \rho'$ in order for there to be any magnetic moment contributions. Once the $\boldsymbol{\pi}$ operators in eq. (5.90) have been applied, the result can be simplified considerably by using eq. (5.29) and the fact that $\mathbf{B_0} = B_0 \hat{\mathbf{z}}$. The result is:

$$\begin{aligned} \Delta E^{\text{int}}_{e\bar{e},E\pm} =& \frac{\beta_0^2 e^2}{4m^3} \sum_{\nu' s'} \sum_{\lambda} \int d^3\mathbf{k} \Big\{ \langle \nu, s| \left[(2\nu'+1) \sigma_z f_{\mathbf{k}\lambda,z} + f_{\mathbf{k}\lambda,z} \right] |\nu', s'\rangle \\ &\times \langle \nu', s'| \, \frac{1}{2} \left[\sigma^{(-)} f^{(+)} + \sigma^{(+)} f^{(-)} \right]^* + \sigma_z f^*_{\mathbf{k}\lambda,z} \, |\nu, s\rangle \Big\} + \text{H.c.} \end{aligned} \tag{5.91}$$

The only non-zero contribution arises for $\nu = \nu'$ and $s = s'$

$$\Delta E^{\text{int}}_{e\bar{e},E\pm} = \frac{\beta_0^2 e^2}{4m^3} \sum_{\lambda} \int d^3\mathbf{k} \left[(2\nu+1) \sigma_z f_{\mathbf{k}\lambda,z} + f_{\mathbf{k}\lambda,z} \right] \sigma_z f^*_{\mathbf{k}\lambda,z} + \text{H.c.} \tag{5.92}$$

Since $\sigma_z\sigma_z$ is equal to a unit matrix, the only spin-dependent term from above is:

$$\Delta E^{\text{int}}_{e\bar{e},E\pm} = \frac{\beta_0^2 e^2}{4m^3}\sum_\lambda \int d^3\mathbf{k}\sigma_z |f_{\mathbf{k}\lambda,z}|^2 + \text{H.c.} \tag{5.93}$$

giving finally

$$\Delta E^{\text{int}}_{e\bar{e},E\pm} = -\frac{e^3 B_0}{4m^3}\sigma_z \sum_\lambda \int d^3\mathbf{k}|f_{\mathbf{k}\lambda,z}|^2 \,. \tag{5.94}$$

The sum of this and eq. (5.89) gives the final answer for the particle-antiparticle shift:

$$\Delta E^{\text{int}}_{e\bar{e}} = \frac{e^3 B_0}{4m^3}\sigma_z \sum_\lambda \int d^3\mathbf{k}|f_{\mathbf{k}\lambda,z}|^2 \,. \tag{5.95}$$

5.3.4 Summary

The sum of eqs. (5.58), (5.67) and (5.95) yields the energy shift of an electron coupled to a quantized electromagnetic field described through mode functions $\mathbf{f}_{\mathbf{k}\lambda}$. The magnetic moment shift $\Delta\mu_\perp$ for $\mathbf{B}_0$ normal to the interface is extracted from this via $\Delta E = -\Delta\mu_\perp(\sigma_z B_0)$. The result is:

$$\begin{aligned}\Delta\mu_\perp = -\frac{e^3}{4m^3}\sum_\lambda \int d^3\mathbf{k}\Bigg[&|f_{\mathbf{k}\lambda,z}|^2 + \frac{|(\nabla\times\mathbf{f}_{\mathbf{k}\lambda})_x|^2}{\omega^2} + \frac{|(\nabla\times\mathbf{f}_{\mathbf{k}\lambda})_y|^2}{\omega^2} \\ &+ \frac{1}{\omega^2}\left(f_{\mathbf{k}\lambda,x}\frac{\partial^2 f^*_{\mathbf{k}\lambda,y}}{\partial x\partial y} + f_{\mathbf{k}\lambda,y}\frac{\partial^2 f^*_{\mathbf{k}\lambda,x}}{\partial x\partial y} - f_{\mathbf{k}\lambda,y}\frac{\partial^2 f^*_{\mathbf{k}\lambda,y}}{\partial x^2} - f_{\mathbf{k}\lambda,x}\frac{\partial^2 f^*_{\mathbf{k}\lambda,x}}{\partial y^2} + \text{H.c.}\right)\Bigg].\end{aligned} \tag{5.96}$$

Some of the terms may be assigned a physical meaning as follows. The terms containing the curl operator originate from the magnetic part of the quantized field inducing a change in the electron's spin state, while the terms containing derivatives are shifts induced by the spatial variation of the quantized field across the cyclotron orbit of the electron.

We note that our derivation and the resulting eq. (5.96) can of course not be used to calculate the anomalous magnetic moment in free space. While one could obtain a crude an estimate by cutting off the integral over photon frequencies at $\omega \sim m$, which would give the correct order of magnitude e^3/m, a correct calculation would require second-quantization of the electron, not just the photon.

Finally, we note that the corresponding shift $\Delta\mu_\parallel$ for $\mathbf{B}_0$ directed parallel to the interface can be obtained from the above by cycling indices (i.e. rotating the surface). The modes for the non-dispersive surface shown in eq. (3.16) or those for the plasma surface shown in eqs. (3.50) and (3.32) can now be used directly in this equation. While this looks a formidable task, we shall see in the next section that analytic continuation in the k_z plane along the lines of that used in Chapter 4 allows one to evaluate the integrals relatively easily, and furthermore that this analytic continuation provides a unique perspective on the physics of the vacuum field near an interface.

5.4 Calculation of shift

5.4.1 Non-dispersive dielectric

We are now ready to substitute the modes (3.16) into the magnetic moment shift (5.96). Before doing this, we make a few simplifications to make the calculation shorter. Firstly, our system is xy symmetric, so we can freely change $x \leftrightarrow y$ in any particular term. Secondly, the contributions of the terms in the second line of (5.96) turn out to be purely real, so the effect of adding the Hermitian conjugate is just to multiply these terms by two. Making these simplifications, we have

$$\Delta\mu_\perp = -\frac{e^3}{4m^3}\sum_\lambda \int d^3\mathbf{k}\left[|f_{\mathbf{k}\lambda,z}|^2 + 2\frac{|(\nabla\times\mathbf{f}_{\mathbf{k}\lambda})_x|^2}{\omega^2} + \frac{4}{\omega^2}\left(f_{\mathbf{k}\lambda,x}\frac{\partial^2 f^*_{\mathbf{k}\lambda,y}}{\partial x\partial y} - f_{\mathbf{k}\lambda,x}\frac{\partial^2 f^*_{\mathbf{k}\lambda,x}}{\partial y^2}\right)\right]. \tag{5.97}$$

This means we have, in principle, eight integrals to do (the four terms above for each of the two polarizations). This is in contrast to the mass shift calculated in Chapter 4 where we just had one (since the TE polarization dropped out for the case considered). In appendix A.3, we consider each of these terms and show that the method we used in section 4.2.1 to determine the mass shift means the contribution of each term can be completely described by a very simple function of the wave vector[5]. Using the functions listed in appendix A.3, after some algebra we find for both components of the magnetic moment shift near a non-dispersive surface

$$\Delta\mu_\perp^{\text{nondisp}} = -\frac{e^3}{32\pi^2 m^3}\int_0^\infty dk_\parallel k_\parallel \int_C dk_z \frac{1}{k^3}\Big[\left(2k_\parallel^2 - k_z^2\right)R^L_{\mathbf{k},\text{TE}}(n^2) + \left(2k_\parallel^2 + k_z^2\right)R^L_{\mathbf{k},\text{TM}}(n^2)\Big]e^{2ik_z z}, \tag{5.98a}$$

$$\Delta\mu_\parallel^{\text{nondisp}} = -\frac{e^3}{32\pi^2 m^3}\int_0^\infty dk_\parallel k_\parallel \int_C dk_z \frac{1}{2k^3}\Big[\left(3k_\parallel^2 + 2k_z^2\right)R^L_{\mathbf{k},\text{TE}}(n^2) + \left(3k_\parallel^2 - 2k_z^2\right)R^L_{\mathbf{k},\text{TM}}(n^2)\Big]e^{2ik_z z}, \tag{5.98b}$$

where the angular integration in the polar co-ordinate system $\{k_x = k_\parallel\cos\phi,\ k_y = k_\parallel\sin\phi\}$ has been carried out immediately, and the curve C is that shown in figure 5.4. The shift (5.98b) for $\mathbf{B}_0$ directed parallel to the interface was doing by cycling indices in (5.96). We note in particular that since the calculation that led to these exactly follows the method shown in section 4.2.1, eqs. (5.98) are already the renormalized magnetic moment shifts[6]

[5] And, as we shall see, the set of functions shown in table A.1 of appendix A.3 provides a useful point of contact with the noise current approach considered in Chapter 7

[6] Throughout this chapter, Chapter 6 and Chapter 7 we will not explicitly include the subscript 'ren' for notational simplicity. It is to be understood that all magnetic moment shifts from here onwards are renormalized.

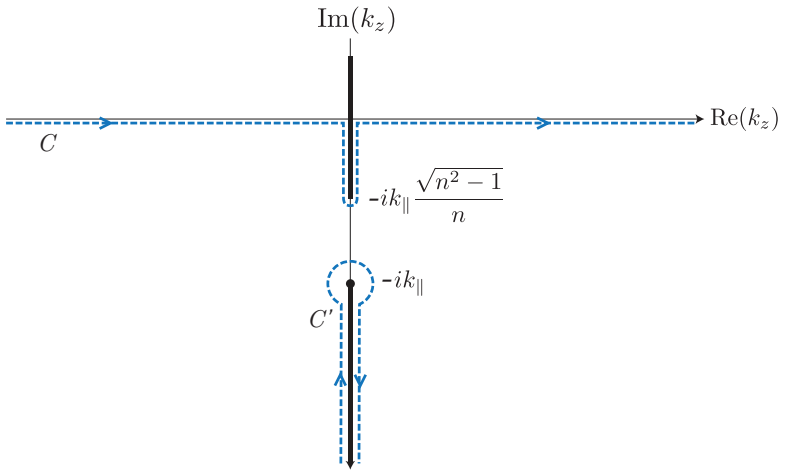

Figure 5.4: Integration paths in the complex k_z plane to be used for calculation of the magnetic moment shift near a non-dispersive surface of refractive index n.

obtained by subtracting the free-space magnetic moment.

The odd power of $k = \sqrt{k_z^2 + k_\parallel^2}$ in the denominators of the integrands of eqs. (5.98) means we have branch points in the complex k_z plane at $k_z = \pm ik_\parallel$ for both expressions. We choose to place the corresponding branch cuts in the regions $|k_z| > k_\parallel$, as shown in figure 5.4. This choice is made so that we may do an analytic continuation of the integrals in the same fashion as for the mass shift described in Chapter 4.

In section 4.2.1 we evaluated the integrals for the mass shift by deforming C into the lower complex plane and picking up a double pole at $k_z = -ik_\parallel$. The presence of the branch cut in the integrand of (5.98a) complicates the analogous process for the magnetic moment matters. As a first naive approach we simply deform the contour C to C', giving

$$\Delta\mu_\perp^{\text{nondisp}} = -\frac{e^3}{32\pi^2 m^3}\int_0^\infty dk_\parallel k_\parallel \int_{C'} dk_z \frac{1}{k^3}\Big[\left(2k_\parallel^2 - k_z^2\right) R^L_{\mathbf{k},\text{TE}}(n^2) + \left(2k_\parallel^2 + k_z^2\right) R^L_{\mathbf{k},\text{TM}}(n^2)\Big] e^{2ik_z z}, \quad (5.99a)$$

$$\Delta\mu_\parallel^{\text{nondisp}} = -\frac{e^3}{32\pi^2 m^3}\int_0^\infty dk_\parallel k_\parallel \int_{C'} dk_z \frac{1}{2k^3}\Big[\left(3k_\parallel^2 + 2k_z^2\right) R^L_{\mathbf{k},\text{TE}}(n^2) + \left(3k_\parallel^2 - 2k_z^2\right) R^L_{\mathbf{k},\text{TM}}(n^2)\Big] e^{2ik_z z}, \quad (5.99b)$$

as shown in figure 5.4. However, the evaluation of the integral over the vanishingly small circle around $k_z = -ik_\parallel$ proves technically awkward, so we take a different approach. Initially specializing to $\Delta\mu_\perp^{\text{nondisp}}$, we subtract the point $k_z = -ik_\parallel$ from the reflection coefficients and evaluate its contribution separately via

$$\Delta\mu_\perp^{\text{nondisp}} = \Delta\mu_{\perp,\text{main}}^{\text{nondisp}} + \Delta\mu_{\perp,\text{main}}^{\text{sep}}\,, \quad (5.100)$$

with

$$\Delta\mu_{\perp,\text{main}}^{\text{nondisp}} = -\frac{e^3}{4m^3}\frac{1}{(2\pi)^2}\int_0^\infty dk_\parallel k_\parallel \int_{C'} dk_z \frac{1}{2k^3} \times \Big\{ \left(2k_\parallel^2 - k_z^2\right)\left[R^L_{\mathbf{k},\text{TE}}(n^2) - R^L_{\mathbf{k},\text{TE}}(n^2)(k_z \to -ik_\parallel)\right] + \left(2k_\parallel^2 + k_z^2\right)\left[R^L_{\mathbf{k},\text{TM}}(n^2) - R^L_{\mathbf{k},\text{TM}}(n^2)(k_z \to -ik_\parallel)\right]\Big\} e^{2ik_z z} \,, \quad (5.101a)$$

$$\Delta\mu_{\perp,\text{sep}}^{\text{nondisp}} = -\frac{e^3}{4m^3}\frac{1}{(2\pi)^2}\int_0^\infty dk_\parallel k_\parallel \int_{C'} dk_z \frac{1}{2k^3}\Big\{ \left(2k_\parallel^2 - k_z^2\right) R^L_{\mathbf{k},\text{TE}}(n^2)(k_z \to -ik_\parallel) + \left(2k_\parallel^2 + k_z^2\right) R^L_{\mathbf{k},\text{TM}}(n^2)(k_z \to -ik_\parallel)\Big\} e^{2ik_z z} \,. \quad (5.101b)$$

Using the explicit form of the reflection coefficients (A.5), we have for the non-dispersive dielectric

$$R^L_{\mathbf{k},\text{TE}}(n^2)(k_z \to -ik_\parallel) = 0, \qquad R^L_{\mathbf{k},\text{TM}}(n^2)(k_z \to -ik_\parallel) = \frac{n^2-1}{n^2+1}, \quad (5.102)$$

giving

$$\Delta\mu_{\perp,\text{sep}}^{\text{nondisp}} = -\frac{e^3}{4m^3}\frac{1}{(2\pi)^2}\frac{n^2-1}{n^2+1}\int_0^\infty dk_\parallel k_\parallel \int_{C'} dk_z \frac{1}{2k^3}\left(2k_\parallel^2 + k_z^2\right) e^{2ik_z z} \,. \quad (5.103)$$

The branch cut between $k_z = \pm ik_\parallel \frac{\sqrt{n^2-1}}{n}$ was present due to the appearance of k_z^d in the reflection coefficient. Since this has been eliminated we can now deform the contour C' appearing in eq. (5.103) to be straight along the real k_z axis. This allows the integral to be written as

$$\Delta\mu_{\perp,\text{sep}}^{\text{nondisp}} = -\frac{e^3}{4m^3}\frac{1}{(2\pi)^2}\frac{n^2-1}{n^2+1}\int_0^\infty dk_\parallel k_\parallel \int_0^\infty dk_z \frac{1}{k^3}\left(2k_\parallel^2 + k_z^2\right)\cos(2k_z z) \,, \quad (5.104)$$

where the parity properties of the integrand have been used. The integral can be evaluated exactly through Bessel functions (see sections 8.432 and 8.561 of [50]) provided that one does the k_z integral first, the result is

$$\Delta\mu_{\perp,\text{sep}}^{\text{nondisp}} = -\frac{e^3}{16\pi^2 m^3}\frac{n^2-1}{n^2+1}\frac{3}{4z^2} \,. \quad (5.105)$$

Turning our attention to the main integral (5.101a), the first task is to investigate how the square root function behaves on either side of the branch cut in the lower complex k_z plane. Writing $k_z = -i\kappa$ ($\kappa > 0$), one can show that the following holds

$$\int_{C'} dk_z \sqrt{k_z^2 + k_\parallel^2} = -2\int_{k_\parallel}^\infty d\kappa \sqrt{\kappa^2 - k_\parallel^2} + \int_{\text{circle}} dk_z \sqrt{k_z^2 + k_\parallel^2} \,, \quad (5.106)$$

with the integral over circle corresponding to that around the circular path around $k_z = -ik_\parallel$ shown in fig. 5.4. The fact that we have subtracted the singularity at $k_z = -ik_\parallel$ means

that on restoration of the full integrand the second term of (5.106) is zero. Using this and eqs. (5.102) we then have

$$\Delta\mu_{\perp,\text{main}}^{\text{nondisp}} = \frac{e^3}{4m^3}\frac{1}{(2\pi)^2}\int_0^\infty dk_\parallel k_\parallel \int_{k_\parallel}^\infty d\kappa \frac{1}{(\kappa^2-k_\parallel^2)^{3/2}}\Big\{ \left(2k_\parallel^2+\kappa^2\right) R^L_{\mathbf{k},\text{TE}}(n^2) + \left(2k_\parallel^2-\kappa^2\right)\left[R^L_{\mathbf{k},\text{TM}}(n^2) - \frac{n^2-1}{n^2+1}\right]\Big\} e^{2\kappa z} \,. \tag{5.107}$$

Defining a complex frequency $\xi = -i\omega$ and writing $\kappa^2 = k_\parallel^2 + \xi^2$ in polar co-ordinates $\{\xi = \kappa\cos\phi, k_\parallel = \kappa\sin\phi\}$, this can be manipulated to

$$\Delta\mu_{\perp,\text{main}}^{\text{nondisp}} = \frac{e^3}{16\pi^2 m^3}\int_0^\infty d\xi\,\xi\int_1^\infty d\eta\Big\{ \left(3\eta^2-2\right) R^L_{\mathbf{k},\text{TE}}(n^2) + \left(\eta^2-2\right)\left(R^L_{\mathbf{k},\text{TM}}(n^2) - \frac{n^2-1}{n^2+1}\right)\Big\} e^{2\xi\eta z} \,, \tag{5.108}$$

where $\eta = k_z/\omega$ is the complex angle of incidence of radiation upon the surface. This form is particularly useful because, for isotropic media, the reflection coefficients depend only on ξ. The subtracted term is, in these variables, given by the two-dimensional limit $\{\eta\to\infty, \xi\to 0\}$ of the TM reflection coefficient, so in order for the above to hold these two limits must commute in *both*[7] reflection coefficients. This turns out to be true for all but one case, which we shall discuss in section 5.4.2. Combining this with the result of the separate integral (5.105), we reach the final result for the magnetic moment shift when the applied magnetic field $\mathbf{B}_0$ is directed perpendicular to the interface

$$\Delta\mu_{\perp}^{\text{nondisp}} = \frac{e^3}{16\pi^2 m^3}\Bigg\{ \int_0^\infty d\xi\,\xi\int_1^\infty d\eta\Big[\left(3\eta^2-2\right) R^L_{\mathbf{k},\text{TE}}(n^2) + \left(\eta^2-2\right)\left(R^L_{\mathbf{k},\text{TM}}(n^2) - \frac{n^2-1}{n^2+1}\right)\Big] e^{2\xi\eta z} - \frac{n^2-1}{n^2+1}\frac{3}{4z^2}\Bigg\} \,. \tag{5.109}$$

An identical calculation beginning from (5.99b) yields the result for the situation when the magnetic field is directed parallel to the interface:

$$\Delta\mu_{\parallel}^{\text{nondisp}} = \frac{e^3}{16\pi^2 m^3}\Bigg\{ \frac{1}{2}\int_0^\infty d\xi\,\xi\int_1^\infty d\eta\Big[\left(\eta^2-3\right) R^L_{\mathbf{k},\text{TE}}(n^2) + \left(5\eta^2-3\right)\left(R^L_{\mathbf{k},\text{TM}}(n^2) - \frac{n^2-1}{n^2+1}\right)\Big] e^{2\xi\eta z} - \frac{n^2-1}{n^2+1}\frac{1}{z^2}\Bigg\} \,. \tag{5.110}$$

[7] See eq. (5.101a) – the TE reflection coefficient also has the point $k_z = -ik_\parallel$ subtracted from it. We could have chosen to transform $R^L_{\mathbf{k},\text{TE}}(n^2)$ to the new variables ξ and η, in which case we would have had to subtract the $\{\eta\to\infty, \xi\to 0\}$ limit. In the case of the non-dispersive reflection coefficient the limits commute and the value of the limit is zero so eq. (5.108) still stands, but this will not always be the case when we consider other models of the surface.

The non-dispersive reflection coefficients in the integration variables ξ and η are

$$R^L_{\mathbf{k},\mathrm{TE}}(n^2) = \frac{\eta - \sqrt{(n^2-1)+\eta^2}}{\eta + \sqrt{(n^2-1)+\eta^2}} \quad , \quad R^L_{\mathbf{k},\mathrm{TM}}(n^2) = \frac{\eta n^2 - \sqrt{(n^2-1)+\eta^2}}{\eta n^2 + \sqrt{(n^2-1)+\eta^2}} \, . \tag{5.111}$$

which is an advantageous form since these are independent of ξ. The integrals (5.109) and (5.110) can be carried out exactly. Evaluating them using MATHEMATICA we find

$$\begin{aligned}\Delta\mu_\perp^{\mathrm{nondisp}} = &- \frac{e^3}{32\pi^2 m^3 z^2} \frac{1}{(n^4-1)^{3/2}} \Bigg[\sqrt{n^4-1}(5 - 2n + n^2 - 2n^3 - 3n^4 + n^5) \\ &- n^4 \sqrt{n^2-1}\,(1+2n^2) \operatorname{arctanh}\left(\frac{(n-1)\sqrt{1+n^2}}{1+(n-1)n}\right) \\ &+ 2\,(n^2-1)\,(1+n^2)^{5/2} \ln\left(n + \sqrt{n^2-1}\right) \Bigg] \, , \end{aligned} \tag{5.112a}$$

$$\begin{aligned}\Delta\mu_\parallel^{\mathrm{nondisp}} = &- \frac{e^3}{192\pi^2 m^3 z^2} \frac{1}{(n^4-1)^{3/2}} \Bigg[\sqrt{n^4-1}(26 - 9n + 8n^2 - 23n^3 - 3n^4 + n^5) \\ &+ 3n^4 \sqrt{n^2-1}\,(2-3n^2) \operatorname{arctanh}\left(\frac{(n-1)\sqrt{1+n^2}}{1+(n-1)n}\right) \\ &+ 9\,(n^2-1)\,(1+n^2)^{5/2} \ln\left(n + \sqrt{n^2-1}\right) \Bigg] \, . \end{aligned} \tag{5.112b}$$

All previous literature on the surface dependence of the magnetic moment uses the idea of a 'perfect reflector' ($n \to \infty$) the describe the surface [39]. So, as a consistency check with these we take a large n expansion of our results (5.112), finding

$$\Delta\mu_\perp^{\mathrm{nondisp}} = -\frac{e^2}{4\pi}\frac{e}{2m}\left[\frac{n}{4\pi m^2 z^2} - \frac{1}{4\pi m^2 z^2} + \mathcal{O}(1/n)\right] \, , \tag{5.113a}$$

$$\Delta\mu_\parallel^{\mathrm{nondisp}} = -\frac{e^2}{4\pi}\frac{e}{2m}\left[\frac{n}{24\pi m^2 z^2} + \frac{1}{4\pi m^2 z^2} + \mathcal{O}(1/n)\right] \, . \tag{5.113b}$$

We have leading terms which rise linearly in n. This appears to be unphysical, as it would suggest that the magnetic moment could be increased arbitrarily by increasing the refractive index n of the surface. However, as we shall explain in section 5.4.3, this apparent problem is an inevitable consequence of the unrealistic assumption of a dispersionless medium. A curious observation to note is that the next-to-leading terms independent of n in eqs. (5.113), if taken on their own, do in fact reproduce the results of the perfect-reflector case, which are the highlighted terms in fig. 5.3[8].

To track down the source of the discrepancies between the results of perfect reflector model and those of the large refractive-index limit of the non-dispersive model, we use a similar approach to that taken in section 4.2.1 and evaluate the integrals with the limit

[8] The extra factor of 4π arises from ref. [39]'s use of CGS units.

$n \to \infty$ taken *before* the limit $k_z \to -ik_\parallel$. Going back to eq. (5.98a) and taking the $n \to \infty$ limits of the reflection coefficients, we have for the perpendicular component of the shift

$$\Delta\mu_\perp^{\mathrm{PM}} = -\frac{e^3}{4m^3}\frac{1}{(2\pi)^2}\int_0^\infty dk_\parallel k_\parallel \int_C dk_z \frac{k_z^2}{k^3} e^{2ik_z z} \,. \tag{5.114}$$

Just as in eq. (5.103), the branch cut due to the presence of k_z^d in the reflection coefficients has now been eliminated, so we may deform the contour to run along the real k_z axis. Thus the shift is given by

$$\Delta\mu_\perp^{\mathrm{PM}} = -\frac{e^3}{4m^3}\frac{2}{(2\pi)^2}\int_0^\infty dk_\parallel k_\parallel \int_0^\infty dk_z \frac{k_z^2}{k^3} \cos(2k_z z) \,. \tag{5.115}$$

The integral is evaluated in the same way as eq. (5.104). An identical calculation yields $\Delta\mu_\parallel^{\mathrm{PM}}$, the results are

$$\Delta\mu_\perp^{\mathrm{PM}} = \frac{e^2}{4\pi}\frac{e}{2m}\frac{1}{4\pi m^2 z^2} = -\Delta\mu_\parallel^{\mathrm{PM}} \,. \tag{5.116}$$

This reproduces the next-to-leading terms in eqs. (5.113a) and (5.113b), and the results of [39] highlighted in fig. 5.3. We emphasise that this does not agree with the result if the $n \to \infty$ limit is taken *after* the limit $k_z \to -ik_\parallel$.

5.4.2 Plasma

In this section we will calculate the shift in the magnetic moment of an electron that is localized near a plasma surface described by the model discussed in section 3.3. We neglect the influence of the magnetic field upon the charge carriers inside the medium, which is justified as we ultimately consider the weak-field limit. Just as in the corresponding calculation for the mass shift found in section 4.2.2, we begin by splitting the magnetic moment shift near a plasma surface $\Delta\mu_\perp^{\mathrm{plasma}}$ into contributions from the bulk (TE and TM) modes and those from the surface plasmon

$$\Delta\mu_\perp^{\mathrm{plasma}} = \Delta\mu_\perp^{\mathrm{bulk}} + \Delta\mu_\perp^{\mathrm{sp}} \,. \tag{5.117}$$

Substituting the surface plasmon modes (3.50) into the expression for the magnetic moment shift (5.96), we find for the contribution of the surface plasmon

$$\Delta\mu_\perp^{\mathrm{sp}} = -\frac{e^3}{8\pi m^3}\int_0^\infty dk_\parallel k_\parallel \frac{2k_\parallel^2 - \kappa^2}{p(k_\parallel)\kappa^2} e^{2\kappa z}, \tag{5.118a}$$

$$\Delta\mu_\parallel^{\mathrm{sp}} = -\frac{e^3}{8\pi m^3}\int_0^\infty dk_\parallel k_\parallel \frac{3k_\parallel^2 + 2\kappa^2}{2p(k_\parallel)\kappa^2} e^{2\kappa z}, \tag{5.118b}$$

where the second equation follows from cycling Cartesian co-ordinates in (5.96). The contribution from TE and TM modes is found by substituting the modes (3.32) into the

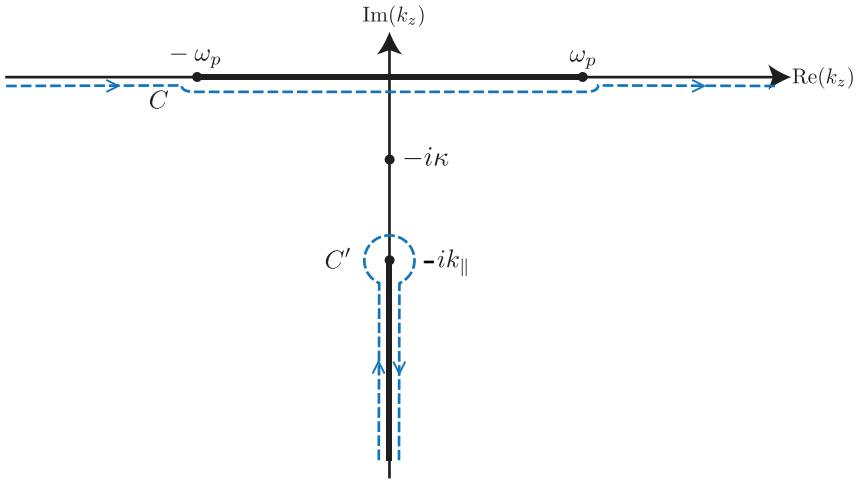

Figure 5.5: Integration paths in the complex k_z plane to be used for calculation of the magnetic moment shift near a plasma surface.

magnetic moment shift in terms of mode functions (5.96) and following an identical method to that shown in section 5.4.1. The result is

$$\Delta\mu_\perp^{\text{bulk}} = -\frac{e^3}{4m^3}\frac{1}{(2\pi)^2}\int_0^\infty dk_\parallel k_\parallel \int_C dk_z \frac{1}{2k^3}\Big[\left(2k_\parallel^2 - k_z^2\right) R^L_{\mathbf{k},\text{TE}}(\epsilon_p) + \left(2k_\parallel^2 + k_z^2\right) R^L_{\mathbf{k},\text{TM}}(\epsilon_p)\Big] e^{2ik_z z}\,, \quad (5.119)$$

where the contour C runs under the cut from $-\omega_p$ to ω_p, as shown in fig. 5.5. Following the approach we took for the non-dispersive dielectric, the contour C shown in fig. 5.5 is deformed to C' running along the cut and around the point $k_z = -ik_\parallel$, however this time we pick up a pole contribution along the way. Splitting the result into 'cut' and 'pole' contributions

$$\Delta\mu_\perp^{\text{bulk}} = \Delta\mu_{\perp\text{cut}}^{\text{bulk}} + \Delta\mu_{\perp\text{pole}}^{\text{bulk}}\,. \quad (5.120)$$

The pole is the same one we already discussed in section 4.2.2, and whose residue is shown in eq. (4.59). Thus we may use the residue theorem to find

$$\Delta\mu_{\perp\text{pole}}^{\text{bulk}} = -\frac{e^3}{4m^3}\frac{1}{(2\pi)}\int_0^\infty dk_\parallel k_\parallel \frac{1}{2\omega_{sp}^3}\left[\left(2k_\parallel^2 - \kappa^2\right)\mathcal{S}\right] e^{2\kappa z}\,, \quad (5.121)$$

where $\mathcal{S}$ is as defined in eq. (4.59). The contribution along the cut is

$$\Delta\mu_{\perp\text{cut}}^{\text{bulk}} = -\frac{e^3}{4m^3}\frac{1}{(2\pi)^2}\int_0^\infty dk_\parallel k_\parallel \int_{C'} dk_z \frac{1}{2k^3}\Big[\left(2k_\parallel^2 - k_z^2\right) R^L_{\mathbf{k},\text{TE}}(\epsilon_p) + \left(2k_\parallel^2 + k_z^2\right) R^L_{\mathbf{k},\text{TM}}(\epsilon_p)\Big] e^{2ik_z z}\,, \quad (5.122)$$

with C' as shown in fig. (5.5). This, combined with the cut contribution (5.121) and the surface plasmon contribution (5.118a) gives us the whole magnetic moment shift for a

magnetic field directed perpendicular to the interface

$$\Delta\mu_{\perp}^{\text{plasma}} = \Delta\mu_{\perp\text{cut}}^{\text{bulk}} + \Delta\mu_{\perp\text{pole}}^{\text{bulk}} + \Delta\mu_{\perp}^{\text{sp}} \,. \tag{5.123}$$

Just as in the calculation for the mass shift in section 4.2.2, we find that the contribution of the pole in the bulk modes cancels with the contribution of the surface plasmon mode: $\Delta\mu_{\perp\text{pole}}^{\text{bulk}} + \Delta\mu_{\perp}^{\text{sp}} = 0$. This gives for the entire energy shift

$$\Delta\mu_{\perp}^{\text{plasma}} = \Delta\mu_{\perp\text{cut}}^{\text{bulk}} \,, \tag{5.124}$$

finally giving via eq. (5.122),

$$\Delta\mu_{\perp}^{\text{plasma}} = -\frac{e^3}{32\pi^2 m^3}\int_0^\infty dk_\parallel k_\parallel \int_{C'} dk_z \frac{1}{k^3}\Big[\left(2k_\parallel^2 - k_z^2\right) R^L_{\mathbf{k},\text{TE}}(\epsilon_p) + \left(2k_\parallel^2 + k_z^2\right) R^L_{\mathbf{k},\text{TM}}(\epsilon_p)\Big] e^{2ik_z z}, \tag{5.125a}$$

$$\Delta\mu_{\parallel}^{\text{plasma}} = -\frac{e^3}{32\pi^2 m^3}\int_0^\infty dk_\parallel \int_{C'} dk_z \frac{k_\parallel}{2k^3}\Big[\left(3k_\parallel^2 + 2k_z^2\right) R^L_{\mathbf{k},\text{TE}}(\epsilon_p) + \left(3k_\parallel^2 - 2k_z^2\right) R^L_{\mathbf{k},\text{TM}}(\epsilon_p)\Big] e^{2ik_z z}, \tag{5.125b}$$

where

$$R^L_{\mathbf{k},\text{TE}}(\epsilon_p) = \frac{k_z - \sqrt{k_z^2 - \omega_p^2}}{k_z + \sqrt{k_z^2 - \omega_p^2}} \quad , \quad R^L_{\mathbf{k},\text{TM}}(\epsilon_p) = \frac{k_z\left(1 - \frac{\omega_p^2}{k_z^2 + k_\parallel^2}\right) - \sqrt{k_z^2 - \omega_p^2}}{k_z\left(1 - \frac{\omega_p^2}{k_z^2 + k_\parallel^2}\right) + \sqrt{k_z^2 - \omega_p^2}} \,, \tag{5.126}$$

and the result $\Delta\mu_{\parallel}^{\text{plasma}}$ for B_0 directed parallel to the surface was obtained in an identical way to $\Delta\mu_{\perp}^{\text{plasma}}$. We note in particular that these can be obtained from the magnetic moment shifts (5.99) for a non-dispersive surface by making the replacement $n^2 \to \epsilon_p$.

The next step is to evaluate the integrals (5.125). In the non-dispersive calculation we subtracted the point $k_z = -ik_\parallel$ from the reflection coefficients and evaluated its contribution separately. In the final expression for our results (5.108) this manifested itself as the need to take a two-dimensional limit of both reflection coefficients, with the condition that these limits must commute. Writing the TE plasma reflection coefficient in terms of the variables η and ξ defined immediately prior to (5.108), we find

$$R^L_{\mathbf{k},\text{TE}}(\epsilon_p) = \frac{\xi\eta - \sqrt{\omega_p^2 + \eta\xi^2}}{\xi\eta + \sqrt{\omega_p^2 + \eta\xi^2}} \,. \tag{5.127}$$

The limits $\eta \to \infty$ and $\xi \to 0$ of this object do not commute – these were precisely the limits on which the validity of equation (5.108) and the calculation preceding it were dependent. This means that attempting to evaluate the TE part of eqs. (5.125) via our subtraction method is not appropriate. Consequently, we use an alternative method to evaluate the

TE contribution to the magnetic moment near a plasma surface. We emphasize that this complication is a purely technical aspect of how we actually evaluate the integrals (5.125) – this is *not* a demonstration of any violation of our observation that the results for the plasma model can be obtained from the non-dispersive integrals simply by replacing the dielectric function.

The TE reflection coefficient for plasma takes a particularly simple form so we proceed to directly evaluate the TE term from eq. (5.119), in which the contour is directly along the real axis. The term is

$$\Delta\mu_{\perp,\mathrm{TE}}^{\mathrm{plasma}} = -\frac{e^3}{32\pi^2\omega_p^2 m^3}\int_0^\infty dk_\parallel \int_{-\infty}^\infty dk_z \, \frac{k_\parallel(2k_\parallel^2 - k_z^2)}{(k_\parallel^2 + k_z^2)^{3/2}} \left(2k_z^2 - \omega_p^2 - 2k_z\sqrt{k_z^2 - \omega_p^2}\right) e^{2ik_z z}, \tag{5.128}$$

where the reflection coefficient has been written out explicitly using eq. (5.126) and the branch cut is placed between the branch points at $\pm\omega_p$, as shown in fig. 5.5. Care must be taken when evaluating this integral due to the physical constraint that $\mathrm{sgn}(k_z) = \mathrm{sgn}(k_z^d)$. The order of integration matters – the integral is convergent only if the k_z integration is done first. To circumvent this restriction we introduce a cutoff Λ in the $k_\parallel$ integral. This improves the convergence of the double integral so that we are allowed to interchange the order of integrations. The $k_\parallel$ integral can then be calculated exactly and yields:

$$\begin{aligned}\Delta\mu_{\perp,\mathrm{TE}}^{\mathrm{plasma}} = -\frac{e^3}{32\pi^2\omega_p^2 m^3} \lim_{\Lambda\to\infty} \int_{-\infty}^\infty dk_z \\ \times \left[(2\Lambda - 5|k_z|)\left(2k_z^2 - \omega_p^2 - 2k_z\sqrt{k_z^2 - \omega_p^2}\right) e^{2ik_z z} + \mathcal{O}(1/\Lambda)\right].\end{aligned} \tag{5.129}$$

We first consider the term with the square root. For the contribution from the region $|k_z| > \omega_p$, we have

$$-\frac{e^3}{32\pi^2\omega_p^2 m^3}\left\{\int_{-\infty}^{-\omega_p} dk_z + \int_{\omega_p}^\infty dk_z\right\}(2\Lambda - 5|k_z|)\left(-2k_z\sqrt{k_z^2 - \omega_p^2}\right) e^{2ik_z z}\,. \tag{5.130}$$

Noting that $k_z\sqrt{k_z^2 - \omega_p^2}$ is even in k_z because of the physical constraint $\mathrm{sgn}(k_z) = \mathrm{sgn}\sqrt{k_z^2 - \omega_p^2}$, we can simplify this to

$$= -\frac{e^3}{16\pi^2\omega_p^2 m^3}\int_{\omega_p}^\infty dk_z \cos(2k_z z)(2\Lambda - 5|k_z|)\left(-2k_z\sqrt{k_z^2 - \omega_p^2}\right)\,. \tag{5.131}$$

Next we consider the region $|k_z| < \omega_p$, where $k_z^d = \sqrt{k_z^2 - \omega_p^2}$ is imaginary. As shown in fig. 5.5, the integration path runs underneath the cut, which means that the factor $k_z\sqrt{\omega_p^2 - k_z^2}$ is now odd in k_z. Applying the constraint $\mathrm{sgn}(k_z) = \mathrm{sgn}\sqrt{k_z^2 - \omega_p^2}$ to the vicinity of $k_z \approx \omega_p$, we are directed to choosing the sign of the square root such that in

the lower half-plane $\sqrt{k_z^2-\omega_p^2} = -i\sqrt{\omega_p^2-k_z^2}$. This leads to the integral analogous to eq. (5.131) but from the region $|k_z| < \omega_p$ as

$$-\frac{e^3}{16\pi^2\omega_p^2 m^3}\int_0^{\omega_p} dk_z\,(2\Lambda-5k_z)\left(-2k_z\sqrt{\omega_p^2-k_z^2}\right)\sin(2k_z z)\,. \tag{5.132}$$

The rest of eq. (5.129) is a trivial integral, and combining this with eqs. (5.131) and (5.132) gives:

$$\begin{aligned}= -\frac{e^3}{16\pi^2 m^3}\lim_{\Lambda\to\infty}\Bigg\{&\frac{1}{\omega_p^2}\int_0^{\omega_p} dk_z\,\left[(2k_z^2-\omega_p^2)\cos(2k_z z)-2k_z\sqrt{\omega_p^2-k_z^2}\sin(2k_z z)\right](2\Lambda-5k_z)\\ &+\frac{1}{\omega_p^2}\int_{\omega_p}^{\infty} dk_z\cos(2k_z z)\left(2k_z^2-\omega_p^2-2k_z\sqrt{k_z^2-\omega_p^2}\right)(2\Lambda-5k_z)\Bigg\}.\end{aligned} \tag{5.133}$$

The integrals proportional to Λ each give expressions with the Bessel function $J_2(2\omega_p z)$, $\sin(2\omega_p z)$, and $\cos(2\omega_p z)$, but all together they conspire to add up to zero. Defining

$$\begin{aligned}\mathcal{I}_{\mathrm{TE}} \equiv \frac{1}{\omega_p^2}\Bigg\{&\int_0^{\omega_p} dk_z k_z\left[(2k_z^2-\omega_p^2)\cos(2k_z z)-2k_z\sqrt{\omega_p^2-k_z^2}\sin(2k_z z)\right]\\ &+\int_{\omega_p}^{\infty} dk_z\,k_z\cos(2k_z z)\left((2k_z^2-\omega_p^2)-2k_z\sqrt{k_z^2-\omega_p^2}\right)\Bigg\}\,,\end{aligned} \tag{5.134}$$

we therefore have

$$\Delta\mu_{\perp,\mathrm{TE}}^{\mathrm{plasma}} = \frac{5e^3}{16\pi^2 m^3}\mathcal{I}_{\mathrm{TE}} \quad\text{and}\quad \Delta\mu_{\parallel,\mathrm{TE}}^{\mathrm{plasma}} = \frac{e^3}{8\pi^2 m^3}\mathcal{I}_{\mathrm{TE}}\,, \tag{5.135}$$

where the case for $\mathbf{B}_0$ parallel to the interface has been evaluated in exactly the same way. The integral $\mathcal{I}_{\mathrm{TE}}$ may be evaluated analytically in MATHEMATICA; one finds

$$\begin{aligned}\mathcal{I}_{\mathrm{TE}} = \frac{1}{4z^2}+\frac{3}{4z^4\omega_p^2}-\frac{4z\omega_p^3}{15}+\frac{\pi\omega_p Y_1(-2\omega_p z)}{2z}\\ +\frac{3\pi Y_2(-2\omega_p z)}{4z^2}-\frac{\pi H_2(2\omega_p z)}{4z^2}+\frac{\pi\omega_p H_3(2\omega_p z)}{2z},\end{aligned} \tag{5.136}$$

where Y_n is the nth Bessel function of the second kind, and H_n is the nth Struve function. This result displays the expected behaviour that $\lim_{z\to-\infty}\mathcal{I}_{\mathrm{TE}} = 0$, i.e. that there is no magnetic moment shift due to a surface that is infinitely far away. The 'perfect-mirror' limit of this object is

$$\lim_{|\omega_p z|\to\infty}\mathcal{I}_{\mathrm{TE}} = \frac{1}{4z^2}, \tag{5.137}$$

which means that for the plasma surface the TE modes do not result in unlimited growth of the magnetic moment shift as one tends towards the perfect reflector limit, in contrast to what was observed for the non-dispersive dielectric in eqs. (5.113a) and (5.113b).

The TM contribution can be found from eq. (5.125a) in precisely the same way as for the non-dispersive case, namely by subtracting the $k_z \to -ik_\parallel$ limit of the reflection

coefficient, changing variables to complex frequency $\xi = -i\omega$ and writing $(ik_z)^2 = k_\parallel^2 + \xi^2$ in polar co-ordinates $\{\xi = (ik_z)\eta, k_\parallel = (ik_z)\sqrt{1-\eta^2}\}$. The result is

$$\Delta\mu_{\perp,\mathrm{TM}}^{\mathrm{plasma}} = \frac{e^3}{16\pi^2 m^3}\left\{\int_0^\infty d\xi\,\xi\int_1^\infty d\eta\,\left(\eta^2-2\right)\left(R^L_{\mathbf{k},\mathrm{TM}}(\epsilon_p)-1\right)e^{2\xi\eta z} - \frac{3}{4z^2}\right\}. \quad (5.138)$$

Replacing the integration over η with one over $\kappa = \eta\xi$ we find

$$\Delta\mu_{\perp,\mathrm{TM}}^{\mathrm{plasma}} = \frac{e^3}{16\pi^2 m^3}\left\{\int_0^\infty d\xi\int_\xi^\infty d\kappa\frac{\kappa^2-2\xi^2}{\xi^2}\left(R^L_{\mathbf{k},\mathrm{TM}}(\epsilon_p)-1\right)e^{2\kappa z} - \frac{3}{4z^2}\right\}, \quad (5.139)$$

where

$$R^L_{\mathbf{k},\mathrm{TM}}(\epsilon_p) = \frac{\kappa\epsilon(\xi)-\sqrt{\xi^2(\epsilon(\xi)-1)+\kappa^2}}{\kappa\epsilon(\xi)+\sqrt{\xi^2(\epsilon(\xi)-1)+\kappa^2}} = \frac{\omega_p^2\kappa+\xi^2(\kappa-\sqrt{\omega_p^2+\kappa^2})}{\omega_p^2\kappa+\xi^2(\kappa+\sqrt{\omega_p^2+\kappa^2})}\,. \quad (5.140)$$

We now change the order of integration, which means that $\int_0^\infty d\xi\int_\xi^\infty d\kappa \to \int_0^\infty\int_0^\kappa d\xi$. Then, the ξ integration is elementary, the result after scaling κ to $s = \kappa/\omega_p$ is

$$\Delta\mu_{\perp,\mathrm{TM}}^{\mathrm{plasma}} = \frac{e^3}{16\pi^2 m^3}\left\{-\frac{3}{4z^2}+2\omega_p^2\int_0^\infty ds\,e^{2s\omega_p z}\frac{1+t^2(s)}{t^2(s)\left[2+t^2(s)\right]^{3/2}}\right.$$
$$\left.\times\left[2t(s)-\left(1+2t^2(s)\right)\operatorname{arccot}(t(s))\right]\right\}, \quad (5.141a)$$

$$\Delta\mu_{\parallel,\mathrm{TM}}^{\mathrm{plasma}} = \frac{e^3}{16\pi^2 m^3}\left\{-\frac{1}{z^2}+\omega_p^2\int_0^\infty ds\,e^{2s\omega_p z}\frac{1+t^2(s)}{t^2(s)\left[2+t^2(s)\right]^{3/2}}\right.$$
$$\left.\times\left[3t(s)-\left(5+3t^2(s)\right)\operatorname{arccot}(t(s))\right]\right\}, \quad (5.141b)$$

with the abbreviation

$$t(s) \equiv \sqrt{\sqrt{1+\frac{1}{s^2}}-1}\,, \quad (5.142)$$

and where the analogous result for $\mathbf{B}_0$ parallel to the surface is also shown. We now have the entire magnetic moment shift of an electron near a plasma surface given through eqs. (5.141) and (5.135) by

$$\Delta\mu_\perp^{\mathrm{plasma}} = \frac{5e^3}{16\pi^2 m^3}\mathcal{I}_{\mathrm{TE}} + \Delta\mu_{\perp,\mathrm{TM}}^{\mathrm{plasma}}, \quad (5.143a)$$

$$\Delta\mu_\parallel^{\mathrm{plasma}} = \frac{e^3}{8\pi^2 m^3}\mathcal{I}_{\mathrm{TE}} + \Delta\mu_{\parallel,\mathrm{TM}}^{\mathrm{plasma}}. \quad (5.143b)$$

The integrals (5.141) which constitute the TM part are done numerically – the results for $\mathbf{B}_0$ perpendicular to the interface are shown in fig 5.6 alongside the perfect reflector shift for comparison.

The asymptotic behavior of the integrals (5.141) for small and large $\omega_p z$ shows some of the important physical qualities of the plasma model. Beginning with large $\omega_p z$, the

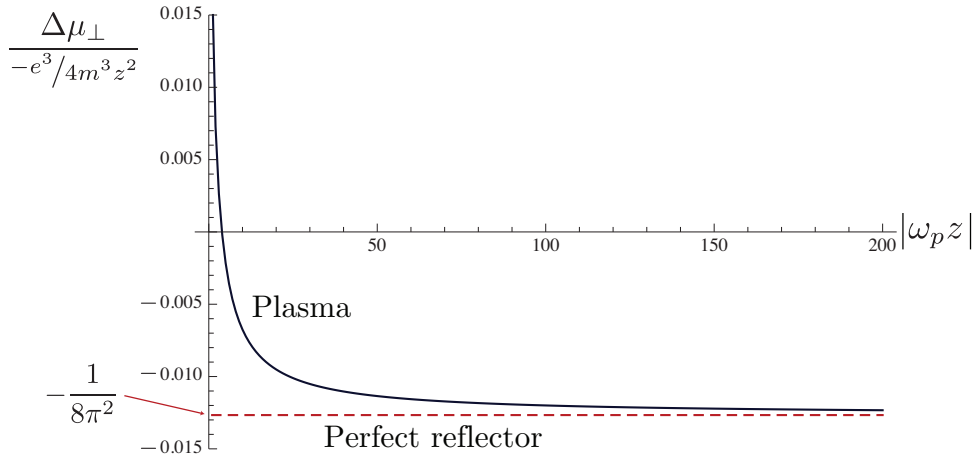

Figure 5.6: Magnetic moment shift for $\mathbf{B}_0$ directed perpendicular to the interface for the plasma and perfect reflector models as a function of the dimensionless parameter $|\omega_p z|$.

integrals from eqs. (5.141) contribute terms of order $1/(\omega_p z^3)$, meaning that the dominant TM contributions are given by the $1/z^2$ terms outside the integrals in (5.141). The TE contribution for large $\omega_p z$ is easily found from eqs (5.135) via eq. (5.137). Combining the TE and TM contributions gives

$$\Delta\mu_\perp^{\text{plasma}}(|\omega_p z| \to \infty) = \frac{e^3}{16\pi^2 m^3}\left(\frac{5}{4z^2} - \frac{3}{4z^2}\right) = \frac{e^3}{32\pi^2 m^3 z^2}\,, \tag{5.144a}$$

$$\Delta\mu_\parallel^{\text{plasma}}(|\omega_p z| \to \infty) = \frac{e^3}{16\pi^2 m^3}\left(\frac{1}{2z^2} - \frac{1}{z^2}\right) = -\frac{e^3}{32\pi^2 m^3 z^2}\,, \tag{5.144b}$$

in agreement with the perfect-mirror calculation, and also of course with the n-independent terms from eqs. (5.113). We are seeing that, just as in the self-energy calculation, the shifts for the plasma and perfect reflector models agree in the limit $|\omega_p z| \to \infty$, and both disagree with the $n \to \infty$ limit of the non-dispersive model. This is another demonstration of the fact that exclusion of evanescent modes from the start of the calculation will give different results to a taking a 'no-evanescent-modes' limit of the shift using a model which explicitly includes them, which as we argued in section 4.2.4 is down to the fundamentally different low-frequency response of conductors and dielectrics.

To find the small $|\omega_p z|$ asymptotics we first note from [50] that (5.136) may be written

$$\mathcal{I}_{\text{TE}}(|\omega_p z| \ll 1) = -\frac{\omega_p^2}{16}\left[1 + 4\gamma_E + 4\ln(-\omega_p z)\right]\,, \tag{5.145}$$

where γ_E is the Euler constant ≈ 0.577. To find the small $|\omega_p z|$ asymptotics of the TM contribution we scale the integration variable s in eqs. (5.141a) and (5.141b) to a new variable equalling $s\omega_p z$, and then expand for small $\omega_p z$. The resulting series may then be integrated term-by-term and turns out to be dominant over the TE part, giving for the

total magnetic moment shift

$$\Delta\mu_{\perp}^{\text{plasma}}(|\omega_p z| \ll 1) = \frac{e^3}{4m^3z^2}\left\{\frac{1}{16\sqrt{2}\pi}\frac{1}{\omega_p z} + \mathcal{O}(\omega_p z)\right\}, \tag{5.146a}$$

$$\Delta\mu_{\parallel}^{\text{plasma}}(|\omega_p z| \ll 1) = \frac{e^3}{4m^3z^2}\left\{\frac{5}{32\sqrt{2}\pi}\frac{1}{\omega_p z} + \mathcal{O}(\omega_p z)\right\}. \tag{5.146b}$$

This $1/z^3$ dependence is not seen when no surface plasmons are present (in the non-dispersive case, for example), so it is reasonable to suppose that appearance of a $1/z^3$ term arises from the interaction of the electron with the surface plasmon. We have an explicit expression (5.118) for the contribution of surface plasmon modes, so we can check this supposition by looking at the magnetic moment shift that is attributable to these modes only. Taking eq. (5.118a) and substituting in the explicit expressions (3.39a) and (3.44) for the imaginary z component of the wave-vector $\kappa \equiv ik_z$, we find

$$\Delta\mu_{\perp}^{\text{sp}} = \frac{1}{4\pi\sqrt{2}\omega_p^4}\int_0^\infty dk_\parallel k_\parallel \left[\frac{\left(2k_\parallel^2 + \omega_p^2 - \sqrt{4k_\parallel^4+\omega_p^4}\right)\left(\sqrt{4k_\parallel^4+\omega_p^4} - 2k_\parallel^2\right)}{4k_\parallel^4+\omega_p^4}\right]^{1/2}$$
$$\times \left(2k_\parallel^4 + k_\parallel^2\left(\omega_p^2 + \sqrt{4k_\parallel^4+\omega_p^4}\right) + 2\omega_p^2\left(\omega_p^2 + \sqrt{4k_\parallel^4+\omega_p^4}\right)\right) e^{2z\sqrt{\sqrt{k_\parallel^4+\omega_p^4/4}-\omega_p^2/2}}, \tag{5.147}$$

Letting

$$\alpha = -z\sqrt{\sqrt{k_\parallel^4+\omega_p^4/4}-\omega_p^2/2}\,, \tag{5.148}$$

this becomes

$$\Delta\mu_{\perp}^{\text{sp}} = \frac{1}{4\pi z^5\omega_p^3}\int_0^\infty d\alpha\, e^{-2\alpha}\sqrt{\alpha\left(\alpha^2+z^2\omega_p^2\right)\left(\alpha+\sqrt{\alpha^2+z^2\omega_p^2}\right)}$$
$$\times\left[3\alpha\left(-\alpha+\sqrt{\alpha^2+z^2\omega_p^2}\right) - 2z^2\omega_p^2\right]. \tag{5.149}$$

Expanding for small $|\omega_p z|$, we find the leading term of the above is given by a trivial integral,

$$\Delta\mu_{\perp}^{\text{sp}}(|\omega_p z| \ll 1) = \frac{e^3}{16m^3\sqrt{2}\pi z^3\omega_p}\int_0^\infty dx\, x^2 e^{-2x} = -\frac{e^3}{64m^3\sqrt{2}\pi z^3\omega_p}, \tag{5.150}$$

reproducing eq. (5.146a), which confirms the fact that at small distances the interaction is dominated by the electrostatic interaction of the electron with the surface plasmon. The corresponding shift for $\mathbf{B}_0$ parallel to the surface behaves in exactly the same way – taking the surface plasmon part of the shift given by eq. (5.118a) on its own and evaluating the integral asymptotically for small $|\omega_p z|$ reproduces that found from the small $|\omega_p z|$ asymptotics of the entire shift (5.146b).

5.4.3 Dispersive dielectric

We would now like to consider the magnetic moment shift near more realistic surfaces. The first surface we will investigate is that described by the dispersive dielectric function discussed in section 4.2.3, which is

$$\epsilon_{\text{disp}}(k_z, k_\parallel) = 1 - \Theta(z)\frac{\omega_p^2}{k_z^2 + k_\parallel^2 - \omega_T^2} \,. \tag{5.151}$$

As discussed in section 4.2.3, a surface described by this dielectric function does not admit a mode expansion of the electromagnetic field, so we cannot derive a mode expansion in the same way as we did for the non-dispersive dielectric in section 3.2, or the plasma surface in section 3.3. However, we note that our expressions (5.99) for the magnetic moment shift near a non-dispersive surface $\epsilon(\omega) = n^2$ and (5.125) for that near a plasma surface $\epsilon(\omega) = \epsilon_p(\omega)$ are the same upon insertion of the appropriate dielectric function n^2 or $\epsilon_p(\omega)$. This leads one to strongly suspect that the formulae may have more general applicability, as we discussed in detail in section 4.2.3. Proceeding, we write down an expression for an arbitrary dielectric function $\epsilon(k_z, k_\parallel)$

$$\Delta\mu_\perp = -\frac{e^3}{32\pi^2 m^3}\int_0^\infty dk_\parallel k_\parallel \int_{C'} dk_z \frac{1}{k^3}\Big\{ \left(2k_\parallel^2 - k_z^2\right) R^L_{\mathbf{k},\text{TE}}\left[\epsilon(k_z, k_\parallel)\right] + \left(2k_\parallel^2 + k_z^2\right) R^L_{\mathbf{k},\text{TM}}\left[\epsilon(k_z, k_\parallel)\right] \Big\} e^{2ik_z z}, \tag{5.152a}$$

$$\Delta\mu_\parallel = -\frac{e^3}{32\pi^2 m^3}\int_0^\infty dk_\parallel k_\parallel \int_{C'} dk_z \frac{1}{2k^3}\Big\{ \left(3k_\parallel^2 + 2k_z^2\right) R^L_{\mathbf{k},\text{TE}}\left[\epsilon(k_z, k_\parallel)\right] + \left(3k_\parallel^2 - 2k_z^2\right) R^L_{\mathbf{k},\text{TM}}\left[\epsilon(k_z, k_\parallel)\right] \Big\} e^{2ik_z z}, \tag{5.152b}$$

which reproduces the non-dispersive shifts (5.109) and (5.110) for $\epsilon(k_z, k_\parallel) \to n^2$, and the plasma shifts (5.125) for $\epsilon(k_z, k_\parallel) \to \epsilon_p(k_z, k_\parallel)$. As discussed in section 4.2.3, there is strong justification for that validity of integrals (5.152) as expressions for the shift in the magnetic moment near a general surface. In particular, we would like to insert the dispersive dielectric function $\epsilon_{\text{disp}}(k_z, k_\parallel)$ given by eq. (5.151) into these, the validity of which is facilitated by the fact that the integration path in the k_z plane is unchanged by the introduction of the parameter ω_T, as shown in figure 5.7. This means we have for the

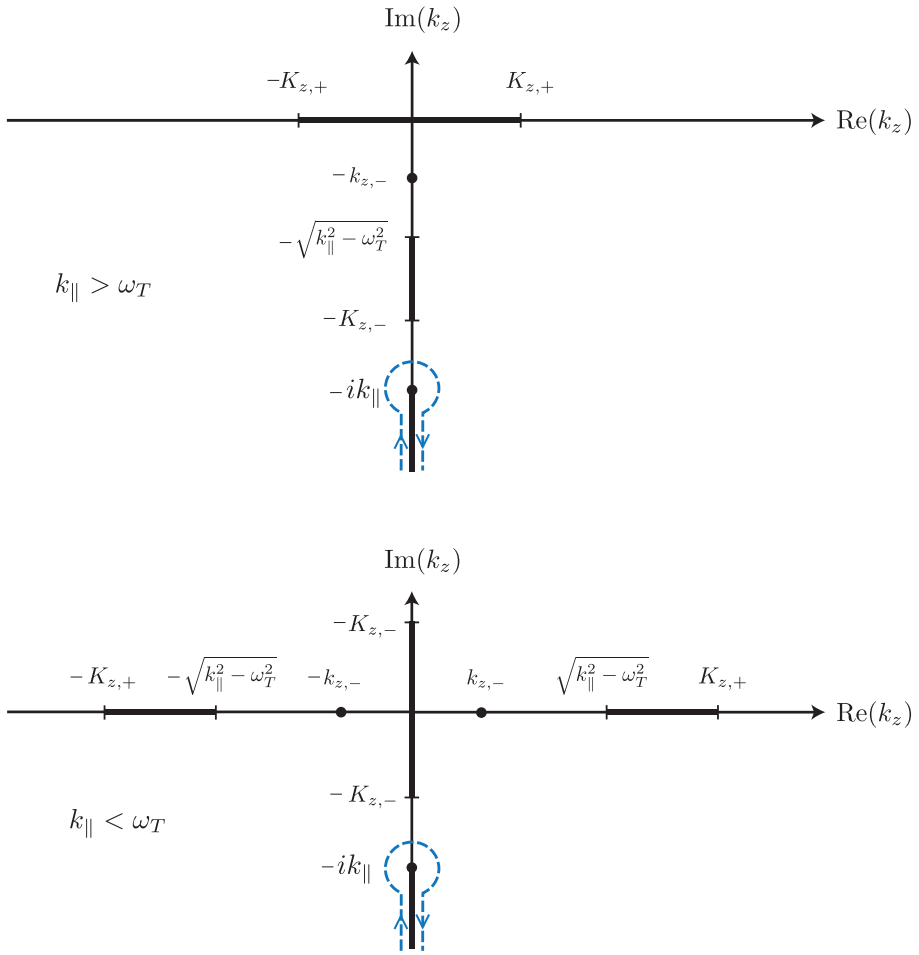

Figure 5.7: Complex k_z plane for $1/\omega$ multiplied by the dispersive dielectric reflection coefficient, with branch points and poles written via eqs. (4.87).

magnetic moment shift near a dispersive dielectric described by the permittivity (5.151)

$$\Delta\mu_\perp^{\text{disp}} = -\frac{e^3}{32\pi^2 m^3}\int_0^\infty dk_\parallel k_\parallel \int_{C'} dk_z \frac{1}{k^3}\Big\{ \left(2k_\parallel^2 - k_z^2\right) R^L_{\mathbf{k},\text{TE}}\left[\epsilon_{\text{disp}}(k_z,k_\parallel)\right] + \left(2k_\parallel^2 + k_z^2\right) R^L_{\mathbf{k},\text{TM}}\left[\epsilon_{\text{disp}}(k_z,k_\parallel)\right]\Big\} e^{2ik_z z}, \tag{5.153a}$$

$$\Delta\mu_\parallel^{\text{disp}} = -\frac{e^3}{32\pi^2 m^3}\int_0^\infty dk_\parallel k_\parallel \int_{C'} dk_z \frac{1}{2k^3}\Big\{ \left(3k_\parallel^2 + 2k_z^2\right) R^L_{\mathbf{k},\text{TE}}\left[\epsilon_{\text{disp}}(k_z,k_\parallel)\right] + \left(3k_\parallel^2 - 2k_z^2\right) R^L_{\mathbf{k},\text{TM}}\left[\epsilon_{\text{disp}}(k_z,k_\parallel)\right]\Big\} e^{2ik_z z}. \tag{5.153b}$$

Defining a complex frequency $\xi = -i\omega$, writing $(ik_z)^2 = k_\parallel^2 + \xi^2$ in polar co-ordinates $\{\xi = (ik_z)\eta, k_\parallel = (ik_z)\sqrt{1-\eta^2}\}$ and taking our usual approach of considering the $\{\xi \to$

$0, \eta \to \infty\}$ limit of the reflection coefficients separately, we manipulate eqs. (5.153) to

$$\Delta\mu_\perp^{\text{disp}} = \frac{e^3}{16\pi^2 m^3}\left\{\int_0^\infty d\xi\,\xi\int_1^\infty d\eta\Big[\left(3\eta^2-2\right)R^L_{\mathbf{k},\text{TE}}\left[\epsilon_{\text{disp}}(\xi)\right] + \left(\eta^2-2\right)\left(R^L_{\mathbf{k},\text{TM}}\left[\epsilon_{\text{disp}}(\xi)\right] - \frac{\omega_p^2}{\omega_p^2+2\omega_T^2}\right)\Big]e^{2\xi\eta z} - \frac{\omega_p^2}{\omega_p^2+2\omega_T^2}\frac{3}{4z^2}\right\}, \tag{5.154a}$$

$$\Delta\mu_\parallel^{\text{disp}} = \frac{e^3}{16\pi^2 m^3}\left\{\frac{1}{2}\int_0^\infty d\xi\,\xi\int_1^\infty d\eta\Big[\left(\eta^2-3\right)R^L_{\mathbf{k},\text{TE}}\left[\epsilon_{\text{disp}}(\xi)\right] + \left(5\eta^2-3\right)\left(R^L_{\mathbf{k},\text{TM}}\left[\epsilon_{\text{disp}}(\xi)\right] - \frac{\omega_p^2}{\omega_p^2+2\omega_T^2}\right)\Big]e^{2\xi\eta z} - \frac{\omega_p^2}{\omega_p^2+2\omega_T^2}\frac{1}{z^2}\right\}, \tag{5.154b}$$

where the dielectric function and reflection coefficients are given by

$$\epsilon_{\text{disp}}(\xi) = 1 + \Theta(z)\frac{\omega_p^2}{\xi^2+\omega_T^2}\,, \tag{5.155a}$$

$$R^L_{\mathbf{k},\text{TE}}\left[\epsilon_{\text{disp}}(\xi)\right] = \frac{\eta - \sqrt{\epsilon_{\text{disp}}(\xi)-1+\eta^2}}{\eta + \sqrt{\epsilon_{\text{disp}}(\xi)-1+\eta^2}}\,, \tag{5.155b}$$

$$R^L_{\mathbf{k},\text{TM}}\left[\epsilon_{\text{disp}}(\xi)\right] = \frac{\eta\epsilon_{\text{disp}}(\xi) - \sqrt{\epsilon_{\text{disp}}(\xi)-1+\eta^2}}{\eta\epsilon_{\text{disp}}(\xi) + \sqrt{\epsilon_{\text{disp}}(\xi)-1+\eta^2}}\,. \tag{5.155c}$$

We evaluate eqs. (5.154) numerically, and find a peak in the magnetic moment shift relative to the perfect-reflector result. To facilitate the discussion of this peak and the comparison of different models, we now choose to write the dielectric function in terms of the static limit of the dielectric susceptibility,

$$\chi(0) = \epsilon(0) - 1 = \omega_p^2/\omega_T^2\,. \tag{5.156}$$

We find peaks in $\Delta\mu_\perp$ and $\Delta\mu_\parallel$ at $\sqrt{\chi(0)} \approx 2$, with the height of the peak being inversely proportional to $\omega_T z$, as shown in fig. 5.8 for the case where the external magnetic field $\mathbf{B}_0$ is perpendicular to the interface. We also plot the corresponding shift for the non-dispersive case, where $\chi(0)_{\text{nondisp}} = n^2 - 1$. If the plot were continued to very large values of $\chi(0)$, the graphs for the two models would very slowly converge into one linearly-rising curve. By contrast, the result for the perfect reflector, also shown in fig. 5.8, is much smaller and has the opposite sign.

The peak appears if the choice of parameters is such that $|\omega_T z| \lesssim 0.07$ for $\mathbf{B}_0$ perpendicular, and $\lesssim 0.25$ for $\mathbf{B}_0$ parallel to the surface. For smaller values of $|\omega_T z|$, the peak moves closer to $\sqrt{\chi(0)} \equiv \omega_p/\omega_T \approx 2$, and increases in height. To gauge the enhancement that dispersion brings to the shift we calculate the ratio of the height of the dispersive peak to the non-dispersive result at the same $\chi(0)$, and find

$$\frac{\Delta\mu_\perp^{\text{disp}}}{\Delta\mu_\perp^{\text{nondisp}}} \approx \frac{30.3\,\text{eVnm}}{|\omega_T z|}\,, \quad \frac{\Delta\mu_\parallel^{\text{disp}}}{\Delta\mu_\parallel^{\text{nondisp}}} \approx \frac{81.6\,\text{eVnm}}{|\omega_T z|}\,. \tag{5.157}$$

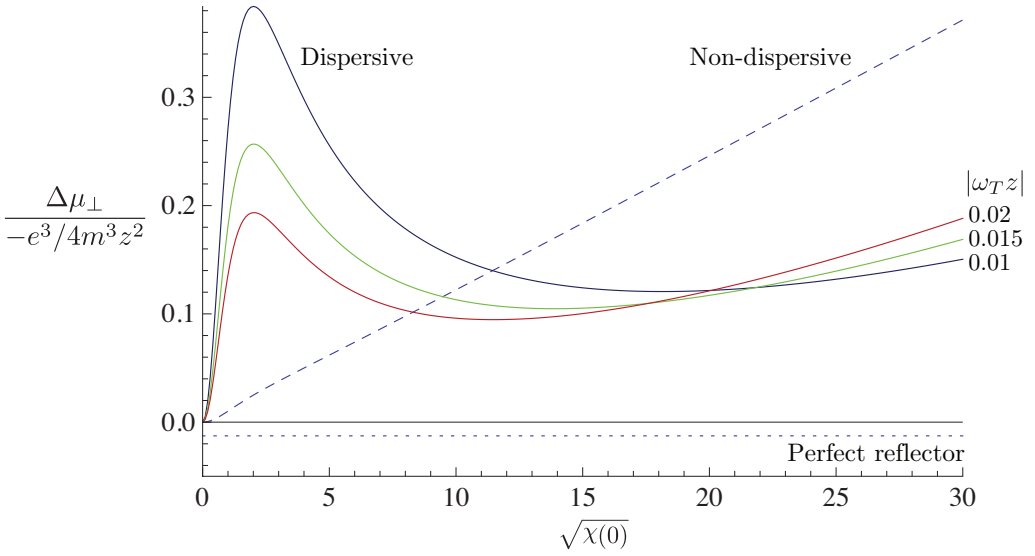

Figure 5.8: Magnetic moment shift for dispersive and non-dispersive dielectric models as a function of static susceptibility, for the case of the magnetic field $\mathbf{B}_0$ perpendicular to the surface and $|\omega_T z| = \{0.01, 0.015, 0.02.\}$

A typical value for the frequency ω_T in a metal is on the order of a few eV (see, for example, [75]), meaning that a significant enhancement relative to the non-dispersive case would be observed only at extremely small (sub-nanometer) distances z. However, restricting oneself to considering the properties of only elemental solids would be short-sighted. Structures engineered on the nanoscale can have transverse resonance frequencies ω_T significantly smaller than any ordinary material — examples include an InSb semiconductor grating with ω_T (and ω_p) in the range of a few meV [76]. These types of materials are at a focal point of strong contemporary interest in low-frequency plasmonics. With appropriate assumptions about the approximation of a part of such a structure as a planar surface[9] we find that for distances z of a few tens of nanometres one may get an enhancement factor on the order of 10^3 relative to the non-dispersive case. While such distances are on the very edge of experimental feasibility, the constantly-improving level of sophistication of manipulation and control of microscopic objects means that these effects may come to the fore in the near future.

The apparent problem of the behaviour of the non-dispersive result in the limit of large refractive index, $n \to \infty$, can be clarified by comparing it with the behaviour of the dispersive shift at large $\chi(0)$. In this regime the shift for the dispersive dielectric model becomes linear in $\sqrt{\chi(0)}$ and agrees with the non-dispersive results; so for large

[9] Since the size (Compton wavelength) of the electron is by far the smallest length scale in the problem, almost any surface in close proximity to an electron could be viewed as being planar.

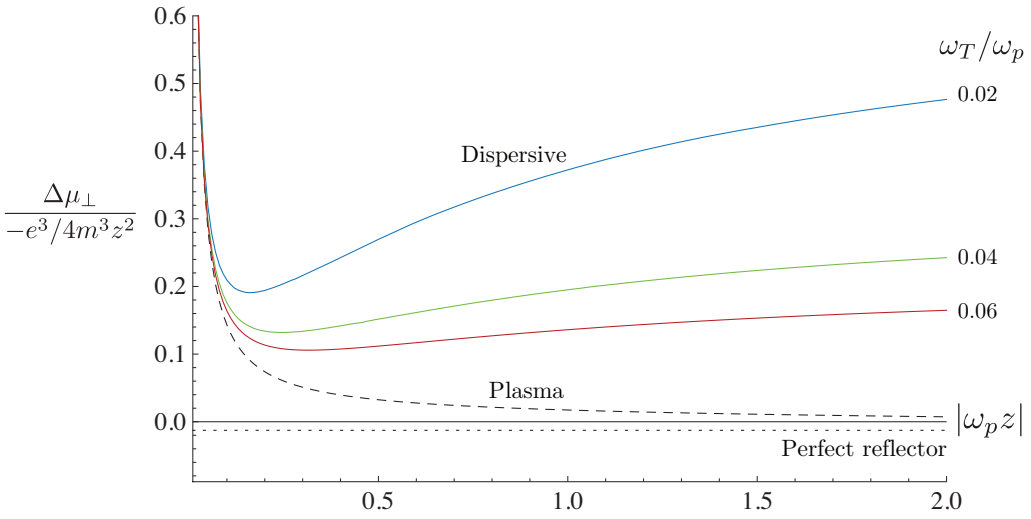

Figure 5.9: Magnetic moment shift for dispersive dielectric and plasma models as a function of scaled distance $|\omega_p z|$ from the surface, for the case of the magnetic field $\mathbf{B}_0$ perpendicular to the surface and $\omega_T/\omega_p = \{0.02, 0.04, 0.06.\}$

$\chi(0)$ the two models are equivalent. The crucial additional observation is to note that for a non-dispersive dielectric with large $\chi(0)$ we have $\chi(0) \approx n^2$, which is to say that a large refractive index necessarily implies a large static susceptibility. Therefore, in the non-dispersive model one cannot sensibly make a distinction between an arbitrarily large refractive index and an arbitrarily large static susceptibility. Investigation of the dispersive dielectric has shown that the latter interpretation is the correct one — the magnetic moment shift grows with increasing static susceptibility, but an arbitrarily large static susceptibility is, of course, physically impossible. So while the shift in the non-dispersive case does indeed increase without bound as the refractive index n is increased, this is not due any problem with the calculation, but is in fact the result of the static susceptibility growing without bound and an inevitable consequence of the unrealistic exclusion of dispersion from the model.

Consideration of the shifts in terms of the static susceptibility also emphasizes the close relationship between plasma and perfect reflector models. In both of these models the static susceptibility is infinite right from the start, which means that their results do agree in the limit $\omega_p \to \infty$.

The differences between the four models discussed above very clearly show that in order to predict the magnetic moment shift for a given set-up, one must choose a model which is physically appropriate for the low-frequency behaviour of electromagnetic response of the material at hand, just as we found with the mass shift in Chapter 4. In other

words, it matters whether the material is a conductor or an insulator. These two classes of material are not obtainable as limiting cases of each other because the conductor models ignore the existence of evanescent modes (which is a direct consequence of their static susceptibilities being infinite). The calculations for each class of model diverge from each other because of non-commutation of a variety of limits of the reflection coefficient, namely between the static limit ($k_z \to -ik_\parallel$) and whichever limit we have to take in order to compare models. For example, we note that the $n \to \infty$ and $k_z \to -ik_\parallel$ limits of the non-dispersive TE reflection coefficient do not commute, which leads to the $n \to \infty$ limit of the result for a non-dispersive dielectric to disagree with the perfect reflector result. A further important example is that the limit of vanishing transverse resonance frequency, $\omega_T \to 0$, and the static limit $k_z \to -ik_\parallel$ of the dispersive TE reflection coefficient do not commute, which means that taking $\omega_T \to 0$ ($\chi(0) \to \infty$) in the dispersive dielectric results will not reproduce the plasma results, while naive comparison of the dielectric functions (3.26) and (4.86) suggests that they should. The commutation (or lack thereof) between the various limits of the reflection coefficients was summarized in Chapter 4 by fig. 4.9 – the same analysis applies here, except of course now results connected by solid arrows have magnetic moment shifts which agree as limiting cases, rather than mass shifts.

For the plasma model, we found a $1/z^3$ dependence of the magnetic moment shift at small distances, i.e. small $|\omega_p z|$, and that the leading $1/z^3$ term can be found either by determining the asymptotics of the complete shift, or by considering only the part due to the interaction with just surface plasmons. The asymptotics of the integrals for the shift in the dispersive dielectric case are too awkward to analyse directly. Instead we give the results one obtains by considering only the interaction with the surface polariton, in the same way as was done for the surface plasmon in the plasma model. In order to do this, one needs to know the dispersion relation for the surface polariton, which we obtain by solving eq. (3.42) with the dispersive dielectric function (5.151). We find

$$\tilde{\omega}_{\rm sp}^2 = k_\parallel^2 + \frac{1}{2}(\omega_p^2 + \omega_T^2) - \sqrt{k_\parallel^4 - k_\parallel^2\omega_T^2 + \frac{1}{4}(\omega_p^2 + \omega_T^2)^2}\ . \tag{5.158}$$

Repeating the normalization process detailed in section 3.3.2 but with the dispersive dielectric function (5.151), the normalization factor $\tilde{p}(k_\parallel)$ analogous to that shown in eq. (3.49) is found to be

$$\tilde{p}(k_\parallel) = \frac{\epsilon_p^2(\tilde{\omega}_{\rm sp})\sqrt{-(1+\epsilon_p^2(\tilde{\omega}_{\rm sp}))}}{\epsilon_p^4(\tilde{\omega}_{\rm sp}) - 1}\ , \tag{5.159}$$

which is then inserted into eqs. (5.118a) and (5.118b). Following the method by which we determined (5.150), we evaluate these integrals for small $|\omega_p z|$ by changing variables such

that the z-dependence is brought out of the integrals, Taylor expanding for small $|\omega_p z|$ and the integrating term-by-term. We find

$$\Delta\mu_\perp(|\omega_p z| \ll 1) \approx \frac{e^3}{64\pi\sqrt{2}m^3 z^3}\frac{1}{\sqrt{2\omega_T^2+\omega_p^2}}\,, \tag{5.160a}$$

$$\Delta\mu_\parallel(|\omega_p z| \ll 1) \approx \frac{5e^3}{128\pi\sqrt{2}m^3 z^3}\frac{1}{\sqrt{2\omega_T^2+\omega_p^2}}\,. \tag{5.160b}$$

Surprisingly, for these short-distances $|\omega_p z| \ll 1$, we find that the $\omega_T \to 0$ limits of eqs. (5.160) *do* agree with the corresponding results for the plasma, eqs. (5.146), unlike the results for general distances $\omega_p z \gtrsim 1$. This is because these results depend only on the surface plasmon part of the mode functions and electrostatic interactions, but there is no reflection of travelling photon modes, and hence any non-commutation of limits in the reflection coefficient does not come into play.

5.4.4 Damped dispersive dielectric

The final model we wish to consider is the damped dispersive dielectric, whose dielectric function is given by eq. (4.84)

$$\epsilon_\gamma(\mathbf{r},\omega) = 1 - \Theta(z)\frac{\omega_p^2}{\omega^2-\omega_T^2+i\omega\gamma}\,. \tag{5.161}$$

As discussed in section 4.2.5 for the mass shift, our integrals in the k_z plane become ambiguous for such a dielectric function, so we proceed by transforming our integrals from the k_z plane to the ω plane. Taking our integrals for the magnetic moment shift (5.152) for any undamped dielectric function $\epsilon_{\gamma\to 0}(k_z,k_\parallel)$ and transforming to the ω plane we find

$$\begin{aligned}\Delta\mu_\perp = -\frac{e^3}{32\pi^2m^3}\int_0^\infty dk_\parallel \int_{C'_\omega} d\omega\, \frac{k_\parallel}{k_z\omega^2}\Big\{ &\left(3k_\parallel^2-\omega^2\right) R^L_{\mathrm{TE}}\left[\epsilon_{\gamma\to 0}(\omega)\right] \\ &+\left(k_\parallel^2+\omega^2\right) R^L_{\mathrm{TM}}\left[\epsilon_{\gamma\to 0}(\omega)\right]\Big\} e^{2ik_z z}\,,\end{aligned} \tag{5.162a}$$

$$\begin{aligned}\Delta\mu_\parallel = -\frac{e^3}{32\pi^2m^3}\int_0^\infty dk_\parallel \int_{C'_\omega} d\omega\, \frac{k_\parallel}{2k_z\omega^2}\Big\{ &\left(k_\parallel^2+2\omega^2\right) R^L_{\mathrm{TE}}\left[\epsilon_{\gamma\to 0}(\omega)\right] \\ &+\left(5k_\parallel^2-2\omega^2\right) R^L_{\mathrm{TM}}\left[\epsilon_{\gamma\to 0}(\omega)\right]\Big\} e^{2ik_z z}\,,\end{aligned} \tag{5.162b}$$

where the contour C'_ω is that shown in fig. 5.10. The formulae (5.162) can be simplified by subtracting the principal part of the integrand's Laurent expansion around $\omega = 0$ and re-adding it as a separate integral. For example, the separate integral for $\Delta\mu_\perp$ as shown in eq. (5.162a) is given by

$$\Delta\mu_\perp^{\mathrm{sep}} = -\frac{e^3}{32\pi^2m^3}\int_0^\infty dk_\parallel \int_{C'_\omega} d\omega \frac{k_\parallel^2}{\omega^2} R^L_{\mathrm{TM}}(0) e^{2k_\parallel z} \tag{5.163}$$

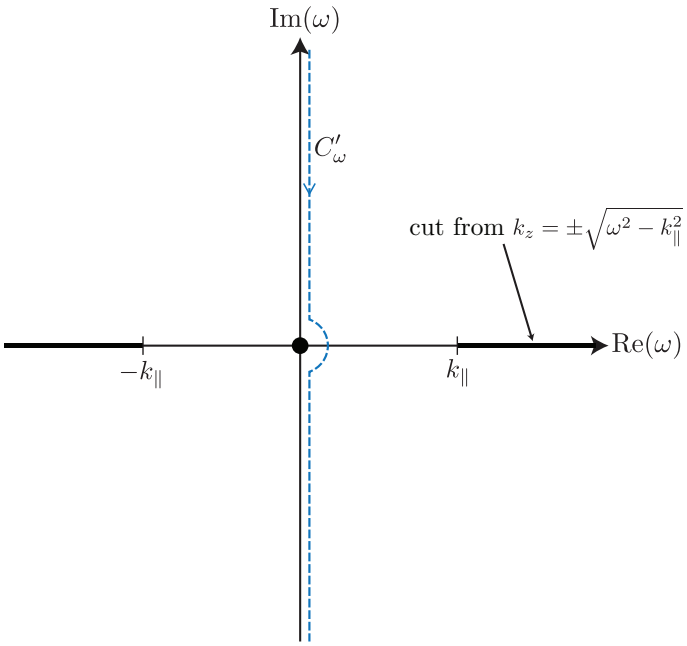

Figure 5.10: Contour C'_ω required to evaluate magnetic moment shifts in the ω plane.

The integrand of $\Delta\mu_\perp^{\text{sep}}$ at $\omega = 0$ has no poles or branch cuts in the right hand side of the ω plane. Thus we may close the contour C'_ω in either the right half plane using a semicircle of a large radius R, the contribution from which vanishes as $R \to \infty$. The closed contour encircles no poles, so the value of the integral is zero. The same result is found for the subtraction $\Delta\mu_\parallel^{\text{sep}}$ from eq. (5.162b).

Using the fact that the integrands of (5.162) are even in ω and re-writing the integrals in terms of the complex frequency $\xi = i\omega$, we obtain

$$\Delta\mu_\perp = \frac{e^3}{16\pi^2 m^3}\int_0^\infty dk_\parallel \int_0^\infty d\xi\, \frac{k_\parallel}{\xi^2}\left\{\frac{e^{2\sqrt{k_\parallel^2+\xi^2}z}}{\sqrt{k_\parallel^2+\xi^2}}\Big[\left(3k_\parallel^2+\xi^2\right) R_{\text{TE}}^L\left[\epsilon_{\gamma\to 0}(\omega)\right] + \left(k_\parallel^2-\xi^2\right) R_{\text{TM}}^L\left[\epsilon_{\gamma\to 0}(\omega)\right]\Big] - e^{2k_\parallel z} k_\parallel R_{\text{TM}}^L(0)\right\}, \tag{5.164a}$$

$$\Delta\mu_\parallel = \frac{e^3}{16\pi^2 m^3}\int_0^\infty dk_\parallel \int_0^\infty d\xi\, \frac{k_\parallel}{2\xi^2}\left\{\frac{e^{2\sqrt{k_\parallel^2+\xi^2}z}}{\sqrt{k_\parallel^2+\xi^2}}\Big[\left(k_\parallel^2-2\xi^2\right) R_{\text{TE}}^L\Big[\epsilon_{\gamma\to 0}(\omega)\Big] + \left(5k_\parallel^2+2\xi^2\right) R_{\text{TM}}^L\left[\epsilon_{\gamma\to 0}(\omega)\right]\Big] - 5e^{2k_\parallel z} k_\parallel R_{\text{TM}}^L(0)\right\}. \tag{5.164b}$$

If we attempt to include damping by making the replacement $[\epsilon_{\gamma\to 0}(\omega)] \to [\epsilon_\gamma(\omega)]$ in the same manner as for the mass shift in section 4.2.5, the integrands of (5.162) are no longer even in ω. One then needs to evaluate an integral over both positive and negative imaginary frequency. The damped reflection coefficient has poles in the lower-half plane, which means

that the portion of the integral over negative imaginary frequency does not represent an absorbing medium. This is clearly problematic; it is related to the way in which one includes absorption. Our investigation of the magnetic moment using the noise current technique Chapter 7 turns out to have the same kind of problem, which ultimately suggests that one may need to carry out a full Huttner-Barnett description of the medium [32] where each degree of freedom is individually canonically quantized in order to unambiguously calculate the magnetic moment of an electron near a dispersive and absorbing surface.

5.5 Experimental relevance

Expressing magnetic moment shifts as relative shifts $\Delta\mu/\mu$ to the Dirac magnetic moment $\mu = e/2m$, we have for the perpendicular component of the non-dispersive shift in SI units:

$$\frac{\Delta\mu_{\perp}^{\text{nondisp}}}{\mu} = \frac{\hbar}{c^3\epsilon_0}\frac{e^2}{16\pi^2 m^2 z^2} f(n) \approx \frac{10^{-11}\text{nm}^2}{z^2} , \tag{5.165}$$

where $f(n)$ is the remaining part of Eq. (5.112a), and is of order unity. For a distance $z \approx 1$nm, eqs. (5.157) (and the discussions following them) show that the enhancement due to the inclusion of dispersion can be of order 10^4 under favourable conditions. Thus, we have a magnetic moment shift of up to one part in 10^7. The current experimental accuracy for $g/2$ in free space is on the order of one part in 10^{12} [29], so that the shift calculated here would compare very favourably to this. As the distance increases to the order of a micron the effect decreases towards the limits of current experimental accuracy. For example, an electron 0.1μm away from the same surface as above would have its magnetic moment shifted by only one part in 10^{11}.

This leads one to ask if the current best techniques for measuring the g factor would be suitable for making a measurement of the surface dependent shift of the magnetic moment. Since one of the sticking points in such experiments is that sufficiently accurate measurement of the externally applied magnetic field B_0 is mostly impossible, g-factor experiments usually do not measure the magnetic moment directly, but instead they find its ratio to either a known magnetic moment, or to the cyclotron frequency of the particle under consideration. In case of the latter for surface-dependent magnetic moments shifts one would need to take into account the shift in cyclotron frequency of a particle near a surface, which arises due to the position-dependent self-energy of the particle as shown in Chapter 4 and reported elsewhere [39, 48, 47]. Crucially, the leading term of the surface-dependent cyclotron frequency shift is of order $\alpha/(mz)$ and thus much bigger than the magnetic moment shift which is of order $\alpha/(mz)^2$. So, an experiment which adapts

the techniques used for measuring the free-space g factor to find its surface dependent part would effectively be measuring the change due to the surface in its self-energy, not in its magnetic moment. While direct experimental confirmation of a shift in the self-energy would, of course, be interesting in its own right, its existence represents a significant obstacle to isolation and observation of the magnetic moment shift. We will discuss some additional aspects of the experimental viability of either measurement in Chapter 6, where we consider a more realistic situation, namely an electron in a trap.

5.6 Summary and conclusions

Beginning from perturbation theory in the Dirac equation, we have found an expression (5.96) for the magnetic moment of an electron in a quantized field in terms of the mode functions $\mathbf{f}_{\mathbf{k}\lambda}$ of that field, as defined through eq. (2.39). The formula (5.96) is

$$\Delta\mu_\perp = -\frac{e^3}{4m^3}\sum_\lambda \int d^3\mathbf{k}\Bigg[|f_{\mathbf{k}\lambda,z}|^2 + \frac{|(\nabla\times\mathbf{f}_{\mathbf{k}\lambda})_x|^2}{\omega^2} + \frac{|(\nabla\times\mathbf{f}_{\mathbf{k}\lambda})_y|^2}{\omega^2} + \frac{1}{\omega^2}\left(f_{\mathbf{k}\lambda,x}\frac{\partial^2 f^*_{\mathbf{k}\lambda,y}}{\partial x\partial y} + f_{\mathbf{k}\lambda,y}\frac{\partial^2 f^*_{\mathbf{k}\lambda,x}}{\partial x\partial y} - f_{\mathbf{k}\lambda,y}\frac{\partial^2 f^*_{\mathbf{k}\lambda,y}}{\partial x^2} - f_{\mathbf{k}\lambda,x}\frac{\partial^2 f^*_{\mathbf{k}\lambda,x}}{\partial y^2} + \text{H.c.}\right)\Bigg]. \quad (5.166)$$

Using the mode functions (3.16) for a non-dispersive dielectric, and the mode functions (3.32) and (3.50) for a plasma surface, we have calculated a shift in the magnetic moment for each surface that is attributable to a surface by finding the difference between the free-space value of the above expression and that with the surface present. Importantly, we found that each shift can be obtained from the same equation (5.164) simply by inserting the appropriate dielectric function, and hence appropriate reflection coefficients $R^L_{\mathbf{k}\lambda}$. We have then reasoned that our formula is also applicable to an undamped dispersive dielectric defined by dielectric function (5.151), as well as investigating the relationship between our work and the previously considered 'perfect reflector' models [39]. Our results for the various models can be found as outlined in table (5.1).

Model	**Result**
Perfect reflector	(5.116)
Non-dispersive dielectric	(5.112)
Plasma surface	(5.143)
Dispersive dielectric	(5.154)

Table 5.1: Locations of magnetic moment results.

For the dispersive dielectric we found a peak in the magnitude of the shift which can be tuned by judicious choice of parameters, as shown in fig. 5.8. We have shown that under favorable conditions the magnetic moment shift may be significant to current and future precision measurements of the electron's anomalous magnetic moment, however we remind the reader that the mass shift obtained in Chapter 4 is likely to be a more significant effect in real g-2 experiments such as those being done at Harvard [29].

Finally we outlined an issue with extracting results for the magnetic moment shift near a damped dispersive surface, which we will discuss in greater detail in Chapter 7.

Chapter 6

Confinement

"The electron is not completely stupid..."

- Prof. Wolfgang Lange
1962-2012

6.1 Introduction

In Chapter 5 we found the shift in the spin magnetic moment of an electron near a variety of surfaces. Aside from the magnetic field that we apply in order to find the energy shift that is due to the magnetic moment, the electron was a free particle. Precision measurements of the magnetic moment are not made under such conditions – the electron is usually confined by some trapping potential (see, for example, [29]).

In this chapter we address this by extending our method to investigate the magnetic moment shift of an electron that is subject to harmonic confinement in the directions parallel to a non-dispersive interface. We again subject the electron to constant magnetic field in order to be able to obtain the magnetic moment as the coefficient of the terms in the energy shift that are linear in this field, so our physical setup is that shown in fig. 6.1, where we have chosen to direct the magnetic field perpendicular to the plane in which the electron is trapped.

We will calculate the energy shift of the two spin states that is attributable to the surface. Just as in Chapter 5, our restriction to one-loop effects for an electron whose wave function does not overlap with the surface means that we can work with a first-quantized electron sitting in a second-quantized photon field. We will again work in the non-relativistic approximation, which means that we must find the eigenstates of the Schrödinger equation for this system.

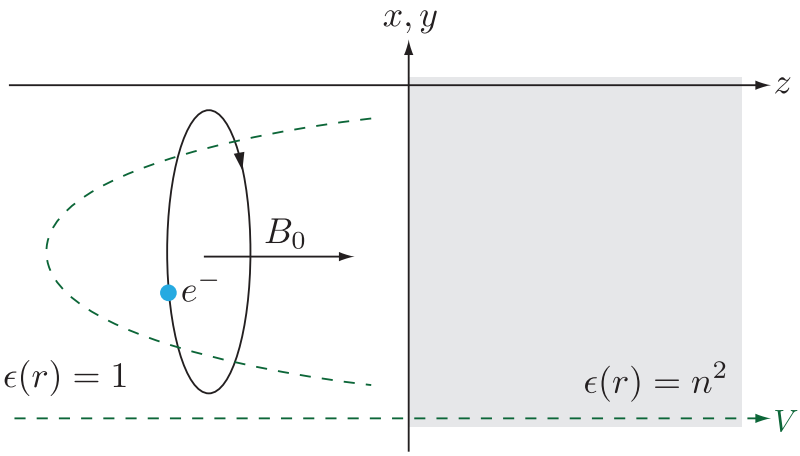

Figure 6.1: Physical setup for an electron confined near a surface, with the horizontal axis representing both the z co-ordinate (solid lines) and the potential (dashed lines)

6.2 Schrödinger eigenstates

We would like to take a non-relativistic approximation of the Dirac equation eq. (5.3) so that we can work with the Schrödinger eingenstates of the electron. In Chapter 5 we used the Dirac Hamiltonian H_D directly within second-order perturbation theory using the Dirac eigenstates for an electron in a constant magnetic field [73]. The Dirac eigenstates for an electron which is confined within a harmonic potential *as well as* a constant magnetic field are not known – finding the eigenstates for even the special case with no magnetic field is fraught with difficulty [77]. Consequently, we begin this calculation by taking the Foldy-Wouthuysen transformation [72] of the Dirac Hamiltonian, which will furnish us with the relevant Schrödinger Hamiltonian to any desired order in $1/m$, to which we can add the well-known Schrödinger Hamiltonians for the interaction with the magnetic field and the confining potential. Care must be taken since several successive applications of the transformation must be applied. As shown in Appendix D the result, in agreement with [39], is

$$H_S \equiv H_0 + H_1 + H_2, \tag{6.1}$$

with

$$H_0 = H_{\text{rad}} + \frac{\boldsymbol{\pi}^2}{2m} - \frac{e}{2m}\boldsymbol{\sigma}\cdot\mathbf{B}_0 + V_{\text{image}}, \tag{6.2}$$

$$H_1 = \frac{e^2}{2m}\mathbf{A}_Q^2 + \frac{e^3}{4m^3}\mathbf{A}_Q^2\boldsymbol{\sigma}\cdot\mathbf{B}_0, \tag{6.3}$$

$$H_2 = -\frac{e}{m}\mathbf{A}_Q\cdot\boldsymbol{\pi} - \frac{e}{2m}\boldsymbol{\sigma}\cdot\mathbf{B}_Q + \frac{e}{8m^2}\boldsymbol{\sigma}\cdot(\boldsymbol{\pi}\times\mathbf{E}_Q - \mathbf{E}_Q\times\boldsymbol{\pi}), \tag{6.4}$$

where $\mathbf{E}_Q = -\frac{\partial \mathbf{A}_Q}{\partial t}$ and $\mathbf{B}_Q = \nabla \times \mathbf{A}_Q$ are the electric and magnetic fields associated with the quantized vector potential, $\boldsymbol{\pi} = \mathbf{p} - e\mathbf{A}_0$ is the canonical momentum and V_{image} is the electrostatic image potential of the electron. H_0 is the unperturbed Hamiltonian, H_1 and H_2 are the parts contributing in first-order and second-order perturbation theory respectively.

Equation (6.1) can be used to derive the magnetic moment shift for a free electron, with results in agreement with [39, 58]. Here we additionally apply a harmonic confinement

$$V_H = \frac{m\omega_H^2}{2}(x^2 + y^2), \tag{6.5}$$

as shown in fig. (6.1). This means that the unperturbed Hamiltonian is now

$$H_0^H = H_{\text{rad}} + \frac{\boldsymbol{\pi}^2}{2m} - \frac{e}{2m}\boldsymbol{\sigma} \cdot \mathbf{B}_0 + V_{\text{image}} + V_H, \tag{6.6}$$

and the second-order perturbative expansion is

$$\Delta E = \sum_\lambda \int d^3k \left[\langle \Psi_e, 0 | H_1 | \Psi_e, 0 \rangle + \sum_{\Psi_e'} \frac{\langle \Psi_e', 1_{\mathbf{k}\lambda} | H_2 | \Psi_e, 0 \rangle |^2}{E - E'} \right], \tag{6.7}$$

where as usual $1_{\mathbf{k}\lambda}$ indicates a photon with wave vector $\mathbf{k}$ and polarisation λ, and Ψ_e represents the state of the electron which is coupled to the classical field B_0 *and* confined by V_H. The states Ψ_e are the Schrödinger eigenstates of an electron subject to a constant magnetic field and a confining potential.

We consider an electron sitting in a magnetic field B_0 directed along the z direction. The electron is also subjected to a harmonic confinement in the xy plane, with frequency ω_H. From eq. (5.16) the Schrödinger Hamiltonian is then

$$\begin{aligned} H_H &= \frac{\left(p_x + \frac{eB_0}{2}y\right)^2}{2m} + \frac{\left(p_y - \frac{eB_0}{2}x\right)^2}{2m} + \frac{p_z^2}{2m} + \frac{m\omega_H^2}{2}(x^2 + y^2) \\ &= \frac{p_x^2 + p_y^2 + p_z^2}{2m} + \frac{m\Omega^2}{2}(x^2 + y^2) - \frac{eB_0}{2m}L_z \,, \end{aligned} \tag{6.8}$$

where L_z is the z-component of the angular momentum operator $L_z = xp_y - p_x y$, and we define

$$\Omega^2 = \omega_H^2 + \left(\frac{eB_0}{2m}\right)^2 . \tag{6.9}$$

As an aside we note that if the electron were confined in the z direction ($V_H \to \frac{m\omega_H^2}{2}z^2$) very little would change in (6.8) relative to the case with no trapping potential. The Hamiltonian would be separable into an xy-dependent part identical to the unbound case and a part which depends on z. This means that the only modification of the wave function would be multiplication by a z dependent part. We are only interested in the energy shifts

of the spin states, so the precise wave function in the z direction (i.e. that which is along the magnetic field) does not matter, as long as the electron is confined far enough away from the surface that there is no wave function overlap.

Proceeding, we follow [74] by introducing

$$\begin{aligned} \hat{x} &= \frac{1}{\sqrt{2m\Omega}}(\hat{b}_x + \hat{b}_x^\dagger), & \hat{p}_x &= i\sqrt{\frac{m\Omega}{2}}(\hat{b}_x^\dagger - \hat{b}_x), \\ \hat{y} &= \frac{1}{\sqrt{2m\Omega}}(\hat{b}_y + \hat{b}_y^\dagger), & \hat{p}_y &= i\sqrt{\frac{m\Omega}{2}}(\hat{b}_y^\dagger - \hat{b}_y), \end{aligned} \tag{6.10}$$

which are analogous to the operators (5.17) used in the unbound case. Using eqs. (6.10), the Hamiltonian may be written as

$$H_H = \frac{\Omega}{2}(\hat{b}_x^\dagger \hat{b}_x + \hat{b}_x \hat{b}_x^\dagger + \hat{b}_y^\dagger \hat{b}_y + \hat{b}_y \hat{b}_y^\dagger) - \frac{ieB_0}{2m}(\hat{b}_x \hat{b}_y^\dagger - \hat{b}_y \hat{b}_x^\dagger) + \frac{\hat{p}_z^2}{2m} ,$$

where p_z has been promoted to an operator $\hat{p}_z$, with eigenvalue p_z. Further defining the operators for right and left-circular quanta

$$\hat{b}_R = \frac{1}{\sqrt{2}}\left(\hat{b}_x - i\hat{b}_y\right) \qquad \hat{b}_L = \frac{1}{\sqrt{2}}\left(\hat{b}_x + i\hat{b}_y\right) , \tag{6.11}$$

one finds

$$H_H = \frac{\Omega}{2}(\hat{b}_R^\dagger \hat{b}_R + \hat{b}_R \hat{b}_R^\dagger + \hat{b}_L^\dagger \hat{b}_L + \hat{b}_L \hat{b}_L^\dagger) + \frac{eB_0}{2m}(\hat{b}_L \hat{b}_L^\dagger - \hat{b}_R \hat{b}_R^\dagger) + \frac{\hat{p}_z^2}{2m} . \tag{6.12}$$

Taking advantage of the commutation relation $[\hat{b}_R, \hat{b}_R^\dagger] = 1 = [\hat{b}_L, \hat{b}_L^\dagger]$ this can be written as

$$H_H = \left(\Omega - \frac{eB_0}{2m}\right)\hat{b}_R^\dagger \hat{b}_R + \left(\Omega + \frac{eB_0}{2m}\right)\hat{b}_L^\dagger \hat{b}_L + \Omega + \frac{\hat{p}_z^2}{2m} . \tag{6.13}$$

Since our $e < 0$, the limit $\omega_H \to 0$ is equivalent to the limit $\Omega \to -\frac{eB_0}{2m}$. In this limit, the above Hamiltonian becomes

$$H_H(\omega_H \to 0) = -\frac{eB_0}{m}\left(\hat{b}_R^\dagger \hat{b}_R + \frac{1}{2}\right) + \frac{\hat{p}_z^2}{2m} = H_S , \tag{6.14}$$

which is the usual statement of the Landau-quantized Schrödinger Hamiltonian H_S, given by eq. (5.20). The energy eigenvalues of H_c for an eigenstate $|n_L\rangle \otimes |n_R\rangle = |n_L, n_R\rangle$ are

$$E_H = \left(\Omega - \frac{eB}{2m}\right) n_R + \left(\Omega + \frac{eB}{2m}\right) n_L + \Omega + \frac{p_z^2}{2m} . \tag{6.15}$$

It is useful to define

$$\Delta_R \equiv \Omega - \frac{eB_0}{2m}, \qquad \Delta_L \equiv \Omega + \frac{eB_0}{2m} \qquad \to \qquad \Delta_i \equiv \Omega - h_i \frac{eB_0}{2m}, \tag{6.16}$$

where h_i denotes the handedness of the Landau states via

$$h_R = +1, \qquad h_L = -1, \tag{6.17}$$

so that the Hamiltonian may be written as

$$\begin{aligned} H_H &= \Delta_L \hat{b}_L \hat{b}_L^\dagger + \Delta_R \hat{b}_R \hat{b}_R^\dagger + \Omega + \frac{p_z^2}{2m} \\ &= \Omega + \frac{p_z^2}{2m} + \sum_{i=L,R} \Delta_i \hat{b}_i \hat{b}_i^\dagger \,. \end{aligned} \tag{6.18}$$

The canonical momenta can be written in terms of $\hat{b}_R$ and $\hat{b}_L$ via eqs. (6.10)

$$\hat{\pi}_x = \hat{p}_x + \frac{eB_0}{2}\hat{y} = \frac{i}{2}\sqrt{\frac{m}{\Omega}}\left[\Delta_R(\hat{b}_R^\dagger - \hat{b}_R) + \Delta_L(\hat{b}_L^\dagger - \hat{b}_L)\right], \tag{6.19a}$$

$$\hat{\pi}_y = \hat{p}_y - \frac{eB_0}{2}\hat{x} = \frac{1}{2}\sqrt{\frac{m}{\Omega}}\left[\Delta_R(\hat{b}_R^\dagger + \hat{b}_R) - \Delta_L(\hat{b}_L^\dagger + \hat{b}_L)\right], \tag{6.19b}$$

and of course $\hat{\pi}_z = \hat{p}_z$. These equations deliver the non-zero matrix elements

$$\langle n_R', n_L' | \pi_x | n_R, n_L \rangle \,, \quad \langle n_R', n_L' | \pi_y | n_R, n_L \rangle \,, \quad \text{with} \quad (n_R' = n_R \pm 1, n_L' = n_L \pm 1), \tag{6.20}$$

listed in appendix B.2. The electromagnetic field is, as usual, written in terms of mode functions $\mathbf{f}_{\mathbf{k}\lambda}$ via (2.39)

$$\hat{\mathbf{A}}(\mathbf{r}, t) = \sum_\lambda \int d^3\mathbf{k} \left[\hat{a}_{\mathbf{k}\lambda} e^{-i\omega_k t}\mathbf{f}_{\mathbf{k}\lambda}(\mathbf{r}, \omega) + \hat{a}_{\mathbf{k}\lambda}^\dagger e^{i\omega_k t}\mathbf{f}_{\mathbf{k}\lambda}^*(\mathbf{r}, \omega)\right] \,, \tag{6.21}$$

where $\hat{a}_{\mathbf{k}\lambda}$ and $\hat{a}_{\mathbf{k}\lambda}^\dagger$ are creation and annihilation operators for photons of wavenumber k and polarization λ. They are normalized so that the Hamiltonian for the radiation field is in the canonical form

$$H_{\text{rad}} = \sum_\lambda \int d^3\mathbf{k}\, \omega_k \left(\hat{a}_{\mathbf{k}\lambda}^\dagger \hat{a}_{\mathbf{k}\lambda} + \frac{1}{2}\right) \,. \tag{6.22}$$

The mode functions $\mathbf{f}_{\mathbf{k}\lambda}$ for the quantized field near a non-dispersive dielectric are shown in eqs (3.16). Using second order perturbation theory, we can use the modes to derive the energy shift (3.16) of the vacuum state that is attributable to the quantized field. While in previous calculations we found a magnetic moment shift by simply Taylor-expanding the energy shift for small B_0 and extracting the linear term, here there are difficulties stemming from the additional confinement by the harmonic potential. The main consequence of this is that there is a proliferation of terms of different types, many of which turn out to be of no interest to any real experiment. For these reasons we consider which asymptotic regime we are interested in before doing any explicit calculations.

6.3 Asymptotic regimes

In section 5.1.4 we noted that our calculations for the free electron are always in the non-retarded regime

$$\frac{eB_0}{m} \ll \frac{c}{z} \,, \tag{6.23}$$

where we have temporarily switched back to S.I. units meaning that both sides of the above equation are in Hz. Typical magnetic field strengths used in experiments with trapped electrons are relatively strong, usually of Tesla order [78, 79], giving

$$\frac{eB_0}{m} \sim 10^{11}\text{Hz} \,. \tag{6.24}$$

Combined with eq. (6.23), this constrains z to be $\ll$ 3mm, which is comfortably within the reach of modern trapping technology. The only other frequency scale in the problem the trap frequency ω_H, which we will estimate for two possible settings. The first of these is an electron in a Penning trap, for which the closest analogue of our trap frequency is the magnetron motion, which is of order 100kHz (see, for example, [29]). The second is an electron bound to a nucleus, for a hydrogen atom the frequency of the 'trap' is a few eV $\sim 10^{15}$Hz. We then have three cases to look at

1. $\omega_H \ll \frac{eB_0}{m} \ll \frac{c}{z}$

   The constraint $\omega_H \ll \frac{eB_0}{m}$ means that Penning traps are the most relevant type of binding potential, as explained above. But, since ω_H is necessarily small, the trapping potential is very weak so one expects no significantly new behavior relative to the free space case.

2. $\frac{eB_0}{m} \ll \omega_H \ll \frac{c}{z}$

   We now have $\omega_H \gg \frac{eB_0}{m}$, meaning that an electron bound to an atom is the most relevant physical system. But we now have the additional condition that $\omega_H \ll \frac{c}{z}$ which, for the atomic trap frequency of 10^{15}Hz corresponds to a distance $z \ll$ 100nm, which is a much less realistically obtainable atom-surface distance than that in the next regime discussed.

3. $\frac{eB_0}{m} \ll \frac{c}{z} \ll \omega_H$

   Again the most relevant physical system is an atomic electron. But we now have trap frequency vs distance constraint is now $\omega_H \gg \frac{c}{z}$ which corresponds to a distance $z \gg$ 100nm. This means we can consider larger distances which are within reach of experiments. The upper limit on the distance is imposed by the fundamental constraint $\frac{eB_0}{m} \ll \frac{c}{z}$, which corresponds to $z \ll$ 3mm as noted above.

For these reasons we choose to consider our integrals in the third asymptotic regime ($\frac{eB_0}{m} \ll \frac{c}{z} \ll \omega_H$), which we shall express in natural units as $|\omega_H z| \gg 1$ or, equivalently, $|\Delta_i z| \gg 1$.

6.4 Evaluation of the energy shift

As in previous calculations, it is important to note the multipole expansion of $\mathbf{A}_Q$ given by (5.34) is significant since it may generate additional factors of B_0, which of course is important when attempting to extract a magnetic moment.

The only first term in H_1 has no σ_z dependence so is discarded. Taking the second term only, we find:

$$\begin{aligned}\Delta E^{(1)}_{\sigma_z} &= \frac{e^3}{4m^3}\sigma_z B_0 \langle 0, n_L, n_R, s| \mathbf{A}_Q^2 |0, n_L, n_R, s\rangle \\ &= \frac{e^3}{4m^3}\sigma_z B_0 \int d^3\mathbf{k} \sum_\lambda \left(|f_x|^2 + |f_y|^2 + |f_z|^2\right) \ . \end{aligned} \tag{6.25}$$

Using Maxwell's equations in the absence of sources we can manipulate the second-order contribution H_2 to

$$H_2 = -\frac{e}{m}\mathbf{A}_Q \cdot \boldsymbol{\pi} - \frac{e}{4m^2}\boldsymbol{\sigma}\cdot(\mathbf{E}_Q \times \boldsymbol{\pi}) - \frac{e}{2m}\boldsymbol{\sigma}\cdot\mathbf{B}_Q + \frac{ie}{8m^2}\boldsymbol{\sigma}\cdot\frac{\partial \mathbf{B}_Q}{\partial t} \ . \tag{6.26}$$

In the dipole approximation (where the field operators $\mathbf{A}_Q$, $\mathbf{E}_Q$ and $\mathbf{B}_Q$ do not act on the Landau levels) the first two terms of eq. (6.26) can only contribute when $s = s'$, and the second two can only contribute when $s \neq s'$. The contribution of the first two terms of eq. (6.26) in second-order perturbation theory is

$$\Delta E^{(2)}_{\text{dip}} = \frac{e^2}{m^2}\int d^3\mathbf{k} \sum_\lambda \sum_{n'_R, n'_L} \frac{|\langle n'_R, n'_L; 1_{\mathbf{k},\lambda}| \left(\mathbf{A}_Q + \frac{\boldsymbol{\sigma}\times\mathbf{E}}{4m}\right)\cdot\boldsymbol{\pi}\, |n_R, n_L; 0\rangle|^2}{-\omega + E_{n_L,n_R} - E_{n'_L,n'_R}} \ . \tag{6.27}$$

Evaluating the four contributions to the sum over Landau levels ($n'_R = n_R \pm 1$, $n'_L = n_L \pm 1$), and defining a generalized summation symbol

$$\tilde{\sum} \equiv \int d^3\mathbf{k} \sum_{\lambda=\text{TE,TM}} \sum_{i=L,R} \ , \tag{6.28}$$

the part of the energy shift proportional to σ_z may be written as

$$\Delta E^{(2)}_{\text{dip},\sigma_z} = -\frac{e^2}{8m^2}\sigma_z \tilde{\sum} \omega h_i (|f_x|^2 + |f_y|^2) \frac{\Delta_i^2}{\Omega}\left(\frac{\Delta_i(2n_i+1) - \omega}{\omega^2 - \Delta_i^2}\right), \tag{6.29}$$

where, along the lines of eqs. (5.56) and the discussions following them, some terms have been discarded because their polarization vectors mean they are trivially zero under the angular part of $d^3\mathbf{k}$ when written in the system of spherical polar co-ordinates shown in eqs. (5.56).

Moving on to the second two terms of eq. (6.26)

$$\begin{aligned}\Delta E^{(2)}_{\text{spin}} =& \frac{e^2}{2m^2}\int d^3\mathbf{k} \sum_\lambda \sum_{s'=\uparrow,\downarrow} \frac{|\langle 1_{\mathbf{k},\lambda}, s'| \frac{i}{4m}\boldsymbol{\sigma}\cdot\frac{\partial \mathbf{B}_Q}{\partial t} - \boldsymbol{\sigma}\cdot\mathbf{B}_Q |0, s\rangle|^2}{-\omega - E_{s'} + E_s} \\ =& \frac{e^2}{4m^2}\int d^3\mathbf{k} \frac{1}{\omega}\sum_\lambda \sum_{s'=\uparrow,\downarrow} \frac{|\langle s'| \left(\frac{i}{4m}\frac{\partial}{\partial t} - 1\right)\boldsymbol{\sigma}\cdot(\nabla\times\mathbf{f})\, |s\rangle|^2}{-\omega - E_{s'} + E_s} \ , \end{aligned} \tag{6.30}$$

where

$$E_\uparrow = -\frac{eB_0}{2m}, \qquad E_\downarrow = \frac{eB_0}{2m}. \tag{6.31}$$

We require the shift in the difference in energies between the two spin states, which is

$$\Delta E^{(2)}_{\text{spin},\sigma_z} = \frac{\sigma_z}{2}\left[\Delta E^{(2)}_{\text{spin}}(s=\downarrow) - \Delta E^{(2)}_{\text{spin}}(s=\uparrow)\right] . \tag{6.32}$$

It is useful to use eq. (5.28) to rewrite the operators appearing in eq. (6.30) as

$$\boldsymbol{\sigma}\cdot(\nabla\times\mathbf{f}) = \frac{1}{2}\left[\sigma^{(-)}(\nabla\times\mathbf{f})^{(+)} + \sigma^{(+)}(\nabla\times\mathbf{f})^{(-)}\right] + \sigma_z f_z . \tag{6.33}$$

Using this to evaluate the shifts for $s' = \uparrow, \downarrow$, we find

$$\Delta E^{(2)}_{\text{spin}}(s'=\uparrow) = \frac{e^2}{4m^2}\int d^3\mathbf{k}\sum_\lambda \frac{1}{-\omega + {}^{eB_0}\!/_m}\left(1+\frac{\omega}{4m}\right)^2 \left|(\nabla\times\mathbf{f}^*)_x - i(\nabla\times\mathbf{f}^*)_y\right|^2 \tag{6.34}$$

$$\Delta E^{(2)}_{\text{spin}}(s'=\downarrow) = \frac{e^2}{4m^2}\int d^3\mathbf{k}\sum_\lambda \frac{1}{-\omega - {}^{eB_0}\!/_m}\left(1+\frac{\omega}{4m}\right)^2 \left|(\nabla\times\mathbf{f}^*)_x + i(\nabla\times\mathbf{f}^*)_y\right|^2 . \tag{6.35}$$

Inserting these into eq. (6.32) and again dropping some terms which are odd under $\int d^3\mathbf{k}$, we find

$$\Delta E^{(2)}_{\text{spin},\sigma_z} = -\sigma_z\frac{e^3B_0}{4m^3}\int d^3\mathbf{k}\sum_\lambda \left(1+\frac{\omega}{4m}\right)^2 \frac{1}{\left(\frac{eB_0}{m}\right)^2-\omega^2}\left[|(\nabla\times\mathbf{f}^*)_x|^2 + |(\nabla\times\mathbf{f}^*)_y|^2\right] . \tag{6.36}$$

We have now found all the terms which, in the dipole approximation, are proportional to σ_z. We can check for consistency with the unbound case by taking the limits $\omega_T \to 0$ and $B_0 \to 0$ of (6.29) and (6.36), extracting the coefficient of B_0 and comparing to the first line of (5.96) (i.e. the magnetic moment shift excluding the quadrupole terms). Beginning with the same-spin ($s = s'$) transitions, the prefactor of eq. (6.29) becomes

$$\begin{aligned}\lim_{\omega_H\to 0}\left[-\frac{e^2}{8m^2}\sigma_z\sum_{i=L,R}\omega h_i\frac{\Delta_i^2}{\Omega}\left(\frac{\Delta_i(2n_i+1)-\omega}{\omega^2-\Delta_i^2}\right)\right] \\ = -\frac{e^3}{16m^3}\sigma_z B_0\sum_{i=L,R}h_i(1+h_i)^2 = -\frac{e^3}{4m^3}\sigma_z B_0 ,\end{aligned} \tag{6.37}$$

with the same result if small B_0 is taken before small ω_H. So we have for the unbound limit of the magnetic moment arising from (6.29)

$$\Delta E^{(2)}_{\text{dip},\sigma_z}(\text{unbound limit}) = -\frac{e^3}{4m^3}\int d^3\mathbf{k}\sum_\lambda \sigma_z B_0(|f_x|^2 + |f_y|^2) \tag{6.38}$$

The first order term (6.25) is independent of ω_H and already linear in B_0, so we can combine this with the unbound limit of the dipole terms (6.38) to find

$$\Delta E_{\mathrm{dip},\sigma_z} = -\frac{e^3}{4m^3}\sigma_z B_0 \int d^3\mathbf{k} \sum_\lambda |f_z^2| \,, \tag{6.39}$$

in agreement with eq. (5.95), which is the part of the magnetic moment shift that is due to same-spin transitions in the dipole approximation. Similarly, taking a small B_0 expansion of (6.36) yields the spin flip part of the unbound magnetic moment eq. (5.67).

We now check for terms that contribute beyond the dipole approximation. Expanding each term of H_2 via eq. (5.34), one finds two additional contributions. The first of these comes from application of the multipole operator to the term in $\boldsymbol{\sigma}\cdot\mathbf{B}_Q$.

$$\Delta E^{(2)}_{\mathrm{quad},1} = \frac{e^2}{2m^2}\tilde{\sum}\frac{1}{E_{LR}}\Big[\langle n_R, n_L; 0|\, \mathbf{A}_Q\cdot\boldsymbol{\pi}\, |n'_R, n'_L; 1_{\mathbf{k},\lambda}\rangle \\ \times \langle n'_R, n'_L; 1_{\mathbf{k},\lambda}|\, [(\mathbf{r}-\mathbf{r}_0)\cdot\nabla]\, \sigma_z B_{Q,z}\, |n_R, n_L; 0\rangle + \text{C.C.}\Big], \tag{6.40}$$

where $E_{LR} \equiv -\omega + E_{n_L,n_R} - E_{n'_L,n'_R}$ and $\boldsymbol{\sigma}\cdot\mathbf{B}_Q \to \sigma_z B_{Q,z}$ has been taken since the term in $\mathbf{A}_Q\cdot\boldsymbol{\pi}$ cannot change the spin state. Similarly, there is a contribution from the application of the multipole operator to the term in $\mathbf{A}_Q\cdot\boldsymbol{\pi}$

$$\Delta E^{(2)}_{\mathrm{quad},2} = \frac{e^2}{2m^2}\tilde{\sum}\frac{1}{E_{LR}}\Big[\langle n_R, n_L; 0|\, [(\mathbf{r}-\mathbf{r}_0)\cdot\nabla]\, \mathbf{A}_Q\cdot\boldsymbol{\pi}\, |n'_R, n'_L; 1_{\mathbf{k},\lambda}\rangle \\ \times \langle n'_R, n'_L; 1_{\mathbf{k},\lambda}|\, \sigma_z B_{Q,z}\, |n_R, n_L; 0\rangle + \text{C.C.}\Big]. \tag{6.41}$$

Inserting the vector potential (6.21) into eqs. (6.40) and (6.41) we find for the contributions proportional to σ_z

$$\Delta E^{(2)}_{\mathrm{quad},1,\sigma_z} = \frac{e^2\sigma_z}{8m^2}\tilde{\sum} h_i \frac{\Delta_i}{\Omega}\frac{\Delta_i - (2n_i+1)\omega}{\omega^2-\Delta_i^2} \\ \times\left(f_y\frac{\partial^2 f_y^*}{\partial x^2} + f_x\frac{\partial^2 f_x^*}{\partial y^2} - f_x\frac{\partial^2 f_y^*}{\partial x\partial y} - f_y\frac{\partial^2 f_x^*}{\partial x\partial y}\right) + \text{C.C.} \tag{6.42}$$

$$\Delta E^{(2)}_{\mathrm{quad},2,\sigma_z} = \frac{e^2}{2m^2}\sigma_z\tilde{\sum}\frac{eB_0}{2m\Omega}\left(n_i+\frac{1}{2}\right)\frac{|(\nabla\times\mathbf{f})_z|^2}{\omega}, \tag{6.43}$$

where we have discarded terms independent of B_0. We now have the entire expression of the part of the energy shift that is proportional to σ_z

$$\Delta E_{\sigma_z} = \Delta E^{(1)}_{\sigma_z} + \Delta E^{(2)}_{\mathrm{dip},\sigma_z} + \Delta E^{(2)}_{\mathrm{spin},\sigma_z} + \Delta E^{(2)}_{\mathrm{quad},1,\sigma_z} + \Delta E^{(2)}_{\mathrm{quad},2,\sigma_z}, \tag{6.44}$$

in terms of the mode functions $f_{\mathbf{k}\lambda}$. We split the shift (6.44) into

$$\Delta E^{a}_{\sigma_z} = \Delta E^{(2)}_{\mathrm{dip},\sigma_z} + \Delta E^{(2)}_{\mathrm{quad},1,\sigma_z}, \tag{6.45}$$

$$\Delta E^{b}_{\sigma_z} = \Delta E^{(1)}_{\sigma_z} + \Delta E^{(2)}_{\mathrm{spin},\sigma_z} + \Delta E^{(2)}_{\mathrm{quad},2,\sigma_z}, \tag{6.46}$$

where $\Delta E^a_{\sigma_z}$ contains the terms that contribute at $\{n'_L, n'_R\} \neq \{n_L, n_R\}$ (i.e. those which have a transition between Landau levels) and $\Delta E^b_{\sigma_z}$ contains the terms that contribute only within the same Landau level $\{n'_L, n'_R\} = \{n_L, n_R\}$.

6.4.1 Transitions between Landau levels

To evaluate $\Delta E^a_{\sigma_z}$, we substitute the non-dispersive modes (3.16) into eqs. (6.29) and (6.42), giving

$$\begin{aligned}\Delta E^{\sigma_z}_{\text{dip}} = &-\frac{e^2}{8m^2}\frac{1}{(2\pi)^3}\sigma_z \sum_{\lambda,i,\vartheta}\int d^2\mathbf{k}_\parallel \Bigg\{ \int_0^\infty dk_z\, \alpha^\vartheta_\lambda [1+|R^L_\lambda|^2] \\ &+ \frac{1}{n^2}\int_{-\infty}^{-\Gamma} dk^d_z \alpha^\vartheta_\lambda |T^R_\lambda|^2 + \vartheta \int_0^\infty dk_z\, \alpha^\vartheta_\lambda R^L_\lambda (e^{2ik_z z} + e^{-2ik_z z}) \\ &+ \frac{\vartheta}{n^2}\int_{-\Gamma}^0 dk^d_z \alpha^\vartheta_\lambda |T^R_\lambda|^2 e^{2ik_z z}\Bigg\} h_i \frac{\Delta_i^2}{\Omega}\frac{\Delta_i(2n_i+1)-\omega}{\omega^2-\Delta_i^2}, \end{aligned} \tag{6.47}$$

$$\begin{aligned}\Delta E^{\sigma_z}_{\text{quad}} = &\frac{e^2}{8m^2}\frac{1}{(2\pi)^3}\sigma_z \sum_{\lambda,i,\vartheta}\int d^2\mathbf{k}_\parallel \Bigg\{ \int_0^\infty dk_z\, \beta^\vartheta_\lambda [1+|R^L_\lambda|^2] \\ &+ \frac{1}{n^2}\int_{-\infty}^{-\Gamma} dk^d_z \beta^\vartheta_\lambda |T^R_\lambda|^2 + \vartheta \int_0^\infty dk_z\, \beta^\vartheta_\lambda R^L_\lambda (e^{2ik_z z} + e^{-2ik_z z}) \\ &+ \frac{\vartheta}{n^2}\int_{-\Gamma}^0 dk^d_z \beta^\vartheta_\lambda |T^R_\lambda|^2 e^{2ik_z z}\Bigg\} \frac{h_i\Delta_i}{\omega\Omega}\frac{\Delta_i-(2n_i+1)\omega}{\omega^2-\Delta_i^2}, \end{aligned} \tag{6.48}$$

with

$$\alpha^+_{\text{TE}} = \frac{k_y^2}{2kk_\parallel^2}, \qquad \alpha^-_{\text{TM}} = \frac{k_x^2k_z^2}{2k^3k_\parallel^2}, \qquad \beta^+_{\text{TE}} = \frac{k_x^2k_y^2}{2kk_\parallel^2} - \frac{k_y^4}{2kk_\parallel^2},$$
$$\{\alpha^-_{\text{TE}}, \alpha^+_{\text{TM}}, \beta^-_{\text{TE}}, \beta^+_{\text{TM}}, \beta^-_{\text{TM}} = 0\}\,. \tag{6.49}$$

and where Γ as defined in eq. (4.30) is the critical value of k^d_z for which medium-incident modes are totally internally reflected and thus become evanescent on the vacuum side. The summation symbol is

$$\sum_{\lambda,i,\vartheta} \equiv \sum_{\lambda=\text{TE,TM}}\sum_{i=L,R}\sum_{\vartheta=\pm1}\,.$$

Exactly following the method used in Chapters 4 and 5, we use the relation $dk^d_z = n^2(k_z/k^d_z)dk_z$ to manipulate the first two of the four terms of eq. (6.47) to

$$\int_0^\infty dk_z\, \alpha^\vartheta_\lambda \left[1+|R^L_\lambda|^2 + \frac{k_z}{k^d_z}|T^R_\lambda|^2\right] = 2\int_0^\infty dk_z\, \alpha^\vartheta_\lambda\,, \tag{6.50}$$

where the equality follows since k_z and k^d_z are here both real. The second two terms in eq. (6.47) contain the z dependent terms and can be written as:

$$\vartheta\int_0^\infty dk_z\, \alpha^\vartheta_\lambda R^L_\lambda (e^{2ik_z z} + e^{-2ik_z z}) + \vartheta\int_0^{i\Gamma/n} dk_z \frac{k_z}{k^d_z}\alpha^\vartheta_\lambda |T^R_\lambda|^2 e^{2ik_z z}\,. \tag{6.51}$$

Restating equation (4.34) (which holds for imaginary k_z only)

$$R^L_{\mathbf{k}\lambda}(n^2)|_{k_z^d=-K} - R^L_{\mathbf{k}\lambda}(n^2)|_{k_z^d=K} = \frac{k_z}{k_z^d} T^R_{\mathbf{k}\lambda}(n^2) T^{R*}_{\mathbf{k}\lambda}(n^2)|_{k_z^d=-K} \,, \tag{6.52}$$

we find that we can manipulate the second integral in (6.51) in such a way that it can be combined with the first, as discussed in detail in section 4.2.1. This means that eq. (6.51) becomes

$$\vartheta \int_C dk_z \, \alpha^\vartheta_\lambda R^L_\lambda e^{2ik_z z} \,, \tag{6.53}$$

with the contour C as shown in Fig. (6.2). Rearranging eq. (6.48) in precisely the same way, we arrive at

$$\begin{aligned} \Delta E^{\sigma_z}_{\text{dip}} = &- \frac{e^2}{8m^2} \frac{1}{(2\pi)^3} \sigma_z \sum_{\lambda,i,\vartheta} \int d^2\mathbf{k}_\parallel \left\{ \vartheta \int_C dk_z \, \alpha^\vartheta_\lambda R^L_\lambda e^{2ik_z z} + 2 \int_0^\infty dk_z \, \alpha^\vartheta_\lambda \right\} \\ &\times \frac{h_i \Delta_i^2}{\Omega} \frac{\Delta_i(2n_i+1) - \omega}{\omega^2 - \Delta_i^2} \end{aligned} \tag{6.54}$$

$$\begin{aligned} \Delta E^{\sigma_z}_{\text{quad}} = &\frac{e^2}{8m^2} \frac{1}{(2\pi)^3} \sum_{\lambda,i,\vartheta} \int d^2\mathbf{k}_\parallel \left\{ \vartheta \int_C dk_z \, \beta^\vartheta_\lambda R^L_\lambda e^{2ik_z z} + 2 \int_0^\infty dk_z \, \beta^\vartheta_\lambda \right\} \\ &\times \frac{h_i \Delta_i}{\Omega\omega} \frac{\Delta_i - (2n_i+1)\omega}{\omega^2 - \Delta_i^2} \,. \end{aligned} \tag{6.55}$$

The second term in the brackets in eqs (6.54) and (6.55) are independent of z, so that they can be seen as the same electromagnetic field fluctuations but in vacuum (i.e. without the dielectric present). For this reason we subtract them as free-space counterterms, leaving for the renormalized position dependent energy shifts

$$\Delta E^{\sigma_z}_{\text{dip,ren}} = - \frac{e^2\sigma_z}{8m^2} \frac{1}{(2\pi)^3} \sum_{\lambda,i,\vartheta} \vartheta \int d^2\mathbf{k}_\parallel \int_C dk_z h_i \frac{\Delta_i^2}{\Omega} \frac{\Delta_i(2n_i+1) - \omega}{\omega^2 - \Delta_i^2} \alpha^\vartheta_\lambda R^L_\lambda e^{2ik_z z}, \tag{6.56}$$

$$\Delta E^{\sigma_z}_{\text{quad, ren}} = \frac{e^2\sigma_z}{8m^2} \frac{1}{(2\pi)^3} \sum_{\lambda,i,\vartheta} \vartheta \int d^2\mathbf{k}_\parallel \int_C dk_z \frac{h_i \Delta_i}{\Omega\omega} \frac{\Delta_i - (2n_i+1)\omega}{\omega^2 - \Delta_i^2} \beta^\vartheta_\lambda R^L_\lambda e^{2ik_z z}. \tag{6.57}$$

Just as in Chapter 5 we will leave subscript 'ren' for renormalized quantities implicit from here onwards. All energy shifts quoted for the rest of this chapter are renormalized unless we specifically state otherwise. The structure of the complex plane is shown in fig. (6.2). There is a branch cut due to $k = \sqrt{k_z^2 + k_\parallel^2}$ in the denominators of all but one of the terms in (6.56) and (6.57); we place this branch cut in the region $k_z = \pm ik_\parallel ... \pm i\infty$. The reflection coefficients have branch points at $k_z = \pm ik_\parallel \frac{\sqrt{n^2-1}}{n}$, we place the corresponding branch cut in between. There is also a pole at $k_z^2 = \Delta_i^2 + k_\parallel^2$ whose position moves through three distinct regions as $k_\parallel$ is integrated over.

For $k_\parallel < \Delta_i$ it is split between two poles on the real axis, for $\Delta_i < k_\parallel < n\Delta_i$ it is split either side of the cut due to k_z^d and finally for $k_\parallel > n\Delta_i$ it is between $-ik_\parallel \frac{\sqrt{n^2-1}}{n}$ and

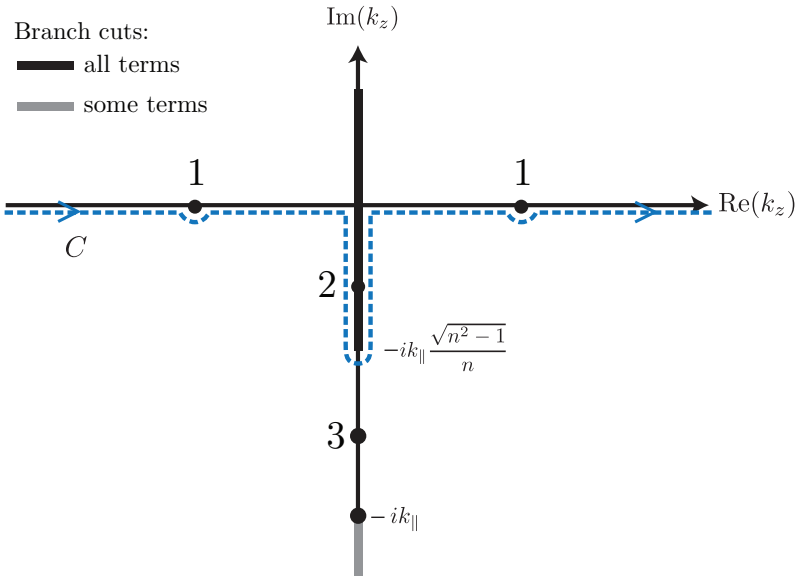

Figure 6.2: Complex k_z plane corresponding to the various terms in eqs. (6.56) and (6.57). The pole at $k_z^2 = \Delta_i^2 - k_\parallel^2$ can appear in one of three regions depending on the relative values of $k_\parallel$, Δ_i and n. These regions are the real axis (shown as points '1'), split either side of the cut due to k_z^d (2), or the imaginary axis between the two cuts (3)

$-ik_\parallel$, as shown in fig. (6.2). On deformation of the contour into the lower-half plane, it is expedient to write the results as contributions from the cut due to k and the pole at $k_z^2 = \Delta_i^2 + k_\parallel^2$

$$\Delta E_{\rm dip}^{\sigma_z} = \Delta E_{\rm dip}^{\rm poles} + \Delta E_{\rm dip}^{\rm cut}, \qquad \Delta E_{\rm quad}^{\sigma_z} = \Delta E_{\rm quad}^{\rm poles} + \Delta E_{\rm quad}^{\rm cut}. \tag{6.58}$$

We further split the contributions from the pole at $k_z = \sqrt{\Delta_i^2 - k_\parallel^2}$ into those from real axis ($k_\parallel < \Delta_i$, denoted as a superscript $<$) and the imaginary axis poles ($k_\parallel > \Delta_i$, superscript $>$). Writing the contributions in terms of the variables

$$x = \frac{\sqrt{\Delta_i^2 - k_\parallel^2}}{\Delta_i} \qquad y = \frac{\sqrt{k_\parallel^2 - \Delta_i^2}}{\Delta_i}, \tag{6.59}$$

we find

$$\Delta E_{\rm dip,\ TE}^{<} = \sum_i \frac{\Gamma_i}{z^2} \int_0^1 dx R_{\rm TE}^{+}(x) \sin(2\zeta_i x), \tag{6.60}$$

$$\Delta E_{\rm dip,\ TE}^{>} = -\sum_i \frac{\Gamma_i}{z^2} \,{\rm Re} \int_0^\infty dy R_{\rm TE}^{-}(y) e^{-2\zeta_i y}, \tag{6.61}$$

$$\Delta E_{\rm dip,\ TM}^{<} = -\sum_i \frac{\Gamma_i}{z^2} \int_0^1 dx\, x^2 R_{\rm TM}^{+}(x) \sin(2\zeta_i x), \tag{6.62}$$

$$\Delta E_{\rm dip,\ TM}^{>} = -\sum_i \frac{\Gamma_i}{z^2} \,{\rm Re} \int_0^\infty dy\, y^2 R_{\rm TM}^{-}(y) e^{-2\zeta_i y}, \tag{6.63}$$

where

$$\zeta_i \equiv -\Delta_i z \qquad \Gamma_i \equiv \frac{e^2}{32\pi m^2 \Omega}\sigma_z h_i \Delta_i^2 \zeta_i^2 n_i, \tag{6.64}$$

and

$$R^{\pm}_{\mathrm{TE}}(x) = \frac{x - \sqrt{x^2 \pm (n^2-1)}}{x + \sqrt{x^2 \pm (n^2-1)}},$$
$$R^{\pm}_{\mathrm{TM}}(x) = \frac{n^2 x - \sqrt{x^2 \pm (n^2-1)}}{n^2 x + \sqrt{x^2 \pm (n^2-1)}}.$$

and similar for $R^{\pm}_{\lambda}(y)$. The TM part of eq. (6.56) also has a contribution from a pole at $k_z = -ik_{\parallel}$, which is the zero frequency or 'static' limit. This turns out to be an elementary integral, the result is

$$\Delta E_{\mathrm{static}} = -\frac{e^2}{256\pi m^2 z^3 \Omega}\frac{n^2-1}{n^2+1}\sum_i h_i \Delta_i (1+2n_i), \tag{6.65}$$

These deliver the dipole part of the shift via:

$$\Delta E^{\mathrm{poles}}_{\mathrm{dip}} = \Delta E^{<}_{\mathrm{dip,\ TE}} + \Delta E^{>}_{\mathrm{dip,\ TE}} + \Delta E^{<}_{\mathrm{dip,\ TM}} + \Delta E^{>}_{\mathrm{dip,\ TM}} + \Delta E^{\mathrm{static}}_{\mathrm{dip}}, \tag{6.66}$$

We do not quote the cut contribution $\Delta E^{\mathrm{cut}}_{\mathrm{dip}}$ here for two reasons. Firstly, up to some prefactors, it is obtained in precisely the same way as in the integrals found in Chapter 5. Secondly, it is negligible in the asymptotic regime considered later on, making its explicit inclusion unnecessary. Moving onto the quadrupole part, we have that the TM polarization does not contribute since $\{\beta^{+}_{\mathrm{TM}}, \beta^{-}_{\mathrm{TM}} = 0\}$. Writing the contributions from the pole at $k_z = \sqrt{\Delta_i^2 - k_{\parallel}^2}$ in the same way as the dipole part we find

$$\Delta E^{<}_{\mathrm{quad}} = -2\sum_i \frac{\Gamma_i}{z^2}\int_0^1 dx (x^2-1) R^{-}_{\mathrm{TE}}(x)\sin(2\zeta_i x), \tag{6.67}$$

$$\Delta E^{>}_{\mathrm{quad}} = -2\sum_i \frac{\Gamma_i}{z^2}\,\mathrm{Re}\int_0^{\infty} dy (y^2+1) R^{+}_{\mathrm{TE}}(y) e^{-2\zeta_i y}. \tag{6.68}$$

There is no equivalent of (6.65) for the quadrupole terms since the TM polarization does not contribute to them, leaving for $\Delta E^{\sigma_z}_{\mathrm{quad}}$

$$\Delta E^{\sigma_z}_{\mathrm{quad}} = \Delta E^{<}_{\mathrm{quad}} + \Delta E^{>}_{\mathrm{quad}}. \tag{6.69}$$

and again we do not quote $\Delta E^{\mathrm{cut}}_{\mathrm{quad}}$. We then have the entire pole contribution

$$\Delta E^{\mathrm{poles}} = \Delta E^{\mathrm{poles}}_{\mathrm{dip}} + \Delta E^{\mathrm{poles}}_{\mathrm{quad}}. \tag{6.70}$$

The integrals (6.60)-(6.63), (6.67) and (6.68) are done asymptotically for large ζ_i. For integrals with $k_{\parallel} < \Delta_i$ this is achieved via repeated integration by parts, and for integrals

with $k_\parallel > \Delta_i$ via a change of variables to $\xi_i = \zeta_i x$ and then Taylor expansion for large ζ_i. The result is

$$\Delta E^{\text{poles}}(\zeta_i \gg 1) = \frac{1}{4\pi}\frac{e^2\sigma_z}{8m^2z^2}\frac{n-1}{n+1}\sum_i \frac{\Delta_i^2}{\Omega}h_i n_i\left[\zeta_i\cos(2\zeta_i) + \mathcal{O}(\zeta_i^0)\right] . \tag{6.71}$$

Finally, one can show that the cut contributions are of higher order in $1/\zeta_i$

$$\Delta E^{\text{cut}}(\zeta_i \gg 1) = \frac{1}{z^2}\mathcal{O}\left(\frac{1}{\zeta^4}\right) . \tag{6.72}$$

6.4.2 Transitions within the same Landau level

Repeating the above analysis for $\Delta E^b_{\sigma_z}$ as defined in eq. (6.46), we first note that the term $\Delta E^{(2)}_{\text{quad},2,\sigma_z}$ is identically zero. This can be seen by noting that, up to constants, eq. (6.43) is

$$\Delta E^{(2)}_{\text{quad},2,\sigma_z} \propto \int d^3\mathbf{k}\frac{|(\nabla\times\mathbf{f})_z|^2}{\omega} . \tag{6.73}$$

The square of any particular component $(\mathbf{f}_{\mathbf{k}\lambda})_i$ of the non-dispersive mode functions (3.16) contains a factor $1/\omega$, which shows that eq. (6.73) is given entirely by a pole at $k_z = -ik_\parallel$. The polarization vectors (A.1) show that $(\nabla\times\mathbf{f}_{\text{TM}})_z = 0$, so we are left with expressions of the same form as (6.56) and (6.57) but with TE contributions only. One can then use the residue theorem to calculate the resulting integral, but the TE reflection coefficient vanishes at $k_z = -ik_\parallel$, so the shift is zero.

Repeating the analysis found in section 6.4.1 on the remaining terms of $\Delta E^b_{\sigma_z}$ as defined in eq. (6.46), we find for the renormalized position-dependent energy shifts

$$\Delta E^{(1)}_{\sigma_z} = \frac{1}{8\pi^2}\frac{e^3}{4m^3}\sigma_z B_0\int_0^\infty dk_\parallel\int_C dk_z\frac{1}{k}\left[R^L_{\text{TE}} + \frac{1}{k^2}\left(k_\parallel^2 - k_z^2\right)R^L_{\text{TM}}\right]e^{2ik_z z} , \tag{6.74a}$$

$$\Delta E^{(2)}_{\text{spin},\sigma_z} = -\frac{1}{8\pi^2}\sigma_z\frac{e^3B_0}{4m^3}\int_0^\infty dk_\parallel\int_C dk_z\left(1+\frac{\omega}{4m}\right)^2\frac{1}{\omega} \times\frac{1}{\left(\frac{eB_0}{m}\right)^2-\omega^2}\left[-R^L_{\text{TE}}k_z^2 + (k_z^2+k_\parallel^2)R^L_{\text{TM}}\right]e^{2ik_z z}, \tag{6.74b}$$

which together constitute $\Delta E^b_{\sigma_z}$ as defined in eq. (6.46) via

$$\Delta E^b_{\sigma_z} = \Delta E^{(1)}_{\sigma_z} + \Delta E^{(2)}_{\text{spin},\sigma_z} + \Delta E^{(2)}_{\text{quad},2,\sigma_z} = \Delta E^{(1)}_{\sigma_z} + \Delta E^{(2)}_{\text{spin},\sigma_z}, \tag{6.75}$$

where we have used the fact that $\Delta E^{(2)}_{\text{quad},2,\sigma_z}$ is identically zero as shown in the discussion immediately following (6.73). The results (6.74) are of course independent of any of the trap parameters, so we do not have the problem seen in section 6.4.1 where the double confinement makes it dangerous to take limits too early. Thus we go ahead and expand

eqs. (6.74) for large m (since we are in the non-relativistic approximation) up to order $1/m^3$. This means that eq. (6.74b) becomes

$$\Delta E^{(2)}_{\text{spin},\sigma_z} = -\frac{1}{8\pi^2}\sigma_z \frac{e^3 B_0}{4m^3}\int_0^\infty dk_\parallel \int_C dk_z \frac{1}{\omega^3}\left[-R^L_{\text{TE}} k_z^2 + (k_z^2+k_\parallel^2) R^L_{\text{TM}}\right] e^{2ik_z z}\,, \quad (6.76)$$

and we also trivially see that

$$\Delta E^b_{\sigma_z}(\zeta_i \gg 1) = \frac{1}{z^2}\mathcal{O}\left(\zeta_i^0\right). \quad (6.77)$$

6.4.3 Total Energy Shift

The cut contributions are all of higher order in ζ_i, so we have for the whole energy shift:

$$\Delta E_{\sigma_z}(\zeta_i \gg 1) = \Delta E^{\text{poles}}(\zeta_i \gg 1) + \mathcal{O}(\zeta_i^0), \quad (6.78)$$

giving for our final result

$$\Delta E_{\sigma_z}(\zeta_i \gg 1) = \frac{1}{4\pi}\frac{e^2\sigma_z}{8m^2 z^2 \Omega}\frac{n-1}{n+1}\sum_i h_i \Delta_i^2 n_i \left[\zeta_i \cos(2\zeta_i) + \mathcal{O}(\zeta_i^0)\right]. \quad (6.79)$$

Using the definition of ζ_i and evaluating the sum over i, the leading term from the above is

$$\Delta E^{(0)}_{\sigma_z}(\zeta_i \gg 1) = \frac{1}{4\pi}\frac{e^2\sigma_z}{8m^2 z \Omega}\frac{n-1}{n+1}\left[n_R \Delta_R^3 \cos(2\Delta_R z) - n_L \Delta_L^3 \cos(2\Delta_L z)\right]. \quad (6.80)$$

This decays with distance from the surface, as of course it must. However, when one attempts to extract a magnetic moment from this, the result behaves in an unexpected way. Expanding this for small B_0 and extracting the coefficient of $\sigma_z B_0$, we find for the magnetic moment shift

$$\Delta\mu^{(0)}(|\omega_H z| \gg 1) = -\frac{e^3(n_L+n_R)}{64\pi m^3}\frac{n-1}{n+1}\omega_H\left[2\omega_H \sin(2\omega_H z) - \frac{3\cos(2\omega_H z)}{z}\right], \quad (6.81)$$

which has the unexpected and unphysical property of oscillating indefinitely as $|z| \to \infty$. To track down the source of this problem, we define $\Lambda \equiv -eB_0/2m > 0$, giving

$$\Omega = \sqrt{\omega_H^2 + \Lambda^2}, \qquad \Delta_i = \sqrt{\omega_H^2+\Lambda^2} + h_i\Lambda\,, \quad (6.82)$$

and look at the behavior of the relevant part of (6.79), namely $\zeta_i \cos(2\zeta_i)/(\Omega z^2)$

$$\frac{\zeta_i}{\Omega z^2}\cos(2\zeta_i) = -\frac{\sqrt{\omega_H^2+\Lambda^2}+h_i\Lambda}{z\sqrt{\omega_H^2+\Lambda^2}}\cos\left[2\left(\sqrt{\omega_H^2+\Lambda^2}+h_i\Lambda\right)z\right]. \quad (6.83)$$

This shows that as Λ varies, both the amplitude and frequency of the oscillation change. This is the source of the term which does not vanish – if the frequency of the oscillatory term were independent of B_0, the linear term in its small B_0 expansion would vanish at $|z| \to \infty$.

A similar B_0 dependence was found in [39] for the energy shift in the retarded regime $\frac{eB_0}{m} \gg \frac{c}{z}$ of an electron near a perfect reflector, the results are shown in expressions 8.14 and 8.15 in our reproduction 5.3 of [39]'s summary of results. We are in the nonretarded regime $\frac{eB_0}{m} \ll \frac{c}{z}$, but simultaneously in a type of retarded regime with respect to the trap frequency ω_H and the distance z since we have $\omega_H \gg \frac{c}{z}$. Loosely speaking, this type of retarded regime $\omega_H \gg \frac{c}{z}$ corresponds to the time it takes for a photon to make a round trip from the electron to the interface and back being long enough for the electron to have moved significantly along its oscillatory path within the trap. This means that the phase is important, which is why we get oscillatory terms. We have already noted that magnetic moments are only strictly defined in the nonretarded regime (see figure 5.3), so what we are seeing in (6.81) is an indication that magnetic moments are also not strictly defined for a trapped electron with $\omega_H \gg \frac{c}{z}$. For this reason we consider the energy shift (6.80) as our final result and will not discuss magnetic moments any further.

We can extract from eq. (6.80) an expression for the shift in the difference of the energies[1] of the two spin states by using the spin eigenvalues $\pm 1/2$.

$$E^{(0)}_{\sigma_z}(\zeta_i \gg 1) = \frac{1}{8\pi}\frac{e^2}{4m^2 z\Omega}\frac{n-1}{n+1}\Big[n_R\Delta_R^3\cos(2\Delta_R z) - n_L\Delta_L^3\cos(2\Delta_L z)\Big], \tag{6.84}$$

We can then express this in units of the unperturbed energy level difference $E = eB_0/m$

$$\frac{E^{(0)}_{\sigma_z}(\zeta_i \gg 1)}{E} = \frac{1}{8\pi}\frac{e}{4mzB_0\Omega}\frac{n-1}{n+1}\Big[n_R\Delta_R^3\cos(2\Delta_R z) - n_L\Delta_L^3\cos(2\Delta_L z)\Big], \tag{6.85}$$

Noting that the defined quantities Δ_i and Ω are frequencies, eq. (6.85) in S.I. units is

$$\frac{E^{(0)}_{\sigma_z}(\zeta_i \gg 1)}{E} = \frac{1}{8\pi}\frac{\hbar}{\epsilon_0 c^4}\frac{e}{4mzB_0\Omega}\frac{n-1}{n+1}\Big[n_R\Delta_R^3\cos(2\Delta_R z) - n_L\Delta_L^3\cos(2\Delta_L z)\Big]. \tag{6.86}$$

As discussed in section 6.3, parameters which are consistent with our choice of asymptotic regime are

$$B_0 \sim \mathrm{T}, \qquad z \sim 10\mu\mathrm{m}, \qquad \omega_H \sim 10^{15}\mathrm{Hz}, \tag{6.87}$$

for which $\Delta_L z/c \approx \Delta_R z/c \approx 30$, meaning that we are at the low end of the region $\Delta_i z/c \gg 1$. Nevertheless, we substitute the values for B_0 and ω_H into (6.86) to find the z dependence for such distances

$$\frac{E^{(0)}_{\sigma_z}(\zeta_i \gg 1)}{E} \approx -(n_R - n_L)\frac{n-1}{n+1}\cdot\frac{10^{-11}\mu\mathrm{m}}{z}\cos(6\mu\mathrm{m}^{-1}z), \quad (0.1\mu\mathrm{m} \ll z \ll 3\mathrm{mm}) \tag{6.88}$$

where z is measured in μm. This z dependence is shown in fig. 6.3, which shows that

[1] It is worth emphasizing the notational trap that E is an energy difference while ΔE is a *shift* in an energy difference

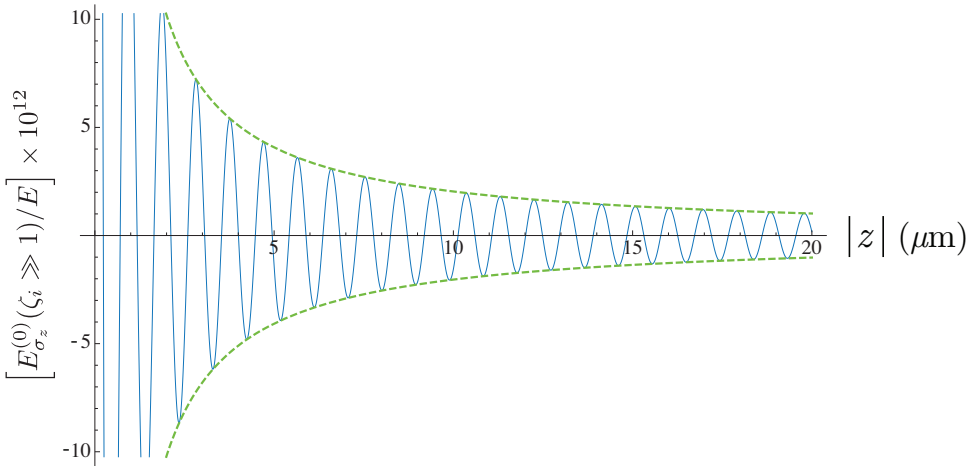

Figure 6.3: Energy shift of the spin states of an atomic electron as a function of distance from a non-dispersive surface with $(n_R - n_L)\frac{n-1}{n+1} \approx 1$, alongside its envelope.

taking $(n_R - n_L)\frac{n-1}{n+1} \approx 1$[2] and a distance z of 10μm gives for the amplitude of the shift

$$\left|\frac{E^{(0)}_{\sigma_z}(\zeta_i \gg 1)}{E}\right| \approx 10^{-12}\,. \tag{6.89}$$

This could in principle be measured in the same fashion as the anomalous Zeeman effect, the energy splitting for which depends on the Bohr magneton μ_B and the strength of the applied magnetic field. Even if one could know the magnetic field to arbitrary accuracy, the current uncertainty in the size of μ_B is around one part in 10^8 [25], so that our shift is around four orders of magnitude smaller than what even an unrealistically perfect experiment could measure. Decreasing the distance to the very edge of our asymptotic regime we could produce a shift which is only two orders of magnitude lower than the uncertainty in μ_B, but these are the conditions under which our approximations begin to break down.

6.5 Summary and conclusions

In this chapter we have calculated the shift in the energy difference between the two spin states of an electron that is confined at a distance $z = -|z|$ away from a non-dispersive half space. We have shown that the most relevant asymptotic regime is where the frequency of

[2]This is justified because the difference between n_R and n_L corresponds to the orbital magnetic quantum number of the electron [74], as can be shown using eqs. (6.10) and the definition $\hat{L}_z = \hat{x}\hat{p}_y - \hat{p}_x\hat{y}$.

the trap ω_H is much larger than $|c/z|$, under which conditions we found for the energy shift

$$\frac{E^{(0)}_{\sigma_z}(|\omega_H z/c| \gg 1)}{E} = \frac{1}{8\pi}\frac{\hbar}{\epsilon_0 c^4}\frac{e}{4mzB_0\Omega}\frac{n-1}{n+1}\left[n_R\Delta_R^3\cos(2\Delta_R z) - n_L\Delta_L^3\cos(2\Delta_L z)\right], \tag{6.90}$$

where

$$\Omega^2 = \omega_H^2 + \left(\frac{eB_0}{2m}\right)^2, \qquad \Delta_R = \Omega - \frac{eB_0}{2m}, \qquad \Delta_L = \Omega + \frac{eB_0}{2m}, \tag{6.91}$$

as given by eqs. (6.9), (6.16) and (6.86). We have described a problem where the oscillatory behavior of the most relevant asymptotic regime of the energy shift means that it is not possible to use such an energy shift to obtain a magnetic moment shift. We have provided estimates of the size of the effect, showing that a measurement is not realistically within the reach of immediately available experiments, but is also not so far out of reach (two to four orders of magnitude) that there is no chance of measurement as experimental techniques and technology continue to improve.

Chapter 7

Noise-current approach

The derivation of the anomalous magnetic moment of an electron near a realistic surface detailed in the previous section represents both a new method and a new result (with the same being partially true for the mass shift). Many different formalisms already exist for the calculation of quantum electrodynamic corrections due to the presence of dielectric media, most notably the Huttner-Barnett model whereby the medium is modeled as a continuum of oscillators coupled to a reservoir that facilitates absorption [32]. In this part of the thesis, we will link our work to that of others by taking another alternative approach based in the macroscopic formulation of Maxwell's equations and their coupling to matter, which we shall call the noise-current approach. This will serve as both a reinforcement of our previous calculations, as well as a hint towards their extension to more realistic media.

7.1 Introduction

The starting point for noise-current quantization of the electromagnetic field in dielectric media is Maxwell's equations in the presence of a homogenous medium

$$\begin{aligned} \nabla \cdot \mathbf{D}(\mathbf{r},t) &= 0, & \nabla \times \mathbf{E}(\mathbf{r},t) &= -\frac{\partial}{\partial t}\mathbf{B}(\mathbf{r},t), \\ \nabla \cdot \mathbf{B}(\mathbf{r},t) &= 0, & \nabla \times \mathbf{B}(\mathbf{r},t) &= \frac{\partial}{\partial t}\mathbf{D}(\mathbf{r},t), \end{aligned} \tag{7.1}$$

where it has immediately been assumed that the medium is non-magnetic (relative permeability of unity). Further assuming that the response of the material to an applied field is linear, the electric displacement is related to the electric field through

$$\mathbf{D}(\mathbf{r},t) = \mathbf{E}(\mathbf{r},t) + \int_0^\infty d\tau \chi(\tau)\mathbf{E}(\mathbf{r},t-\tau), \tag{7.2}$$

where τ corresponds to the temporal delay in the response of the material to the field, $\chi(\tau)$ is a linear response function. Causality requires that the lower limit of the τ integral is

zero, and τ can never be negative. Using Maxwell's equations (7.1), we find the following relation for the vector potential $\mathbf{A}$, in Coulomb gauge[1]

$$\nabla^2\mathbf{A}(\mathbf{r},t) - \frac{\partial}{\partial t^2}\mathbf{A}(\mathbf{r},t) - \int_0^\infty d\tau\chi(\tau)\frac{\partial^2}{\partial t^2}\mathbf{A}(\mathbf{r},t-\tau) = 0\ . \tag{7.3}$$

The fields are Fourier transformed according to the convention[2]

$$\mathbf{X}(\mathbf{r},t) = \int_0^\infty d\omega\, e^{-i\omega t}\mathbf{X}(\mathbf{r},\omega) + \text{c.c.} \qquad (\mathbf{X} = \mathbf{E},\mathbf{D},\mathbf{B},\mathbf{A}), \tag{7.4}$$

which delivers the Fourier-transformed version of eq. (7.2)

$$\mathbf{D}(\mathbf{r},\omega) = \left(\int_0^\infty d\tau\chi(\tau)e^{i\omega\tau} + 1\right)\mathbf{E}(\mathbf{r},\omega) \equiv \epsilon(\omega)\mathbf{E}(\mathbf{r},\omega)\ , \tag{7.5}$$

and the wave equation in Coulomb gauge

$$\nabla^2\mathbf{A}(\mathbf{r},\omega) + \omega^2\epsilon(\omega)\mathbf{A}(\mathbf{r},\omega) = 0\ . \tag{7.6}$$

The task is, as usual, to quantize this theory. When the permittivity is real, the theory can be quantized in the same fashion as in Chapter 3. However, if the permittivity is complex, eq. (7.6) becomes damped, destroying the fundamental equal-time commutator $[\mathbf{A}(\mathbf{r}),\mathbf{E}(\mathbf{r}')] = -i\hbar\delta^\perp(\mathbf{r}-\mathbf{r}')$ [36]. This can be remedied by the introduction of a source on the right hand side of (7.6), interpreted as quantum noise associated with damping. This interpretation is in line with the fluctuation-dissipation theorem [80], which is a very general result from statistical physics concerning the irreversible dissipation of energy into small fluctuations in the properties of a system. The introduction of the source term means that the fundamental commutator is preserved, and the theory may be quantized.

In order to deduce the specific form of the source term, we make a brief detour to the Huttner-Barnett model [32]. This describes the medium-dependent electromagnetic field via its interaction with a harmonic oscillator field representing the polarization of the medium. This polarization field is, in turn, coupled to a continuum of harmonic oscillators representing a reservoir into which energy may flow – this is the means by which absorption is included in the model. The resulting Hamiltonian for the composite matter-field system can be diagonalized, giving [32]

$$H_{\text{HB}} = \sum_\lambda \int d^3\mathbf{k} \int_0^\infty d\omega\ \omega\hat{C}_\lambda^\dagger(\mathbf{k},\omega)\hat{C}_\lambda(\mathbf{k},\omega), \tag{7.7}$$

[1] In this section we are dealing with homogenous media, under which conditions the generalized Coulomb gauge condition $\nabla\cdot[\epsilon(\mathbf{r},\omega)\mathbf{A}(\mathbf{r},\omega)] = 0$ becomes $\nabla\cdot\mathbf{A}(\mathbf{r},\omega) = 0$, which is identical to the standard Coulomb gauge condition.

[2] It may seem strange that the Fourier transform shown is defined only for positive frequency. This is unavoidable as this will lead to the definition of noise-current quanta, which are coupled to polaritons and therefore exist only for positive frequencies.

where $\hat{C}_\lambda(\mathbf{k},\omega)$ and $\hat{C}^\dagger_\lambda(\mathbf{k},\omega)$ obey the bosonic commutation relations

$$\left[\hat{C}_\lambda(\mathbf{k},\omega),\hat{C}^\dagger_{\lambda'}(\mathbf{k}',\omega')\right] = \delta_{\lambda\lambda'}\delta^\perp(\mathbf{k}-\mathbf{k}')\delta(\omega-\omega'), \tag{7.8a}$$

$$\left[\hat{C}_\lambda(\mathbf{k},\omega),\hat{C}_{\lambda'}(\mathbf{k}',\omega')\right] = 0, \tag{7.8b}$$

and are made up of linear combinations of polariton creation and annihilation operators. The vector potential at $t=0$ is [32]

$$\hat{\mathbf{A}}(\mathbf{r},\omega) = \frac{1}{(2\pi)^{3/2}}\frac{1}{\sqrt{\pi}}\sum_\lambda \int d^3\mathbf{k}\int_0^\infty d\omega \left[\frac{\omega\sqrt{\mathrm{Im}[\epsilon(\omega)]}}{\omega^2\epsilon(\omega)-k^2}\hat{C}_\lambda(\mathbf{k},\omega)e^{i\mathbf{k}\cdot\mathbf{r}} + \mathrm{H.c.}\right]\mathbf{e}_\lambda(\mathbf{k}). \tag{7.9}$$

Applying the operator $\nabla^2+\omega^2\epsilon(\omega)$ we have:

$$\left[\nabla^2+\omega^2\epsilon(\omega)\right]\hat{\mathbf{A}}(\mathbf{r},\omega) = \frac{1}{(2\pi)^{3/2}}\frac{1}{\sqrt{\pi}}\sum_\lambda\int d^3\mathbf{k}\int_0^\infty d\omega \times\left[\omega\sqrt{\mathrm{Im}[\epsilon(\omega)]}\hat{C}_\lambda(\mathbf{k},\omega)e^{i\mathbf{k}\cdot\mathbf{r}}+\mathrm{H.c.}\right]\mathbf{e}_\lambda(\mathbf{k}), \tag{7.10}$$

which does not in general satisfy eq. (7.6). Defining the operator

$$\hat{\mathcal{F}}(\mathbf{r},\omega) = -\frac{1}{(2\pi)^{3/2}}\int d^3\mathbf{k}\sum_\lambda \mathbf{e}_\lambda(\mathbf{k})\hat{C}_\lambda(\mathbf{k},\omega)e^{i\mathbf{k}\cdot\mathbf{r}}, \tag{7.11}$$

which satisfies

$$\left[\hat{f}_i(\mathbf{r},\omega),\hat{f}^\dagger_j(\mathbf{r}',\omega')\right] = \delta_{ij}(\mathbf{r}-\mathbf{r}')\delta(\omega-\omega'), \tag{7.12a}$$

$$\left[\hat{f}_i(\mathbf{r},\omega),\hat{f}^\dagger_j(\mathbf{r}',\omega')\right] = 0 = \left[\hat{f}^\dagger_i(\mathbf{r},\omega),\hat{f}^\dagger_j(\mathbf{r}',\omega')\right], \tag{7.12b}$$

we have

$$\left[\nabla^2+\omega^2\epsilon(\omega)\right]\hat{\mathbf{A}}(\mathbf{r}) = -\omega\sqrt{\frac{\mathrm{Im}[\epsilon(\omega)]}{\pi}}\hat{\mathcal{F}}(\mathbf{r},\omega)\,. \tag{7.13}$$

This means that the introduction of a term $\hat{\mathbf{j}}(\mathbf{r},\omega) = -\omega\sqrt{\frac{\mathrm{Im}[\epsilon(\omega)]}{\pi}}\hat{\mathcal{F}}(\mathbf{r},\omega)$ on the right hand side of eq. (7.6) will preserve the fundamental commutator and allow the field to be quantized. To see how this works, we rewrite the wave equation (7.6) in terms of the operator $\hat{\mathbf{A}}(\mathbf{r},\omega)$ as

$$\nabla^2\hat{\mathbf{A}}(\mathbf{r},\omega)+\omega^2\epsilon(\omega)\hat{\mathbf{A}}(\mathbf{r},\omega) = \hat{\mathbf{j}}(\mathbf{r},\omega)\,. \tag{7.14}$$

The solution to the inhomogeneous differential equation (7.14) can be written in terms of the Green's function, defined as the solution to

$$\nabla^2\mathbf{G}(\mathbf{r},\mathbf{r}',\omega)+\omega^2\epsilon(\omega)\mathbf{G}(\mathbf{r},\mathbf{r}',\omega) = \delta^{(3)}(\mathbf{r}-\mathbf{r}'). \tag{7.15}$$

Causality is assured by choosing the retarded Green's function. Since the dependent variable $\hat{\mathbf{A}}$ is a vector, the Green's function has the form of a dyadic tensor with the

properties outlined in appendix (E.1). This delivers the Fourier-transformed field $\hat{\mathbf{A}}(\mathbf{r},\omega)$ as

$$\hat{\mathbf{A}}(\mathbf{r},\omega) = \int d^3\mathbf{r}'\, \mathbf{G}(\mathbf{r},\mathbf{r}',\omega)\cdot\hat{\mathbf{j}}(\mathbf{r}',\omega)\;, \tag{7.16}$$

giving for the configuration-space field

$$\hat{\mathbf{A}}(\mathbf{r},t) = \int_0^\infty d\omega \int d^3\mathbf{r}'\, \mathbf{G}(\mathbf{r},\mathbf{r}',\omega)\cdot\hat{\mathbf{j}}(\mathbf{r}',\omega)e^{-i\omega t} + \text{H.c.}\;. \tag{7.17}$$

where the product is defined via eq. (E.4). The Green's function has a useful property

$$\omega^2 \int d^3\mathbf{r}\epsilon_I(\omega)\mathbf{G}_{il}(\mathbf{r}',\mathbf{r},\omega)\mathbf{G}^*_{jl}(\mathbf{r}'',\mathbf{r},\omega) = -\,\text{Im}\,\mathbf{G}_{ij}(\mathbf{r}',\mathbf{r}'',\omega)\;, \tag{7.18}$$

as proved in appendix E.2. We wish to show that $\hat{\mathbf{j}}(\mathbf{r},\omega) = -\omega\sqrt{\frac{\text{Im}[\epsilon(\omega)]}{\pi}}\hat{\mathcal{F}}(\mathbf{r},\omega)$ is the correct choice of noise operator, i.e. that which ensures the equal-time commutation relation

$$[\hat{\mathbf{A}}(\mathbf{r}),\hat{\mathbf{E}}(\mathbf{r}')] = -i\hbar\delta^\perp(\mathbf{r}-\mathbf{r}') \tag{7.19}$$

is preserved. Using the commutation relations (7.12) and the component-wise statements of the vector potential and the electric field at $t=0$,

$$\hat{A}_i(\mathbf{r}) = \int_0^\infty d\omega \int d^3\mathbf{r}'\, G_{ij}(\mathbf{r},\mathbf{r}',\omega)\hat{j}_j(\mathbf{r}',\omega) + \text{H.c.}\;, \tag{7.20}$$

$$\hat{E}_i(\mathbf{r}) = i\int_0^\infty d\omega\,\omega \int d^3\mathbf{r}'\,\Big[G_{ij}(\mathbf{r},\mathbf{r}',\omega)\hat{j}_j(\mathbf{r}',\omega) - \text{H.c.}\Big]\;, \tag{7.21}$$

it is easy to show that the following holds

$$\begin{aligned}[\hat{A}_i(\mathbf{r}),\hat{E}_k(\mathbf{s})] = &-i\int_0^\infty d\omega \int_0^\infty d\omega'\omega' \int d^3\mathbf{r}' \int d^3\mathbf{s}'\omega\omega' \sqrt{\frac{\text{Im}[\epsilon(\omega)]}{\pi}}\sqrt{\frac{\text{Im}[\epsilon(\omega')]}{\pi}} \\ &\times\Big[G^*_{ji}(\mathbf{r}',\mathbf{r},\omega)G_{kl}(\mathbf{s},\mathbf{s}',\omega')\delta^\perp_{ij}(\mathbf{s}'-\mathbf{r}')\delta(\omega-\omega') \\ &+ G_{ij}(\mathbf{r},\mathbf{r}',\omega)G^*_{lk}(\mathbf{s}',\mathbf{s},\omega')\delta^\perp_{jl}(\mathbf{s}'-\mathbf{r}')\delta(\omega-\omega')\Big]\;.\end{aligned} \tag{7.22}$$

Carrying out the integrals over ω' and $\mathbf{s}'$ we have

$$\begin{aligned}[\hat{A}_i(\mathbf{r}),\hat{E}_k(\mathbf{s})] &= -\frac{i}{\pi}\int_0^\infty d\omega\omega \int d^3\mathbf{r}'\,\text{Im}[\epsilon(\omega)]\Big[G^*_{ji}(\mathbf{r}',\mathbf{r},\omega)G_{kj}(\mathbf{s},\mathbf{r}',\omega) \\ &\quad + G_{ij}(\mathbf{r},\mathbf{r}',\omega)G^*_{jk}(\mathbf{r}',\mathbf{s},\omega)\Big] \\ &= -\frac{i}{\pi}\int_0^\infty d\omega\omega \int d^3\mathbf{r}'\,\text{Im}[\epsilon(\omega)]\Big[G^*_{ij}(\mathbf{r},\mathbf{r}',\omega)G_{kj}(\mathbf{s},\mathbf{r}',\omega) \\ &\quad + G_{ij}(\mathbf{r},\mathbf{r}',\omega)G^*_{kj}(\mathbf{s},\mathbf{r}',\omega)\Big]\;.\end{aligned} \tag{7.23}$$

This is now suitable for simplification via eq. (7.18), the result is

$$[\hat{A}_i(\mathbf{r}),\hat{E}_k(\mathbf{s})] = \frac{1}{\pi}\int_{-\infty}^\infty d\omega\frac{1}{\omega}G_{ij}(\mathbf{r},\mathbf{s},\omega) \tag{7.24}$$

where the property $G^*_{ij}(\mathbf{r},\mathbf{s},\omega) = G_{ij}(\mathbf{r},\mathbf{s},-\omega)$ of the retarded Green's function has been used. In order to evaluate this integral we need to know the specific form of the Green's function, which we shall take to be that for a bulk dielectric, in accordance with the assumptions made in writing down Maxwell's equations (7.1) at the start of this section. The Green's function that satisfies eq. (7.15) for an infinite bulk dielectric may be represented as [81]

$$G_{ij}(\mathbf{r},\mathbf{r}',\omega) = \left[\partial_i\partial_j + \delta_{ij}\omega^2\epsilon(\omega)\right]\frac{1}{\omega^2\epsilon(\omega)}\int\frac{d^3\mathbf{k}}{(2\pi)^3}\frac{e^{i\mathbf{k}\cdot(\mathbf{r}-\mathbf{r}')}}{k^2-\omega^2\epsilon(\omega)}\,, \tag{7.25}$$

Comparison of this with (7.24) shows that we require the following ω integrals

$$\int_{-\infty}^{\infty} d\omega\frac{1}{\omega}\frac{1}{k^2-\omega^2\epsilon(\omega)}, \qquad\qquad \int_{-\infty}^{\infty} d\omega\frac{\omega}{k^2-\omega^2\epsilon(\omega)}, \tag{7.26}$$

where, to conform with the definition of $\mathbf{G}$ as a retarded Green's function, the poles at $\omega^2 = k^2/\epsilon(\omega)$ are displaced below the real ω axis. The first integral in (7.26) has a pole at $\omega = 0$, which must be treated as a principal part. Closing the contour in the upper half plane, we find that the large semicircle does not contribute due to the physical requirement that the medium become transparent at high frequencies $\epsilon(\omega\to\infty) = 1$. Since $\epsilon(\omega)$ is analytic and without zeroes in the upper half-plane, the only remaining contribution is from the residue at $\omega = 0$

$$\int_{-\infty}^{\infty} d\omega\frac{1}{\omega}\frac{1}{k^2-\omega^2\epsilon(\omega)} = \frac{i\pi}{k^2}, \tag{7.27}$$

The second integral in (7.26) has no poles, but the contribution around the large semicircle is non-zero. Parameterizing the integral via $\omega = Re^{i\theta}$ we find

$$\int_{-\infty}^{\infty} d\omega\frac{\omega}{k^2-\omega^2\epsilon(\omega)} = -i\lim_{R\to\infty}\int_0^{\pi} d\theta\frac{R^2e^{2i\theta}}{k^2-R^2e^{2i\theta}\epsilon(Re^{i\theta})} = i\pi, \tag{7.28}$$

giving

$$[A_i(\mathbf{r}), E_k(\mathbf{s})] = i\left[\frac{\partial_i\partial_k}{k^2}+\delta_{ik}\right]\int\frac{d^3\mathbf{k}}{(2\pi)^3}e^{i\mathbf{k}\cdot(\mathbf{r}-\mathbf{s})} = -i\delta^{\perp}_{ik}(\mathbf{r}-\mathbf{s}), \tag{7.29}$$

as required. So, introduction of a current source

$$\hat{\mathbf{j}}(\mathbf{r},\omega) = -\omega\sqrt{\frac{\mathrm{Im}[\epsilon(\omega)]}{\pi}}\hat{\mathcal{F}}(\mathbf{r},\omega) \tag{7.30}$$

on the right hand side of eq. (7.6) ensures preservation of the fundamental commutator $[A_i(\mathbf{r}), E_k(\mathbf{s})] = -i\delta^{\perp}_{ik}(\mathbf{r}-\mathbf{s})$, in agreement with [36][3]. Consequently, the final expression of the field at time $t = 0$ to be used in calculations of radiative corrections is

$$\hat{\mathbf{A}}(\mathbf{r}) = \frac{1}{\sqrt{\pi}}\int_0^{\infty} d\omega\,\omega\int d^3\mathbf{r}'\sqrt{\epsilon_I(\omega)}\mathbf{G}(\mathbf{r},\mathbf{r}',\omega)\cdot\hat{\mathbf{a}}^p(\mathbf{r}',\omega) + \text{H.c.}, \tag{7.31}$$

[3]Care must be taken when comparing to ref [36] due to a different sign convention for $\hat{\mathbf{j}}(\mathbf{r},\omega)$

where $\epsilon_I(\omega) = \mathrm{Im}[\epsilon(\omega)]$ and we have renamed $\hat{\mathcal{F}}(\mathbf{r},\omega) \to \hat{\mathbf{a}}^p(\mathbf{r},\omega)$ in order to reflect its interpretation as the annihilation operator for the (transverse) polariton excitations. It is possible to generalize (7.31) to multilayer systems since these can be subdivided into elements where the permittivity does not vary with space [81]. The generalization is achieved by introducing the Green's function satisfying

$$\nabla^2\mathbf{G}(\mathbf{r},\mathbf{r}',\omega) + \omega^2\epsilon(\mathbf{r},\omega)\mathbf{G}(\mathbf{r},\mathbf{r}',\omega) = \delta^{(3)}(\mathbf{r}-\mathbf{r}'), \tag{7.32}$$

and introducing noise sources in each layer, meaning that the commutation relation (7.19) is preserved within each element, and the vector potential (7.31) becomes [36]

$$\hat{\mathbf{A}}(\mathbf{r}) = \frac{1}{\sqrt{\pi}}\int_0^\infty d\omega\,\omega \int d^3\mathbf{r}'\sqrt{\epsilon_I(\mathbf{r}',\omega)}\mathbf{G}(\mathbf{r},\mathbf{r}',\omega)\cdot\hat{\mathbf{a}}^p(\mathbf{r}',\omega) + \text{H.c.}\,. \tag{7.33}$$

7.2 Mass Shift

We can now couple the vector potential (7.33) to an electron in order to derive radiative corrections of the same type as in Chapters 4 and 5. Starting with the mass shift, we need to consider

$$\Delta E = \frac{e^2}{m^2}\sum_{p_{\text{int}}} \frac{|\,\langle \mathbf{p}_{\text{int}}; 1_j(\mathbf{r},\omega)|\,\mathbf{p}\cdot\mathbf{A}\,|\mathbf{p};0\rangle\,|^2}{\frac{\mathbf{p}^2}{2m} - \left(\frac{\mathbf{p}_{\text{int}}^2}{2m}+\omega\right)} \tag{7.34}$$

as shown in section 4.2. The intermediate one-polariton state generated by the application of the operator $\hat{a}_j^{p\dagger}(\mathbf{r},\omega)$ is written as $|1_j(\mathbf{r},\omega)\rangle$. In the no-recoil approximation eq. (7.34) becomes

$$\Delta E = -\frac{e^2}{m^2}\langle p_i^2\rangle|\,\langle 1_j(\mathbf{r},\omega)|\,\hat{A}_i(\mathbf{r})\,|0\rangle\,|^2\frac{1}{\omega}\,. \tag{7.35}$$

Using eq. (E.4), the component-wise version of eq. (7.33) is:

$$\hat{A}_i(\mathbf{r}) = \frac{1}{\sqrt{\pi}}\int_0^\infty d\omega\,\omega\int d^3\mathbf{r}'\sqrt{\epsilon_I(\mathbf{r}',\omega)}\mathbf{G}_{ij}(\mathbf{r},\mathbf{r}',\omega)\hat{a}_j^p(\mathbf{r}',\omega) + \text{H.c.}\,, \tag{7.36}$$

giving for the energy shift

$$\begin{aligned}
\Delta E &= -\frac{e^2}{m^2}\langle p_i^2\rangle|\,\langle 1_j(\mathbf{r}',\omega)|\,\hat{A}_i(\mathbf{r})\,|0\rangle\,|^2\frac{1}{\omega}\\
&= -\frac{e^2}{\pi m^2}\langle p_i^2\rangle\left|\int_0^\infty d\omega\,\omega\int d^3\mathbf{r}'\sqrt{\epsilon_I(\mathbf{r}',\omega)}\mathbf{G}_{ij}(\mathbf{r},\mathbf{r}',\omega)\right|^2\frac{1}{\omega}\\
&= -\frac{e^2}{\pi m^2}\langle p_i^2\rangle\int_0^\infty d\omega\,\omega\int d^3\mathbf{r}'\epsilon_I(\mathbf{r}',\omega)\mathbf{G}_{ij}(\mathbf{r},\mathbf{r}',\omega)\mathbf{G}^*_{ji}(\mathbf{r}',\mathbf{r},\omega)\,,
\end{aligned} \tag{7.37}$$

where the third line follows from the second via orthogonality of the polariton states. This may be simplified using symmetry relation (E.11) and eq. (7.18). The result is:

$$\Delta E = \frac{e^2}{\pi m^2}\langle p_i^2\rangle\int_0^\infty\frac{d\omega}{\omega}\,\mathrm{Im}\,\mathbf{G}_{ii}(\mathbf{r},\mathbf{r},\omega)\,. \tag{7.38}$$

Using the property $G^*_{ij}(\mathbf{r},\mathbf{s},\omega) = G_{ij}(\mathbf{r},\mathbf{s},-\omega)$ of the retarded Green's function we may also write (7.38) as

$$\Delta E = \frac{e^2}{2\pi m^2}\langle p_i^2\rangle \int_{-\infty}^{\infty} \frac{d\omega}{\omega}\mathbf{G}_{ii}(\mathbf{r},\mathbf{r},\omega)\ . \tag{7.39}$$

Thus, all we need to find the mass shift in a particular system is the Green's function for that system. The determination of the electromagnetic Green's function is, in general, a very complex problem. However, three geometries have Green's functions which may be expressed in reasonably compact analytical forms. These are: planar surface, cylinder, sphere and symmetrically layered versions thereof. Since we have already obtained results via explicit mode expansion for the mass shift and magnetic moment of an electron near a single-layered planar surface, it is instructive to re-derive these using the noise-current approach, which means we need the Green's function for the same system considered in section 4.2.1, namely a medium filling the space $z > 0$ and vacuum in the region $z < 0$. We place an electron in the region $z < 0$. In order to calculate the effects of the coupling of the vector potential (7.33) to this electron we require only the $z < 0$ part of the Green's function, which is most naturally and usefully written as [36, 37, 81, 82]

$$\mathbf{G}_{ij}(\mathbf{r},\mathbf{r}',\omega) = \begin{cases} \mathbf{G}^{\rm vac}_{ij}(\mathbf{r},\mathbf{r}',\omega) + \mathbf{G}^{R}_{ij}(\mathbf{r},\mathbf{r}',\omega) & \text{if } z,z' < 0 \\ \mathbf{G}^{T}_{ij}(\mathbf{r},\mathbf{r}',\omega) & \text{if } z < 0,\ z' > 0 \end{cases}, \tag{7.40}$$

where $\mathbf{G}^{\rm vac}$ is the Green's function for unbounded vacuum, and $\mathbf{G}^R$ and $\mathbf{G}^T$ are Green's functions describing medium-influenced propagation from vacuum to vacuum (reflection) and dielectric to vacuum (transmission), respectively. $\mathbf{G}^R$ and $\mathbf{G}^T$ collectively comprise the so-called scattering Green's function.

We begin by calculating the component of the mass shift proportional to $\langle p_\perp^2\rangle$. From eq. (7.38) we have

$$\Delta E_\perp = \frac{e^2}{\pi m^2}\langle p_\perp^2\rangle \int_0^{\infty} \frac{d\omega}{\omega}\,\mathrm{Im}\,\mathbf{G}_{zz}(\mathbf{r},\mathbf{r},\omega)\ . \tag{7.41}$$

We note from eq. (7.40) that at $\mathbf{r} = \mathbf{r}'$ we may immediately ignore $\mathbf{G}^T$. Additionally, $\mathbf{G}^{\rm vac}$ is, by construction, z-independent so is also dropped, leaving only $\mathbf{G}^R$

$$\Delta E_{\rm ren\perp} = \frac{e^2}{\pi m^2}\langle p_\perp^2\rangle \int_0^{\infty} \frac{d\omega}{\omega}\,\mathrm{Im}\,\mathbf{G}^R_{zz}(\mathbf{r},\mathbf{r},\omega)\ . \tag{7.42}$$

The Green's function is compactly expressed by taking advantage of translational invariance parallel to the interface by defining

$$\mathbf{G}(\mathbf{r},\mathbf{r}',\omega) = \frac{1}{(2\pi)^2}\int d^2\mathbf{k}_\parallel e^{i\mathbf{k}_\parallel\cdot(\mathbf{r}_\parallel-\mathbf{r}'_\parallel)}\mathbf{G}(\mathbf{k}_\parallel,z,z',\omega)\ . \tag{7.43}$$

We require $\mathbf{G}_{zz}(\mathbf{r},\mathbf{r}',\omega)$ only, which we will express via $\mathbf{G}_{zz}(\mathbf{k}_\parallel,z,z',\omega)$, which is [37, 51, 81][4]

$$\mathbf{G}^R_{zz}(\mathbf{k}_\parallel,z,z,\omega) = -\frac{i}{2k_z(\omega,k_\parallel)}\frac{k_\parallel^2}{k^2}R^L_{\mathbf{k},\mathrm{TM}}(\omega,k_\parallel)e^{2ik_z(\omega,k_\parallel)z} \tag{7.44}$$

with the reflection coefficient as listed in appendix A.2, and where the notation $k_z(\omega,k_\parallel)$ emphasizes the fact that k_z is here simply a shorthand for $k_z=\sqrt{\omega^2-k_\parallel^2}$. Thus the mass shift is

$$\Delta E_z = -\frac{e^2}{\pi m^2}\frac{\langle p_z^2\rangle}{(2\pi)^2}\,\mathrm{Im}\int_0^\infty\frac{d\omega}{\omega}\int d^2\mathbf{k}_\parallel\frac{i}{2k_z(\omega,k_\parallel)}\frac{k_\parallel^2}{k^2}R^L_{\mathbf{k},\mathrm{TM}}(\omega,k_\parallel)e^{2ik_z(\omega,k_\parallel)z}\,. \tag{7.45}$$

Transforming to spherical polar co-ordinates defined by $k_x=k_\parallel\sin\phi$, $k_y=k_\parallel\cos\phi$, doing the angular integration and simplifying, this becomes

$$\Delta E_z = -\frac{e^2}{4\pi^2m^2}\langle p_z^2\rangle\,\mathrm{Re}\int_0^\infty\frac{d\omega}{\omega^3}\int_0^\infty dk_\parallel\frac{k_\parallel^3}{k_z(\omega,k_\parallel)}R^L_{\mathbf{k},\mathrm{TM}}(\omega,k_\parallel)e^{2ik_z(\omega,k_\parallel)z}\,. \tag{7.46}$$

If we had begun this calculation using the formulation (7.39) of the mass shift, we would have had to specify carefully around which side to circumvent the pole at $\omega=0$. The same pole in (7.46) should be treated by considering the ω integration to start at some infinitesimal value of ω as in

$$\Delta E_z = -\frac{e^2}{4\pi^2m^2}\langle p_\perp^2\rangle\lim_{\delta\to0}\mathrm{Re}\int_\delta^\infty\frac{d\omega}{\omega^3}\int_0^\infty dk_\parallel\frac{k_\parallel^3}{k_z(\omega,k_\parallel)}R^L_{\mathbf{k},\mathrm{TM}}(\omega,k_\parallel)e^{2ik_z(\omega,k_\parallel)z}\,. \tag{7.47}$$

While formula (7.47) looks cumbersome, it is advantageous with respect to that which we would have found using (7.39) because it explicitly includes the taking of a real part, which turns out to be useful in showing its relation to the mode expansion approach to the mass shift. In the formulation based on (7.39) we would not have a real part, rather we would have to consider the parity properties of the ω integrand, which turns out to be much more awkward.

7.2.1 Non-dispersive

We would like to show that formula (7.47) reproduces the k_z plane contour integral (4.39) found through mode expansion. The non-dispersive dielectric has $\epsilon(\omega)=n^2$, in which case the reflection coefficient is

$$R^L_{\mathrm{TM}}(\omega,k_\parallel) = \frac{n^2\sqrt{\omega^2-k_\parallel^2}-\sqrt{n^2\omega^2-k_\parallel^2}}{n^2\sqrt{\omega^2-k_\parallel^2}+\sqrt{n^2\omega^2-k_\parallel^2}} = \frac{n^2k_z(\omega,k_\parallel)-k_z^d(\omega,k_\parallel)}{n^2k_z(\omega,k_\parallel)+k_z^d(\omega,k_\parallel)}\,. \tag{7.48}$$

[4] Care must be taken when comparing this work with [37] because we have $\mathrm{Im}\,k_z<0$, while they have $\mathrm{Im}\,k_z>0$.

The integrand of eq. (7.47) can be real or imaginary depending on the value of ω. As a consequence of this it proves useful to split the integral over ω into three parts. First we have the region $\delta < \omega < k_\parallel/n$

$$\Delta E^{\text{nondisp}}_{z,1} = -\frac{e^2}{4\pi^2 m^2}\langle p_z^2\rangle \lim_{\delta\to 0} \operatorname{Re}\int_\delta^{k_\parallel/n} \frac{d\omega}{\omega^3}\int_0^\infty dk_\parallel \frac{k_\parallel^3}{k_z(\omega,k_\parallel)} R^L_{\mathbf{k},\mathrm{TM}}(\omega,k_\parallel) e^{2ik_z(\omega,k_\parallel)z}. \tag{7.49}$$

In this region k_z is imaginary and the reflection coefficient is real, so the real part of this integral is zero. The next region is $k_\parallel/n < \omega < k_\parallel$

$$\Delta E^{\text{nondisp}}_{z,2} = -\frac{e^2}{4\pi^2 m^2}\langle p_z^2\rangle \operatorname{Re}\int_{k_\parallel/n}^{k_\parallel} \frac{d\omega}{\omega^3}\int_0^\infty dk_\parallel \frac{k_\parallel^3}{k_z(\omega,k_\parallel)} R^L_{\mathbf{k},\mathrm{TM}}(\omega,k_\parallel) e^{2ik_z(\omega,k_\parallel)z}, \tag{7.50}$$

where taking the limit $\delta \to 0$ is trivial since the integral is manifestly independent of δ. Here k_z is imaginary and k_z^d is real, meaning the reflection coefficient is complex. Letting $k_z = -i\kappa = -i\sqrt{k_\parallel^2 - \omega^2}$, we have

$$\begin{aligned}\Delta E^{\text{nondisp}}_{z,2} &= -\frac{e^2}{4\pi^2 m^2}\langle p_z^2\rangle \operatorname{Re}\int_{k_\parallel/n}^{k_\parallel} \frac{d\omega}{\omega^3}\int_0^\infty dk_\parallel \frac{ik_\parallel^3}{\kappa(\omega,k_\parallel)} R^L_{\mathrm{TM}}(\kappa,k_\parallel) e^{-2\kappa(\omega,k_\parallel)z} \\ &= -\frac{e^2}{8\pi^2 m^2}\langle p_z^2\rangle \int_{k_\parallel/n}^{k_\parallel} \frac{d\omega}{\omega^3}\int_0^\infty dk_\parallel \frac{k_\parallel^3}{\kappa(\omega,k_\parallel)} \left[R^L_{\mathrm{TM}}(\kappa,k_\parallel) - R^{L*}_{\mathrm{TM}}(\kappa,k_\parallel)\right] e^{2\kappa(\omega,k_\parallel)z}. \end{aligned} \tag{7.51}$$

Since k_z is here imaginary, we have $k_z = -i\kappa$ where the branch is chosen to preserve the physical constraint that the shift must vanish as $z \to -\infty$. Changing variables via $\omega = \sqrt{k_\parallel^2 + k_z^2} = \sqrt{k_\parallel^2 - \kappa^2}$ gives

$$\begin{aligned}\Delta E^{\text{nondisp}}_{z,2} = -\frac{e^2}{8\pi^2 m^2}\langle p_z^2\rangle \int_0^{-k_\parallel\frac{\sqrt{n^2-1}}{n}} d\kappa \int_0^\infty dk_\parallel \frac{k_\parallel^3}{(k_\parallel^2-\kappa^2)^2} \\ \times \left[R^L_{\mathrm{TM}}(\kappa,k_\parallel) - R^{L*}_{\mathrm{TM}}(\kappa,k_\parallel)\right] e^{2\kappa z}. \end{aligned} \tag{7.52}$$

Inspection of the reflection coefficient (7.48) shows that for k_z imaginary and k_z^d real, taking the conjugate is equivalent to taking $k_z^d \to -k_z^d$.

$$\begin{aligned}\Delta E^{\text{nondisp}}_{z,2} = -\frac{e^2}{8\pi^2 m^2}\langle p_z^2\rangle \int_0^{-k_\parallel\frac{\sqrt{n^2-1}}{n}} d\kappa \int_0^\infty dk_\parallel \frac{k_\parallel^3}{(k_\parallel^2-\kappa^2)^2} \\ \times \left[R^L_{\mathrm{TM}}(\kappa,k_z^d) - R^L_{\mathrm{TM}}(\kappa,-k_z^d)\right] e^{2\kappa z}. \end{aligned} \tag{7.53}$$

Remembering that $\operatorname{Im} k_z < 0$, we have that the first term represents an integral running from the origin down to $-ik_\parallel\frac{\sqrt{n^2-1}}{n}$ in the complex k_z plane, which we displace slightly to the left so that it may be considered as an analytic continuation of the integral along the real k_z axis which we will determine next. Similarly, the second term represents an integral running from $-ik_\parallel\frac{\sqrt{n^2-1}}{n}$ to zero, displaced slightly to the right.

Finally, we have for $\omega > k_\parallel$

$$\Delta E_{z,3}^{\text{nondisp}} = -\frac{e^2}{4\pi^2 m^2}\langle p_z^2\rangle \,\text{Re}\int_{k_\parallel}^{\infty}\frac{d\omega}{\omega^3}\int_0^\infty dk_\parallel \frac{k_\parallel^3}{k_z(\omega,k_\parallel)} R^L_{\mathbf{k},\text{TM}}(\omega,k_\parallel)e^{2ik_z(\omega,k_\parallel)z}$$
$$= -\frac{e^2}{8\pi^2 m^2}\langle p_z^2\rangle \int_{-\infty}^{\infty}dk_z\int_0^\infty dk_\parallel \frac{k_\parallel^3}{(k_z^2+k_\parallel^2)^2} R^L_{\mathbf{k},\text{TM}}(\omega,k_\parallel)e^{2ik_z z}, \tag{7.54}$$

where the change of variable $\omega = \sqrt{k_z^2 + k_\parallel^2}$ has been made.

Thus, the entire mass shift is given by the sum of integrals (7.52) and (7.54), which together are identical to the contour integral (4.39) derived through mode expansion.

7.2.2 General surface

For reasons that will become clear, we begin our discussion of dispersive models with the dielectric function introduced in the discussion of realistic models of the response of the surface found in sec. 4.2.3, namely

$$\epsilon_\gamma(\omega) = 1 - \frac{\omega_p^2}{\omega^2 - \omega_T^2 + i\gamma\omega}\,, \tag{7.55}$$

where ω_p is the plasma frequency, ω_T is the position of an absorption resonance, and $\gamma > 0$ is the damping parameter which determines the width of this resonance. The integral we wish to evaluate is given by eq. (7.47), which we restate here for convenience

$$\Delta E_z = -\frac{e^2}{4\pi^2 m^2}\langle p_\perp^2\rangle \,\text{Re}\int_{\delta}^{\infty}\frac{d\omega}{\omega^3}\int_0^\infty dk_\parallel \frac{k_\parallel^3}{k_z(\omega,k_\parallel)} R^L_{\mathbf{k},\text{TM}}(\omega,k_\parallel)e^{2ik_z(\omega,k_\parallel)z}, \tag{7.56}$$

The dielectric function ϵ_γ is part of a broader class of dielectric functions which satisfy the Kramers-Kronig relations (2.67), for which the poles in R^L_{TM} are in the lower half of the complex ω plane. Thus, our contour is as shown in fig. (7.1). We close the contour

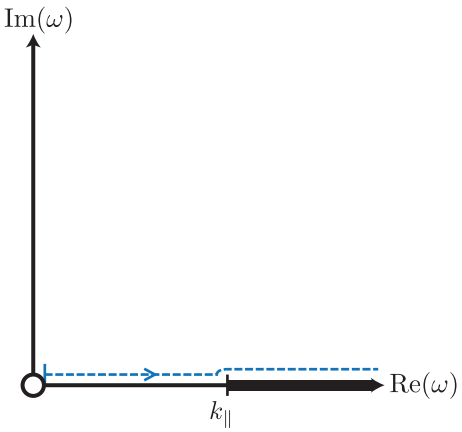

Figure 7.1: ω-plane contour for integral (7.56) for a damped, dispersive dielectric.

in the first quadrant so that we have contributions from the imaginary axis and from the quarter-circle around the pole at $\omega = 0$. The former does not contribute since in that region we have for imaginary $\omega = i\xi$ ($\xi > 0$):

$$\Delta E_z^{\xi} = -\frac{e^2}{\pi m^2}\frac{\langle p_z^2\rangle}{(2\pi)^2}\left[\mathrm{Re}\int_\delta^\infty \frac{d\xi}{\xi^3}\int_0^\infty dk_\parallel \frac{k_\parallel^3}{i\sqrt{\xi^2+k_\parallel^2}} R_{\mathrm{TM}}^L(i\xi,k_\parallel)e^{2\sqrt{\xi^2+k_\parallel^2}z}\right], \tag{7.57}$$

where

$$R_{\mathrm{TM}}^L(i\xi,k_\parallel) = \frac{\epsilon(i\xi)\sqrt{\xi^2+k_\parallel^2}-\sqrt{\epsilon(i\xi)\xi^2+k_\parallel^2}}{\epsilon(i\xi)\sqrt{\xi^2+k_\parallel^2}+\sqrt{\epsilon(i\xi)\xi^2+k_\parallel^2}}, \tag{7.58}$$

and δ is the radius if the small circle around $\omega = 0$. All dielectric functions that we will consider have $\epsilon(i\xi) \in \mathbb{R}^+$, so the reflection coefficient is real on the imaginary ω axis, showing that $\Delta E_z^{\xi} = 0$. The contribution at $\omega = 0$ is evaluated through the residue theorem. Carrying out the $k_\parallel$ integral as well, we have for the result

$$\Delta E_z = \frac{e^2}{16\pi m^2 z}\left\{\frac{[\epsilon(0)-1][1+2\epsilon(0)]}{[1+\epsilon(0)]^2}+\frac{[1+\epsilon(0)]\epsilon''(0)-2\epsilon'(0)^2}{2z^2[1+\epsilon(0)]^3}\right\}\langle p_z^2\rangle, \tag{7.59}$$

where the primes denote derivatives[5] with respect to ω. This formula represents a generalization of our previous work to damped media, and also reproduces the undamped models considered before. The latter fact warrants further investigation since inspection of eq. (7.33) shows that if an undamped dielectric function ($\epsilon_I(\omega) = 0$) were inserted at that point in the calculation, there would be no polariton excitations and the shift would vanish, in clear disagreement with the results of eq. (7.59) upon insertion of a real permittivity. This means that it is instructive to investigate precisely how and why undamped results can be obtained from a formalism whose foundations rest entirely on the inclusion of damping, and how this relates to Chapter 4 where we used a direct first-principles mode expansion to obtain results for undamped media.

7.2.3 Undamped dispersive dielectric

An undamped dispersive dielectric is described by the following permittivity

$$\epsilon_{\mathrm{disp}}(\omega) = 1 - \frac{\omega_p^2}{\omega^2-\omega_T^2}, \tag{7.60}$$

which we insert into eq. (7.56) to give the mass shift near an undamped dispersive dielectric

$$\Delta E_z = -\frac{e^2}{4\pi^2 m^2}\langle p_\perp^2\rangle\,\mathrm{Re}\int_\delta^\infty \frac{d\omega}{\omega^3}\int_0^\infty dk_\parallel \frac{k_\parallel^3}{k_z(\omega,k_\parallel)} R_{\mathbf{k},\mathrm{TM}}^L(\epsilon_{\mathrm{disp}})e^{2ik_z(\omega,k_\parallel)z}, \tag{7.61}$$

[5] We remind the reader that here and throughout we use primes to denote derivatives of ϵ – this should not be confused with the common notation $\epsilon' = \mathrm{Re}\,\epsilon$ and $\epsilon'' = \mathrm{Im}\,\epsilon$.

The TM reflection coefficient $R^L_{\mathbf{k},\mathrm{TM}}(\epsilon_{\mathrm{disp}})$ listed in (A.5) has two positive frequency poles, the positions of which are given by

$$\omega_\pm = \left\{ k_\parallel^2 + \frac{1}{2}(\omega_p^2 + \omega_T^2) \pm \left[k_\parallel^4 - k_\parallel^2 \omega_T^2 + \frac{1}{4}\left(\omega_p^2 + \omega_T^2\right)^2 \right]^{1/2} \right\}^{1/2}, \tag{7.62}$$

where $\omega_-(\omega_T = 0) = \omega_{\mathrm{sp}}$ is the surface plasmon frequency of the material. The reflection coefficient also has three positive-frequency branch points, located at $\omega = \omega_T$ and

$$\Omega_\pm = \frac{1}{\sqrt{2}} \left\{ k_\parallel^2 + \omega_p^2 + \omega_T^2 \pm \left[k_\parallel^4 + 2k_\parallel^2 \left(\omega_p^2 - \omega_T^2\right) + \left(\omega_p^2 + \omega_T^2\right)^2 \right]^{1/2} \right\}^{1/2}. \tag{7.63}$$

The various possible relative positions of the poles and branch points are summarized in fig. (7.2) – we place the branch cuts in the shaded areas, as shown in fig. (7.3).

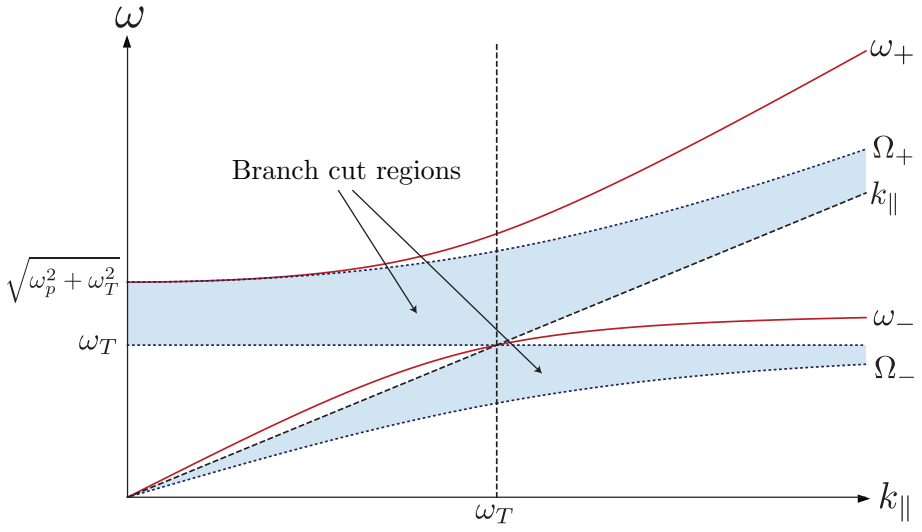

Figure 7.2: Positions of the poles and branch points of $R^L_{\mathbf{k},\mathrm{TM}}(\epsilon_{\mathrm{disp}})$ along the real ω axis for an undamped dispersive dielectric.

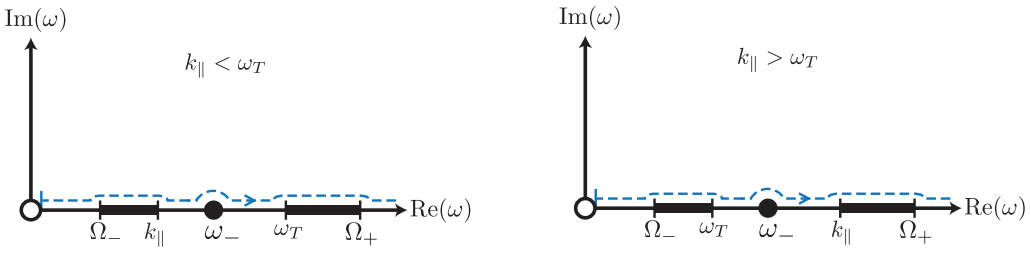

Figure 7.3: ω-plane contour for an undamped dispersive dielectric

The subtlety is in precisely how the poles (7.62) should be dealt with. The pole at $\omega = 0$ was dealt with by restricting the range of integration, which we deduced was the correct way to proceed based on what one would have to do in alternative formulation of the whole

problem, namely the full-range ω integral (7.39) rather than its half-range counterpart (7.38). However, there is nothing to say that the poles (7.62) should be treated the same way as that at $\omega = 0$ – in fact they should not. This is because of a previously mentioned quality that the noise-current approach has, which is that it necessarily requires a damped surface. This means that the undamped cases can only be viewed as particular limits of the damped case, which means that these poles must be displaced an infinitesimal amount below the real axis, or, equivalently, the contour must be displaced the corresponding amount above the real axis, as shown in figure (7.3). Closing the contour into the upper half-plane, then discarding the contribution along the imaginary axis and evaluating the quarter residue around $\omega = 0$ of course gives the same result as obtained by inserting the dielectric function (7.60) into eq. (7.59). We emphasize that eq. (7.59) was derived using a method which specifically relied on the material in question being damped, but we have shown that by using the correct pole prescription the formula (7.59) is equally applicable to undamped media.

An important part of our previous work obtaining the mass shift via mode expansion was that we included specific and separate expressions of the surface plasmon modes. Analytic continuation of the integrals over TE and TM modes in the complex k_z plane led to a cancellation of the surface plasmon modes with the pole in the TM reflection coefficient at the surface plasmon frequency. The noise-current method seems to completely circumvent this step, so the question is then precisely how this happens. We shall see that the contour integral in the ω plane encapsulates this step, without ever explicitly referring to surface plasmon modes.

To show this we transform the integral (7.56) from the complex ω plane into the complex k_z plane, giving

$$\Delta E_z = -\frac{e^2}{4\pi^2 m^2}\langle p_\perp^2 \rangle \lim_{\delta\to 0} \mathrm{Re} \int_C dk_z \int_0^\infty dk_\parallel \frac{k_\parallel^3}{(k_z^2 + k_\parallel^2)^2} R^L_{\mathbf{k},\mathrm{TM}}(k_z, k_\parallel) e^{2ik_z z}, \tag{7.64}$$

where the curve C is that shown in fig. 7.5. The poles $k_{z,\pm}$ and branch points $K_{z,\pm}$ of $R^L_{\mathbf{k},\mathrm{TM}}(\epsilon_{\mathrm{disp}})$ in the k_z plane are located at

$$k_{z,\pm} = \sqrt{\omega_\pm^2 - k_\parallel^2}, \qquad\qquad K_{z,\pm} = \sqrt{\Omega_\pm^2 - k_\parallel^2}, \tag{7.65}$$

so it is evident that under certain conditions these may move onto the imaginary axis, as shown in figs 7.4, which together correspond to the form of the k_z plane shown in figure 7.5. Taking initially the case where $k_\parallel > \omega_T$, in a similar way to the non-dispersive dielectric we have that the act of taking the real part removes all contributions which run directly along the imaginary axis, leaving only those parts which are displaced slightly (i.e. those

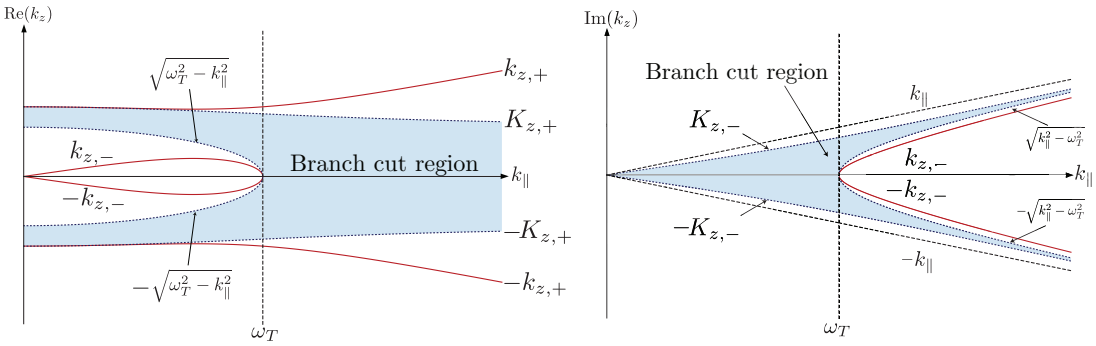

(a) Real axis **(b)** Imaginary axis

Figure 7.4: Positions of the poles and branch points of $R^L_{\mathbf{k},\mathrm{TM}}(\epsilon_{\mathrm{disp}})$ along the real and imaginary k_z axes for an undamped dispersive dielectric.

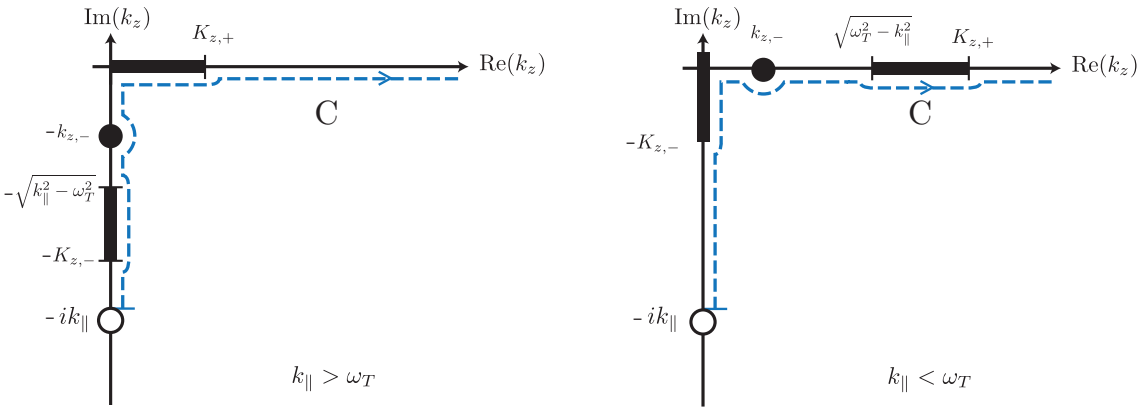

Figure 7.5: k_z-plane contour for an undamped dispersive dielectric.

around poles or branch cuts), as shown in fig. 7.6(b). We have that the real-axis integral is even in k_z, so we may extend it over the whole real axis and introduce a factor of $\frac{1}{2}$ as shown in fig. 7.6(c). This integral represents the contributions of the TE and TM travelling modes previously encountered in the mode expansion, and the integrals around poles and branch cuts on the imaginary axis represent the contribution of bound states of the system (surface plasmons, for example), previously considered as entirely separate types of mode. In order to actually evaluate the energy shift, we deform the real axis integral into the lower half plane where of course it picks up contributions from encirclement of the pole and the branch cut. However, due to opposite winding and the introduction of the factor of $\frac{1}{2}$ from extension of the real axis integral over the whole real line, these contributions cancel with the explicit bound state contributions arising from the original contour as shown in fig. 7.6(d), leaving only the contribution from the residue at $k_z = -ik_\parallel$ shown in fig. 7.6(e). This cancellation is the analogue of the surface plasmon cancellation detailed in section 4.2.2. The case with $k_\parallel < \omega_T$ is simplified in an identical way, again resulting in the whole

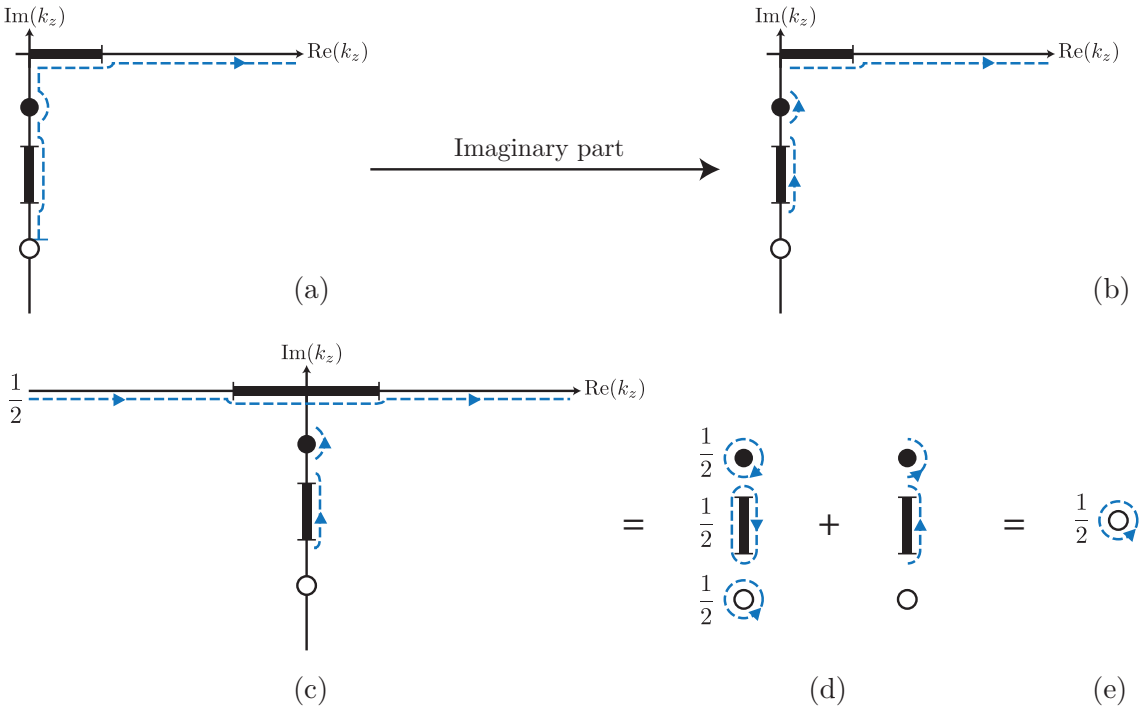

Figure 7.6: (continuation of fig. 7.5) Schematic illustration of the method by which the mass shift derived via the noise-current approach for a dispersive dielectric reproduces that found by mode expansion for the case $k_{\parallel} > \omega_T$.

contribution being from the residue at $k_z = -ik_{\parallel}$.

7.2.4 Summary

We have shown that the noise-current approach to calculation of the mass shift of an electron near a surface reproduces the corresponding results found through mode expansion. Further to this, we have demonstrated that the contour in the ω plane required to calculate the mass shift in the noise-current approach contains all the various mode structure (cancellation of surface plasmon modes, etc) that we observed in the mode expansion method.

7.3 Magnetic Moment

7.3.1 Introduction

We will now calculate the magnetic moment shift of an electron near a surface using the noise-current approach, so that we may compare the results to those obtained by mode expansion in Chapter 5. From eqs (5.33) and (5.39), we have for the interaction energy

that gives rise to the magnetic moment

$$\Delta E_{\text{int}} = e^2 \sum_{\nu' s'} \frac{|\langle \nu, s; 0| (H_0 + E_\nu) \boldsymbol{\alpha} \cdot \mathbf{A}(\mathbf{r}) (H_0 + E_{\nu'}) |\nu', s'; 1_j(\mathbf{r}', \omega)\rangle|^2}{(E_\nu - E_{\nu'} - \omega) 2E_\nu (E_\nu + m) 2E_{\nu'} (E_{\nu'} + m)}, \tag{7.66}$$

where α_i is given by eq. (5.5). Using eq. (7.33) and introducing an infinitesimal δ in the same way as in (7.47), this becomes

$$\Delta E_{\text{int}} = \frac{e^2}{\pi} \lim_{\delta \to 0} \sum_{\nu' s'} \int_\delta^\infty d\omega\, \omega^2 \int d^3\mathbf{r}' \epsilon_I(\mathbf{r}', \omega) \times \frac{|\langle \nu, s; 0| (H_0 + E_\nu) \boldsymbol{\alpha} \cdot \left[\mathbf{G}^R(\mathbf{r}, \mathbf{r}', \omega) \cdot \hat{\mathbf{a}}^p(\mathbf{r}, \omega)\right] (H_0 + E_{\nu'}) |\nu', s'; 1_j(\mathbf{r}', \omega)\rangle|^2}{(E_\nu - E_{\nu'} - \omega) 2E_\nu (E_\nu + m) 2E_{\nu'} (E_{\nu'} + m)}. \tag{7.67}$$

Using eq. (E.4), the operator part is written in component form as

$$\mathbf{G}^R(\mathbf{r}, \mathbf{r}', \omega) \cdot \hat{\mathbf{a}}^p(\mathbf{r}, \omega) = G^R_{ij}(\mathbf{r}, \mathbf{r}', \omega) \hat{a}^p_j \hat{\mathbf{r}}_i \equiv \mathbf{F}(\mathbf{r}, \mathbf{r}', \omega) \hat{a}^p_j, \tag{7.68}$$

where $\mathbf{F}(\mathbf{r}, \mathbf{r}, \omega) \equiv G^R_{ij}(\mathbf{r}, \mathbf{r}, \omega) \hat{\mathbf{r}}_i$ is a vector, and throughout we leave the sum over j implied. Through orthogonality of the polariton eigenstates, we must have $\mathbf{r} = \mathbf{r}'$. However, in contrast to the mass shift calculation, we will see that we have to take derivatives of $\mathbf{F}(\mathbf{r}, \mathbf{r}', \omega)$ with respect to $\mathbf{r}$. We could do the entire calculation before applying the operator $\hat{\mathbf{a}}^p(\mathbf{r}, \omega)$, but this is very cumbersome. We avoid this issue by saying that derivatives of $\mathbf{F}(\mathbf{r}, \mathbf{r}, \omega)$ with respect to the components of $\mathbf{r}$ act only on the first argument, i.e.

$$\frac{\partial \mathbf{F}(\mathbf{r}, \mathbf{r}, \omega)}{\partial r_i} \equiv \lim_{\mathbf{r}' \to \mathbf{r}} \left[\frac{\partial \mathbf{F}(\mathbf{r}, \mathbf{r}', \omega)}{\partial r_i}\right]. \tag{7.69}$$

With this definition, the shift is obtained from

$$\Delta E_{\text{int}} = \frac{e^2}{\pi} \lim_{\delta \to 0} \sum_{\nu' s'} \int_\delta^\infty d\omega \omega^2 \int d^3\mathbf{r} \epsilon_I(\mathbf{r}, \omega) \frac{|\langle \nu, s| (H_0 + E_\nu) \boldsymbol{\alpha} \cdot \mathbf{F}(\mathbf{r}, \mathbf{r}, \omega) (H_0 + E_{\nu'}) |\nu', s'\rangle|^2}{(E_\nu - E_{\nu'} - \omega) 2E_\nu (E_\nu + m) 2E_{\nu'} (E_{\nu'} + m)}. \tag{7.70}$$

The matrix element and energy denominators are identical to eq. (5.39) with $\mathbf{f}_{\mathbf{k}\lambda}(\mathbf{r}, \omega) \to \mathbf{F}(\mathbf{r}, \mathbf{r}, \omega)$. Thus, we can significantly shorten the calculation by appealing to the fact that much of the analysis in section 5.3 holds for any vector in place of $\mathbf{f}_{\mathbf{k}\lambda}(\mathbf{r}, \omega)$. The only step which relies on the specific form of the mode functions is the elimination of various terms due to their being zero under $\int d^3\mathbf{k}$. This section concerns layered planar media only, for which the Green's function is analytically known. For these calculations all the same terms can be dropped. That this must happen can be seen by comparing the Green's function (E.17) with the table of coefficients A.1 used to streamline the process of taking products of mode functions. Taking, for example, the $|\mathbf{f}_{\mathbf{k}\lambda,z}(\mathbf{r}, \omega)|^2$ term we have from A.1

$$|\mathbf{f}_{\mathbf{k}\lambda,z}(\mathbf{r}, \omega)|^2 \propto \frac{k_\parallel^2}{k^2}. \tag{7.71}$$

We note also the following property of the zz component of the reflected part of the Green's function (E.17)

$$\mathbf{G}^R_{zz}(\mathbf{k}_\parallel, z, z', \omega) \propto \frac{k_\parallel^2}{k^2}, \tag{7.72}$$

which demonstrates that the product of component i and (the conjugate of) component j of the mode functions has the same function of k multiplying it as component G_{ij} of the Green's function. In other words, the Green's function can be constructed from the mode functions $\mathbf{f}_{\mathbf{k}\lambda}(\mathbf{r}, \omega)$. Thus, we can say by direct analogy to eq. (5.96) that the shift in terms of the vector $\mathbf{F}(\mathbf{r}, \mathbf{r}, \omega)$ is given by

$$\Delta\mu_\perp = -\frac{e^3}{4m^3}\frac{1}{\pi}\int_\delta^\infty d\omega\,\omega^2 \int d^3\mathbf{r}\,\epsilon_I(\mathbf{r},\omega)\Bigg[|F_z|^2 + \frac{|(\nabla\times\mathbf{F})_x|^2}{\omega^2} + \frac{|(\nabla\times\mathbf{F})_y|^2}{\omega^2} + \frac{1}{\omega^2}\left(F_x\frac{\partial^2 F_y^*}{\partial x\partial y} + F_y\frac{\partial^2 F_x^*}{\partial x\partial y} - F_y\frac{\partial^2 F_y^*}{\partial x^2} - F_x\frac{\partial^2 F_x^*}{\partial y^2} + \text{H.c.}\right)\Bigg], \tag{7.73}$$

where we have abbreviated $\mathbf{F}(\mathbf{r}, \mathbf{r}, \omega) \equiv \mathbf{F}$. As was done in section 5.4 we can simplify by noting that pairs of terms that differ by $x \leftrightarrow y$ must give the same contribution due to the xy symmetry of the problem, and we also note that each term in (7.73) contributes a real number, so that we can replace the Hermitian conjugation with a factor of two. Making these simplifications we are left with

$$\Delta\mu_\perp = -\frac{e^3}{4m^3}\frac{1}{\pi}\int_\delta^\infty d\omega\,\omega^2 \int d^3\mathbf{r}\,\epsilon_I(\mathbf{r},\omega) \times\left[|F_z|^2 + 2\frac{|(\nabla\times\mathbf{F})_x|^2}{\omega^2} + \frac{4}{\omega^2}\left(F_x\frac{\partial^2 F_y^*}{\partial x\partial y} - F_x\frac{\partial^2 F_x^*}{\partial y^2}\right)\right]. \tag{7.74}$$

From eq. (7.68), we have

$$\mathbf{F}(\mathbf{r}, \mathbf{r}, \omega) \equiv G_{ij}(\mathbf{r}, \mathbf{r}, \omega)\hat{\mathbf{r}}_i, \tag{7.75}$$

so that, for example,

$$F_z(\mathbf{r}, \mathbf{r}, \omega) = G_{ij}(\mathbf{r}, \mathbf{r}, \omega)\hat{\mathbf{r}}_i \cdot \hat{\boldsymbol{z}} = G_{zj}(\mathbf{r}, \mathbf{r}, \omega). \tag{7.76}$$

Due to the tensor nature of $\mathbf{G}$ it is more transparent to write the curl out in terms of its constituent derivatives rather than leave it as a curl as was done in section 5.4. Inserting (7.76) into eq. (7.74) and expanding out the curl term we have

$$\Delta\mu_\perp = -\frac{e^3}{4m^3}\frac{1}{\pi}\int_\delta^\infty d\omega\,\omega^2 \int d^3\mathbf{r}\,\epsilon_I(\mathbf{r},\omega) \times\Bigg[|G_{zj}|^2 + \frac{2}{\omega^2}\left(\left|\frac{\partial G_{zj}}{\partial y}\right|^2 + \left|\frac{\partial G_{yj}}{\partial z}\right|^2 - \frac{\partial G_{zj}}{\partial y}\frac{\partial G_{jy}^*}{\partial z} - \frac{\partial G_{yj}}{\partial z}\frac{\partial G_{jz}^*}{\partial y}\right) + \frac{4}{\omega^2}\left(G_{xj}\frac{\partial^2 G_{jy}^*}{\partial x\partial y} - G_{jx}\frac{\partial^2 G_{xj}^*}{\partial y^2}\right)\Bigg], \tag{7.77}$$

where we have again abbreviated $G_{ij}(\mathbf{r},\mathbf{r},\omega) \equiv G_{ij}$. Further abbreviating

$$\partial_\gamma^{(l)} \equiv \frac{\partial}{\partial x_i}\frac{\partial}{\partial x_j}...\frac{\partial}{\partial x_l} \qquad \left(\text{e.g.} \quad \partial_{xyz}^3 = \frac{\partial}{\partial x}\frac{\partial}{\partial y}\frac{\partial}{\partial z}\right) \tag{7.78}$$

the magnetic moment shift is finally written as

$$\begin{aligned}\Delta\mu_\perp = -\frac{e^3}{4m^3}\frac{1}{\pi}\int_\delta^\infty d\omega\,\omega^2 \int d^3\mathbf{r}\,\epsilon_I(\mathbf{r},\omega) \\ \times\Bigg[|G_{zj}|^2 + \frac{2}{\omega^2}\Big(|\partial_y G_{zj}|^2 + |\partial_z G_{yj}|^2 - (\partial_y G_{zj})(\partial_z G_{yj}^*) - (\partial_z G_{yj})(\partial_y G_{zj}^*)\Big) \\ + \frac{4}{\omega^2}\left(G_{xj}^*\partial_{xy}^2 G_{yj} - G_{xj}\partial_{yy}^2 G_{xj}^*\right)\Bigg],\end{aligned} \tag{7.79}$$

where the symmetry relation (E.11) has been used. This is an expression which is nearly suitable for simplification via the integral relation (7.18), however there is one subtlety that needs to be addressed. The main difference between eq. (7.79) and the corresponding expression for the mass shift (7.37) is the presence of spatial derivatives. This means that in order to apply (7.18) we have to apply the derivative operator first. To do this we assume that the electron is sitting in vacuum. This is not just to make the calculation simpler – consideration of radiative corrections to microscopic systems embedded in macroscopic materials would necessitate the inclusion of local field effects [83]. This assumption has the useful consequence that the spatial dependence of the Green's function on the vacuum side of the interface must be either a plane wave or a damped exponential, meaning that the components of the reflected Green's function are necessarily eigenfunctions of any spatial derivative operator.

The final step in the simplification of (7.79) is to note that for real k_z one has to take $k_z \to -k_z$ in the reflected part of the Green's function upon interchange of the indices $\mathbf{r}$ and $\mathbf{r}'$, which is essentially the analogue of the process by which an extra minus sign is generated in products of mode functions as detailed in appendix A.3 eqs. (A.17) and (A.18). As an aside, we note that if one happens to miss this subtlety when taking the mode expansion approach, the entire process of transformation of the integrals into a single contour integral breaks down. The fact that this always works is a consequence of the completeness of the modes (as shown explicitly for non-dispersive and plasma media), so if this does not work one is naturally led to realize that there has been a mistake. If one misses this subtlety in the noise-current approach the only consequences are a few different signs in the simplification of (7.79), which will lead one to get reasonable-seeming but wrong results. This is a telling example of the mode expansion approach being more physically transparent and intuitive than other approaches.

Proceeding, we use the assumptions above to rewrite the shift as

$$\Delta\mu_\perp = \frac{e^3}{4m^3}\frac{1}{\pi}\int_\delta^\infty d\omega\ \mathrm{Im}\left[G_{zz} + \frac{2}{\omega^2}\left(G_{zz}k_y^2 - G_{yy}k_z^2 + G_{zy}k_yk_z - G_{yz}k_yk_z\right) - \frac{4}{\omega^2}\left(G_{xy}k_xk_y - G_{xx}k_y^2\right)\right]. \tag{7.80}$$

We now let $\mathbf{G}(\mathbf{r},\mathbf{r}',\omega) \to \mathbf{G}^R(\mathbf{r},\mathbf{r}',\omega)$ for the same reasons as that which took eq. (7.41) to eq. (7.42) in the calculation of the mass shift, which were that the vacuum component of $\mathbf{G}(\mathbf{r},\mathbf{r}',\omega)$ is independent of z, so is subtracted to effect our usual approach to renormalization via subtraction of terms which would remain without the presence of the surface. We then have

$$\Delta\mu_\perp = \frac{e^3}{4m^3}\frac{1}{\pi}\int_\delta^\infty d\omega\ \mathrm{Im}\left[G^R_{zz} + \frac{2}{\omega^2}\left(G^R_{zz}k_y^2 - G^R_{yy}k_z^2 + G^R_{zy}k_yk_z - G_{yz}k_yk_z\right) - \frac{4}{\omega^2}\left(G^R_{xy}k_xk_y - G_{xx}k_y^2\right)\right]. \tag{7.81}$$

This cannot be extended over the whole frequency axis in the same way as (7.39) for the mass shift because its extra power of ω means it has different parity properties.

We are now ready to substitute the explicit dyadic Green's function for planar media, found in appendix E.3.2. After some algebra, the result is found to be

$$\Delta\mu_\perp = -\frac{e^3}{4m^3}\frac{1}{2\pi^2}\int_\delta^\infty d\omega\int_0^\infty dk_\parallel\ \mathrm{Re}\left\{\frac{k_\parallel}{2k_z\omega^2}\left[\left(2k_\parallel^2 - k_z^2\right)R^L_{\mathrm{TE}}(\omega) + \left(2k_\parallel^2 + k_z^2\right)R^L_{\mathrm{TM}}(\omega)\right]e^{2ik_zz}\right\}, \tag{7.82}$$

where the angular integration over ϕ defined by $\{k_x = k_\parallel\cos\phi,\ k_y = k_\parallel\sin\phi\}$ has been evaluated already.

7.3.2 Evaluating the shift

The principal difference between the expressions for the magnetic moment shift (7.82) and the mass shift (7.46) is the extra power of ω appearing in the denominator. This is completely inconsequential in the reproduction of the k_z plane contour. For example, in the case of a non-dispersive dielectric the above expression can be easily shown to be equivalent to the contour integral (5.98a) obtained from mode expansion by an identical method to that used to show that the noise-current mass shift result (7.47) in section 7.2 is equivalent to the contour integral (4.39) obtained by mode expansion. The extra power of ω only has an effect once the contour is deformed into the lower half-plane where it introduces a branch point at $k_z = -ik_\parallel$, whence the method is identical to section 5.4.

The extra power of ω does however have significant consequences in the ω plane, which, as we have seen in section 4.2.5, is the most appropriate setting in which to calculate radiative corrections near absorbing surfaces. Completing the contour in the upper half-plane and changing variables to $\xi = -i\omega$, we have for the magnetic moment shift

$$\Delta\mu_\perp = -\frac{e^3}{4m^3}\frac{1}{(2\pi)^2}\,\mathrm{Re}\int_{C_\delta} d\xi \int_0^\infty dk_\parallel k_\parallel \frac{e^{2\sqrt{\xi^2+k_\parallel^2}z}}{\xi^2\sqrt{\xi^2+k_\parallel^2}} \times \left[\left(3k_\parallel^2+\xi^2\right)R^L_{\mathrm{TE}}(\xi) + \left(k_\parallel^2-\xi^2\right)R^L_{\mathrm{TM}}(\xi)\right] = \int_{C_\delta} d\xi f(\xi), \tag{7.83}$$

where the contour C_δ is that shown in fig. 7.7(a). All the dielectric functions that we

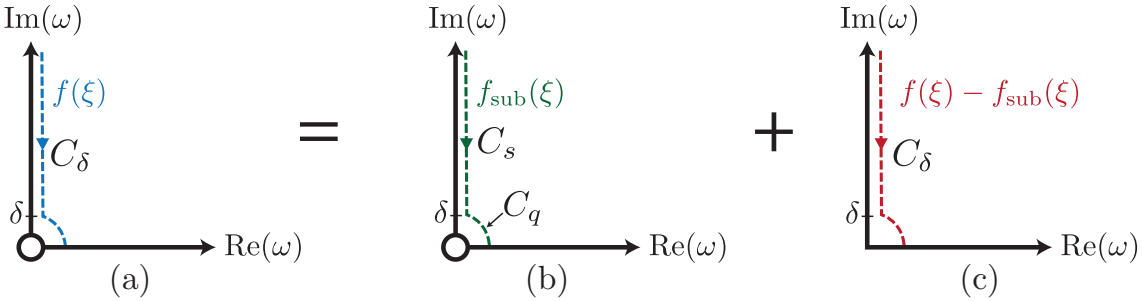

Figure 7.7: Illustrations in the complex ω plane of the process by which we deal with the pole at $\omega = 0$ in magnetic moment calculations. The colors emphasize the fact that the integrands are different for each contour.

consider have $\epsilon(i\xi) \in \mathbb{R}^+$, so the portion of the integral that is along the imaginary frequency axis is *not* zero, in contrast to the mass shift. This makes the treatment of the pole at $\omega = 0$ considerably more awkward. As shown in figure 7.7(b), we begin by subtracting from the integrand the part which diverges as $\xi \to 0$, which corresponds to subtracting the principal part of its Laurent series about $\xi = 0$. For *undamped* dielectric functions (we will come back to this point) the integral over the subtraction $f_{\mathrm{sub}}(\xi)$ is

$$\int_{C_\delta} d\xi f_{\mathrm{sub}}(\xi) = -\frac{e^3}{4m^3}\frac{1}{(2\pi)^2}\,\mathrm{Re}\int_{C_\delta} d\xi \int_0^\infty dk_\parallel \frac{k_\parallel^2}{\xi^2} R^L_{\mathrm{TM}}(0)e^{2k_\parallel z}\,. \tag{7.84}$$

The residue of this at $\xi = 0$ is zero, which means that the integral is not suitable for evaluation through the residue theorem. Instead we parameterize the quarter circle C_q by letting $\omega = \delta e^{i\varphi}$, with $\varphi = \pi/2 ... 0$. In terms of ξ, this corresponds to letting $\xi = -i\delta e^{i\phi}$

with $\phi = 0...{}^{-\pi}/_{2}$ so that the quarter circle part of (7.84) becomes

$$\begin{aligned}\int_{C_q} d\xi f_{\text{sub}}(\xi) &= \frac{e^3}{4m^3}\frac{1}{(2\pi)^2}\,\text{Re}\int_0^{-\pi/2} d\phi\;\delta\int_0^{\infty} dk_\parallel \frac{k_\parallel e^{i\phi}}{\delta^2 e^{2i\phi}} R^L_{\text{TM}}(0)e^{2k_\parallel z}\\ &= \frac{e^3}{4m^3}\frac{1}{(2\pi)^2}\int_0^{-\pi/2} d\phi\;\delta\int_0^{\infty} dk_\parallel \frac{k_\parallel}{\delta^2}\cos(\phi) R^L_{\text{TM}}(0)e^{2k_\parallel z}\\ &= \frac{e^3}{4m^3}\frac{1}{(2\pi)^2}\frac{1}{4\delta z^3} R^L_{\text{TM}}(0)\;. \end{aligned} \tag{7.85}$$

The part of integral (7.84) that is straight down the imaginary axis (contour C_s in fig. 7.7(b)) is

$$\begin{aligned}\int_{C_s} d\xi f_{\text{sub}}(\xi) &= \frac{e^3}{4m^3}\frac{1}{(2\pi)^2}\,\text{Re}\int_\delta^{\infty} d\xi\int_0^{\infty} dk_\parallel \frac{k_\parallel^2}{\xi^2} R^L_{\text{TM}}(0)e^{2k_\parallel z}\\ &= -\frac{e^3}{4m^3}\frac{1}{(2\pi)^2}\frac{1}{4\delta z^3} R^L_{\text{TM}}(0)\;. \end{aligned} \tag{7.86}$$

Thus we find for the integral along the whole contour C_δ

$$\int_{C_\delta} d\xi f_{\text{sub}}(\xi) = \int_{C_q} d\xi f_{\text{sub}}(\xi) + \int_{C_s} d\xi f_{\text{sub}}(\xi) = 0\;, \tag{7.87}$$

for all δ. So we have shown that the integral shown in fig. 7.7(b) is zero, meaning that the whole contribution is given by the integral shown in fig. 7.7(c). Since the pole at $\omega = 0$ is not present in the integral shown in 7.7(c), we may freely deform the contour C_δ to run straight along the imaginary frequency axis, as shown fig. 7.8(c).

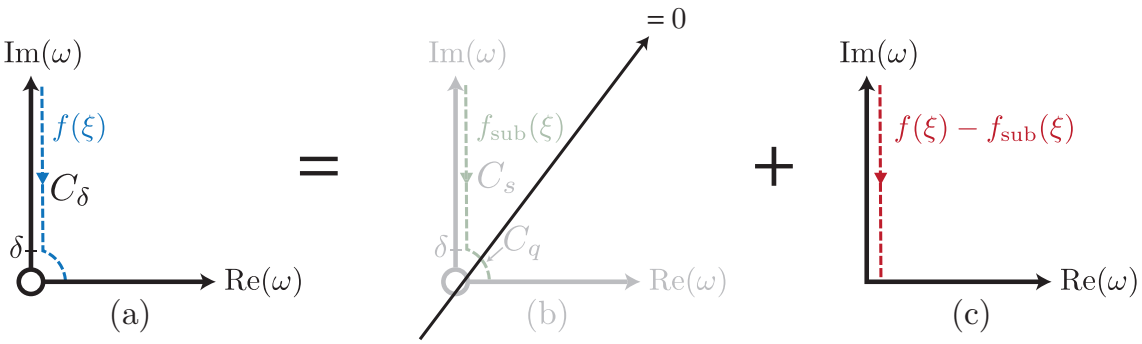

Figure 7.8: (continuation of fig. 7.7) Illustrations in the complex ω plane of the process by which we deal with the pole at $\omega = 0$ in magnetic moment calculations. Part (b) has been removed as a consequence of (7.87).

In summary, we have shown that the pole in eq. (7.83) should be treated by subtracting $\int_{C_\delta} d\xi f_{\text{sub}}(\xi)$ from eq. (7.83) and then deforming the contour C_δ to run straight along the imaginary axis, giving

$$\begin{aligned}\Delta\mu_\perp = &\frac{e^3}{4m^3}\frac{1}{(2\pi)^2}\int_0^{\infty} d\xi\int_0^{\infty} dk_\parallel k_\parallel\\ &\times\left\{\frac{e^{2\sqrt{\xi^2+k_\parallel^2}z}}{\xi^2\sqrt{\xi^2+k_\parallel^2}}\left[\left(3k_\parallel^2+\xi^2\right)R^L_{\text{TE}}+\left(k_\parallel^2-\xi^2\right)R^L_{\text{TM}}\right]-\frac{k_\parallel}{\xi^2}R^L_{\text{TM}}(0)e^{2k_\parallel z}\right\},\end{aligned} \tag{7.88}$$

where it has been observed that the integrand is real for all dielectric functions with $\epsilon(i\xi) \in \mathbb{R}^+$, and is integrated directly over real ξ, so the result is necessarily real. This agrees with the result (5.164a) found through mode expansion.

7.3.3 Damping

In our derivation of (7.88) we assumed in eq. (7.84) that the surface does not have a damping parameter γ in its permittivity. If we lift that assumption and take the permittivity to be

$$\epsilon_\gamma(\mathbf{r},\omega) = 1 - \Theta(z)\frac{\omega_p^2}{\omega^2 - \omega_T^2 + i\omega\gamma}, \tag{7.89}$$

we have for eq. (7.83)

$$\begin{aligned}\Delta\mu = -\frac{e^3}{4m^3}\frac{1}{(2\pi)^2}\,\mathrm{Re}\int_{C_\delta} d\xi \int_0^\infty dk_\parallel k_\parallel \frac{e^{2\sqrt{\xi^2+k_\parallel^2}z}}{\xi^2\sqrt{\xi^2+k_\parallel^2}} \\ \times\left[\left(3k_\parallel^2+\xi^2\right)R_{\mathrm{TE}}^{\gamma L}(\xi) + \left(k_\parallel^2-\xi^2\right)R_{\mathrm{TM}}^{\gamma L}(\xi)\right] = \int_{C_\delta} d\xi f(\xi),\end{aligned} \tag{7.90}$$

where we have written $R_\lambda^L(\xi) \to R_\lambda^{\gamma L}(\xi)$ to emphasize that we are considering a damped surface. Following the method we used in the previous section, we subtract from the integrand the principal part of its Laurent series about $\xi = 0$, giving for the subtracted part of the integral

$$\int_{C_\delta} d\xi f_{\mathrm{sub}}^\gamma(\xi) = -\frac{e^3}{4m^3}\frac{1}{(2\pi)^2}\,\mathrm{Re}\int_{C_\delta} d\xi \int_0^\infty dk_\parallel \frac{k_\parallel^2}{\xi^2}\left(R_{\mathrm{TM}}^{\gamma L}(0) + \xi R_{\mathrm{TM}}^{\gamma L'}(0)\right)e^{2k_\parallel z}, \tag{7.91}$$

where the prime denotes a derivative with respect to ξ. The contour C_δ is given by the sum of C_q and C_s, as shown in fig. (7.7). Considering the part of the second term of (7.91) that is integrated over C_s, we have

$$-\frac{e^3}{4m^3}\frac{1}{(2\pi)^2}\,\mathrm{Re}\int_\delta^\infty d\xi \int_0^\infty dk_\parallel \frac{k_\parallel^2}{\xi} R_{\mathrm{TM}}^{\gamma L'}(0) e^{2k_\parallel z}, \tag{7.92}$$

which diverges logarithmically at its upper limit, so making a subtraction along the lines of that done in section 7.3.2 does not work if the dielectric function has $\gamma \neq 0$. This problem was not seen in the mass shift (7.56) because of its differing overall power of ω which meant that the integral along the imaginary frequency axis vanished when we took the real part of the integrand. This, alongside the related problems detailed in section 5.4.4, may indicate that one needs to do a full Huttner-Barnett quantization [31, 32] in order to calculate the magnetic moment of an electron near an absorbing surface.

7.4 Born series approach

The main utility of the noise-current approach is its description of the surface solely through its electromagnetic Green's function. This makes it amenable to extension to more complex systems than an infinite half-space. In this section we outline how the Green's function for the electromagnetic field near an arbitrarily shaped object can be calculated perturbatively through the use of a Born series, and then compare this with the exact results obtained thus far.

7.4.1 The Born series

It is familiar from scattering theory that amplitudes can be calculated perturbatively through the use of the Born series. For example, the Schrödinger equation

$$\left(\nabla^2 + k^2\right)\psi(\mathbf{r}) = 2mV(\mathbf{r})\psi(\mathbf{r}) \qquad (k^2 = 2mE), \tag{7.93}$$

has a solution which is the sum of the general solution to the corresponding homogeneous differential equation

$$\left(\nabla^2 + k^2\right)\psi_0(\mathbf{r}) = 0, \tag{7.94}$$

and of a particular solution, here written in terms of the Green's function $G(\mathbf{r}-\mathbf{r}')$

$$\psi_S(\mathbf{r}) = 2m\int d^3\mathbf{r}' G(\mathbf{r}-\mathbf{r}')V(\mathbf{r}')\psi(\mathbf{r}'), \tag{7.95}$$

where $G(\mathbf{r}-\mathbf{r}')$ is defined as the solution to

$$\left(\nabla^2 + k^2\right)G(\mathbf{r}-\mathbf{r}') = \delta^{(3)}(\mathbf{r}-\mathbf{r}'), \tag{7.96}$$

giving for the whole solution

$$\psi(\mathbf{r}) = \psi_0(\mathbf{r}) + 2m\int d^3\mathbf{r}' G(\mathbf{r}-\mathbf{r}')V(\mathbf{r}')\psi(\mathbf{r}'). \tag{7.97}$$

This is an integral form of the Schrödinger equation. Its advantage over the differential form is that it can be solved iteratively. The zeroth order solution (no scattering) is given simply by $\psi(\mathbf{r}) = \psi_0(\mathbf{r})$. The first order solution is obtained by inserting the zeroth order solution into eq. (7.97), which gives:

$$\psi_1(\mathbf{r}) = \psi_0(\mathbf{r}) + 2m\int d^3\mathbf{r}' G(\mathbf{r}-\mathbf{r}')V(\mathbf{r}')\psi_0(\mathbf{r}'). \tag{7.98}$$

The second order solution is obtained by inserting the first order solution into eq. (7.97). This procedure can be repeated an arbitrary number of times, meaning that full the solution

can be written

$$\psi(\mathbf{r}) = \psi_0(\mathbf{r}) + 2m \int d^3\mathbf{r}' G(\mathbf{r}-\mathbf{r}')V(\mathbf{r}')\psi_0(\mathbf{r}') + (2m)^2 \int d^3\mathbf{r}' \int d^3\mathbf{r}'' G(\mathbf{r}-\mathbf{r}')V(\mathbf{r}')G(\mathbf{r}'-\mathbf{r}'')V(\mathbf{r}'')\psi_0(\mathbf{r}'') + ... \quad (7.99)$$

Thus, to obtain $\psi(\mathbf{r})$ to a specified order in the scattering potential $V(\mathbf{r})$, we only require knowledge of the Green's function $G(\mathbf{r}-\mathbf{r}')$, and the solution of the homogenous equation (7.94).

7.4.2 Application to noise-current QED

In section 7.1 we saw that the noise-current approach to QED in media is based upon the following differential equation

$$\nabla^2\hat{\mathbf{A}}(\mathbf{r},\omega) + \omega^2\epsilon(\mathbf{r},\omega)\hat{\mathbf{A}}(\mathbf{r},\omega) = \hat{\mathbf{j}}(\mathbf{r},\omega), \quad (7.100)$$

which is solved via the Green's function

$$\nabla^2\mathbf{G}(\mathbf{r},\mathbf{r}',\omega) + \omega^2\epsilon(\mathbf{r},\omega)\mathbf{G}(\mathbf{r},\mathbf{r}',\omega) = \delta^{(3)}(\mathbf{r}-\mathbf{r}'). \quad (7.101)$$

Since, in general, the Green's function for a particular geometry is not known analytically, it is worth finding a way of expressing the Green's function in terms of a perturbation from one of the very few geometries for which the exact Green's function can be written down. Following [84], this can be done by considering the Green's function $\mathbf{G}(\mathbf{r},\mathbf{r}',\omega)$ as being made up of an analytically known Green's function $\mathbf{G}^{(0)}(\mathbf{r},\mathbf{r}',\omega)$ and an additional contribution resulting from the difference between the two. This implies the relations

$$\nabla^2\mathbf{G}(\mathbf{r},\mathbf{r}',\omega) + \omega^2\epsilon(\mathbf{r},\omega)\mathbf{G}(\mathbf{r},\mathbf{r}',\omega) = \delta^{(3)}(\mathbf{r}-\mathbf{r}'), \quad (7.102a)$$

$$\nabla^2\mathbf{G}^{(0)}(\mathbf{r},\mathbf{r}',\omega) + \omega^2\epsilon^{(0)}(\mathbf{r},\omega)\mathbf{G}^{(0)}(\mathbf{r},\mathbf{r}',\omega) = \delta^{(3)}(\mathbf{r}-\mathbf{r}'), \quad (7.102b)$$

where $\epsilon^{(0)}(\mathbf{r},\omega)$ is the dielectric function which describes the geometry for which the Green's function is analytically known, and $\epsilon(\mathbf{r},\omega)$ is the dielectric function of the whole system. Subtracting these equations from each other, we get:

$$\nabla^2\delta\mathbf{G}(\mathbf{r},\mathbf{r}',\omega) + \omega^2\epsilon^{(0)}(\mathbf{r},\omega)\delta\mathbf{G}(\mathbf{r},\mathbf{r}',\omega) = -\omega^2\delta\epsilon(\mathbf{r},\omega)\left[\delta\mathbf{G}(\mathbf{r},\mathbf{r}',\omega) + \mathbf{G}^{(0)}(\mathbf{r},\mathbf{r}',\omega)\right], \quad (7.103)$$

where $\delta\mathbf{G}(\mathbf{r},\mathbf{r}',\omega) = \mathbf{G}(\mathbf{r},\mathbf{r}',\omega) - \mathbf{G}^{(0)}(\mathbf{r},\mathbf{r}',\omega)$, and $\delta\epsilon(\mathbf{r},\omega) = \epsilon(\mathbf{r},\omega) - \delta\epsilon^{(0)}(\mathbf{r},\omega)$. This is an inhomogeneous differential equation for some function $\delta\mathbf{G}(\mathbf{r},\mathbf{r}',\omega)$, formally similar to eq. (7.93). Thus we can solve it using the method of the Green's function (even though the

function we are solving for is itself another Green's function), and construct a Born series expansion for $\delta\mathbf{G}(\mathbf{r},\mathbf{r}',\omega)$. The Green's function $\tilde{\mathbf{G}}(\mathbf{r},\mathbf{r}',\omega)$ for the differential equation (7.103) satisfies

$$\nabla^2\tilde{\mathbf{G}}(\mathbf{r},\mathbf{r}',\omega)+\omega^2\epsilon^{(0)}(\mathbf{r},\omega)\tilde{\mathbf{G}}(\mathbf{r},\mathbf{r}',\omega)=\delta^{(3)}(\mathbf{r}-\mathbf{r}'), \tag{7.104}$$

which, on comparison with eq. (7.102b) shows that

$$\tilde{\mathbf{G}}(\mathbf{r},\mathbf{r}',\omega)=\mathbf{G}^{(0)}(\mathbf{r},\mathbf{r}',\omega)\ . \tag{7.105}$$

Thus the solution to eq. (7.103) may be written as

$$\delta\mathbf{G}(\mathbf{r},\mathbf{r}',\omega)=-\omega^2\int d^3\mathbf{s}\mathbf{G}^{(0)}(\mathbf{r},\mathbf{s},\omega)\delta\epsilon(\mathbf{s},\omega)\left[\delta\mathbf{G}(\mathbf{s},\mathbf{r}',\omega)+\mathbf{G}^{(0)}(\mathbf{s},\mathbf{r}',\omega)\right], \tag{7.106}$$

so for the whole Green's function $\mathbf{G}(\mathbf{r},\mathbf{r}',\omega)=\mathbf{G}^{(0)}(\mathbf{r},\mathbf{r}',\omega)+\delta\mathbf{G}(\mathbf{r},\mathbf{r}',\omega)$ we have

$$\mathbf{G}(\mathbf{r},\mathbf{r}',\omega)=\mathbf{G}^{(0)}(\mathbf{r},\mathbf{r}',\omega)-\omega^2\int d^3\mathbf{s}\mathbf{G}^{(0)}(\mathbf{r},\mathbf{s},\omega)\delta\epsilon(\mathbf{s},\omega)\mathbf{G}(\mathbf{s},\mathbf{r}',\omega), \tag{7.107}$$

which is of the same form as eq. (7.97). This means we can solve it in the same iterative way, giving for the Born series

$$\begin{aligned}\mathbf{G}(\mathbf{r},\mathbf{r}',\omega)&=\mathbf{G}^{(0)}(\mathbf{r},\mathbf{r}',\omega)-\omega^2\int d^3\mathbf{s}_1\,\mathbf{G}^{(0)}(\mathbf{r},\mathbf{s}_1,\omega)\delta\epsilon(\mathbf{s}_1,\omega)\mathbf{G}^{(0)}(\mathbf{s}_1,\mathbf{r}',\omega)\\&+\omega^4\int d^3\mathbf{s}_1\int d^3\mathbf{s}_2\,\mathbf{G}^{(0)}(\mathbf{r},\mathbf{s}_1,\omega)\delta\epsilon(\mathbf{s}_1,\omega)\mathbf{G}^{(0)}(\mathbf{s}_1,\mathbf{s}_2,\omega)\delta\epsilon(\mathbf{s}_2,\omega)\mathbf{G}^{(0)}(\mathbf{s}_2,\mathbf{r}',\omega)+\ldots\end{aligned} \tag{7.108}$$

This shows that the Green's function representing propagation from $\mathbf{r}$ to $\mathbf{r}'$ in a region with an arbitrarily spatially varying dielectric function $\epsilon(\mathbf{r},\omega)$ is represented by a sum of multiple scatterings from a 'potential' given by the difference between $\epsilon(\mathbf{r},\omega)$ and the dielectric function $\epsilon^{(0)}(\mathbf{r},\omega)$ of a system for which the Green's function is analytically known. Equation (7.108) is exact, but in order to only have to deal with a tractable number of terms it is necessarily to consider a system whose geometry deviates only slightly[6] from that with an analytically known Green's function. We also note that since the dielectric contrast $\delta\epsilon(\mathbf{s},\omega)$ is necessarily zero in the region where the Green's function is analytically known, the integral over $d^3\mathbf{s}$ shown in eq. (7.107) may be restricted to the region where an arbitrarily shaped perturbing body exists.

[6] Precisely how far the geometry should be allowed to deviate is not easily quantifiable. One would need to define a 'geometric deviation' as a function of both permittivity and spatial extent, since either (or both) of these properties are desirable in the approximation of a Green's function.

7.4.3 Slab

As an initial demonstrative case, we consider a slab of material which extends from $z = 0$ to $z = L$, and which is infinite in the x and y directions. An electron sits in the region $z < 0$. In the limit $L \to \infty$ this system is the same half-space as previously considered. The Green's function for all L is analytically known, but we shall consider it perturbatively to demonstrate the method. The dielectric function is:

$$\epsilon(\mathbf{r},\omega) = \begin{cases} 1 & \text{if } z < 0, \\ \epsilon_s(\omega) & \text{if } 0 < z < L, \\ 1 & \text{if } z > L, \end{cases} \tag{7.109}$$

which is considered as a perturbation to a vacuum background $\epsilon^{(0)}(\mathbf{r},\omega) = 1$. So the dielectric contrast is

$$\delta\epsilon(\mathbf{r},\omega) = \epsilon(\mathbf{r},\omega) - 1 = \begin{cases} 0 & \text{if } z < 0, \\ \epsilon_s(\omega) - 1 & \text{if } 0 < z < L, \\ 0 & \text{if } z > L, \end{cases} \tag{7.110}$$

From eq. (7.108), the first-order correction to the Green's function is given by

$$\Delta^{(1)}\mathbf{G}(\mathbf{r},\mathbf{r}',\omega) = -\omega^2 \int d^3\mathbf{s}\, \mathbf{G}^{(0)}(\mathbf{r},\mathbf{s},\omega)\delta\epsilon(\mathbf{s},\omega)\mathbf{G}^{(0)}(\mathbf{s},\mathbf{r}',\omega). \tag{7.111}$$

On substitution of the explicit dielectric contrast, this reduces to

$$\Delta^{(1)}\mathbf{G}(\mathbf{r},\mathbf{r}',\omega) = -\omega^2(\epsilon_s(\omega) - 1) \int d^2\mathbf{s}_\parallel \int_0^L d\mathbf{s}_z\, \mathbf{G}^{(0)}(\mathbf{r},\mathbf{s},\omega)\mathbf{G}^{(0)}(\mathbf{s},\mathbf{r}',\omega), \tag{7.112}$$

where $\mathbf{G}^{(0)}(\mathbf{r},\mathbf{r}',\omega)$ is the vacuum Green's function. We shall consider only the zz component because this is a short calculation which gives a Green's function that can be used to determine a physical quantity, namely the component of the mass shift proportional to $\langle p_\perp^2 \rangle$ as given by eq. (7.42). We have:

$$\Delta^{(1)}\mathbf{G}_{zz}(\mathbf{r},\mathbf{r}',\omega) = -\omega^2(\epsilon_s(\omega) - 1) \int d^2\mathbf{s}_\parallel \int_0^L d\mathbf{s}_z\, \mathbf{G}^{(0)}_{zi}(\mathbf{r},\mathbf{s},\omega)\mathbf{G}^{(0)}_{zi}(\mathbf{r}',\mathbf{s},\omega), \tag{7.113}$$

where the symmetry relation (E.11) has been used. Defining

$$\mathcal{G}^2_{ij}(\mathbf{r},\mathbf{r}',\omega) \equiv \int d^2\mathbf{s}_\parallel \int_0^L d\mathbf{s}_z\, \mathbf{G}^{(0)}_{ij}(\mathbf{r},\mathbf{s},\omega)\mathbf{G}^{(0)}_{ij}(\mathbf{r}',\mathbf{s},\omega), \tag{7.114}$$

we note from eq. (7.113) that we need $\mathcal{G}^2_{zx}(\mathbf{r},\mathbf{r}',\omega)$ and $\mathcal{G}^2_{zz}(\mathbf{r},\mathbf{r}',\omega)$ (with the contribution from $\mathcal{G}^2_{zy}(\mathbf{r},\mathbf{r}',\omega)$ being necessarily equal to $\mathcal{G}^2_{zx}(\mathbf{r},\mathbf{r}',\omega)$ through xy symmetry). We are

only interested in the region $r_z < s_z$, since that is where the electron is, so from appendix E.3 we have for the required Green's functions

$$G^{(0)}_{zx}(\mathbf{r},\mathbf{s},\omega) = \frac{1}{\omega^2}\int \frac{d^2\mathbf{k}_\parallel}{(2\pi)^2} e^{i\mathbf{k}_\parallel\cdot(\mathbf{r}_\parallel-\mathbf{s}_\parallel)}(-k_x k_z)\frac{ie^{ik_z(r_z-s_z)}}{2k_z}, \tag{7.115a}$$

$$G^{(0)}_{zz}(\mathbf{r},\mathbf{s},\omega) = \frac{1}{\omega^2}\int \frac{d^2\mathbf{k}_\parallel}{(2\pi)^2} e^{i\mathbf{k}_\parallel\cdot(\mathbf{r}_\parallel-\mathbf{s}_\parallel)}k_\parallel^2\frac{ie^{ik_z(r_z-s_z)}}{2k_z}, \tag{7.115b}$$

First considering the zx contribution we have

$$\mathcal{G}^2_{zx}(\mathbf{r},\mathbf{r}',\omega) = -\frac{1}{4\omega^4}\int d^2\mathbf{s}_\parallel \int_0^L d\mathbf{s}_z \int \frac{d^2\mathbf{k}_\parallel}{(2\pi)^2}\int \frac{d^2\mathbf{p}_\parallel}{(2\pi)^2} e^{i\mathbf{k}_\parallel\cdot(\mathbf{r}_\parallel-\mathbf{s}_\parallel)}e^{i\mathbf{p}_\parallel\cdot(\mathbf{r}'_\parallel-\mathbf{s}_\parallel)} \times k_x e^{ik_z(r_z-s_z)}p_x e^{ip_z(r'_z-s_z)}, \tag{7.116}$$

where $p_z \equiv \sqrt{\omega^2-p_\parallel^2}$. The $\mathbf{s}_\parallel$ integration is trivial and results in a factor of $(2\pi)^2\delta^{(2)}(\mathbf{k}_\parallel + \mathbf{p}_\parallel)$, which can be used to do the $\mathbf{p}_\parallel$ integral. The result is

$$\mathcal{G}^2_{zx}(\mathbf{r},\mathbf{r}',\omega) = \frac{1}{4\omega^4}\int_0^L d\mathbf{s}_z \int \frac{d^2\mathbf{k}_\parallel}{(2\pi)^2} e^{i\mathbf{k}_\parallel\cdot(\mathbf{r}_\parallel-\mathbf{r}'_\parallel)}k_x^2 e^{-2ik_z s_z}e^{ik_z(r_z+r'_z)}. \tag{7.117}$$

The $\mathbf{s}_z$ integral is elementary, giving the final result for the zx contribution as

$$\mathcal{G}^2_{zx}(\mathbf{r},\mathbf{r}',\omega) = \frac{i}{8\omega^4}\int \frac{d^2\mathbf{k}_\parallel}{(2\pi)^2} e^{i\mathbf{k}_\parallel\cdot(\mathbf{r}_\parallel-\mathbf{r}'_\parallel)}\frac{k_x^2}{k_z}(e^{-2ik_z L}-1)e^{ik_z(r_z+r'_z)}. \tag{7.118}$$

Calculation of the zz contribution works in exactly the same way, the result is

$$\mathcal{G}^2_{zz}(\mathbf{r},\mathbf{r}',\omega) = -\frac{i}{8\omega^4}\int \frac{d^2\mathbf{k}_\parallel}{(2\pi)^2} e^{i\mathbf{k}_\parallel\cdot(\mathbf{r}_\parallel-\mathbf{r}'_\parallel)}\frac{k_\parallel^4}{k_z^3}(e^{-2ik_z L}-1)e^{ik_z(r_z+r'_z)}. \tag{7.119}$$

We have from eq. (7.113)

$$\begin{aligned}\Delta^{(1)}\mathbf{G}_{zz}(\mathbf{r},\mathbf{r}',\omega) &= -\omega^2(\epsilon_s(\omega)-1)\left[\mathcal{G}^2_{zx}(\mathbf{r},\mathbf{r}',\omega)+\mathcal{G}^2_{zx}(\mathbf{r},\mathbf{r}',\omega)|_{k_x\to k_y}+\mathcal{G}^2_{zz}(\mathbf{r},\mathbf{r}',\omega)\right]\\ &= \frac{i(\epsilon_s(\omega)-1)}{8\omega^2}\int \frac{d^2\mathbf{k}_\parallel}{(2\pi)^2} e^{i\mathbf{k}_\parallel\cdot(\mathbf{r}_\parallel-\mathbf{r}'_\parallel)}\frac{k_\parallel^2}{k_z}\left(\frac{k_\parallel^2}{k_z^2}-1\right)(e^{-2ik_z L}-1)e^{ik_z(r_z+r'_z)}.\end{aligned} \tag{7.120}$$

Writing this in the same form as eq. (7.43), we finally have:

$$\Delta^{(1)}\mathbf{G}_{zz}(\mathbf{k}_\parallel,r_z,r'_z,\omega) = \frac{i(\epsilon_s(\omega)-1)}{8\omega^2}\frac{k_\parallel^2}{k_z}\left(\frac{k_\parallel^2}{k_z^2}-1\right)(e^{-2ik_z L}-1)e^{ik_z(r_z+r'_z)}. \tag{7.121}$$

We now check this for agreement with the exact Green's function for this system. Similarly to eq. (7.40) we write the exact Green's function as

$$\mathbf{G}^{\text{slab}}_{zz}(\mathbf{r},\mathbf{r}',\omega) = \begin{cases}\mathbf{G}^{v}_{zz}(\mathbf{r},\mathbf{r}',\omega)+\mathbf{G}^{R,\text{slab}}_{zz}(\mathbf{r},\mathbf{r}',\omega) & \text{for } r_z, r'_z < 0,\\ \mathbf{G}^{T,\text{slab}}_{z}(\mathbf{r},\mathbf{r}',\omega) & \text{for } r_z < 0,\ r'_z > 0.\end{cases} \tag{7.122}$$

While in principle the transmitted component should be taken into account, all our calculations of radiative corrections have only required the Green's function at $\mathbf{r}=\mathbf{r}'$, with both points being located away from the surface in vacuum. Thus we only need

$$\mathbf{G}^{\text{slab}}_{zz}(\mathbf{r},\mathbf{r},\omega) = \mathbf{G}^{v}_{zz}(\mathbf{r},\mathbf{r},\omega)+\mathbf{G}^{R,\text{slab}}_{zz}(\mathbf{r},\mathbf{r},\omega) \quad \text{for } r_z, r'_z < 0. \tag{7.123}$$

From eq. (7.108) our approximate Green's function is

$$\mathbf{G}_{zz}(\mathbf{k}_\parallel, r_z, r_z, \omega) = \mathbf{G}^v_{zz}(\mathbf{k}_\parallel, r_z, r_z, \omega) + \Delta^{(1)}\mathbf{G}_{zz}(\mathbf{k}_\parallel, r_z, r_z, \omega) + \mathcal{O}\left[(\epsilon_s(\omega)-1)^2\right]. \quad (7.124)$$

Since we have found the approximate Green's function only in the region $r_z < 0$, we expect

$$\mathbf{G}^{R,\text{slab}}_{zz}(\mathbf{k}_\parallel, r_z, r_z, \omega) = \Delta^{(1)}\mathbf{G}_{zz}(\mathbf{k}_\parallel, r_z, r_z, \omega) + \mathcal{O}\left[(\epsilon_s(\omega)-1)^2\right]. \quad (7.125)$$

From appendix E.3.2, we have the zz component of the reflected Green's function for general layered media as

$$\mathbf{G}^R_{zz}(\mathbf{k}_\parallel, r_z, r_z, \omega) = -\frac{i}{2k_z} e^{2ik_z r_z} \tilde{R}^L_{\text{TM}} \frac{k_\parallel^2}{k^2}. \quad (7.126)$$

Comparing eqs. (7.121) and (7.126), the relation we expect to find is

$$\tilde{R}^L_{\text{TM}} = \frac{\epsilon_s(\omega)-1}{4}\left(1 - \frac{k_\parallel^2}{k_z^2}\right)(e^{-2ik_z L} - 1) + \mathcal{O}\left[(\epsilon_s(\omega)-1)^2\right]. \quad (7.127)$$

The reflection coefficient is given by eq. (A.6) as

$$\tilde{R}^L_{\text{TM}} = \frac{R^{vs}_{\text{TM}} + R^{sv}_{\text{TM}} e^{2ik_z^s L}}{1 + R^{vs}_{\text{TM}} R^{sv}_{\text{TM}} e^{2ik_z^s L}}, \quad (7.128)$$

where R^{vs}_{TM} and R^{sv}_{TM} represent the TM reflection coefficients for modes travelling vacuum-to-slab and slab-to-vacuum respectively. k_z^s is the z component of the wave vector inside the slab,

$$k_z^s = \sqrt{\epsilon_s(\omega)(k_z^2 + k_\parallel^2) - k_\parallel^2}. \quad (7.129)$$

Expanding $\tilde{R}^L_{\text{TM}}$ for small values of $\epsilon_s(\omega) - 1$ yields eq. (7.127), as expected.

Reproduction of the exact Green's function in the half-space limit $\{l_1 \to 0, l_2 \to \infty\}$ is slightly trickier. As $l_2 \to \infty$, eq. (7.121) oscillates rapidly. To deal with this we subtract a small imaginary part $q > 0$ from k_z and let $q \to 0$ at the end of the calculation. For example, eq. (7.117) becomes

$$\begin{aligned}
\mathcal{G}^2_{zx}(\mathbf{r}, \mathbf{r}', \omega, \text{half-space}) &= \frac{1}{4\omega^4} \lim_{q\to 0} \int_0^\infty d\mathbf{s}_z \int \frac{d^2\mathbf{k}_\parallel}{(2\pi)^2} e^{i\mathbf{k}_\parallel \cdot (\mathbf{r}_\parallel - \mathbf{r}'_\parallel)} k_x^2 e^{-2i(k_z - iq)s_z} e^{ik_z(r_z + r'_z)} \\
&= \frac{1}{4\omega^4} \lim_{q\to 0} \int \frac{d^2\mathbf{k}_\parallel}{(2\pi)^2} e^{i\mathbf{k}_\parallel \cdot (\mathbf{r}_\parallel - \mathbf{r}'_\parallel)} k_x^2 \frac{1}{2i(k_z - iq)} e^{ik_z(r_z + r'_z)} \\
&= -\frac{i}{8\omega^4} \int \frac{d^2\mathbf{k}_\parallel}{(2\pi)^2} e^{i\mathbf{k}_\parallel \cdot (\mathbf{r}_\parallel - \mathbf{r}'_\parallel)} \frac{k_x^2}{k_z} e^{ik_z(r_z + r'_z)}.
\end{aligned} \quad (7.130)$$

Taking the same approach with $\mathcal{G}^2_{zz}$, and using eq. (7.120) we arrive at

$$\Delta^{(1)}\mathbf{G}_{zz}(\mathbf{r}, \mathbf{r}', \omega, \text{half-space}) = -\frac{i(\epsilon_s(\omega)-1)}{8\omega^2} \int \frac{d^2\mathbf{k}_\parallel}{(2\pi)^2} e^{i\mathbf{k}_\parallel \cdot (\mathbf{r}_\parallel - \mathbf{r}'_\parallel)} \frac{k_\parallel^2}{k_z} \left(\frac{k_\parallel^2}{k_z^2} - 1\right) e^{ik_z(r_z + r'_z)}. \quad (7.131)$$

From appendix E.3.2, the zz component of the reflected part of the exact Green's function of the half-space is

$$\mathbf{G}^R_{zz}(\mathbf{k}_\parallel, r_z, r_z, \omega) = -\frac{i}{2k_z} e^{2ik_z r_z} R^L_{\mathrm{TM}} \frac{k_\parallel^2}{k^2}. \tag{7.132}$$

Comparing this and eq. (7.131), the approximation is valid if the following holds

$$R^L_{\mathrm{TM}} = \frac{\epsilon_s(\omega) - 1}{4} \left(\frac{k_\parallel^2}{k_z^2} - 1 \right) + \mathcal{O}\left[(\epsilon_s(\omega) - 1)^2 \right], \tag{7.133}$$

which can be shown to be true using the explicit form of the reflection coefficient listed in eqs. A.5. Since physical quantities such as the mass shift and magnetic moment depend only on a frequency integral over the Green's function, the agreement between the approximate Green's function found via the Born series and the exact Green's function in the appropriate limit necessarily means that the mass shift and magnetic moment results for *non*-dispersive media found in sections 4.2.1 and 5.4.1 can be obtained from the approximate Green's function (7.131). This is not true in general for dispersive media because the calculation of physical quantities requires an integration over all ω, where $\epsilon_s(\omega) - 1$ is not necessarily small. For a non-dispersive dielectric there is no problem, one can simply let $\epsilon_s(\omega) = n^2 \approx 1$, but for dispersive media the issue is more complicated. The method is clearly unsuitable for a plasma

$$\epsilon_s(\omega) \to \epsilon_p(\omega) = 1 - \frac{\omega_p^2}{\omega^2}, \tag{7.134}$$

due to its pole at $\omega = 0$. Because of this, we consider an undamped dispersive dielectric as the test-case for a dispersive medium

$$\epsilon_s(\omega) \to \epsilon_{\mathrm{disp}}(\omega) = 1 - \frac{\omega_p^2}{\omega^2 - \omega_T^2} \quad \text{with} \quad \omega_p \ll \omega_T. \tag{7.135}$$

Our (unrenormalized) expression (7.41) for the perpendicular component of the mass shift in terms of the Green's function is

$$\begin{aligned} \Delta E_\perp &= \frac{e^2}{\pi m^2} \langle p_\perp^2 \rangle \int_0^\infty \frac{d\omega}{\omega} \operatorname{Im} \mathbf{G}_{zz}(\mathbf{r}, \mathbf{r}, \omega) \\ &= \frac{e^2}{\pi m^2} \langle p_\perp^2 \rangle \int_0^\infty \frac{d\omega}{\omega} \operatorname{Im} \left[\mathbf{G}^{(0)}(\mathbf{r}, \mathbf{r}', \omega) + \Delta^{(1)}\mathbf{G}(\mathbf{r}, \mathbf{r}', \omega) + ... \right]. \end{aligned} \tag{7.136}$$

As usual, we renormalize by subtracting all quantities which would be present in free space. Here this corresponds to subtracting $\mathbf{G}^{(0)}(\mathbf{r}, \mathbf{r}', \omega)$, giving

$$\Delta E_{\mathrm{ren}\perp} = \frac{e^2}{\pi m^2} \langle p_\perp^2 \rangle \int_0^\infty \frac{d\omega}{\omega} \operatorname{Im} \left[\Delta^{(1)}\mathbf{G}(\mathbf{r}, \mathbf{r}', \omega) + ... \right]. \tag{7.137}$$

We now insert the Green's function (7.121) into the expression for the mass shift (7.41) to

find a first-order approximation to the perpendicular part of the mass shift

$$\Delta E_{\mathrm{ren}\perp}(\epsilon_s(\omega)\approx 1) = \frac{e^2}{16\pi^2 m^2}\langle p_\perp^2\rangle \,\mathrm{Re}\int_0^\infty d\omega \frac{\epsilon_s(\omega)-1}{\omega^3} \times \int_0^\infty dk_\parallel \frac{k_\parallel^3}{k_z}\left(\frac{k_\parallel^2}{k_z^2}-1\right)(e^{-2ik_z L}-1)e^{2ik_z r_z}. \quad (7.138)$$

This may be evaluated through the residue theorem in an identical way to that shown in section 7.2.2, the result is

$$\Delta E_{\mathrm{ren}\perp}(\epsilon_s(\omega)\approx 1) = \frac{e^2}{128\pi m^2 z^3(L-z)^3}\Big[6Lz^2(L-z)^2(\epsilon_s(0)-1) + L\left(L^2-3Lz+3z^2\right)\epsilon_s''(0)\Big]\langle p_\perp^2\rangle. \quad (7.139)$$

A consistency check is to take a non-dispersive slab ($\epsilon_s(0)=n^2$, $\epsilon_s''(0)=0$) and $L\to\infty$, giving

$$\Delta E_{\mathrm{ren}\perp}(n^2\approx 1, L\to\infty) = \langle p_\perp^2\rangle \frac{3e^2}{64\pi m^2 z}(n^2-1)\,, \quad (7.140)$$

so that we may check for agreement with the mass shift near a non-dispersive half-space obtained in Chapter 4, the result being given by eq. (4.47) as

$$\Delta E_{\mathrm{ren}\perp}^{\mathrm{nondisp}} = \langle p_\perp^2\rangle \frac{e^2}{16\pi m^2 z}\frac{2n^4-n^2-1}{(n^2+1)^2}\,, \quad (7.141)$$

which for $n^2\approx 1$ becomes

$$\Delta E_{\mathrm{ren}\perp}^{\mathrm{nondisp}}(n^2\approx 1) = \left[\frac{\partial}{\partial(n^2)}\Delta E_{\mathrm{NonDisp},z}\right]_{n^2=1} + \mathcal{O}(n^2-1)^2 = \langle p_\perp^2\rangle \frac{3e^2}{64\pi m^2 z}(n^2-1) + \mathcal{O}(n^2-1)^2\,, \quad (7.142)$$

in agreement with (7.140). Similarly, we can insert the dispersive dielectric function (7.135) into (7.139) to find:

$$\Delta E_{\mathrm{Disp},\perp}(\epsilon_{\mathrm{disp}}(0)\approx 1) = \frac{\omega_p^2 z^3 + \omega_p^2(L-z)^2\left(L-z+3L\omega_T^2 z^2\right)}{64\pi\omega_T^4 z^3(L-z)^3}\langle p_\perp^2\rangle + \mathcal{O}(\epsilon_{\mathrm{disp}}(0)-1)^2. \quad (7.143)$$

In the limit of large L, this becomes

$$\Delta E_{\mathrm{Disp},\perp}(\epsilon_{\mathrm{disp}}(0)\approx 1, L\to\infty) = \frac{\omega_p^2(1+3\omega_T^2 z^2)}{64\pi\omega_T^4 z^3}\langle p_\perp^2\rangle. \quad (7.144)$$

The corresponding exact result was obtained in Chapter 4 and is given by eq. (4.88)

$$\Delta E_{\mathrm{ren}}^{\mathrm{disp}} = \frac{e^2}{16\pi m^2}\frac{\omega_p^2}{\left(\omega_p^2+2\omega_T^2\right)^2}\left[\frac{1}{z^3}+\frac{1}{z}(2\omega_p^2+3\omega_T^2)\right]\langle p_\perp^2\rangle. \quad (7.145)$$

As we have already noted, the Born series approximation is only valid when $\omega_p \ll \omega_T$. Under these conditions the exact result becomes

$$\Delta E_{\mathrm{ren}}^{\mathrm{disp}}(\omega_p\ll\omega_T) = \frac{\omega_p^2(1+3\omega_T^2 z^2)}{64\pi\omega_T^4 z^3}\langle p_\perp^2\rangle + \mathcal{O}(\omega_p^2). \quad (7.146)$$

in agreement with the Born series approximation (7.144).

7.5 Summary and conclusions

In this chapter we have shown that the mass shift calculated in chapter Chapter 4 and the magnetic moment shift calculated in Chapter 5 can be rederived using the noise-current approach to QED in dielectric media. In sections 7.2 and 7.3 we showed the method by which our previous results for undamped media may be recovered as limiting cases of formulae whose derivations relied on the medium being damped. In section 7.3.3 we encountered the same difficulty concerning the calculation of a magnetic moment near a dispersive surface that we found using the mode expansion in section 5.4.4. Finally, in section (7.4), we provided a brief discussion of how the noise-current approach can be used to calculate, under suitable conditions, the effects of an arbitrarily shaped medium upon an electron in its vicinity.

Chapter 8

Summary

In this thesis we have derived shifts of the mass and magnetic moment of an electron near a realistic surface, relevant to ultra-precise experimental tests of fundamental physics. We noted that results for different models of the electromagnetic response of the surface do not agree in the expected limiting cases due to their drastically different behavior at low frequency, which led to the conclusion that one must carefully choose an suitable model of the surface when considering quantum electrodynamic surface effects. As a consequence of this, we have shown that obtaining rough estimates by modeling a surface as a perfect reflector is not necessarily appropriate. We have found that the use of a dispersive surface may make the magnetic moment shift significantly larger than previous perfect-reflector estimates suggest, so much so that its measurement is on the verge of experimental viability.

We then extended our model to calculation of radiative corrections to an electron bound in a harmonic potential near a surface, finding that the notion of a magnetic moment is not particularly well-defined in such a system. This caused us to consider the change in the energy difference of the spin states instead, in which we found an oscillatory behavior stemming from retardation effects between the oscillator potential and the surface.

We then reinforced our mode expansion results by recalculating them using a semi-phenomenological 'noise-current' approach, with agreement in all cases. On comparison of the two methods we found that the mode expansion approach has the advantage of being more physically intuitive and traceable, but the noise-current approach has the advantage of being purpose-built around dispersive media.

Possible extensions to this work would be consideration of non-planar surfaces, perhaps with a view to specifically tuning the shape of a surface in order to maximize radiative corrections to an electron (or atom) held near it. This could lead to novel devices for controlling and enhancing the properties of microscopic systems.

Appendix A

Modes

A.1 Polarization vectors

A.1.1 TE and TM modes

The polarization vectors referred to throughout this thesis are:

$$\hat{\mathbf{e}}_{\mathrm{TE}} = \frac{1}{k_{\|}}(k_y, -k_x, 0), \qquad \hat{\mathbf{e}}_{\mathrm{TM}} = \frac{1}{kk_{\|}}(k_x k_z, k_y k_z, -k_{\|}^2). \tag{A.1}$$

A.1.2 Surface plasmon modes

The polarisation vectors for the surface plasmon modes are given by eq. (3.41)

$$\mathbf{e}^L(\kappa) = \hat{\mathbf{k}}_{\|} - i\frac{k_{\|}^2}{\kappa}\hat{z}, \tag{A.2a}$$

$$\mathbf{e}^R(\kappa^d) = \hat{\mathbf{k}}_{\|} + i\frac{k_{\|}^2}{\kappa^d}\hat{z}\ . \tag{A.2b}$$

The following products are used in the simplification of eq. (3.48)

$$|\mathbf{e}^L(\kappa)|^2 = 1 + \frac{k_{\|}^2}{\kappa^2}, \qquad |\mathbf{e}^R(\kappa^d)|^2 = 1 + \frac{k_{\|}^2}{\kappa^{d2}},$$
$$|\mathbf{k}^L \times \mathbf{e}^L(\kappa)|^2 = \frac{\omega_{\mathrm{sp}}^4}{\kappa^2}, \qquad |\mathbf{k}^R \times \mathbf{e}^R(\kappa)|^2 = \frac{(\omega_{\mathrm{sp}}^2 - \omega_p^2)^2}{\kappa^{d2}}, \tag{A.3}$$

where

$$\mathbf{k}^L = ik_x\hat{x} + ik_y\hat{y} + \kappa, \qquad \mathbf{k}^R = ik_x\hat{x} + ik_y\hat{y} - \kappa^d\ . \tag{A.4}$$

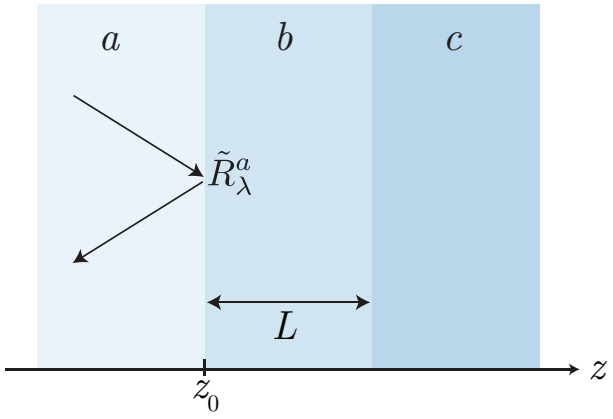

Figure A.1: Layered reflection coefficient example

A.2 Fresnel Coefficients

The full set of reflection and transmission coefficients for an interface with vacuum on the left and a medium described by dielectric function $\epsilon(k_z, k_\parallel)$ on the right are

$$\begin{aligned} R^L_{\mathbf{k},\mathrm{TE}} &= \frac{k_z - k^d_z}{k_z + k^d_z}, & T^L_{\mathbf{k},\mathrm{TE}} &= \frac{2k_z}{k_z + k^d_z}, \\ R^L_{\mathbf{k},\mathrm{TM}} &= \frac{\epsilon(k_z,k_\parallel)k_z - k^d_z}{\epsilon(k_z,k_\parallel)k_z + k^d_z}, & T^L_{\mathbf{k},\mathrm{TM}} &= \frac{2\sqrt{\epsilon(k_z,k_\parallel)}k_z}{\epsilon(k_z,k_\parallel)k_z + k^d_z}, \\ R^R_{\mathbf{k},\lambda} &= -R^L_{\mathbf{k},\lambda}, & T^R_{\mathbf{k},\lambda} &= \frac{k^d_z}{k_z} T^L_{\mathbf{k},\lambda}\,. \end{aligned} \tag{A.5}$$

These can be combined to form a reflection coefficient for a layered medium [81, 85, 86]. For example, the reflection coefficient for the interface shown in fig. (A.1) is

$$\tilde{R}^a_{\mathbf{k},\lambda} = \frac{R^{ab}_{\mathbf{k},\lambda} + R^{bc}_{\mathbf{k},\lambda} e^{2ik^b_z L}}{1 + R^{ab}_{\mathbf{k},\lambda} R^{bc}_{\mathbf{k},\lambda} e^{2ik^b_z L}} e^{-2ik^a_z z_0}\,, \tag{A.6}$$

where media a and c extend infinitely in the direction normal to the surface of b, which is a slab of thickness L. R^{ij}_λ denotes the reflection coefficient for λ-polarised radiation propagating from medium i to medium j, which are given by generalized versions of eqs. (A.5)

$$R^{ij}_{\mathbf{k},\mathrm{TE}} = \frac{k^i_z - k^j_z}{k^i_z + k^j_z}, \qquad R^{ij}_{\mathbf{k},\mathrm{TM}} = \frac{\epsilon_j(k_z,k_\parallel)k^i_z - \epsilon_i(k_z,k_\parallel)k^j_z}{\epsilon_j(k_z,k_\parallel)k^i_z + \epsilon_i(k_z,k_\parallel)k^j_z}\,. \tag{A.7}$$

Since any layered system can be broken down into smaller systems such as this, a reflection coefficient for an arbitrary number of layers can be found by repeated use of eq. (A.6). It is worth noting that while the phase factor $e^{-2ik^a_z z_0}$ is arbitrary, its counterpart in the layered transmission coefficient $\tilde{T}_{\mathbf{k},\lambda}$ (see, for example, [85]) means that conservation of energy

$$|\tilde{R}_{\mathbf{k},\lambda}|^2 + |\tilde{T}_{\mathbf{k},\lambda}|^2 = 1, \tag{A.8}$$

is preserved independently of any particular choice of z_0.

A.3 Products of Mode Functions

The non-dispersive modes are (3.16)

$$\mathbf{f}^L_{\mathbf{k}\lambda}(\mathbf{r},\omega) = \frac{1}{(2\pi)^{3/2}}\frac{1}{\sqrt{2\omega}}\left[\Theta(-z)\left(e^{i\mathbf{k}\cdot\mathbf{r}}\hat{\mathbf{e}}_{\mathbf{k}\lambda} + R^L_{\mathbf{k}\lambda}e^{i\bar{\mathbf{k}}\cdot\mathbf{r}}\hat{\bar{\mathbf{e}}}_{\mathbf{k}\lambda}\right) + \Theta(z)T^L_{\mathbf{k}\lambda}e^{i\mathbf{k}^d\cdot\mathbf{r}}\hat{\mathbf{e}}_{\mathbf{k}^d\lambda}\right], \tag{A.9a}$$

$$\mathbf{f}^R_{\mathbf{k}\lambda}(\mathbf{r},\omega) = \frac{1}{(2\pi)^{3/2}}\frac{1}{n(\mathbf{r})}\frac{1}{\sqrt{2\omega}}\left[\Theta(z)\left(e^{i\mathbf{k}^d\cdot\mathbf{r}}\hat{\mathbf{e}}_{\mathbf{k}^d\lambda} + R^R_{\mathbf{k}\lambda}e^{i\bar{\mathbf{k}}^d\cdot\mathbf{r}}\hat{\bar{\mathbf{e}}}_{\mathbf{k}^d\lambda}\right) + \Theta(-z)T^R_{\mathbf{k}\lambda}e^{i\mathbf{k}\cdot\mathbf{r}}\hat{\mathbf{e}}_{\mathbf{k}\lambda}\right], \tag{A.9b}$$

We are only ever interested in the region $z<0$, so it is of obvious utility to define

$$\mathbf{f}^I_{\mathbf{k}\lambda}(\mathbf{r},\omega) = \frac{1}{(2\pi)^{3/2}}\frac{1}{\sqrt{2\omega}}\left(e^{i\mathbf{k}\cdot\mathbf{r}}\hat{\mathbf{e}}_{\mathbf{k}\lambda} + R^L_{\mathbf{k}\lambda}e^{i\bar{\mathbf{k}}\cdot\mathbf{r}}\hat{\bar{\mathbf{e}}}_{\mathbf{k}\lambda}\right), \tag{A.10a}$$

$$\mathbf{f}^T_{\mathbf{k}\lambda}(\mathbf{r},\omega) = \frac{1}{(2\pi)^{3/2}}\frac{1}{\sqrt{2\omega}}T^R_{\mathbf{k}\lambda}e^{i\mathbf{k}\cdot\mathbf{r}}\hat{\mathbf{e}}_{\mathbf{k}\lambda}. \tag{A.10b}$$

We require mode sums over products of the form:

$$\sum_{\lambda=\mathrm{TE,TM}}\int d^3\mathbf{k}|f_{\mathbf{k}\lambda,i}|^2, \qquad i=\{x,y,z\}. \tag{A.11}$$

Taking, for example, the first term in eq. (5.97) and considering only the region $z<0$, we need

$$\sum_{\lambda=\mathrm{TE,TM}}\int d^3\mathbf{k}|f_{\mathbf{k}\lambda,z}|^2 = \sum_{\lambda=\mathrm{TE,TM}}\int d^3\mathbf{k}\left[|\mathbf{f}^I_{\mathbf{k}\lambda,z}(\mathbf{r},\omega)|^2 + \frac{1}{n^2}|\mathbf{f}^T_{\mathbf{k}\lambda}(\mathbf{r},\omega)|^2\right]. \tag{A.12}$$

Using the explicit polarization vectors (A.1) we have that in this case there is no TE contribution, and the TM contribution is given by:

$$|\mathbf{f}^I_{\mathbf{k}\lambda,z}(\mathbf{r},\omega)|^2 = \frac{1}{(2\pi)^3}\frac{1}{2\omega}\frac{k_\parallel^2}{k^2}\left[1+|R^L_{\mathbf{k},\mathrm{TM}}|^2 + R^L_{\mathbf{k},\mathrm{TM}}(e^{2ik_zz}+e^{-2ik_zz})\right], \tag{A.13}$$

$$|\mathbf{f}^T_{\mathbf{k}\lambda,z}(\mathbf{r},\omega)|^2 = \frac{1}{(2\pi)^3}\frac{1}{2\omega}\frac{k_\parallel^2}{k^2}|T^R_{\mathbf{k},\mathrm{TM}}|^2\begin{cases}1 & \text{if } k_z \text{ is real}\\ e^{2|k_z|z} & \text{if } k_z \text{ is imaginary,}\end{cases} \tag{A.14}$$

where the possibility of a right-incident mode suffering total internal reflection at the boundary has been considered. All the various terms in eq. (5.97) can be written in the same way, but terms that contain factors of k_z require a little more care. To show this, we consider the TE part of the $|(\nabla\times\mathbf{f}_{\mathbf{k}\lambda})_x|^2$ term in eq. (5.97). One finds

$$|(\nabla\times\mathbf{f}^I_{\mathbf{k}\lambda})_{x,\mathrm{TE}}|^2 = \frac{1}{(2\pi)^3}\frac{1}{2\omega}\frac{k_x^2}{k_\parallel^2}\left[1+|R^L_{\mathbf{k},\mathrm{TE}}|^2 - R^L_{\mathbf{k},\mathrm{TE}}(e^{2ik_zz}+e^{-2ik_zz})\right], \tag{A.15}$$

$$|(\nabla\times\mathbf{f}^T_{\mathbf{k}\lambda})_{x,\mathrm{TE}}|^2 = \frac{1}{(2\pi)^3}\frac{1}{2\omega}\frac{k_x^2}{k_\parallel^2}|T^R_{\mathbf{k},\mathrm{TE}}|^2\begin{cases}k_z^2 & \text{if } k_z \text{ is real,}\\ |k_z|^2e^{2|k_z|z} & \text{if } k_z \text{ is imaginary.}\end{cases} \tag{A.16}$$

The minus sign next to $R^L_{\mathbf{k},\mathrm{TE}}$ appears to be troublesome, since the method outlined in section 4.2.1 is reliant on the coefficients of $R^L_{\mathbf{k},\mathrm{TE}}$ and $e^{2|k_z|z}$ being equal. The simple (but easy to miss) resolution of this is found by noting that for k_z pure imaginary, $|k_z|^2 = -k_z^2$. So

$$|(\nabla \times \mathbf{f}^I_{\mathbf{k}\lambda})_x|^2 = \frac{1}{(2\pi)^3}\frac{1}{2\omega}\frac{k_x^2 k_z^2}{k_\parallel^2}\left[1 + |R^L_{\mathbf{k},\mathrm{TE}}|^2 - R^L_{\mathbf{k},\mathrm{TE}}(e^{2ik_z z} + e^{-2ik_z z})\right], \tag{A.17}$$

$$|(\nabla \times \mathbf{f}^T_{\mathbf{k}\lambda})_{x,\mathrm{TE}}|^2 = \frac{1}{(2\pi)^3}\frac{1}{2\omega}\frac{k_x^2 k_z^2}{k_\parallel^2}|T^R_{\mathbf{k},\mathrm{TE}}|^2 \begin{cases} 1 & \text{if } k_z \text{ is real,} \\ -e^{2|k_z|z} & \text{if } k_z \text{ is imaginary.} \end{cases} \tag{A.18}$$

So we have that the coefficients of $R^L_{\mathbf{k},\mathrm{TE}}$ and $e^{2|k_z|z}$ are equal, meaning the method outlined in section 4.2.1 still applies. That method also shows that this coefficient completely specifies the shift once the free-space counter term as been subtracted. So, we can summarize the contribution of each term by this coefficient, i.e.

$$\begin{aligned} |\mathbf{f}_{\mathbf{k}\mathrm{TM},z}(\mathbf{r},\omega)|^2 \quad &\text{is summarized by} \quad \frac{k_\parallel^2}{k^2}, \\ |(\nabla \times \mathbf{f}_{\mathbf{k}\mathrm{TE}})_x|^2 \quad &\text{is summarized by} \quad -\frac{k_x^2 k_z^2}{k_\parallel^2}, \end{aligned}$$

and then to get the shift due to a term of polarization λ we simply multiply the coefficient by $\frac{1}{(2\pi)^3}\frac{1}{2\omega}R^L_{\mathbf{k},\lambda}e^{2ik_z z}$, insert it into eq. (5.97) and evaluate the integral. The full set of coefficients are shown in table A.1.

Term	Polarization	Coefficient
$\lvert\mathbf{f}_{\mathbf{k}\lambda,z}(\mathbf{r},\omega)\rvert^2$	TE	0
	TM	$\frac{k_\parallel^2}{k^2}$
$\lvert(\nabla \times \mathbf{f}_{\mathbf{k}\lambda})_x\rvert^2$	TE	$-\frac{k_x^2 k_z^2}{k_\parallel^2}$
	TM	$\frac{k_y^2 k^2}{k_\parallel^2}$
$f_{\mathbf{k}\lambda,x}\frac{\partial^2 f^*_{\mathbf{k}\lambda,y}}{\partial x \partial y}$	TE	$\frac{k_x^2 k_y^2}{k_\parallel^2}$
	TM	$\frac{k_x^2 k_y^2 k_z^2}{k^2 k_\parallel^2}$
$f_{\mathbf{k}\lambda,x}\frac{\partial^2 f^*_{\mathbf{k}\lambda,x}}{\partial y^2}$	TE	$-\frac{k_y^4}{k_\parallel^2}$
	TM	$\frac{k_x^2 k_y^2 k_z^2}{k^2 k_\parallel^2}$

Table A.1: Coefficients that summarize the contribution to the magnetic moment shift of each term in (5.97).

Appendix B

Matrix Elements

B.1 Free electron

The matrix elements of the canonically conjugate momentum (5.19) are

$$\langle \nu+1|\, \pi_x \,|\nu\rangle = i\beta_0\sqrt{\nu+1}, \tag{B.1a}$$

$$\langle \nu-1|\, \pi_x \,|\nu\rangle = -i\beta_0\sqrt{\nu}, \tag{B.1b}$$

$$\langle \nu+1|\, \pi_y \,|\nu\rangle = \beta_0\sqrt{\nu+1}, \tag{B.1c}$$

$$\langle \nu-1|\, \pi_y \,|\nu\rangle = \beta_0\sqrt{\nu}\,. \tag{B.1d}$$

and those for the defined quantities (5.28) are

$$\langle \nu+1|\, \pi_+ \,|\nu\rangle = 2i\beta_0\sqrt{\nu+1}, \tag{B.2a}$$

$$\langle \nu-1|\, \pi_- \,|\nu\rangle = -2i\beta_0\sqrt{\nu}\,. \tag{B.2b}$$

We also need the matrix elements of the position operator. Noting that [87]

$$x = \frac{1}{2\beta_0}(b_R + b_L + \hat{b}_R^\dagger + \hat{b}_L^\dagger) = x_0 + \frac{1}{2\beta_0}(b_R + \hat{b}_R^\dagger)\,, \tag{B.3}$$

$$y = \frac{i}{2\beta_0}(b_R - b_L - \hat{b}_R^\dagger + \hat{b}_L^\dagger) = y_0 + \frac{i}{2\beta_0}(b_R - \hat{b}_R^\dagger)\,, \tag{B.4}$$

we have

$$\langle \nu+1|\, (x-x_0) \,|\nu\rangle = \frac{1}{2\beta_0}\sqrt{\nu+1}, \tag{B.5a}$$

$$\langle \nu-1|\, (x-x_0) \,|\nu\rangle = \frac{1}{2\beta_0}\sqrt{\nu}, \tag{B.5b}$$

$$\langle \nu+1|\, (y-y_0) \,|\nu\rangle = -\frac{i}{2\beta_0}\sqrt{\nu+1}, \tag{B.5c}$$

$$\langle \nu-1|\, (y-y_0) \,|\nu\rangle = \frac{i}{2\beta_0}\sqrt{\nu}\,. \tag{B.5d}$$

B.2 Confined electron

Using

$$\hat{\pi}_x = \hat{p}_x + \frac{eB_0}{2}\hat{y} = \frac{i}{2}\sqrt{\frac{m}{\Omega}}\left[\Delta_R(\hat{b}_R^\dagger - \hat{b}_R) + \Delta_L(\hat{b}_L^\dagger - \hat{b}_L)\right], \tag{B.6a}$$

$$\hat{\pi}_y = \hat{p}_y - \frac{eB_0}{2}\hat{x} = \frac{1}{2}\sqrt{\frac{m}{\Omega}}\left[\Delta_R(\hat{b}_R^\dagger + \hat{b}_R) - \Delta_L(\hat{b}_L^\dagger + \hat{b}_L)\right], \tag{B.6b}$$

we have

$$\begin{aligned}
\langle n_i + 1|\, \pi_x \,|n_i\rangle &= \frac{i}{2}\sqrt{\frac{m}{\Omega}}\Delta_i\sqrt{n_i+1}, \\
\langle n_i - 1|\, \pi_x \,|n_i\rangle &= -\frac{i}{2}\sqrt{\frac{m}{\Omega}}\Delta_i\sqrt{n_i}, \\
\langle n_i + 1|\, \pi_y \,|n_i\rangle &= h_i\sqrt{\frac{m}{\Omega}}\Delta_i\sqrt{n_i+1}, \\
\langle n_i - 1|\, \pi_y \,|n_i\rangle &= h_i\sqrt{\frac{m}{\Omega}}\Delta_i\sqrt{n_i},
\end{aligned} \tag{B.7}$$

where definition (6.17) of h_i has been used. It is also useful to have the matrix elements of the displacement operator in the directions parallel to the surface:

$$\begin{aligned}
\langle n_i + 1|\, (x - x_0) \,|n_i\rangle &= \frac{1}{2\sqrt{m\Omega}}\sqrt{n_i+1}, \\
\langle n_i - 1|\, (x - x_0) \,|n_i\rangle &= \frac{1}{2\sqrt{m\Omega}}\sqrt{n_i}, \\
\langle n_i + 1|\, (y - y_0) \,|n_i\rangle &= -h_i\frac{i}{2\sqrt{m\Omega}}\sqrt{n_i+1}, \\
\langle n_i - 1|\, (y - y_0) \,|n_i\rangle &= h_i\frac{i}{2\sqrt{m\Omega}}\sqrt{n_i}.
\end{aligned} \tag{B.8}$$

Appendix C

The Schrödinger equation with an anisotropic mass

We wish to investigate the cyclotron frequency of the electron, which means we must consider its eigenstates in a constant magnetic field $\mathbf{B}_0$. In section 5.2 we saw that the Schrödinger Hamiltonian for an electron in a magnetic field B_0 directed along $\hat{z}$ can be written as

$$H_S = \frac{(p_x + \frac{eB_0}{2}y)^2}{2m} + \frac{(p_y - \frac{eB_0}{2}x)^2}{2m} + \frac{p_z^2}{2m}. \tag{C.1}$$

In Chapter 4 we saw that the presence of a surface can change the mass of the electron, and that this change in mass is dependent upon the direction of the electron's momentum – the electron has an anisotropic mass. We would like to investigate how this anisotropy affects the cyclotron frequency, so we modify the Hamiltonian (C.1) to

$$H^A_{S,z} = \frac{(p_x + \frac{eB_0}{2}y)^2}{2m_x} + \frac{(p_y - \frac{eB_0}{2}x)^2}{2m_y} + \frac{p_z^2}{2m_z}, \tag{C.2}$$

where the subscript z specifies that the magnetic field is directed along z. Just as in section 5.2 we introduce annihilation and creation operators and rewrite the positions and momenta in terms of those. We write

$$\begin{aligned} x &= \frac{1}{\beta_x\sqrt{2}}(\hat{b}_x + \hat{b}_x^\dagger), & p_x &= \frac{i\beta_x}{\sqrt{2}}(\hat{b}_x^\dagger - \hat{b}_x), \\ y &= \frac{1}{\beta_y\sqrt{2}}(\hat{b}_y + \hat{b}_y^\dagger), & p_y &= \frac{i\beta_y}{\sqrt{2}}(\hat{b}_y^\dagger - \hat{b}_y), \end{aligned} \tag{C.3}$$

where

$$\beta_x^2 = -\frac{eB_x}{2}\sqrt{\frac{m_x}{m_y}}, \qquad \beta_y^2 = -\frac{eB_y}{2}\sqrt{\frac{m_y}{m_x}}. \tag{C.4}$$

The operators $\hat{b}_x, \hat{b}_x^\dagger, \hat{b}_y$ and $\hat{b}_y^\dagger$ are combined to form creation and annihilation operators for right and left-circular quanta

$$\begin{aligned} \hat{b}_R &= \frac{1}{\sqrt{2}}(\hat{b}_x - i\hat{b}_y) \ , \quad \hat{b}_R^\dagger = \frac{1}{\sqrt{2}}(\hat{b}_x^\dagger + i\hat{b}_y^\dagger) \ , \\ \hat{b}_L &= \frac{1}{\sqrt{2}}(\hat{b}_x + i\hat{b}_y) \ , \quad \hat{b}_L^\dagger = \frac{1}{\sqrt{2}}(\hat{b}_x^\dagger - i\hat{b}_y^\dagger) \ . \end{aligned} \tag{C.5}$$

in exact analogy to the isotropic case considered in section 5.2. The Hamiltonian which results from combination of (C.3), (C.4) and (C.5) is

$$H_{S,z}^A = -\frac{eB_0}{2\sqrt{m_x m_y}}\left(2\hat{b}_R^\dagger \hat{b}_R + 1\right) + \frac{p_z^2}{2m_z} = \omega_c^{xy}\left(\hat{b}_R^\dagger \hat{b}_R + \frac{1}{2}\right) + \frac{p_z^2}{2m_z} \ , \tag{C.6}$$

where the cyclotron frequency ω_c^{xy} has been identified as the eigenfrequency of the Landau levels

$$\omega_c^{xy} = \left|\frac{eB_0}{\sqrt{m_x m_y}}\right| \ . \tag{C.7}$$

None of the above discussion made explicit reference to the orientation of the surface, so we may cycle indices to find the corresponding relation for a magnetic field directed along the $\hat{x}$ direction

$$H_{S,x}^A = \omega_c^{yz}\left(\hat{b}_R^\dagger \hat{b}_R + \frac{1}{2}\right) + \frac{p_x^2}{2m_x} \ , \tag{C.8}$$

with

$$\omega_c^{yz} = \left|\frac{eB_0}{\sqrt{m_y m_z}}\right| . \tag{C.9}$$

We now introduce the surface, with, as usual, its normal directed along $\hat{z}$. This introduces an asymmetry between (C.6) and (C.8) because the electrostatic image potential V_{image} cannot depend on x or y since the system is translation invariant in these directions, giving

$$H_{S,\perp}^A = \omega_c^{xy}\left(\hat{b}_R^\dagger \hat{b}_R + \frac{1}{2}\right) + \frac{p_z^2}{2m_z} + V_{\text{image}}(z) \ , \tag{C.10}$$

$$H_{S,\parallel}^A = \omega_c^{yz}\left(\hat{b}_R^\dagger \hat{b}_R + \frac{1}{2}\right) + \frac{p_x^2}{2m_x} + V_{\text{image}}(z) \ . \tag{C.11}$$

For a magnetic field directed perpendicular to the interface, the cyclotron frequency is ω_c^{xy} as given by (C.7). Translational invariance along the surface means that the shifts in the masses m_x and m_y must be equal, meaning that eq. (C.7) becomes

$$\omega_c^{xy} = \left|\frac{eB_0}{m_\parallel}\right| . \tag{C.12}$$

Equation (C.10) then makes the Schrödinger equation separable into parallel (x, y) and perpendicular (z) co-ordinates meaning that the image potential $V_{\text{image}}(z)$ decouples. Conversely, eq. (C.11) is separable only into x and (y, z) co-ordinates, but the $V_{\text{image}}(z)$ affects the latter, so that the image potential does not decouple from the cyclotron motion.

The electrostatic potential $V_{\text{image}}(z)$ varies as the electron moves under the influence of the magnetic field, so that the path it takes is skewed relative to the circular cyclotron orbit found for magnetic fields directed perpendicular to the interface. As shown in [39], this extra distortion from $V_{\text{image}}(z)$ has much more of an effect than the mass shift itself, so one cannot claim that a measurement of the cyclotron frequency in a field directed parallel to the interface is a measurement of the mass shift.

Appendix D

Foldy-Wouthuysen Transformation

The Foldy-Wouthuysen (FW) transformation [72] is a unitary transformation to be applied to the Dirac Hamiltonian (5.31) which delivers a non-relativistic approximation up to arbitrary order in e/m.

The Dirac equation for a particle coupled to a field $\mathbf{A}_Q$ given by eq. (5.31) as

$$i\frac{\partial}{\partial t}\Psi = [\boldsymbol{\alpha}\cdot(\mathbf{p} - e\mathbf{A}_Q)] + e\Phi + \beta m]\Psi. \tag{D.1}$$

The electron near the dielectric is coupled to two fields: $\mathbf{A}_0$, which is the magnetic vector potential corresponding to the classical magnetic field $\mathbf{B}_0$ applied along the z axis, and $\mathbf{A}_Q$, which is the quantized field described by the mode functions, so that $\mathbf{A}_Q = \mathbf{A}_0 + \mathbf{A}_0$. The potential term $e\Phi$ becomes the image potential V. Also, the Hamiltonian of the photon field must be added, this is denoted H_{rad} and is given by eq. (3.14). So, the Dirac Hamiltonian H to be considered is:

$$H = \beta m + V + \boldsymbol{\alpha}\cdot(\mathbf{p} - e\mathbf{A}_0 - e\mathbf{A}_Q) + H_{rad}. \tag{D.2}$$

The Hamiltonian can be written as a sum of 'even' ($\mathcal{E}$) and 'odd' ($\mathcal{O}$) parts as:

$$H = \beta m + \mathcal{O} + \mathcal{E},$$
$$\text{where} \quad \mathcal{E} = V + H_{rad}, \quad \text{and} \quad \mathcal{O} = \boldsymbol{\alpha}\cdot(\mathbf{p} - e\mathbf{A}_0 - e\mathbf{A}_Q) \equiv \boldsymbol{\alpha}\cdot\boldsymbol{\pi}, \tag{D.3}$$

where as usual the $\boldsymbol{\pi}$ operator has been defined. An 'odd' operator couples the upper two components of a Dirac spinor to the lower two, while an 'even' one does not. The FW transformation aims to eliminate this coupling by removing odd operators. This means that through the FW transformation, the four component Dirac spinor can be reduced to its upper two components and the Dirac Hamiltonian is transformed into a Schrödinger Hamiltonian that contains appropriate relativistic corrections. This can be

done exactly for a free particle. For a particle in a field there is in general no representation for which the Hamiltonian is exactly even [72]. However, the odd part of the Hamiltonian can be eliminated to the required order by the use of successive applications of the FW transformation.

The required unitary transformation U_1 is [72]

$$U_1 = e^{\frac{\beta\mathcal{O}}{2m}} \qquad U_1^\dagger = e^{-\frac{\beta\mathcal{O}}{2m}} \,. \tag{D.4}$$

One can show by taking a unitary transform of the Schrödinger equation that the unitary-transformed Hamiltonian is given by

$$H_1 = U_1 H U_1^\dagger - i U_1 \frac{\partial U_1^\dagger}{\partial t}. \tag{D.5}$$

In the Schrödinger picture U_1 is time independent, so this reduces to

$$H_1 = U_1 H U_1^\dagger = U_1(\beta m + \mathcal{O} + \mathcal{E})U_1^\dagger = U_1(\beta m + \mathcal{O})U_1^\dagger + U_1 \mathcal{E} U_1^\dagger. \tag{D.6}$$

Using the definitions of $\mathcal{E}$ and $\mathcal{O}$, the following commutation and anticommutation relations can be shown to hold

$$\{\beta m + \mathcal{O}, \beta\mathcal{O}\} = 0, \tag{D.7a}$$

$$[\beta\mathcal{O}, \mathcal{E}] = \beta[\mathcal{O}, \mathcal{E}], \tag{D.7b}$$

$$[\beta\mathcal{O}, [\beta\mathcal{O}, \mathcal{E}]] = -[\mathcal{O}, [\mathcal{O}, \mathcal{E}]], \tag{D.7c}$$

$$[\beta\mathcal{O}, [\beta\mathcal{O}, [\beta\mathcal{O}, \mathcal{E}]]] = -\beta[\mathcal{O}, [\mathcal{O}, [\mathcal{O}, \mathcal{E}]]]. \tag{D.7d}$$

Expressing the exponential as a power series and using the commutation relation (D.7a), a short calculation shows that the odd part of eq. (D.6) satisfies

$$U_1(\beta m + \mathcal{O})U_1^\dagger = (\beta m + \mathcal{O}) \left[\mathbb{1} - \frac{\beta\mathcal{O}}{m} + \frac{1}{2!}\left(\frac{\beta\mathcal{O}}{m}\right)^2 + ... \right], \tag{D.8}$$

Using the fact that $(\beta\mathcal{O})^2 = -(\alpha\cdot\pi)^2 = -\mathcal{O}^2$, this series is can be written as the sum of two series, one with even powers of $\mathcal{O}$ and one with odd powers of $\mathcal{O}$; these are the expansions of trigonometric functions

$$\begin{aligned} U_1(\beta m + \mathcal{O})U_1^\dagger &= (\beta m + \mathcal{O}) \left[\mathbb{1} - \frac{1}{2!}\left(\frac{\mathcal{O}}{m}\right)^2 + \frac{1}{4!}\left(\frac{\mathcal{O}}{m}\right)^4 + ... - \frac{\beta\mathcal{O}}{m} + \beta\frac{1}{3!}\left(\frac{\mathcal{O}}{m}\right)^3 + ... \right] \\ &= (\beta m + \mathcal{O}) \left[\cos\left(\frac{\theta}{m}\right) - \beta \sin\left(\frac{\theta}{m}\right) \right]. \end{aligned} \tag{D.9}$$

Expanding to order $1/m^3$ we have

$$\begin{aligned} U_1(\beta m + \mathcal{O})U_1^\dagger &\approx \beta m - \frac{1}{2}\beta\frac{\mathcal{O}^2}{m} + \frac{1}{24}\beta\frac{\mathcal{O}^4}{m^3} + \beta\frac{\mathcal{O}^2}{m} - \frac{1}{6}\beta\frac{\mathcal{O}^4}{m^3} + \mathcal{O} - \frac{1}{2}\frac{\mathcal{O}^3}{m^2} - \mathcal{O} + \frac{1}{6}\frac{\mathcal{O}^3}{m^2} \\ &= \beta m + \frac{1}{2}\beta\frac{\mathcal{O}^2}{m} - \frac{1}{3}\frac{\mathcal{O}^3}{m^2} - \frac{1}{8}\beta\frac{\mathcal{O}^4}{m^3}, \end{aligned} \tag{D.10}$$

where, importantly, the terms lowest order in $1/m$ (aside from βm which is the part of the Hamiltonian to which corrections are being applied) have cancelled out - the lowest order odd terms have been eliminated.

The even part of eq. (D.6) is

$$U_1 \mathcal{E} U_1^\dagger = e^{\frac{\beta \mathcal{O}}{2m}} \mathcal{E} e^{-\frac{\beta \mathcal{O}}{2m}}. \tag{D.11}$$

This can be expanded using the Baker-Campbell-Hausdorff relation:

$$e^A B e^{-A} = B + [A, B] + \frac{1}{2!}[A, [A, B]] + \frac{1}{3!}[A, [A, [A, B]]] + ... \tag{D.12}$$

(see, for example, [88]). Then, to order $1/m^3$

$$U_1 \mathcal{E} U_1^\dagger = \mathcal{E} + \frac{1}{2m}[\beta \mathcal{O}, \mathcal{E}] + \frac{1}{8m^2}[\beta \mathcal{O}, [\beta \mathcal{O}, \mathcal{E}]] + \frac{1}{48m^3}[\beta \mathcal{O}, [\beta \mathcal{O}, [\beta \mathcal{O}, \mathcal{E}]]]. \tag{D.13}$$

Using the commutation relations (D.7b) to (D.7d), this can be written:

$$U_1 \mathcal{E} U_1^\dagger = \mathcal{E} + \frac{\beta}{2m}[\mathcal{O}, \mathcal{E}] - \frac{1}{8m^2}[\mathcal{O}, [\mathcal{O}, \mathcal{E}]] - \frac{\beta}{48m^3}[\mathcal{O}, [\mathcal{O}, [\mathcal{O}, \mathcal{E}]]]. \tag{D.14}$$

The total Hamiltonian H_1 shown in eq. (D.6) can then be written using eqs (D.10) and (D.14):

$$\begin{aligned} H_1 = U_1(\beta m + \mathcal{O})U_1^\dagger + U_1 \mathcal{E} U_1^\dagger =& \beta m + \frac{1}{2}\beta \frac{\mathcal{O}^2}{m} - \frac{1}{3}\frac{\mathcal{O}^3}{m^2} - \frac{1}{8}\beta \frac{\mathcal{O}^4}{m^3} + \mathcal{E} + \frac{\beta}{2m}[\mathcal{O}, \mathcal{E}] \\ & - \frac{1}{8m^2}[\mathcal{O}, [\mathcal{O}, \mathcal{E}]] - \frac{\beta}{48m^3}[\mathcal{O}, [\mathcal{O}, [\mathcal{O}, \mathcal{E}]]]. \end{aligned} \tag{D.15}$$

Grouping terms by the power to which $\mathcal{O}$ is raised

$$\begin{aligned} H_1 = \beta m + & \mathcal{E} + \frac{1}{2}\beta \frac{\mathcal{O}^2}{m} - \frac{1}{8m^2}[\mathcal{O}, [\mathcal{O}, \mathcal{E}]] - \frac{1}{8}\beta \frac{\mathcal{O}^4}{m^3} \\ & + \frac{\beta}{2m}[\mathcal{O}, \mathcal{E}] - \frac{1}{3}\frac{\mathcal{O}^3}{m^2} - \frac{\beta}{48m^3}[\mathcal{O}, [\mathcal{O}, [\mathcal{O}, \mathcal{E}]]], \end{aligned} \tag{D.16}$$

shows that H_1 can be written as $H_1 = \beta m + \mathcal{O}_1 + \mathcal{E}_1$ where:

$$\mathcal{O}_1 = \frac{\beta}{2m}[\mathcal{O}, \mathcal{E}] - \frac{1}{3}\frac{\mathcal{O}^3}{m^2} - \frac{\beta}{48m^3}[\mathcal{O}, [\mathcal{O}, [\mathcal{O}, \mathcal{E}]]], \tag{D.17}$$

is odd, and

$$\mathcal{E}_1 = \mathcal{E} + \frac{1}{2}\beta \frac{\mathcal{O}^2}{m} - \frac{1}{8m^2}[\mathcal{O}, [\mathcal{O}, \mathcal{E}]] - \frac{1}{8}\beta \frac{\mathcal{O}^4}{m^3}, \tag{D.18}$$

is even.

Another unitary transformation $U_2 = e^{\frac{\beta \mathcal{O}_1}{2m}}$ is then applied to H_1 to further eliminate odd operators into higher order terms. This will yield a Hamiltonian $H_2 = \beta m + \mathcal{O}_2 + \mathcal{E}_2$. This can be done by exact analogy with the first unitary transformation U_1 since it is just the replacements $\mathcal{O} \to \mathcal{O}_1$, $\mathcal{O}_1 \to \mathcal{O}_2$, $\mathcal{E} \to \mathcal{E}_1$ and $\mathcal{E}_1 \to \mathcal{E}_2$. Any odd or even operators

$\mathcal{O}_i$ or $\mathcal{E}_i$ must, by definition, have exactly the same properties with respect to the above analysis, so we can immediately write:

$$H_2 = \beta m + \mathcal{O}_2 + \mathcal{E}_2, \tag{D.19}$$

where

$$\mathcal{O}_2 = \frac{\beta}{2m}[\mathcal{O}_1, \mathcal{E}_1] - \frac{1}{3}\frac{\mathcal{O}_1^3}{m^2} - \frac{\beta}{48m^3}[\mathcal{O}_1, [\mathcal{O}_1, [\mathcal{O}_1, \mathcal{E}_1]]], \tag{D.20a}$$

$$\mathcal{E}_2 = \mathcal{E}_1 + \frac{1}{2}\beta\frac{\mathcal{O}_1^2}{m} - \frac{1}{8m^2}[\mathcal{O}_1, [\mathcal{O}_1, \mathcal{E}_1]] - \frac{1}{8}\beta\frac{\mathcal{O}_1^4}{m^3}. \tag{D.20b}$$

$\mathcal{O}_1$ contains a factor of $1/m$ throughout, so the final two terms of both $\mathcal{O}_2$ and $\mathcal{E}_2$ are of order higher than $1/m^3$, meaning they can be dropped. This gives:

$$\mathcal{O}_2 = \frac{\beta}{2m}[\mathcal{O}_1, \mathcal{E}_1], \tag{D.21a}$$

$$\mathcal{E}_2 = \mathcal{E}_1 + \frac{1}{2}\beta\frac{\mathcal{O}_1^2}{m}. \tag{D.21b}$$

Substituting equations (D.17) into (D.21a) gives

$$\mathcal{O}_2 = \frac{\beta}{2m}\Bigg[\left(\frac{\beta}{2m}[\mathcal{O}, \mathcal{E}] - \frac{1}{3}\frac{\mathcal{O}^3}{m^2} - \frac{1}{48m^3}[\mathcal{O}, [\mathcal{O}, [\mathcal{O}, \mathcal{E}]]]\right), \tag{D.22}$$

$$\left(\mathcal{E} + \frac{1}{2}\beta\frac{\mathcal{O}^2}{m} - \frac{1}{8m^2}[\mathcal{O}, [\mathcal{O}, \mathcal{E}]] - \frac{1}{8}\beta\frac{\mathcal{O}^4}{m^3}\right)\Bigg]. \tag{D.23}$$

Dropping terms of order $1/m^3$ or higher this becomes

$$\mathcal{O}_2 = \frac{1}{4m^2}[[\mathcal{O}, \mathcal{E}], \mathcal{E}] + \frac{\beta}{8m^3}\left[[\mathcal{O}, \mathcal{E}], \mathcal{O}^2\right] - \frac{\beta}{6m^3}[\mathcal{O}^3, \mathcal{E}]\,. \tag{D.24}$$

Repeating the analysis for $\mathcal{E}_2$ gives

$$\mathcal{E}_2 = \mathcal{E}_1 + \frac{\beta}{8m^3}(\beta[\mathcal{O}, \mathcal{E}])^2\,. \tag{D.25}$$

We have now obtained the even part of H up to order $1/m^3$. We could keep applying the FW transformation to (D.24) in order to eliminate all the terms of lower order than $1/m^3$, but this of course would not affect the even part (D.25). So, the Hamiltonian H can be approximated as the even operator $H = \beta m + \mathcal{E}_2$. which is:

$$H = \beta m + \mathcal{E} + \frac{1}{2}\beta\frac{\mathcal{O}^2}{m} - \frac{\beta}{8}\frac{\mathcal{O}^4}{m^3} - \frac{1}{8m^2}[\mathcal{O}, [\mathcal{O}, \mathcal{E}]] + \frac{\beta}{8m^3}(\beta[\mathcal{O}, \mathcal{E}])^2. \tag{D.26}$$

This Hamiltonian needs to be written in terms of the fields and potentials as set out in eq. (D.2). The $\beta m + \mathcal{E}$ part evaluates trivially. The term $\frac{1}{2}\beta\frac{\mathcal{O}^2}{m}$ may be simplified by noting that

$$\alpha_i\alpha_j = i\sigma_k\epsilon_{ijk}\mathbb{1}_2 + \delta_{ij}, \tag{D.27}$$

giving

$$\mathcal{O}^2 = (\mathbf{p} - e\mathbf{A_0} - e\mathbf{A}_Q)^2 + i\boldsymbol{\alpha}\cdot((\mathbf{p} - e\mathbf{A_0} - e\mathbf{A}_Q)\times(\mathbf{p} - e\mathbf{A_0} - e\mathbf{A}_Q)), \tag{D.28}$$

Since $\mathbf{p}$ and $\mathbf{A}_Q$ do not commute, the second term is not zero, rather we find

$$\frac{1}{2}\beta\frac{\mathcal{O}^2}{m} = \frac{\beta}{2m}[(\mathbf{p} - e\mathbf{A_0} - e\mathbf{A}_Q)^2 - e\boldsymbol{\sigma}\cdot\mathbf{B_0} - e\boldsymbol{\sigma}\cdot\mathbf{B}]. \tag{D.29}$$

Similarly, the fourth term in eq. (D.26) ($-\frac{\beta}{8}\frac{\mathcal{O}^4}{m^3}$) follows immediately from the square of this

$$-\frac{\beta}{8}\frac{\mathcal{O}^4}{m^3} = -\frac{\beta}{8m^3}[(\mathbf{p} - e\mathbf{A_0} - e\mathbf{A}_Q)^2 - e\boldsymbol{\sigma}\cdot\mathbf{B_0} - e\boldsymbol{\sigma}\cdot\mathbf{B}]^2. \tag{D.30}$$

The next term in eq. (D.26) ($\frac{1}{8m^2}[\mathcal{O},[\mathcal{O},\mathcal{E}]]$) contains a large amount of hidden structure. Firstly considering $[\mathcal{O},\mathcal{E}]$, we have:

$$\begin{aligned}[\mathcal{O},\mathcal{E}] &= [\boldsymbol{\alpha}\cdot\boldsymbol{\pi}, V + H_{rad}] \\ &= [\boldsymbol{\alpha}\cdot(\mathbf{p} - e\mathbf{A_0} - e\mathbf{A}_Q), V] + [\boldsymbol{\alpha}\cdot(\mathbf{p} - e\mathbf{A_0} - e\mathbf{A}_Q), H_{rad}].\end{aligned} \tag{D.31}$$

$\mathbf{A_0}$ and $\mathbf{A}_Q$ do not contain any operators which act on V, so they commute with V. $\mathbf{p} = -i\nabla$ does not commute with V because it contains a derivative which acts on V as detailed below. Similarly, $\mathbf{p}$ and $\mathbf{A_0}$ commute with H_{rad}, but $\mathbf{A}_Q$ does not. Loosely, this is because $\mathbf{A}_Q$ and H_{rad} both contain the photon creation and annihilation operators, which do not commute. For these reasons, $[\mathcal{O},\mathcal{E}]$ reduces to:

$$[\mathcal{O},\mathcal{E}] = [\boldsymbol{\alpha}\cdot\mathbf{p}, V] - e[\boldsymbol{\alpha}\cdot\mathbf{A}_Q, H_{rad}]. \tag{D.32}$$

A short calculation shows that $[\boldsymbol{\alpha}\cdot\mathbf{p}, V] = -i\boldsymbol{\alpha}\cdot\varphi\nabla V$. When considering the second term of (D.32), it is useful to invoke Ehrenfest's theorem and write $\dot{\mathbf{A}}_Q = -i[\mathbf{A}_Q, H_{rad}] = -\mathbf{E}_Q$. So $[\mathbf{A}_Q, H_{rad}] = -i\mathbf{E}_Q$, meaning equation (D.32) can be written as:

$$[\mathcal{O},\mathcal{E}] = i\boldsymbol{\alpha}\cdot(e\mathbf{E}_Q - \nabla V) \tag{D.33}$$

The whole commutator $[\mathcal{O},[\mathcal{O},\mathcal{E}]]$ is then

$$[\mathcal{O},[\mathcal{O},\mathcal{E}]] = ie[\boldsymbol{\alpha}\cdot\boldsymbol{\pi}, \boldsymbol{\alpha}\cdot\mathbf{E}_Q] - i[\boldsymbol{\alpha}\cdot\boldsymbol{\pi}, \boldsymbol{\alpha}\cdot\nabla V]. \tag{D.34}$$

The following identity holds for F and G which commute with the α_i but not with each other

$$[\alpha\cdot F, \alpha\cdot G] = i\sigma\cdot(F\times G) - i\sigma\cdot(G\times F) + [F_i, G_i]. \tag{D.35}$$

This, alongside the facts that $[p_i, E_{Qi}] = 0$ and $[A_{0i}, E_{Qi}] = 0$ can be used to simplify the first term of eq. (D.34), giving

$$[\alpha\cdot\boldsymbol{\pi}, \alpha\cdot\mathbf{E}_Q] = i\sigma\cdot(\boldsymbol{\pi}\times\mathbf{E}_Q - \mathbf{E}_Q\times\boldsymbol{\pi}) - e[A_{Qi}, E_{Qi}]. \tag{D.36}$$

Similarly, the second term of eq. (D.34) simplifies to

$$[\boldsymbol{\alpha}\cdot\boldsymbol{\pi}, \boldsymbol{\alpha}\cdot\nabla V] = i\sigma\cdot(\boldsymbol{\pi}\times\nabla V - \nabla V\times\boldsymbol{\pi}) - i\nabla^2 V, \tag{D.37}$$

where $[p_i, \nabla_i V]\varphi = -i\nabla^2 V\varphi$ has been used. Thus the whole term is:

$$\begin{aligned}-\frac{1}{8m^2}[\mathcal{O},[\mathcal{O},\mathcal{E}]] = \frac{e}{8m^2}\sigma\cdot[(\boldsymbol{\pi}\times\mathbf{E}_Q) - (\mathbf{E}_Q\times\boldsymbol{\pi})] \\ + \frac{e}{8m^2}\sigma\cdot\left[\left(\boldsymbol{\pi}\times-\frac{\nabla V}{e}\right) - \left(-\frac{\nabla V}{e}\times\boldsymbol{\pi}\right)\right] \\ + \frac{1}{8m^2}(\nabla^2 V + ie^2[A_{Qi}, E_{Qi}]).\end{aligned} \tag{D.38}$$

The final term of eq. (D.26) to be considered is $\frac{\beta}{8m^3}(\beta[\mathcal{O},\mathcal{E}])^2$. From eq. (D.33), $[\mathcal{O},\mathcal{E}] = i\alpha(e\mathbf{E}_Q - \nabla V)$. Recalling that $\{\alpha,\beta\} = 0$ we find

$$\frac{\beta}{8m^3}(\beta[\mathcal{O},\mathcal{E}])^2 = \frac{\beta e^2}{8m^3}\left(\mathbf{E}_Q - \frac{\nabla V}{e}\right)^2. \tag{D.39}$$

Inserting eqs (D.29), (D.30), (D.38) and (D.39) into (D.26) gives

$$\begin{aligned}H =& \beta m + \mathcal{E} + \frac{\beta}{2m}[(\mathbf{p} - e\mathbf{A_0} - e\mathbf{A}_Q)^2 - e\sigma\cdot\mathbf{B_0} - e\sigma\cdot\mathbf{B}_Q] \\ &- \frac{\beta}{8m^3}[(\mathbf{p} - e\mathbf{A_0} - e\mathbf{A}_Q)^2 - e\sigma\cdot\mathbf{B_0} - e\sigma\cdot\mathbf{B}_Q]^2 \\ &+ \frac{e}{8m^2}\sigma\cdot[(\boldsymbol{\pi}\times\mathbf{E}_Q) - (\mathbf{E}_Q\times\boldsymbol{\pi})] + \frac{e}{8m^2}\sigma\cdot\left[\left(\boldsymbol{\pi}\times-\frac{\nabla V}{e}\right) - \left(-\frac{\nabla V}{e}\times\boldsymbol{\pi}\right)\right] \\ &+ \frac{1}{8m^2}(\nabla^2 V + ie^2[A_{Qi}, E_{Qi}]) + \frac{\beta e^2}{8m^3}\left(\mathbf{E}_Q - \frac{\nabla V}{e}\right)^2,\end{aligned} \tag{D.40}$$

which is the required Hamiltonian (D.26) in terms of the electromagnetic fields and image potential.

To simplify the term from (D.40) that contains a commutator, we note from [40] that the following relation holds in generalized Coulomb gauge

$$[A_i(\mathbf{r}), E_i(\mathbf{r}')] = -i\delta^{(3)}(\mathbf{r}-\mathbf{r}') + i\nabla_i\nabla_i' G(\mathbf{r},\mathbf{r}'), \tag{D.41}$$

where $G(\mathbf{r},\mathbf{r}')$ is the Green's function of the Poisson equation

$$\nabla^2 G(\mathbf{r},\mathbf{r}') = \delta^{(3)}(\mathbf{r}-\mathbf{r}'), \tag{D.42}$$

which, for a half space with both $\mathbf{r}$ and $\mathbf{r}'$ on the vacuum side, can be written

$$G(\mathbf{r},\mathbf{r}') = G^{(0)}(\mathbf{r},\mathbf{r}') + G_R(\mathbf{r},\mathbf{r}'), \tag{D.43}$$

where $G^{(0)}(\mathbf{r},\mathbf{r}')$ is the Green's function for the free Poisson equation and $G_R(\mathbf{r},\mathbf{r}')$ is the reflected part of the Green's function. Substituting this into eq. (D.41) and using (D.42), we find

$$ie^2[A_i(\mathbf{r}), E_i(\mathbf{r}')] = -e^2\nabla_i\nabla_i' G_R(\mathbf{r},\mathbf{r}'), \tag{D.44}$$

giving for the term of (D.40) that contains the commutator

$$\frac{1}{8m^2}\left(\nabla^2 V + ie^2[A_{Qi}, E_{Qi}]\right) = \frac{1}{8m^2}\left(\nabla^2 V - e^2\nabla^2 G_R(\mathbf{r},\mathbf{r})\right). \tag{D.45}$$

The reflected part of the electrostatic Green's function *is* the image potential. We are considering the interaction of an electron with its image, so the interaction energy is found by multiplying the image potential by e^2, meaning that eq. (D.45) vanishes:

$$\frac{1}{8m^2}\left(\nabla^2 V + ie^2[A_{Qi}, E_{Qi}]\right) = 0. \tag{D.46}$$

Proceeding, we group the terms by their contributing order in perturbation theory of the quantized electromagnetic field – i.e. by their order in $\mathbf{A}_Q$ and $\mathbf{E}_Q$. The terms contributing in first-order perturbation theory are

$$H_1 = \frac{e^2}{2m}\mathbf{A}_Q^2 + \frac{e^3}{4m^3}\mathbf{A}_Q^2\boldsymbol{\sigma}\cdot\mathbf{B}_0, \tag{D.47}$$

and those contributing in second-order perturbation theory are

$$H_2 = -\frac{e}{m}\mathbf{A}_Q\cdot\boldsymbol{\pi} - \frac{e}{2m}\boldsymbol{\sigma}\cdot\mathbf{B}_Q + \frac{e}{8m^2}\boldsymbol{\sigma}\cdot(\boldsymbol{\pi}\times\mathbf{E}_Q - \mathbf{E}_Q\times\boldsymbol{\pi}), \tag{D.48}$$

The remaining terms are denoted $V_{\text{electrostatic}}$,

$$H = H_1 + H_2 + V_{\text{electrostatic}}. \tag{D.49}$$

Appendix E

Dyadic Green's Functions

E.1 Dyads

In a Cartesian co-ordinate system, a vector is denoted by:

$$\mathbf{F} = F_i \hat{\mathbf{r}}_i, \tag{E.1}$$

Following [89], we may specify in three dimensions a set of three vector functions $\overline{F}_j$, $j = \{1, 2, 3\}$ through a nine-component object F_{ij}

$$\overline{\mathbf{F}}_j = F_{ij} \hat{\mathbf{r}}_i, \tag{E.2}$$

and from that we can define

$$\overline{\overline{\mathbf{F}}} = \overline{\mathbf{F}}_j \hat{x}_j = F_{ij} \hat{\mathbf{r}}_i \hat{\mathbf{r}}_j, \tag{E.3}$$

which is known as a *dyadic*. In the main text we use the *posterior scalar product*, defined as

$$\overline{\overline{\mathbf{F}}} \cdot \overline{\mathbf{a}} = F_{ij} a_j \hat{\mathbf{r}}_i. \tag{E.4}$$

It is worth noting that in general $\overline{\overline{\mathbf{F}}} \cdot \overline{\mathbf{a}} \neq \overline{\mathbf{a}} \cdot \overline{\overline{\mathbf{F}}}$, the right hand side being known as the anterior scalar product. This difference is of no consequence to our calculations. In the main we text we drop the bars $\overline{\overline{\mathbf{F}}} \to \mathbf{F}$ since whether a quantity is a dyadic or not is easily inferred from context, or is explicitly stated.

E.2 Proof of a useful integral relation

In this section we prove eq. (7.18). We begin by noting that the dyadic Green's function delivers the solution to eq. (7.14), which in component form is

$$\partial_k \partial_k A_i(\mathbf{r}, \omega) + \omega^2 \epsilon(\mathbf{r}, \omega) A_i = j_i(\mathbf{r}, \omega), \tag{E.5}$$

where the solution is obtained from

$$\hat{A}_i(\mathbf{r},\omega) = \int d^3\mathbf{r}'\, \mathbf{G}_{ij}(\mathbf{r},\mathbf{r}',\omega)\hat{j}_j(\mathbf{r}',\omega), \tag{E.6}$$

implying

$$\left[\partial_k\partial_k + \omega^2\epsilon(\mathbf{r},\omega)\right]\mathbf{G}_{ij}(\mathbf{r},\mathbf{r}',\omega) = \delta_{ij}\delta^{(3)}(\mathbf{r}-\mathbf{r}'). \tag{E.7}$$

To prove eq. (7.18) we follow the general approach of [37]. We begin by multiplying both sides of (E.7) by $\mathbf{G}^*_{il}(\mathbf{r},\mathbf{r}'',\omega)$ and integrating over $d^3\mathbf{r}$

$$\int d^3\mathbf{r}\left[\partial_k\partial_k + \omega^2\epsilon(\mathbf{r},\omega)\right]\mathbf{G}_{ij}(\mathbf{r},\mathbf{r}',\omega)\mathbf{G}^*_{il}(\mathbf{r},\mathbf{r}'',\omega) = \mathbf{G}^*_{jl}(\mathbf{r}',\mathbf{r}'',\omega)\ . \tag{E.8}$$

We then integrate parts in the first term on the left hand-side, giving

$$\begin{aligned}-\int d^3\mathbf{r}\left[\partial_k\mathbf{G}_{ij}(\mathbf{r},\mathbf{r}',\omega)\right]\left[\partial_k\mathbf{G}^*_{il}(\mathbf{r},\mathbf{r}'',\omega)\right] &= \mathbf{G}^*_{jl}(\mathbf{r}',\mathbf{r}'',\omega)\\ &\quad -\omega^2\int d^3\mathbf{r}\epsilon(\mathbf{r},\omega)\mathbf{G}_{ij}(\mathbf{r},\mathbf{r}',\omega)\mathbf{G}^*_{il}(\mathbf{r},\mathbf{r}'',\omega).\end{aligned} \tag{E.9}$$

Taking the complex conjugate, making the replacements $\mathbf{r}' \leftrightarrow \mathbf{r}''$ and $j \leftrightarrow l$ and subtracting the resulting equation from the above causes the left hand side to vanish, leaving

$$\omega^2\int d^3\mathbf{r}\left[\epsilon(\mathbf{r},\omega)-\epsilon^*(\mathbf{r},\omega)\right]\mathbf{G}_{ij}(\mathbf{r},\mathbf{r}',\omega)\mathbf{G}^*_{il}(\mathbf{r},\mathbf{r}'',\omega) = -\left[\mathbf{G}_{jl}(\mathbf{r}',\mathbf{r}'',\omega) - \mathbf{G}^*_{lj}(\mathbf{r}'',\mathbf{r}',\omega)\right)], \tag{E.10}$$

where real frequency has been assumed. The Green's function has the symmetry property [90]

$$G_{ij}(\mathbf{r},\mathbf{r}',\omega) = G_{ji}(\mathbf{r}',\mathbf{r},\omega), \tag{E.11}$$

so that we are left with

$$\omega^2\int d^3\mathbf{r}\epsilon_I(\mathbf{r},\omega)\mathbf{G}_{ij}(\mathbf{r},\mathbf{r}',\omega)\mathbf{G}^*_{il}(\mathbf{r},\mathbf{r}'',\omega) = -\operatorname{Im}\mathbf{G}_{jl}(\mathbf{r}',\mathbf{r}'',\omega), \tag{E.12}$$

as required. The works because the integral kernel $\mathbf{K}(\mathbf{r},\mathbf{r}',\omega)$ defined by eqs. (E.5) and (E.6) is reciprocal: $\mathbf{K}(\mathbf{r},\mathbf{r}',\omega) = \mathbf{K}^T(\mathbf{r}',\mathbf{r},\omega)$ [91]. Changing the notation slightly we are left with the form (7.18) used in the main text

$$\omega^2\int d^3\mathbf{r}\epsilon_I(\mathbf{r},\omega)\mathbf{G}_{il}(\mathbf{r}',\mathbf{r},\omega)\mathbf{G}^*_{jl}(\mathbf{r}'',\mathbf{r},\omega) = -\operatorname{Im}\mathbf{G}_{ij}(\mathbf{r}',\mathbf{r}'',\omega)\ . \tag{E.13}$$

E.3 Specific dyadic Green's functions

E.3.1 Vacuum

We now need the explicit vacuum Green's function, which we will put into the form of eq. (7.43) for convenience. This is found from [37]

$$\begin{aligned}\mathbf{G}^v_{ij}(\mathbf{r},\mathbf{r}',\omega) &= \left[\partial^r_i\partial^r_j + \delta_{ij}\omega^2\epsilon(\omega)\right]\frac{1}{\omega^2\epsilon(\omega)}\int\frac{d^3\mathbf{k}}{(2\pi)^3}\frac{e^{i\mathbf{k}\cdot(\mathbf{r}-\mathbf{r}')}}{k^2-\omega^2}\\ &= \left[\partial^r_i\partial^r_j + \delta_{ij}\omega^2\right]\frac{1}{\omega^2}\int\frac{d^2\mathbf{k}_\parallel}{(2\pi)^2}e^{i\mathbf{k}_\parallel\cdot(\mathbf{r}_\parallel-\mathbf{r}'_\parallel)}\int_{-\infty}^{\infty}\frac{dk_z}{2\pi}\frac{e^{ik_z(z-z')}}{k_\parallel^2+k_z^2-\omega^2}.\end{aligned}$$

For $z > z'$ ($z < z'$), the k_z contour can be closed in the upper (lower) half plane. Remembering that the pole in the lower half plane is encircled clockwise (thus generating an additional minus), the residue theorem gives

$$\mathbf{G}^v_{ij}(\mathbf{r},\mathbf{r}',\omega) = \left[\partial^r_i\partial^r_j + \delta_{ij}\omega^2\right]\frac{1}{\omega^2}\int\frac{d^2\mathbf{k}_\parallel}{(2\pi)^2}e^{i\mathbf{k}_\parallel\cdot(\mathbf{r}_\parallel-\mathbf{r}'_\parallel)}\frac{ie^{-ik_z|z-z'|}}{2k_z}. \tag{E.14}$$

The required components are

$$G^v_{zx}(\mathbf{r},\mathbf{r}',\omega) = \frac{1}{\omega^2}\int\frac{d^2\mathbf{k}_\parallel}{(2\pi)^2}e^{i\mathbf{k}_\parallel\cdot(\mathbf{r}_\parallel-\mathbf{r}'_\parallel)}\left[k_xk_z\mathrm{sgn}(z-z')\right]\frac{ie^{-ik_z|z-z'|}}{2k_z}, \tag{E.15a}$$

$$G^v_{zz}(\mathbf{r},\mathbf{r}',\omega) = \frac{1}{\omega^2}\int\frac{d^2\mathbf{k}_\parallel}{(2\pi)^2}e^{i\mathbf{k}_\parallel\cdot(\mathbf{r}_\parallel-\mathbf{r}'_\parallel)}k_\parallel^2\frac{ie^{-ik_z|z-z'|}}{2k_z}, \tag{E.15b}$$

where the fact that, in vacuum, $\omega^2 - k_z^2 = k_\parallel^2$ has been used. We are usually interested in the case $z < 0$, $z' > 0$, for which $|z-z'| = z'-z$, and $\mathrm{sgn}(z-z') = -1$

$$G^v_{zx}(\mathbf{r},\mathbf{r}',\omega) = \frac{1}{\omega^2}\int\frac{d^2\mathbf{k}_\parallel}{(2\pi)^2}e^{i\mathbf{k}_\parallel\cdot(\mathbf{r}_\parallel-\mathbf{r}'_\parallel)}\left[-k_xk_z\right]\frac{ie^{ik_z(z-z')}}{2k_z}, \tag{E.16a}$$

$$G^v_{zz}(\mathbf{r},\mathbf{r}',\omega) = \frac{1}{\omega^2}\int\frac{d^2\mathbf{k}_\parallel}{(2\pi)^2}e^{i\mathbf{k}_\parallel\cdot(\mathbf{r}_\parallel-\mathbf{r}'_\parallel)}k_\parallel^2\frac{ie^{ik_z(z-z')}}{2k_z}. \tag{E.16b}$$

E.3.2 Planar media

Writing the Green's function via eq. (7.43), we have from [37] the reflected part of Green's function in vacuum ($z < 0$) where the space $z > 0$ is filled with a one-layered medium (i.e. a half-space):

$$\mathbf{G}^R_{xx}(\mathbf{k}_\parallel,z,z',\omega) = -\frac{i}{2k_z}e^{ik_z(z+z')}\left(R^L_{\mathrm{TE}}\frac{k_y^2}{k_\parallel^2} - R^L_{\mathrm{TM}}\frac{k_x^2k_z^2}{k^2k_\parallel^2}\right), \tag{E.17a}$$

$$\mathbf{G}^R_{xy}(\mathbf{k}_\parallel,z,z',\omega) = \frac{i}{2k_z}e^{ik_z(z+z')}\left(R^L_{\mathrm{TE}}\frac{k_xk_y}{k_\parallel^2} + R^L_{\mathrm{TM}}\frac{k_xk_yk_z^2}{k^2k_\parallel^2}\right), \tag{E.17b}$$

$$\mathbf{G}^R_{xz}(\mathbf{k}_\parallel,z,z',\omega) = \frac{i}{2k_z}e^{ik_z(z+z')}R^L_{\mathrm{TM}}\frac{k_xk_z}{k^2}, \tag{E.17c}$$

$$\mathbf{G}^R_{zz}(\mathbf{k}_\parallel,z,z',\omega) = -\frac{i}{2k_z}e^{ik_z(z+z')}R^L_{\mathrm{TM}}\frac{k_\parallel^2}{k^2}, \tag{E.17d}$$

where, in contrast with [37], $\mathrm{Re}\, k_z > 0$, $\mathrm{Im}\, k_z < 0$. The remaining five components of $\mathbf{G}^R_{ij}$ may be derived through the symmetry relations

$$\begin{aligned} \mathbf{G}^R_{yx} &= \mathbf{G}^R_{xy}, & \mathbf{G}^R_{yy} &= \mathbf{G}^R_{xx}(k_x \leftrightarrow k_y), & \mathbf{G}^R_{zx} &= -\mathbf{G}^R_{xz}, \\ & & \mathbf{G}^R_{yz} &= \mathbf{G}^R_{xz}(k_x \leftrightarrow k_y), & \mathbf{G}^R_{zy} &= -\mathbf{G}^R_{yz}\,. \end{aligned} \tag{E.18}$$

We do not list the transmitted part of the Green's function since it does not enter into any of our calculations, however we note from [37] that the z component of the wave vector in the medium must obey the same constraints as that in vacuum, in particular $\mathrm{Re}\, k^d_z < 0$. We also note that the Green's function for multilayered systems can be obtained by replacing the reflection coefficients appearing in eqs. (E.17) by the layered reflection coefficients (A.6) [38].

Bibliography

[1] Armin Hermann and Claude W Nash. *The genesis of quantum theory (1899-1913)*. MIT Press Boston, 1971.

[2] Albert Einstein and Otto Stern. Some Arguments for the Assumption of Molecular Agitation at Absolute Zero. *Annalen Phys.*, 40:551–560, 1913.

[3] E. H. Kennard. Zur Quantenmechanik einfacher Bewegungstypen. *Zeitschrift fur Physik*, 44:326–352, April 1927.

[4] M Bauer and P.A Mello. The time-energy uncertainty relation. *Annals of Physics*, 111(1):38 – 60, 1978.

[5] David J Griffiths and Gale Dick. Introduction to quantum mechanics. *Physics Today*, 48:94, 1995.

[6] C. Itzykson and J.B. Zuber. *Quantum Field Theory*. Dover Books on Physics. Dover Publications, 2005.

[7] M. Abramowitz and I.A. Stegun. *Handbook of Mathematical Functions: With Formulas, Graphs, and Mathematical Tables*. Applied mathematics series. Dover Publications, 1964.

[8] S. K. Lamoreaux. Demonstration of the casimir force in the 0.6 to 6 μm range. *Phys. Rev. Lett.*, 78:5–8, Jan 1997.

[9] D. Iannuzzi, M. Lisanti, J. N. Munday, and F. Capasso. New challenges and directions in casimir force experiments. *Proceedings of the 6th Workshop on Quantum Field Theory Under the Influence of External Conditions (QFEXT03)*, 2003.

[10] H.B.G. Casimir. On the Attraction Between Two Perfectly Conducting Plates. *Indag.Math.*, 10:261–263, 1948.

[11] Lev Davidovich Landau, Evgenij Mihajlovič Lifšic, John Bradbury Sykes, John Stewart Bell, MJ Kearsley, and Lev Petrovich Pitaevskii. *Electrodynamics of continuous media*, volume 364. Pergamon press Oxford, 1960.

[12] Marc Thierry Jaekel and Serge Reynaud. Casimir force between partially transmitting mirrors. *J. Phys. I France*, 1(10):1395–1409, 1991.

[13] RL Jaffe and A Scardicchio. Casimir effect and geometric optics. *Physical review letters*, 92(7):070402, 2004.

[14] Kimball A Milton. Casimir energies and pressures for δ-function potentials. *Journal of Physics A: Mathematical and General*, 37(24):6391, 2004.

[15] M. Sparnaay. Measurements of attractive forces between flat plates. *Physica*, 24:751–764, 1958.

[16] Astrid Lambrecht and Serge Reynaud. Comment on "demonstration of the casimir force in the 0.6 to 6 μm range". *Phys. Rev. Lett.*, 84:5672–5672, Jun 2000.

[17] S. K. Lamoreaux. Lamoreaux replies:. *Phys. Rev. Lett.*, 84:5673–5673, Jun 2000.

[18] R. S. Decca, D. López, E. Fischbach, G. L. Klimchitskaya, D. E. Krause, and V. M. Mostepanenko. Tests of new physics from precise measurements of the casimir pressure between two gold-coated plates. *Phys. Rev. D*, 75:077101, Apr 2007.

[19] Willis E. Lamb and Robert C. Retherford. Fine structure of the hydrogen atom by a microwave method. *Phys. Rev.*, 72:241–243, Aug 1947.

[20] H. B. G. Casimir and D. Polder. The influence of retardation on the london-van der waals forces. *Phys. Rev.*, 73:360–372, Feb 1948.

[21] C. I. Sukenik, M. G. Boshier, D. Cho, V. Sandoghdar, and E. A. Hinds. Measurement of the casimir-polder force. *Phys. Rev. Lett.*, 70:560–563, Feb 1993.

[22] E. A. Power and S. Zienau. Coulomb gauge in non-relativistic quantum electrodynamics and the shape of spectral lines. *Philosophical Transactions of the Royal Society of London. Series A, Mathematical and Physical Sciences*, 251(999):427–454, 1959.

[23] V. Sandoghdar, C. I. Sukenik, E. A. Hinds, and Serge Haroche. Direct measurement of the van der waals interaction between an atom and its images in a micron-sized cavity. *Phys. Rev. Lett.*, 68:3432–3435, Jun 1992.

[24] Krzysztof Pachucki. Theory of the lamb shift in muonic hydrogen. *Phys. Rev. A*, 53:2092–2100, Apr 1996.

[25] Peter J. Mohr, Barry N. Taylor, and David B. Newell. Codata recommended values of the fundamental physical constants: 2010. *Rev. Mod. Phys.*, 84:1527–1605, Nov 2012.

[26] K Pachucki, D Leibfried, M Weitz, A Huber, W Knig, and T W Hnsch. Theory of the energy levels and precise two-photon spectroscopy of atomic hydrogen and deuterium. *Journal of Physics B: Atomic, Molecular and Optical Physics*, 29(2):177, 1996.

[27] Savely G. Karshenboim. Precision physics of simple atoms: {QED} tests, nuclear structure and fundamental constants. *Physics Reports*, 422(12):1 – 63, 2005.

[28] Randolf Pohl, Aldo Antognini, François Nez, Fernando D Amaro, François Biraben, João MR Cardoso, Daniel S Covita, Andreas Dax, Satish Dhawan, Luis MP Fernandes, et al. The size of the proton. *Nature*, 466(7303):213–216, 2010.

[29] B. Odom, D. Hanneke, B. D'Urso, and G. Gabrielse. New measurement of the electron magnetic moment using a one-electron quantum cyclotron. *Phys. Rev. Lett.*, 97:030801, Jul 2006.

[30] KM Watson and JM Jauch. Phenomenological quantum electrodynamics. part iii. dispersion. *Physical Review*, 75:1249–1261, 1949.

[31] B. Huttner and S. M. Barnett. Dispersion and loss in a hopfield dielectric. *EPL (Europhysics Letters)*, 18(6):487, 1992.

[32] Bruno Huttner and Stephen M. Barnett. Quantization of the electromagnetic field in dielectrics. *Phys. Rev. A*, 46:4306–4322, Oct 1992.

[33] PW Milonni. Field quantization and radiative processes in dispersive dielectric media. *Journal of Modern Optics*, 42(10):1991–2004, 1995.

[34] Peter D. Drummond. Electromagnetic quantization in dispersive inhomogeneous nonlinear dielectrics. *Phys. Rev. A*, 42:6845–6857, Dec 1990.

[35] T Gruner and D-G Welsch. Correlation of radiation-field ground-state fluctuations in a dispersive and lossy dielectric. *Physical Review A*, 51(4):3246, 1995.

[36] T. Gruner and D.-G. Welsch. Green-function approach to the radiation-field quantization for homogeneous and inhomogeneous kramers-kronig dielectrics. *Phys. Rev. A*, 53:1818–1829, Mar 1996.

[37] Ho Trung Dung, Ludwig Knöll, and Dirk-Gunnar Welsch. Three-dimensional quantization of the electromagnetic field in dispersive and absorbing inhomogeneous dielectrics. *Phys. Rev. A*, 57:3931–3942, May 1998.

[38] Stefan Scheel and Stefan Yoshi Buhmann. Macroscopic quantum electrodynamics-concepts and applications. *Acta Physica Slovaca. Reviews and Tutorials*, 58(5):675–809, 2008.

[39] Gabriel Barton and N.S.J. Fawcett. Quantum Electromagnetics of an Electron Near Mirrors. *Physics Reports*, 170(1):1–95, 1988.

[40] Robert J Zietal. Quantum electrodynamics near material boundaries. *University of Sussex Doctoral Thesis*, 2010.

[41] Roy J. Glauber and M. Lewenstein. Quantum optics of dielectric media. *Phys. Rev. A*, 43(1):467–491, Jan 1991.

[42] C. K. Carniglia and L. Mandel. Quantization of evanescent electromagnetic waves. *Phys. Rev. D*, 3(2):280–296, 1971.

[43] Hanno Hammer. Orthogonality relations for triple modes at dielectric boundary surfaces. *Journal of Modern Optics*, 50(2):207–225, 2003.

[44] G Barton. Quantum mechanics of charged particles near a plasma surface. *J. Phys. A: Math. Gen.*, 10(4):601, 1977.

[45] Michael E. Peskin and Daniel V. Schroeder. *An Introduction to Quantum Field Theory.* Westview Press, Boulder, 1995.

[46] Claudia Eberlein and Dieter Robaschik. Quantum electrodynamics near a dielectric half-space. *Phys. Rev. D*, 73:025009, 2006.

[47] Robert Bennett and Claudia Eberlein. Quantum electrodynamics of a free particle near dispersive dielectric or conducting boundaries. *Phys. Rev. A*, 86:062505, Dec 2012.

[48] Claudia Eberlein and Dieter Robaschik. Inadequacy of perfect-reflector models in cavity qed for systems with low-frequency excitations. *Phys. Rev. Lett.*, 92:233602, 2004.

[49] M Babiker and G Barton. Quantum frequency shifts near a plasma surface. *J. Phys. A: Math. Gen.*, 9(1):129, 1976.

[50] I.S. Gradshteyn and I.M. Ryzhik. *Table of Integrals, Series, and Products, Seventh Edition*. Elsevier, Burlington, MA, USA, 2007.

[51] A. A. Maradudin and D. L. Mills. Scattering and absorption of electromagnetic radiation by a semi-infinite medium in the presence of surface roughness. *Phys. Rev. B*, 11:1392–1415, Feb 1975.

[52] J.D. Jackson. *Classical Electrodynamics*. Wiley, 1998.

[53] S. T. Wu and C. Eberlein. Quantum electrodynamics of an atom in front of a non-dispersive dielectric half-space. *Proc. R. Soc. Lond. A*, 455(1987):2487–2512, 1999.

[54] H. B. G. Casimir and D. Polder. The influence of retardation on the london-van der waals forces. *Phys. Rev.*, 73:360–372, 1948.

[55] PG Etchegoin, EC Le Ru, and M Meyer. An analytic model for the optical properties of gold. *The Journal of chemical physics*, 125:164705, 2006.

[56] P. G. Etchegoin, E. C. Le Ru, and M. Meyer. Erratum: "An analytic model for the optical properties of gold" [J. Chem. Phys. 125, 164705 (2006)]. *The Journal of Chemical Physics*, 127(18):189901, 2007.

[57] G. W. Bennett, B. Bousquet, H. N. Brown, G. Bunce, R. M. Carey, P. Cushman, G. T. Danby, P. T. Debevec, M. Deile, H. Deng, W. Deninger, S. K. Dhawan, V. P. Druzhinin, L. Duong, E. Efstathiadis, F. J. M. Farley, G. V. Fedotovich, S. Giron, F. E. Gray, D. Grigoriev, M. Grosse-Perdekamp, A. Grossmann, M. F. Hare, D. W. Hertzog, X. Huang, V. W. Hughes, M. Iwasaki, K. Jungmann, D. Kawall, M. Kawamura, B. I. Khazin, J. Kindem, F. Krienen, I. Kronkvist, A. Lam, R. Larsen, Y. Y. Lee, I. Logashenko, R. McNabb, W. Meng, J. Mi, J. P. Miller, Y. Mizumachi, W. M. Morse, D. Nikas, C. J. G. Onderwater, Y. Orlov, C. S. Özben, J. M. Paley, Q. Peng, C. C. Polly, J. Pretz, R. Prigl, G. zu Putlitz, T. Qian, S. I. Redin, O. Rind, B. L. Roberts, N. Ryskulov, S. Sedykh, Y. K. Semertzidis, P. Shagin, Yu. M. Shatunov, E. P. Sichtermann, E. Solodov, M. Sossong, A. Steinmetz, L. R. Sulak, C. Timmermans, A. Trofimov, D. Urner, P. von Walter, D. Warburton, D. Winn, A. Yamamoto, and D. Zimmerman. Final report of the e821 muon anomalous magnetic moment measurement at bnl. *Phys. Rev. D*, 73:072003, Apr 2006.

[58] Robert Bennett and Claudia Eberlein. Magnetic moment of an electron near a surface with dispersion. *New Journal of Physics*, 14(12):123035, 2012.

[59] Robert Bennett and Claudia Eberlein. Anomalous magnetic moment of an electron near a dispersive surface. *arXiv preprint arXiv:1304.1480*, 2013.

[60] Julian Schwinger. On quantum-electrodynamics and the magnetic moment of the electron. *Phys. Rev.*, 73:416–417, Feb 1948.

[61] Julian Schwinger. Quantum electrodynamics. iii. the electromagnetic properties of the electron – radiative corrections to scattering. *Phys. Rev.*, 76:790–817, Sep 1949.

[62] J. C. Ward. An identity in quantum electrodynamics. *Phys. Rev.*, 78:182–182, Apr 1950.

[63] Claudia Eberlein and Robert Zietal. Quantum electrodynamics near a dispersive and absorbing dielectric. *Phys. Rev. A*, 86:022111, Aug 2012.

[64] Karl Svozil. Mass and anomalous magnetic moment of an electron between two conducting parallel plates. *Phys. Rev. Lett.*, 54:742–744, 1985.

[65] Maximilian Kreuzer and Karl Svozil. Qed between conducting plates: Corrections to radiative mass and *g-2*. *Phys. Rev. D*, 34:1429–1437, 1986.

[66] M. Bordag. On the apparatus dependence of the anomalous magnetic moment of the electron. *Phys. Lett. B*, 171(1):113 – 117, 1986.

[67] David G. Boulware, Lowell S. Brown, and Taejin Lee. Apparatus-dependent contributions to *g-2* ? *Phys. Rev. D*, 32:729–735, 1985.

[68] Ephraim Fischbach and Norio Nakagawa. Apparatus-dependent contributions to $g-2$ and other phenomena. *Phys. Rev. D*, 30:2356–2370, 1984.

[69] Ephraim Fischbach and Norio Nakagawa. Is (g-2) apparatus-dependent? *Physics Letters B*, 149(6):504 – 508, 1984.

[70] Davis G. Boulware and Lowell S. Brown. Comment on "mass and anomalous magnetic moment of an electron between two conducting parallel plates". *Phys. Rev. Lett.*, 55:133–133, Jul 1985.

[71] Maximilian Kreuzer. Mass and magnetic moment of localised electrons near conductors. *J. Phys. A: Math. Gen.*, 21:3285, 1988.

[72] Leslie L Foldy and Siegfried A Wouthuysen. On the dirac theory of spin 1/2 particles and its non-relativistic limit. *Physical Review*, 78(1):29, 1950.

[73] M. H. Johnson and B. A. Lippmann. Motion in a constant magnetic field. *Phys. Rev.*, 76:828–832, 1949.

[74] Claude Cohen-Tannoudji, Bernard Diu, and Frank Laloë. *Quantum Mechanics, 2 Volume Set*. NewYork: John Wiley & Sons, Inc, 2006.

[75] John P. Walter and Marvin L. Cohen. Frequency- and wave-vector-dependent dielectric function for silicon. *Phys. Rev. B*, 5:3101–3110, 1972.

[76] J. Gómez Rivas, M. Kuttge, H. Kurz, P. Haring Bolivar, and J. A. Sánchez-Gil. Low-frequency active surface plasmon optics on semiconductors. *Appl. Phys. Lett.*, 88(8):082106, 2006.

[77] F Dominguez-Adame and MA González. Solvable linear potentials in the dirac equation. *EPL (Europhysics Letters)*, 13(3):193, 1990.

[78] H. Häffner, T. Beier, N. Hermanspahn, H.-J. Kluge, W. Quint, S. Stahl, J. Verdú, and G. Werth. High-accuracy measurement of the magnetic moment anomaly of the electron bound in hydrogenlike carbon. *Phys. Rev. Lett.*, 85:5308–5311, Dec 2000.

[79] S. Sturm, A. Wagner, M. Kretzschmar, W. Quint, G. Werth, and K. Blaum. g-factor measurement of hydrogenlike $^{28}Si^{13+}$ as a challenge to QED calculations. *Phys. Rev. A*, 87:030501, Mar 2013.

[80] H. Nyquist. Thermal agitation of electric charge in conductors. *Phys. Rev.*, 32:110–113, Jul 1928.

[81] M. S. Tomaš. Green function for multilayers: Light scattering in planar cavities. *Phys. Rev. A*, 51:2545–2559, Mar 1995.

[82] T. Gruner and D.-G. Welsch. Quantum-optical input-output relations for dispersive and lossy multilayer dielectric plates. *Phys. Rev. A*, 54:1661–1677, Aug 1996.

[83] Ho Trung Dung, Stefan Yoshi Buhmann, and Dirk-Gunnar Welsch. Local-field correction to the spontaneous decay rate of atoms embedded in bodies of finite size. *Phys. Rev. A*, 74:023803, Aug 2006.

[84] S.Y. Buhmann and D.-G. Welsch. Born expansion of the Casimir–Polder interaction of a ground-state atom with dielectric bodies. *Applied Physics B*, 82:189–201, 2006.

[85] Ana María Contreras Reyes and Claudia Eberlein. Casimir-polder interaction between an atom and a dielectric slab. *Phys. Rev. A*, 80:032901, Sep 2009.

[86] Claudia Eberlein and Robert Zietal. Interaction of an atom with layered dielectrics. *Phys. Rev. A*, 82:062506, Dec 2010.

[87] Claude Cohen-Tannoudji, Bernard Diu, and Franck Laloe. *Quantum Mechanics*, volume 1. John Wiley and Sons, New York, NY, USA, 1977.

[88] Albert Messiah. *Quantum Mechanics (Dover Republication)*. Dover Books, Mineola, NY , USA, 1999.

[89] Chen-To Tai. *Dyadic Green Functions in Electromagnetic Theory*. IEEE Press, New York, 1994.

[90] C. E. Reed, J. Giergiel, J. C. Hemminger, and S. Ushioda. Dipole radiation in a multilayer geometry. *Phys. Rev. B*, 36:4990–5000, Sep 1987.

[91] Christian Raabe, Stefan Scheel, and Dirk-Gunnar Welsch. Unified approach to qed in arbitrary linear media. *Phys. Rev. A*, 75:053813, May 2007.